ENGINEERING COCRYSTAL AND COCRYSTALLINE SALT SOLUBILITY BY MODULATION OF SOLUTION PHASE CHEMISTRY

by

Lilly Roy

A dissertation submitted in partial fulfillment
of the requirements for the degree of
Doctor of Philosophy
(Pharmaceutical Sciences)
in The University of Michigan
2013

Doctoral Committee:

Associate Professor Naír Rodríguez-Hornedo, Chair
Professor Gordon L. Amidon
Professor Adam J. Matzger
Professor Steven P. Schwendeman
Associate Professor Duxin Sun

This dissertation is dedicated to my family and friends, and to my grandfather who continues to inspire me.

ACKNOWLEDGEMENTS

I would like to thank all of the individuals who have helped and supported me during my graduate studies. I would like to first express my sincerest appreciation of the guidance I have received from my advisor, Dr. Naír Rodríguez-Hornedo. She is an inspirational scientist, an excellent teacher and I would not be the scientist I am today without her mentoring and training. Before coming to the University of Michigan, I enjoyed learning about science but I was not particularly good at planning, or carrying out a scientific study. From our interactions, I learned how to critically review scientific literature, the significance of asking the right questions and the importance of keeping an open mind. I would also like to recognize my dissertation committee members, Dr. Gordon Amidon, Dr. Adam Matzger, Dr. Duxin Sun and Dr. Steve Schwendeman for their valuable guidance, suggestions and critical review of my dissertation work.

My family has supported me tremendously during my graduate studies. My grandfather was continuously encouraging me and kept saying that I was a "much better student than he was". During my first hurdle in graduate school, my candidacy exam, he assured me that my writing would keep getting better and it just takes time and practice. His dissertation has been on my bookshelf as a reminder of how much easier I have it, as I don't have to use a typewriter to put this together. I would like to thank my grandmother for calling me with words of encouragement and sending care packages (at all times of the year) to make sure I had a home-cooked meal every once and awhile. I would like to thank my mom for all of her support, in many ways I have followed in her footsteps by coming here; she too is also a Michigan alumnus. She has always given me so much support in everything I do, and it was my mom who first suggested that I pursue a degree in pharmacy. I would like to thank my Aunt Poppy for her words of wisdom during my thesis writing and for her help with my admissions essays for graduate school. She has always told me how important writing is to progress in any field, which is really some of

the best advice I have received. I would also like to thank my boyfriend Ryan for all of his support during my last two years in graduate school.

This doctoral research was made possible by financial contributions from Pfizer Inc., the Chhotubhai and Savitaben Patel Fellowship, the Norman Weiner Graduate Scholarship, the Fred W. Lyons Fellowship, the Upjohn Fellowship in Pharmaceutics, the University of Michigan College of Pharmacy Fellowship, and the Graduate Student Instructor program. I would also like to thank Barbara-Rodríguez-Spong, for helping to make the Strategic Alliance with Pfizer possible. It was a great experience, and inspired the work presented in the fourth chapter. Thank you to all who gave financial support to this research and my education.

A special thanks to the past and present members of the Rodríguez lab including Sarah Bethune, Adivaraha (Jay) Jayasankar, Neal Huang, Chinmay Maheshwari, David Good, Maya Lipert, Yitan Chen, Fengjuan Cao, Sreenivas Reddy, Phil Zocharski, Crystal Miranda, and Toshiro Fukami. I learned a great deal from all of these students, and their insights, advice, and ideas truly contributed to the learning environment that surrounded me. I could not have picked a better group of people to work with and to be connected to for the rest of my career.

Finally, a note to the reader: parts of the introduction chapter presented in this thesis have been published in the following book chapter

- Roy, L.; Lipert, M.P.; Rodríguez-Hornedo N, Cocrystal Solubility and Thermodynamic Stability. In *Pharmaceutical Salts and Cocrystals*; Wouters, J and Quere, L., Eds; Royal Society of Chemistry: London, UK, 2012, pp. 247-279

TABLE OF CONTENTS

LIST OF FIGURES

LIST OF TABLES

ABSTRACT

ENGINEERING COCRYSTAL AND COCRYSTALLINE SALT SOLUBILITY BY MODULATION OF SOLUTION PHASE CHEMISTRY

by

Lilly Roy

Chair: Naír Rodríguez-Hornedo

There is increasing interest in cocrystal and cocrystalline salts as alternate pharmaceutical solid forms because they provide a range of physicochemical and biopharmaceutical properties. Both cocrystals and cocrystalline salts provide an opportunity to alter not only the lattice chemistry but also the solution chemistry of the parent drug. There are numerous reports of cocrystals and cocrystalline salts that enhance the aqueous solubility and in some cases bioavailability of hydrophobic drugs. The most common method used to characterize the solution behavior of these solid forms is currently powder dissolution. This approach may not identify rapidly transforming metastable cocrystals and cannot be extrapolated to other solution conditions. Cocrystal forms are often evaluated in the presence of additives that affect the solution chemistry of the cocrystal components thereby impacting cocrystal solubility and thermodynamic stability. This dissertation explores the influence of solution chemistry on cocrystal and cocrystalline salt solubility and thermodynamic stability relative to the parent drug and salt respectively. Knowledge of the solution mechanisms that alter the cocrystal component solubilities can be used to anticipate cocrystal solubility and $S_{cocrystal}/S_{drug}$.

The objectives of this work are to (1) to determined the key thermodynamic parameters necessary to rationally select surfactants to modulate cocrystal solubility and $S_{cocrystal}/S_{drug}$ using mathematical models derived from knowledge of the solution-chemistry affecting the cocrystal components (2) to evaluate the contributions of

ionization and micellar solubilization to cocrystal solubility and $S_{cocrystal}/S_{drug}$ in physiologically relevant media (3) to derive mathematical models that describe cocrystalline salt solubility dependence on ionization and the common-ion effect so that the solubility of these solid forms can be characterized using minimal experimental measurements (4) to develop a method to characterize the equilibrium solubility of metastable cocrystalline salts and (5) to examine the relationship between the relative magnitude of $S_{cocrystal}/S_{drug}$ and the observed supersaturation relative to the parent drug.

Surfactant selection to control cocrystal solubility and $S_{cocrystal}/S_{drug}$ was rationalized by the magnitude of drug solubilization (K_s^{drug}) and the preferential solubilization of the drug by the micellar surfactant ($K_s^{drug}>K_s^{coformer}$). The surfactant concentration required to reduce the $S_{cocrystal}/S_{drug}$ by half the original magnitude for a group of surfactants was in order of the surfactant's critical micelle concentration. Both micellar solubilization and ionization are capable of altering $S_{cocrystal}/S_{drug}$. For the case of indomethacin-saccharin, micellar solubilization decreased $S_{cocrystal}/S_{drug}$ while ionization increased $S_{cocrystal}/S_{drug}$. This behavior is expected to occur for other cocrystals composed of a drug that is more hydrophobic than the coformer when the coformer ionizes at lower pH values than the drug ($pK_a^{coformer}<pK_a^{drug}$)

Media reported to simulate physiologically relevant solution conditions affects cocrystal solubility based on the ionization and micellar solubilization of the cocrystal components. Cocrystal solubility can be predicted from the cocrystal component solubilities by deriving solubility models that include component ionization and micellar solubilization. Any media containing physiologically relevant surfactants that preferentially solubilizes the drug component relative to the coformer reduces the $S_{cocrystal}/S_{drug}$ compared to media without the surfactant. Fed state simulated intestinal fluid was found to decrease the $S_{cocrystal}/S_{drug}$ of the indomethacin-saccharin cocrystal due to preferential solubilization of the drug. The indomethacin-saccharin cocrystal achieved higher solution concentrations, which were sustained for a longer period of time (4 hours) during dissolution in FeSSIF relative to acetate buffer, which is at the same pH and ionic strength as FeSSIF without sodium taurocholate and lecithin.

Cocrystalline salts were found to exhibit solubility product behavior and exhibit a different solubility dependence on solution pH and counterion concentration relative to

the parent salt. Equations were derived considering cocrystalline salt dissociation and coformer ionization. These equations described the solubility-pH dependence and the common-ion effect and enable the prediction and anticipation of cocrystalline salt solubility under a wide variety of solution conditions. The common-ion effect on cocrystalline salts is less than that observed for the parent salt, therefore cocrystalline salts may be useful to mitigate the common-ion effect.

Chapter 1

Introduction

Research regarding the biopharmaceutical and physicochemical properties of cocrystals has generated tremendous interest among a range of scientific fields, including chemistry, crystal engineering, materials engineering, and the pharmaceutical sciences. Even though there are increasing examples of cocrystals that offer superior pharmaceutical properties relative to the parent drug, they are currently under-utilized.[1-11] Cocrystals are a class of multicomponent solids containing two or more different molecular components in a single homogenous crystalline phase with a well-defined stoichiometry; they are distinguished from solvates in that the cocrystal components are solids at room temperature.

Hydrogen-bonded assemblies between the neutral molecules of the drug and the cocrystal coformer often guide cocrystal formation, which is why they are of particular interest due to their ability to modify the solubility properties of nonionizable drugs that cannot otherwise form pharmaceutical salts. Currently there are no examples of cocrystal drug forms on the market, but there is a cocrystalline salt marketed as Depakote. Depakote (divalproex sodium) is sodium valproate cocrystallized with valproic acid that was serendipitously discovered to exhibit superior characteristics relative to its components.[12]

Solid-state modifications and formulation design allow for the improvement of the physicochemical properties of a drug substance while maintaining the same chemical entity and pharmacological interaction. Polymorphs, solvates and salts are the common solid forms employed for product development. However, consideration of cocrystals and cocrystalline salts as viable solid forms for development would significantly expand the number and diversity of solid drug forms available, and improve the likelihood of finding a solid form with the required physicochemical properties. A schematic of the different classes of multicomponent solids is shown in Figure 1.1

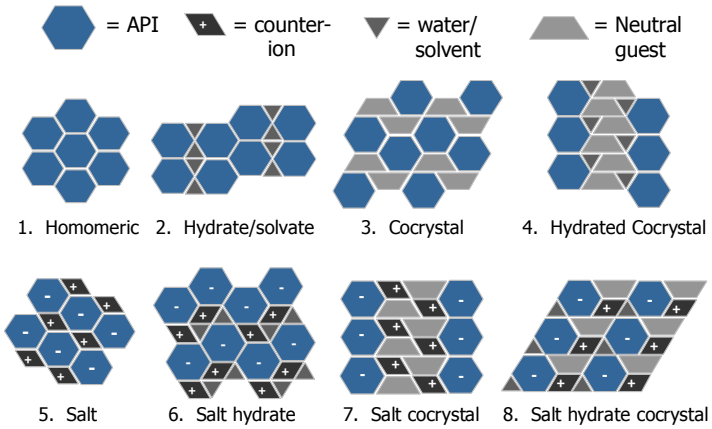

Figure 1.1 Comparison of multicomponent solid form modifications that can be used to alter the properties of a drug product.[13]

It is crucial to know the possible solid-forms of a given drug substance to select the form with optimal biopharmaceutical properties and to avoid unwanted transformations to another form during processing, storage and dosing. Cocrystal-solution phase interactions have a major impact on the solution conditions that promote cocrystal formation or cocrystal solution-mediated transformation to the parent drug. While the role of solution chemistry on the solubility and thermodynamic stability of cocrystals has been investigated,[4,14-17] these concepts are seldom applied to cocrystal synthesis and solubility characterization. This chapter introduces examples of cocrystals that enhance physicochemical properties, the *in silico* methodologies used to guide cocrystal design, rational approaches for screening and synthesizing cocrystals and an introduction to the current understanding of salt and cocrystal solution chemistry. A statement of the research objectives of this thesis will be provided at the conclusion of this chapter.

Cocrystal Physicochemical and Biopharmaceutical properties

It is possible to generate many distinct crystalline forms via cocrystallization of a pharmaceutical free drug or salt. The opportunity to alter the crystalline structures by introduction of a new molecular component that interacts with the drug increases the potential to modify the crystal lattice compared to polymorphs, which are composed of only the drug molecule. Each cocrystalline form exhibits unique physicochemical and biopharmaceutical properties compared to its components and compared to other cocrystals. Cocrystallization has been used to improve properties such as hygroscopicity,

compactability, tensile strength, chemical stability, solubility, dissolution and bioavailability. There are numerous examples that have been published in which cocrystals improve the pharmaceutical properties of the parent drug (or salt); however, there is no correlation between cocrystal design and the desired physicochemical properties. There are however, a few examples in which the cause of a chemical instability or poor tableting was identified within the crystalline lattice, and cocrystallization was specifically pursued to modify the site of interest.[5,11]

Chemical stability

Cocrystals may exhibit improved chemical stability relative to the parent drug due to the rearrangement of the drug molecules in the crystal lattice. For example, cocrystallization of the drug adefovir dipivoxil with saccharin improves the chemical stability. The pivaloyoxymethyl moiety of the drug interacts with the NH group in saccharin which is hypothesized to prevent hydrolysis of the pivaloyoxymethyl moiety in the solid state.[3] A 2:1 miconazole-succinic acid cocrystal exhibited improved chemical stability in the crystalline state and in formulation compared to the free base.[11] The cocrystal had similar chemical stability to the marketed nitrate salt and could be considered as an alternate solid form.

Mechanical properties

Tableting properties of pharmaceutical solids relate to their crystal packing and structure. Cocrystals have been used to design solid forms with improved tableting properties relative to the parent drug.[5] The stable form 1 of paracetamal exhibits poor tableting properties relative to its metastable form 2. Form 2 is proposed to have better tableting properties due to its parallel hydrogen bonded layers in the crystal lattice. Coformers for cocrystallization were selected based on the ability to generate layered solid forms of paracetamol, similar to that of form 2. Cocrystals of paracetamol exhibited tableting superior to both forms, and are thermodynamically stable in the solid state.[5] The tablets formed with paracetamol cocrystals were characterized in terms of breaking force and tensile strength.

Solubility, dissolution and bioavailability

Inadequate solubility of drug candidates is an ongoing issue in drug development and methodologies to improve solubility are commonly pursued. Cocrystals can generate supersaturation with respect to the less soluble parent drug, which is of particular interest for BCS class II drugs (low aqueous solubility, and high permeability) that may exhibit poor bioavailability do to their low aqueous solubility. The indomethacin-saccharin cocrystal was found to achieve higher solution concentrations than the parent drug during dissolution,[1,6] and is 13-65 times more soluble than the parent drug in a range of pH 1-3, as determined by equilibrium solubility measurements.[18] The cocrystal was found to improve bioavailability relative to the unformulated parent drug when dosed in canines.[6] Cocrystals of itraconazole increased drug concentration relative to the free drug, and performed similarly to the marketed amorphous formulation (Sporanox®).[8]

There are several examples of cocrystals that exhibit enhanced bioavailability relative to the parent drug, as measured by an increase in the area under the curve (AUC) of the time course of the drug in the plasma. Zaworotko *et al.* showed that four cocrystals of quercetin had superior bioavailability relative to the parent drug; the highest increase in AUC was achieved by the quercetin:theobromine dihydrate cocrystal and was 10 times higher than that of the parent drug.[9] Mcnamara *et al.* showed that a glutaric acid cocrystal of a poorly soluble development compound, 2-[4-(4-chloro-2-fluorophenoxy)phenyl]pyrimidine-4-carboxamide, enhanced the disk dissolution rate by 18-fold which translated to a 3-fold higher AUC relative to drug when dosed in canines.[7] Other cocrystals reported to increase AUC relative to the parent drug include meloxicam-aspirin (4.4-fold increase in AUC)[2], meloxicam-1-hydroxy-2napthoic acid (1.5-fold increase in AUC)[19], indomethacin-saccharin (1.9-fold increase in AUC)[6] as long as drug and cocrystal were compared using the same formulation.

There are cases in which cocrystals generate higher solution concentrations during dissolution relative to the parent drug, but do not show an improved bioavailability. For example, lamotrigine: nicotinamide monohydrate exhibited a lower AUC and C_{max} when dosed in rats despite demonstrating improved dissolution in water and acidic media (water 0.1 M HCl, pH =1).[20] The cocrystal and drug were dosed in a suspension (5% PEG and 95% Methyl cellulose aqueous solution) without an indication of whether the

cocrystal was thermodynamically stable under these conditions. The carbamazepine:saccharin (CBZ:SAC) cocrystal has a higher solubility than carbamazepine dihydrate,[4] however, the pharmacokinetic parameters determined from a bioavailability study of CBZ:SAC in canines were not statistically different compared to those of the marketed formulation of carbamazepine (Tegretol).[21] None of the reported studies evaluate cocrystal solution chemistry under equilibrium conditions prior to evaluating their pharmacokinetic behavior; the influence of formulation additives on cocrystal solubility and $S_{cocrystal}/S_{drug}$ is not considered prior to adding a cocrystal to a routine formulation. Understanding the effect of formulation additives and biologically relevant solution conditions on cocrystal solubility and $S_{cocrystal}/S_{drug}$ could give insight as to which excipients and which cocrystals will result in the best *in vivo* performance, and may help to guide cocrystal selection.

Cocrystal Formation & Design

Prior to carrying out cocrystal screens, which are costly in material and time, potential coformers can be identified based on molecular recognition interactions. Molecular recognition events are responsible for the self-assembly of two or more components through noncovalent interactions with energetically favorable geometries.[22] A large number of diverse solid forms can be generated by taking advantage of self-assembly, and the resulting molecular arrangement of a drug within a crystal lattice affects its physicochemical properties. Through cocrystallization, it is possible to construct a new three-dimensional, ordered crystal structure using noncovalent interactions between a drug product and a coformer.

The Cambridge Structural Database (CSD) can be used to perform supramolecular retrosynthetic analysis, which involves identifying intermolecular units for a target cocrystal structure. Coformers can be selected to cocrystallize with a drug based on knowledge of geometries and preferred orientations of existing intermolecular interactions. Synthons are the common noncovalent intermolecular interactions of specified geometries identified in the literature that make up the structural units within a supramolecular structure; a few examples of synthons are shown in Figure 1.2.

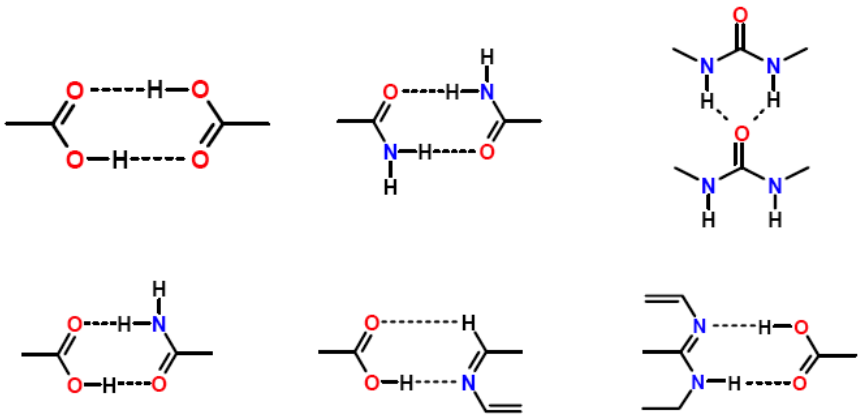

Figure 1.2.Common supramolecular synthons formed from carboxylic acids and amide groups.[23-25]

Synthons can form between identical functional moieties (homosynthon) or different functional moieties (heterosynthon). Cocrystal structures may contain different combinations of homosynthons and heterosynthons. Additionally, these intermolecular interactions may be homomeric, between the same molecule, or heteromeric, between different molecules. Coformers were selected to form cocrystals with carbamazepine based on two design strategies. The first strategy was to maintain the cyclic homomeric carboxamide homosynthon and find coformers that could interact with the exterior hydrogen-bond donors and acceptors. An example of this is the 1:1 cocrystal carbamazepine-saccharin which is shown in Figure 1.3a. The second strategy was to disrupt the carboxamide homosynthon by forming a heteromeric synthon with the carboxamide. This was accomplished by forming a heterosynthon between the carboxamide with a carboxylic acid coformer. An example of the second strategy is the 2:1 carbamazepine-succinic acid cocrystal, which is shown in Figure 1.3b.

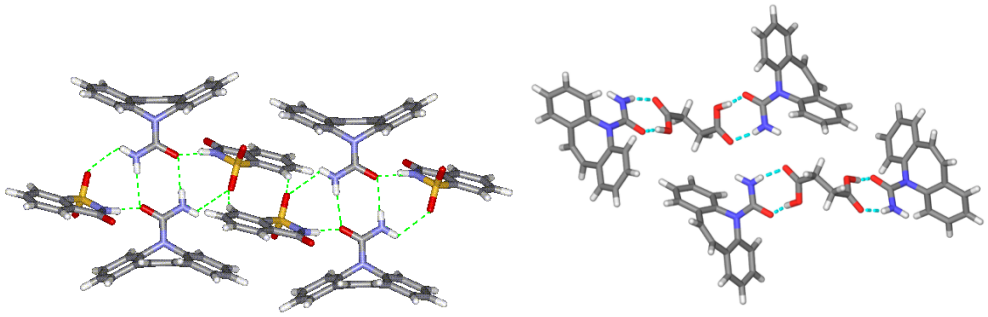

(a) (b)

Figure 1.3. Examples of two strategies to form cocrystals of carbamazepine (a) carbamazepine-saccharin which maintain cyclic carboxamide homosynthon (b) carbamazepine-succinic which disrupts carboxamide homosynthon in favor of a heterosynthon between carboxamide and the dicarboxylic acid.[26]

Coformers are often selected based on functional groups capable of complimentary hydrogen bonding with the drug substance. Due to their directional interactions, hydrogen bonds most strongly influences molecular recognition. Etter and Donohue developed general guidelines to predict hydrogen bond interactions that result in crystal formation.[22,25] These guidelines are based on the analysis of the hydrogen bond interactions and the packing motifs of numerous molecular structures: (1) the hydrogen bonding in the crystal structure will include all acidic hydrogen atoms, (2) all good hydrogen bond acceptors will participate in hydrogen bonding if there is an adequate supply of hydrogen bond donors, (3) hydrogen bonds will preferentially form between the best proton donor and acceptor, and (4) intramolecular hydrogen bonds in a six-membered ring form in preference to intermolecular hydrogen bonds.[22,24,25]

In addition to these rules, the stereochemistry and competing interactions between molecules may need to be considered for cocrystal design. Other considerations in designing stable crystal structures include minimizing electrostatic energies and the free volume within the crystal.[27] Analysis of cocrystal structures from the CSD suggests that components that cocrystallize often have similar shapes and polarities.[28] While these strategies offer a good basis to select coformers for cocrystal screening and synthesis, they are not able to *ab initio* determine the cocrystal structure, molecules that will cocrystallize, conditions that promote cocrystallization or the physicochemical properties of the cocrystals based on their supramolecular structure. Several cocrystals been

discovered by using a combination of supramolecular retrosynthetic analysis and cocrystal screening techniques and are shown in Table 1.1.

Table 1.1 Examples of pharmaceutical cocrystals reported in the literature

Drug	Coformer	Reference
Indomethacin	saccharin, nicotinamide, D/L mandelic, lactamide and benzamide	[1,29]
Carbamazepine	4-aminobenzoic, saccharin, salicylic, succinic, benzoic, ketoglutaric, maleic, glutaric, malonic, oxalic, adipic, (+)-camphoric, 4-hydroxybenzoic, 1-hydroxy-2-napthoic, DL-tartaric, L-tartaric, fumaric, DL-malic, L-malic, acetic, butyric, 5-nitroisphthalic, formic,	[26,30]
Meloxicam	aspirin, 1-hydroxy-1-napthoic acid, salicylic, 4-hydroxybenzoic, glutaric, maleic, L-malic, benzoic, DL-malic, hydrocinnamic, fumaric	[2,31]
Piroxicam	L-tartaric, citric, fumaric, adipic acid, succinic, benzoic, 4-hydroxybenzoic, oxalic, ketoglutaric, salicylic, pyroglutamic acid, DL-tartaric, maleic, DL-malic, L-malic	[32]
Ketoconazole	succinic, fumaric, adipic, oxalic	[33]
Itraconazole	succinic, fumaric, L-malic, L-tartaric, DL-tartaric,	[8]
Lamotrigine	acetamide, nicotinamide, methylparaben	[20]
Curcumin	resorcinol, pyrogallol	[34,35]
Paracetamol	oxalic, theophylline, phenazine, naphthalene	[5]

Screening and Synthesis of Cocrystals

Cocrystals that are less soluble than the parent drug have been made by slurrying the stoichiometric amounts of cocrystal components in a solvent. However, this method will not work for cocrystals that are more soluble than the parent drug. Similar to salts, cocrystal solid-solution equilibria are dictated by solution composition,[36,37] and cocrystal solubility product behavior has been utilized to develop reliable methods for screening synthesis and equilibrium solubility characterization of cocrystals.[4,38] The reaction crystallization method (RCM),[38] is useful for synthesis and screening, and is based on selecting solution conditions that generate supersaturation with respect to cocrystal. The supersaturation, σ, of a cocrystal has been described by

$$\sigma = \left(\frac{\prod c_i^{v_i}}{K_{sp}}\right)^{1/v} \quad (1.1)$$

where Πc_i^{vi} is the product of the cocrystal component concentrations in the supersaturated solution when the activity coefficients are unity, ν_i is the stoichiometric coefficient in the chemical equation or stoichiometric number of cocrystal components, i, is the cocrystal chemical formula $\nu=\Sigma\nu_i$, and K_{sp} is the cocrystal solubility product.[38] Therefore the supersaturation of a 1:1 cocrystal AB is described by

$$\sigma = \left(\frac{[A][B]}{K_{sp}}\right)^{1/2} \quad (1.2)$$

The supersaturation with respect to a 1:1 cocrystal AB is generated by adding the poorly soluble drug A to a solution that is near saturated or saturated with the water-soluble coformer B as shown in Figure 1.4.

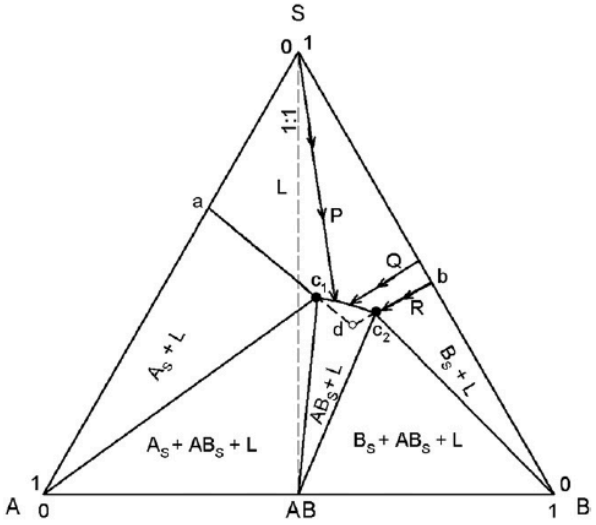

Figure 1.4. Schematic triangular phase solubility diagram showing the different methods by which supersaturation is generated with respect to cocrystal AB for a system where reactants have different solubilities and cocrystal is more soluble than reactants in solutions of equivalent reactant composition (a non-congruently saturating system). Arrows indicate the of solution composition as a result of evaporation of solution of nonequivalent composition of A and B (path P), adding reactant A to solutions at close to saturation with B (path Q) or saturated with B (path R).[30]

The RCM method has been used to successfully discover 27 cocrystals of carbamazepine in both water and ethanol.[30] By creating supersaturation with respect to cocrystal by taking advantage of solubility product behavior, cocrystals can be discovered in solvents in which they are incongruently saturating. Other commonly used methods to

synthesize cocrystals include grinding, solvent drop grinding, and solvo-thermo methods. Cocrystals have also been shown to form spontaneously in the solid-state during storage,[39] as well as from drug and coformer mixtures in the presence of deliquescent additives.[40]

Solubility characterization of metastable cocrystals

Cocrystals that are more soluble than the parent drug may undergo solution-mediated transformation to the less soluble drug, making solubility characterization a challenge. The true cocrystal solubility is underestimated when transformation occurs during dissolution or an apparent solubility measurement in which cocrystal is suspended in an aqueous solution. The drug concentrations observed during these kinetic measurements, is highly dependent on the solution conditions, and cannot be extrapolated to other solution conditions. *Good et al.* developed a method to access the equilibrium cocrystal solubility that takes advantage of the solubility product behavior of a cocrystal. [4] Because cocrystal solubility decreases with coformer concentration, an intersection point exists between the cocrystal and drug solubility curves. According to Gibbs' phase rule, a system with three components (drug, coformer and solution) and three phases (solid cocrystal, solid drug and solution) has one degree of freedom. Therefore the solution concentrations in equilibrium with solid cocrystal and solid drug are invariant holding temperature and pH constant.

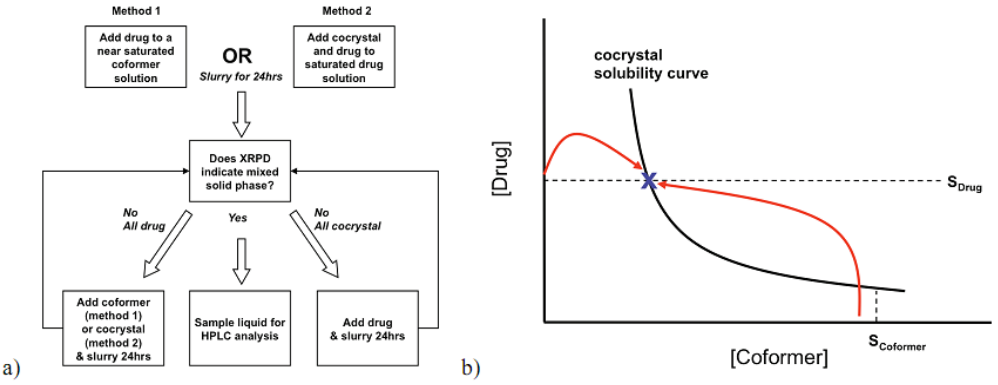

Figure 1.5. (a) Flowchart of method used to approach the eutectic point and determine the equilibrium solution concentrations of cocrystal components at the eutectic (b) Schematic phase solubility diagram illustrating two pathways to the eutectic point (marked X).[4]

As shown in Figure 1.5, the eutectic point can be approached by cocrystal dissolution and precipitation of the parent drug, or by drug dissolution in a coformer rich

solution, which results in cocrystal precipitation. Approaching the eutectic point by cocrystal dissolution can result in supersaturated drug concentrations while approaching the eutectic point by cocrystal precipitation can result in under saturated drug concentrations. Solid phases and solution compositions should be monitored until the solution composition reaches a steady value in the presence of the two solid phases. Convergence of the solution composition from these two methods, i.e. different initial states, establishes that equilibrium is reached. Solid phases can be analyzed in-situ by Raman spectroscopy or by XRPD and FT-IR after isolation of the solids. Solution composition can be analyzed by HPLC. Approaching the equilibrium eutectic point by cocrystal precipitation and dissolution is crucial to obtain the most reliable experimental measurements, especially when the parent drug can withstand a supersaturated state. The eutectic point is a key parameter to measure cocrystal solubility and establish solution conditions for cocrystal synthesis.

Salt Solution Chemistry

Salt formation is one of the most common solid state modifications used to improve the solubility of a poorly soluble drug. There are numerous salt forms available as marketed drug products such as chloroquine phosphate, miconazole nitrate, doxycycline hydrochloride, and diclofenac sodium to name a few. Chloride is the most common counter-ion for a pharmaceutical base.[41] Mathematical equations that describe the solubility and stability regions between free drug and its salt as a function of pH were derived in the 1970s, [42,43] and are widely used to characterize the solubility behavior of salts. An example of a pH-solubility diagram between a salt and its free base is shown in Figure 1.6.

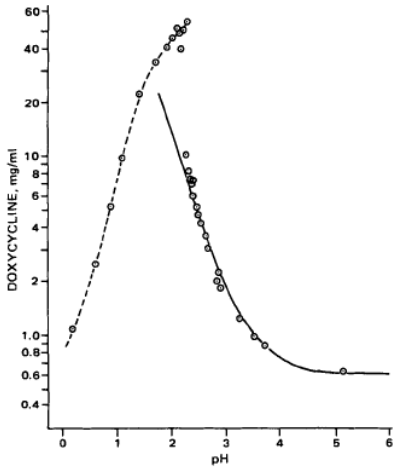

Figure 1.6. The pH-solubility profile of doxycycline (free base and HCl salt) in aqueous hydrochloric acid at 25°C. At pH_{max}= 2.16, both salt and base are in equilibrium with the solution. Below pH_{max}, the salt is the stable solid phase (dashed line). Above this pH, the base is the stable solid phase in equilibrium with solution. The solid line is theoretical according to equation (1.3) using S_{un}^{B}=0.625 mg/ml and pK_a =3.30. Concentration is expressed as free base equivalent.[44]

The solubility of the free base (doxycycline) increases with decreasing pH (increasing $[H^+]$) according to

$$S_T^B = S_{un}^B \left(1 + \frac{[H^+]}{K_a^B}\right) \tag{1.3}$$

where S_{un} is the solubility of the unionized base, K_a^{HA} is the ionization constant of the acid and $[H^+]$ is the concentration of protons in solution.[42] In the example shown in Figure 1.6, the solution pH is decreased using HCl resulting in the precipitation of the HCl salt. The solubility of the salt of the protonated base is

$$S_T^{BH+Cl-} = \sqrt{K_{sp}\left(1+\frac{K_a^B}{[H^+]}\right)} \tag{1.4}$$

where the solubility product, K_{sp}, is defined by the concentrations of the protonated base and the counter-ion Cl^-:

$$K_{sp}=[BH^+][Cl^-] \tag{1.5}$$

Due to solubility product behavior, the solubility of the HCl salt, as measured by the concentration of drug, decreases with increasing solution concentrations of chloride,[45] according to equation (1.5), this is referred to as the common-ion effect. Often this

behavior is observed as a consequence of altering solution pH by the addition of HCl. As more HCl is added to the solution to decrease the solution pH, the solution concentration of chloride increases causing the drop in solubility with pH.

The pH_{max} occurs at the intersection of the salt and free base solubility curves, and is a function of the salt K_{sp}, the drug intrinsic solubility and the drug pK_a according to

$$pH_{max}=pK_a+\log\left(\frac{K_{sp}}{S_{un}}\right) \qquad (1.6)$$

for a free base and its salt.[44] The pH_{max} increases by 1 pH unit with a one unit increase in the free base pKa, or an increase in magnitude of the unionized base solubility, S_{un}. The pH_{max} decreases by 1 pH unit with an increase in magnitude of the salt K_{sp}. Similar mathematical relationships describing the solubility-pH and pH_{max} of a free acid and its salt have also been derived in the literature.[43]

Engineering Cocrystal Solubility via Solution Chemistry

The diverse molecular properties and multicomponent nature of cocrystals provide an extraordinary level of solubility control via solution phase interactions. The molecular processes shown in Figure 1.7 influence the cocrystal solubility and the cocrystal solubility advantage relative to drug ($S_{cocrystal}/S_{drug}$) and include cocrystal dissociation, complexation, ionization and micellar solubilization.

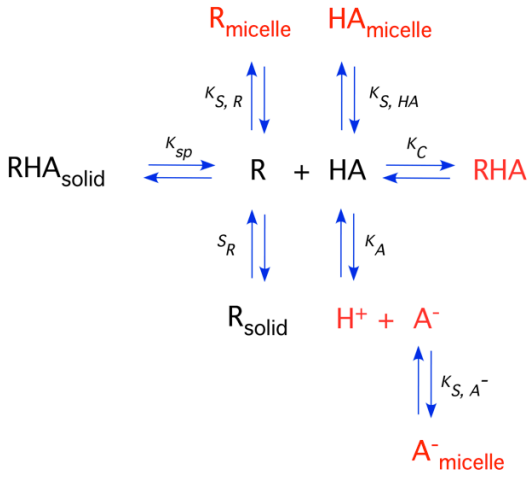

Figure 1.7. Examples of cocrystal solution phase interactions and associated equilibria for a cocrystal RHA of a nonionizable drug (R) and an ionizable coformer (HA) a micellar solution.

Ionization

Several pharmaceutical cocrystals containing molecules with a wide range of ionization behaviors have been reported: acidic drugs with acidic or nonionizable coformers, (indomethacin-saccharin, indomethacin-nicotinamide);[1,29] basic drugs with acidic coformers, (ketoconazole-fumaric acid, miconazole-succinic acid);[11,33] and nonionizable drugs with acidic or amphoteric coformers (paracetamol-oxalic acid, carbamazepine-4aminobenzoic acid).[5,26] The ability to *a priori* predict the solubility-pH dependence of a novel pharmaceutical cocrystal is critical to select coformers to customize the solubility-pH dependence relative to the parent drug.

Mathematical models describing cocrystal pH-solubility dependence have been derived considering the equilibria for cocrystal dissociation and component ionization. For example, the relevant equilibria and equilibrium constants for a 1:1 cocrystal RHA composed of a nonionizable drug (R) and an acidic coformer (HA) are

$$RHA_{solid} \overset{K_{sp}}{\leftrightarrow} R+HA$$

$$K_{sp}=[R][HA] \tag{1.7}$$

$$HA \leftrightarrow H^{+}+A^{-}$$

$$K_a^{HA}=\frac{[H^{+}][A^{-}]}{[HA]} \tag{1.8}$$

where K_{sp} is the solubility product of the cocrystal, K_a is the ionization constant of HA and species without subscripts refer to the solution phase.

The analytical concentration of coformer is the sum of the ionized and nonionized species, which is given by:

$$[HA]_T=[HA]+[A^{-}] \tag{1.9}$$

The cocrystal solubility equals the analytical concentration of drug or coformer in solutions of a stoichiometry equal to that of the cocrystal (no coformer in stoichiometric excess):

$$S_T^{RHA}=[R]_T=[HA]_T \tag{1.10}$$

Based on the mass balances of HA and R, and the equilibrium constants described in equation (1.7) and (1.8), the cocrystal solubility dependence on $[H^{+}]$ is described by

$$S_T^{RHA} = \sqrt{K_{sp}\left(1+\frac{K_a}{[H^+]}\right)} \tag{1.11}$$

This solubility represented by equation (1.11) is referred to as the stoichiometric solubility based on the presented assumptions. The analysis presented applies to dilute solutions in which activities are relatively constant and can be replaced by solution concentrations.

Cocrystal solubility dependence on $[H^+]$ can be predicted from knowledge of the cocrystal solubility product (K_{sp}) and component ionization (K_a). Table 1.2 shows the solubility equations describing the solubility-pH dependence for cocrystals with a range of stoichiometries and ionization properties. Figure 1.8 demonstrates the ability of cocrystals to modify the solubility behavior relative to the parent drug. Theoretical

Table 1.2 Equations describing cocrystal solubility-pH dependence

Cocrystal	Solubility	Equation
RHA 1:1 nonionizable: monoprotic acid	$S_T^{RHA} = \sqrt{K_{sp}\left(1+\frac{K_a}{[H^+]}\right)}$	(1.12)
HDHA 1:1 monoprotic acid: monoprotic acid	$S_T^{HDHA} = \sqrt{K_{sp}\left(1+\frac{K_a^{HD}}{[H^+]}\right)\left(1+\frac{K_a^{HA}}{[H^+]}\right)}$	(1.13)
R_2H_2A 2:1 nonionizable: diprotic acid	$S_T^{R_2H_2A} = \sqrt[3]{\frac{K_{sp}}{4}\left(1+\frac{K_a^{H_2A}}{[H^+]}+\frac{K_a^{H_2A}K_a^{HA^-}}{[H^+]^2}\right)}$	(1.14)
R_2HAB 2:1 nonionizable: amphoteric	$S_T^{R_2HAB} = \sqrt[3]{\frac{K_{sp}}{4}\left(1+\frac{[H^+]}{K_{a1}^{HAB}}+\frac{K_{a2}^{HAB}}{[H^+]}\right)}$	(1.15)
B_2H_2A 2:1 monoprotic base: diprotic acid	$S_T^{B_2H_2A} = \sqrt[3]{\frac{K_{sp}}{4}\left(1+\frac{[H^+]}{K_{a1}^{B}}\right)^2\left(1+\frac{K_a^{H_2A}}{[H^+]}+\frac{K_a^{H_2A}K_a^{HA^-}}{[H^+]^2}\right)}$	(1.16)
$^-ABH^+H_2A$ zwitterion: diprotic acid	$S_T^{\ ^-ABH^+H_2A} = \sqrt{K_{sp}\left(1+\frac{[H^+]}{K_{a1}^{-ABH+}}+\frac{K_{a2}^{-ABH+}}{[H^+]}\right)\left(1+\frac{K_a^{H_2A}}{[H^+]}+\frac{K_a^{H_2A}K_a^{HA^-}}{[H^+]^2}\right)}$	(1.17)

solubility-pH profiles were generated from the equations in Table 1.2, using the K_a values, and cocrystal K_{sp} indicated in the figure. Cocrystals of a nonionizable drug may exhibit a variety of solubility-pH dependencies based on the coformer ionization properties.

For example, the solubility of cocrystal of a nonionizable drug with an acidic coformer increases with increasing pH (Figure 1.8(a)) while cocrystallization with an amphoteric coformer results in a U-shaped cocrystal solubility-pH profile with the minimum solubility occurring between the two coformer pK_a values (Figure 1.8(b)).

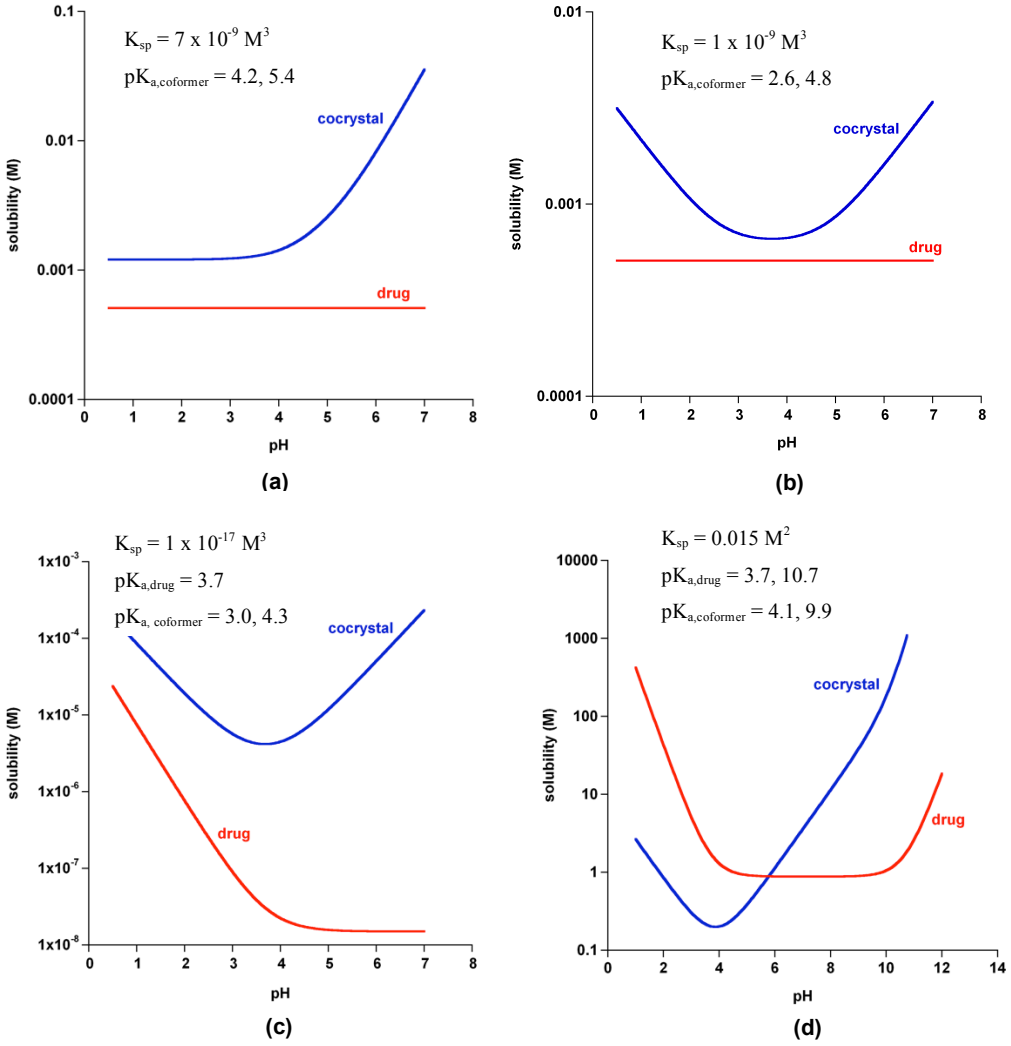

Figure 1.8. Theoretical solubility-pH profiles were calculated for (a) 2:1 R_2H_2A (carbamazepine-succinic acid) cocrystal, (b) 2:1 R_2HAB cocrystal (carbamazepine 4-aminobenzoic acid), (c) 2:1 B_2H_2A cocrystal (itraconazole-L-tartaric acid) and (d) 1:1 $ABH^+H_2X^-$ cocrystal (gabapentin-3-hydroxybenzoic acid) using the equations in Table 1.2. Drug and coformer pK_a values and cocrystal K_{sp} are included in each graph. K_{sp} values were either experimentally determined or estimated from published work.[14]

A U-shaped solubility-pH profile can also be obtained by cocrystallizing a basic drug with an acidic coformer (Figure 1.8(c)) with the minimum solubility occurring between the drug and coformer pK_a values. The pH range in which the minimum

solubility occurs is dependent on the difference between the 2 pK_a values. Often, several cocrystals of a given drug are discovered for which the solubility is not known. The derived cocrystal solubility models shown in Table 1.2 are useful to predict the cocrystal solubility-pH dependence based on the ionization properties of the cocrystal components. The complete cocrystal solubility-pH profile can be characterized from a single solubility measurement to evaluate K_{sp}, when the component ionization constants (K_a) are known.

Micellar solubilization

Pharmaceutical drug forms encounter aqueous solutions containing surfactants during processing, formulation and dissolution. Surfactants are composed of amphiphilic monomers that self-associate above a critical micellar concentration (CMC) to form micelles containing a hydrophobic core in which hydrophobic molecules can partition. Because pharmaceutical cocrystals are often composed of a hydrophobic drug and a hydrophilic coformer, the two components will be solubilized differentially according to the relative hydrophobicities of the components. Recently, we have discovered that micellar surfactants impart thermodynamic stability to otherwise metastable cocrystals when the hydrophobic drug is solubilized preferentially to the hydrophilic coformer.[16,17]

Cocrystals of carbamazepine that were 2-4 times more soluble than the drug in water were found to be thermodynamically stabilized in solutions containing the surfactant sodium lauryl sulfate (SLS) above a critical stabilization concentration (CSC).[16] As shown in Figure 1.9, the cocrystals exhibited a weaker solubility dependence on micellar solubilization compared to the drug resulting in the intersection of the cocrystal and drug solubility curves at the CSC. Above the CSC, the cocrystal is the stable and less soluble phase.

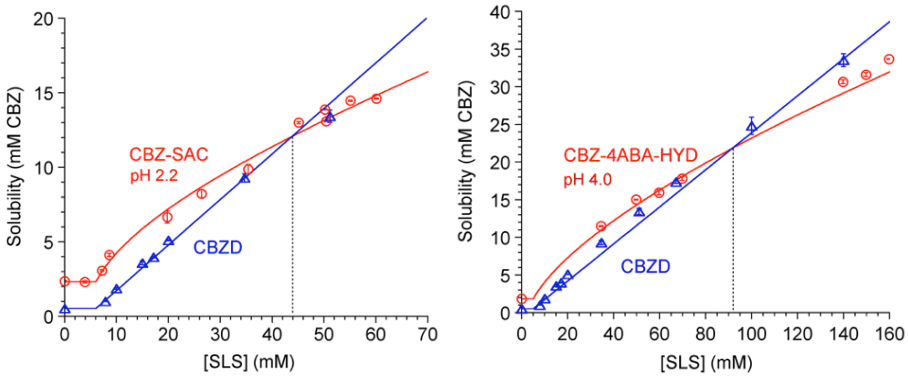

(a) (b)

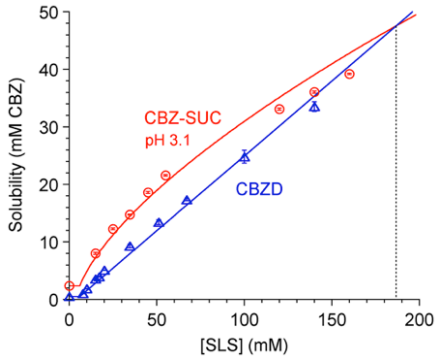

(c)

Figure 1.9. Experimental and predicted influence of SLS on drug (CBZD) solubility and CBZ cocrystal solubilities for (a) CBZ-SAC, (b) CBZ-4-ABA-HYD and (c) CBZ-SUC The experimental solubilities were measured in unbuffered surfactant aqueous solutions. The pH measured at equilibrium is indicated in figure. Symbols (○ cocrystal, Δ drug) represent experimental values. Predicted cocrystal solubilities were calculated according to equations (1.18), (1.21) and (1.20) with K_{sp}, pK_a and K_s values in Table 1.3.[16]

The solubility behaviors of the carbamazepine cocrystals were well described by mathematical models that consider the equilibria for cocrystal dissociation (K_{sp}), component ionization (K_a) and component micellar solubilization (K_s).[15,16] The K_{sp}, pK_a and K_s values used to describe the behavior in Figure 1.9 are shown in Table 1.3.

Table 1.3. Cocrystal K_{sp}, component pK_a and K_s values used to predict cocrystal solubility.[16]

Solid phase	K_{sp} mM^2 or mM^3	pK_a	K_s^{CBZ} mM^{-1}	$K_s^{coformer}$ mM^{-1}
CBZ-SAC (1:1)	2.08	2.0	0.58[a]	0.013
CBZ-4ABA (H) (2:1)	2.56	2.6, 4.8	0.49[b]	0[g]
CBZ-SUC (2:1)	6.15	4.1, 5.6	0.49[b]	0[g]
CBZ (H)	n/a	n/a	0.49 (0 to 140 mM) 0.58 (0 to 50 mM)	n/a

(a) average K_s in lower concentrations of SLS (0 to 50 mM)
(b) average K_s in higher concentrations of SLS (0 to 140 mM)

Solubility equations describing the ionization and micellar solubilization of cocrystals with a variety of ionization behaviors and stoichiometries have been derived and are presented in Table 1.4. As shown in Figure 1.9, the predictive power of the solubility models have been evaluated for cocrystals containing nonionizable drugs with ionizable coformers, including RHA, R_2HAB R_2H_2A, and are in excellent agreement with the observed solubility behaviors. However, the mathematical models have not been

used to quantify the micellar solubilization of cocrystals containing ionizable drugs. The micellar solubilization of cocrystals composed of ionizable drugs should be investigated to demonstrate the applicability of these solubility models to describe the solubility behavior of a wide variety of cocrystals.

Table 1.4 Equations that describe the cocrystal solubility dependence on solution $[H^+]$ and [M] from cocrystal K_{sp}, component K_a and K_s

Cocrystal	Solubility	Equation
RHA 1:1 nonionizable: monoprotic acid	$S_T^{RHA}=\sqrt{K_{sp}\left(1+K_s^R[M]\right)\left(1+\frac{K_a}{[H^+]}+K_s^{HA}[M]\right)}$	(1.18)
HDHA 1:1 monoprotic acid: monoprotic acid	$S_T^{HDHA}=\sqrt{K_{sp}\left(1+\frac{K_a^{HD}}{[H^+]}+K_s^{HD}[M]\right)\left(1+\frac{K_a^{HA}}{[H^+]}+K_s^{HA}[M]\right)}$	(1.19)
R_2H_2A 2:1 nonionizable: diprotic acid	$S_T^{R_2H_2A}=\sqrt[3]{\frac{K_{sp}}{4}\left(1+K_s^R[M]\right)^2\left(1+\frac{K_a^{H_2A}}{[H^+]}+\frac{K_a^{H_2A}K_a^{HA^-}}{[H^+]^2}+K_s^{H_2A}[M]\right)}$	(1.20)
R_2HAB 2:1 nonionizable: amphoteric	$S_T^{R_2HAB}=\sqrt[3]{\frac{K_{sp}}{4}\left(1+K_s^R[M]\right)^2\left(1+\frac{[H^+]}{K_{a1}^{HAB}}+\frac{K_{a2}^{HAB}}{[H^+]}+K_s^{HAB}[M]\right)}$	(1.21)

The key parameters governing cocrystal solubility in the presence of a surfactant are the cocrystal solubility product (K_{sp}), and the preferential solubilization of the drug relative to the coformer ($K_s^{drug} >> K_s^{coformer}$). The underlying mechanism responsible for the stabilization of cocrystals in solutions containing micellar surfactants is the differential solubilization of the cocrystal components as illustrated in Figure 1.10. The hydrophobic drug is preferentially solubilized by micelles relative to the hydrophilic coformer.

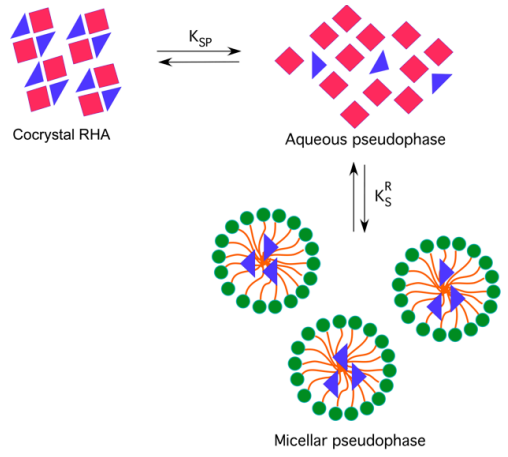

Figure 1.10. Schematic of the cocrystal equilibria and the resulting component distribution between the aqueous and micellar pseudophases. This scheme represents

preferential micellar solubilization of the drug component, leading to excess coformer in the aqueous pseudophase.

As cocrystal solubility increases due to micellar solubilization, the micellar phase becomes enriched with drug leaving the coformer to accumulate in the aqueous pseudophase. The observed solubility in a surfactant solution is the sum of the solubility in the aqueous and micellar phases; the distribution of the cocrystal species between these two pseudophases, explains the reversal of thermodynamic stability between drug and cocrystal at the CSC. Figure 1.11 shows the distribution of the drug solubility (R) compared to the cocrystal solubility (RHA) in micellar and aqueous phases under non-ionizing conditions.

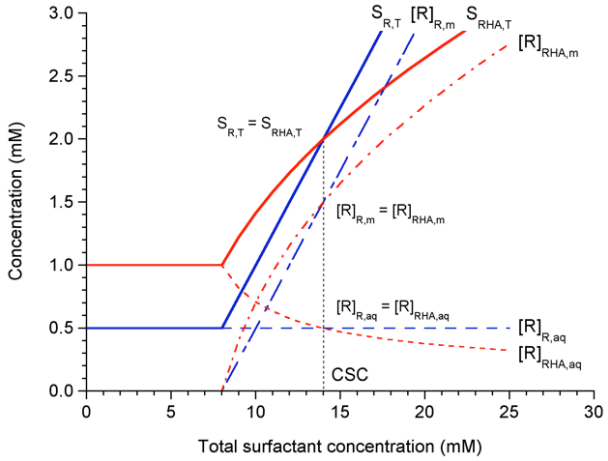

Figure 1.11 Distribution of drug (R) between the aqueous and micellar environments at equilibrium with cocrystal (RHA) and crystal (R) in surfactant solutions. The cocrystal solubility relative to the drug decreases with surfactant concentration. A thermodynamically unstable cocrystal in pure solvent becomes stable at the CSC where all curves intersect. Cocrystal is more soluble than drug below the CSC, cocrystal is equally soluble to drug at the CSC, and cocrystal is less soluble than drug above the CSC. Subscripts aq, m, and t, refer to aqueous, micellar and total. Solubilities and drug distributions were calculated from Equations (4.13) and (4.14) with K_{sp} = 1 mM^{-1}, K_s^R = 0.5 mM^{-1}, K_s^{HA} = 0 mM^{-1}, $S_{R,aq}$ = 0.5 mM, and CMC = 8 mM.[16]

The drug concentration in equilibrium with the drug solid phase in the aqueous phase, ($[R]_{R,aq}$) remains constant regardless of the surfactant concentration in solution, while the drug in the micellar pseudophase ($[R]_{R,m}$) increases linearly with increasing surfactant.

The solution distribution of a cocrystal as a function of surfactant concentration is very different from that of the single component. The drug concentration in equilibrium with the cocrystal solid phase in the aqueous pseudophase ($[R]_{RHA,aq}$) decreases with

increasing surfactant due to the increase of coformer in the aqueous phase. The excess coformer in the aqueous phase is a result of the asymmetric solubilization of the cocrystal components. $[R]_{RHA,aq}$ decreases until the drug concentration is lowered to that of the drug solubility in the aqueous phase, which occurs at the CSC. The drug concentration in equilibrium with the cocrystal solid phase in the micellar pseudophase ($[R]_{RHA,m}$) increases until the CSC where $[R]_{RHA,m}=[R]_{R,m}$. Pharmaceutical cocrystals are often composed of a hydrophobic drug and a hydrophilic coformer;[1,2,7,46] therefore preferential solubilization of the drug component may be widely encountered.

Influence of solution chemistry on cocrystal eutectic points

Eutectic point measurements are used to characterize the equilibrium solubility of cocrystals that are more soluble than the parent drug. The equilibrium at the eutectic point consists of a solution phase at its eutectic composition and two separate solid phases (cocrystal and pure component solid). For a binary cocrystal RHA, composed of a drug R and a coformer HA, there are two eutectic points, RHA solid and pure drug solid (R), and RHA solid and pure coformer solid (HA). The relationships and equations presented in this section pertain to the eutectic between cocrystal and drug. The cocrystal solubility and cocrystal solubility advantage ($S_{cocrystal}/S_{drug}$) can be determined from the solution concentrations in equilibrium at the eutectic.[16,47]

Cocrystal solubility can be calculated from the measured solution concentrations at the eutectic point. This approach is valuable because it uses a thermodynamically accessible equilibrium state to calculate cocrystal solubilities under stoichiometric solution conditions. The stoichiometric solubility of a 1:1 cocrystal can be determined from the analytical drug and coformer concentrations according to

$$\sqrt{[\text{drug}]_{T,eu}[\text{coformer}]_{T,eu}} \tag{1.22}$$

and the stoichiometric solubility of a 2:1 cocrystal can be determined according to

$$\sqrt[3]{\frac{([\text{drug}]_{T,eu})^2[\text{coformer}]_{T,eu}}{4}} \tag{1.23}$$

These equations consider ionization and micellar solubilization of the cocrystal components,[15,16,47] but do not account for solution complexation between the cocrystal components.

The eutectic constant, K_{eu} is a parameter that is calculated from the measured solution concentrations in equilibrium with the eutectic according to:

$$K_{eu}=\frac{[\text{coformer}]_{eu}}{[\text{drug}]_{eu}}=zy^{y/z}\left(\frac{S_{cocrystal}}{S_{drug}}\right)^{\frac{(y+z)}{z}} \quad (1.24)$$

and is a function of $S_{cocrystal}/S_{drug}$ for a cocrystal with a drug:coformer stoichiometry y:z. The relationship for a 1:1 cocrystal is given by

$$K_{eu}=\left(\frac{S_{cocrystal}}{S_{drug}}\right)^{2} \quad (1.25)$$

For a 1:1 cocrystal, measured $[\text{coformer}]_{eu} > [\text{drug}]_{eu}$ indicates $S_{cocrystal}>S_{drug}$, $[\text{coformer}]_{eu} = [\text{drug}]_{eu}$ indicates $S_{cocrystal} = S_{drug}$, and $[\text{coformer}]_{eu} < [\text{drug}]_{eu}$ indicates $S_{cocrystal} < S_{drug}$ based on equation (1.25).

Similar to cocrystal solubility, the cocrystal component eutectic concentrations depend on solution chemistry. Solution mechanisms that increase the equilibrium coformer eutectic concentration relative to the drug increase cocrystal solubility relative to the parent drug based on equation (1.24). It is important to measure both drug and coformer concentrations as an excess of one component will affect the equilibrium concentration of the other. The coformer eutectic-pH dependence has been derived for a variety of different cocrystal types as shown in Table 1.5.

Table 1.5. Equations describing the coformer eutectic-pH dependence from cocrystal K_{sp}, and component K_a.

Cocrystal	Coformer Eutectic	Equation
RHA 1:1 nonionizable: monoprotic acid	$[HA]_{eu}=\frac{K_{sp}}{[R]_{eu}}\left(1+\frac{K_a}{[H^+]}\right)$	(1.26)
HDHA 1:1 monoprotic acid: monoprotic acid	$[HA]_{eu}=\frac{K_{sp}}{[HD]_{eu,aq}}\left(1+\frac{K_a^{HA}}{[H^+]}\right)$	(1.27)
R_2H_2A 2:1 nonionizable: diprotic acid	$[H_2A]_{eu}=\frac{K_{sp}}{[R]_{eu}^{2}}\left(1+\frac{K_a^{H_2A}}{[H^+]}+\frac{K_a^{H_2A}K_a^{HA^-}}{[H^+]^2}\right)$	(1.28)
R_2HAB 2:1 nonionizable: amphoteric	$[H_2A]_{eu}=\frac{K_{sp}}{[R]_{eu}^{2}}\left(1+\frac{[H^+]}{K_{a1}^{HAB}}+\frac{K_{a2}^{HAB}}{[H^+]}\right)$	(1.29)

The equations in Table 1.5 have been used to evaluate cocrystal solubility products and cocrystal solubility-pH dependence from eutectic measurements for cocrystals that are more soluble than the parent drug.[14-16,18,37]

For example, equation (1.27) was used to evaluate the solubility product of the 1:1 indomethacin-saccharin cocrystal (HDHA) from eutectic measurements between drug and cocrystal because it converts to the parent drug under non-ionizing conditions. The indomethacin-saccharin cocrystal solubility product and coformer ionization constants were determined from the measured coformer eutectic-pH dependence according to equation(1.27), as shown in Figure 1.12a. These parameters were also used to generate a solubility-pH profile as shown in Figure 1.12b. The stoichiometric solubilities were calculated from the measured component concentrations in equilibrium at the eutectic according to equation (1.22) and are also shown in Figure 1.12b. The theoretical cocrystal solubility curve was generated using equation (1.13), K_{sp}=1.38x10^{-9} m^2 and K_a^{SAC}=1.6 (determined from the nonlinear regression analysis of the eutectic-pH dependence) and K_a^{IND} = 4.2.[48]

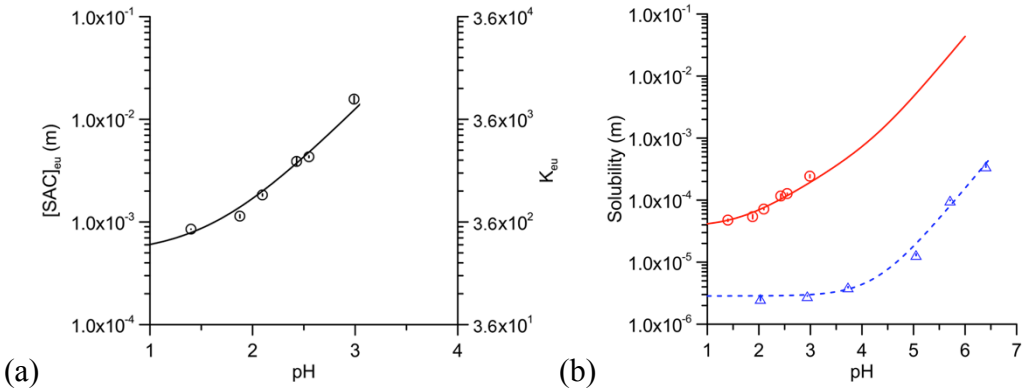

Figure 1.12 (a) Coformer eutectic-pH dependence of indomethacin-saccharin (O). Theoretical $[SAC]_{eu}$ dependence on pH (——) was generated from non-linear regression analysis of the data according to equation (1.26), the evaluated parameters were coformer pK_a= 1.6, and K_{sp}= 1.38x10^{-9} m^2.[18] (b) Stoichiometric cocrystal solubility-pH dependence predicted from equation (1.11) (——) was compared to the cocrystal solubility (○) determined from eutectic-pH measurements. The measured drug solubility (Δ) followed Henderson-Hasselbach behavior (pK_a^{IND} = 4.2).[18]

Micellar solubilization increases the cocrystal concentrations in equilibrium at the eutectic and both drug and coformer eutectic concentrations exhibit a linear dependence on micellar solubilization.[15] The intersection of the drug and coformer eutectic points occurs at the CSC. The micellar solubilization constant of a nonionizable drug (R) can be calculated from the drug eutectic concentration dependence on surfactant concentration according to

$$[R]_{eu,T}=[R]_{eu,aq}\left(1+K_s^R[M]\right) \quad (1.30)$$

where $[R]_{eu,aq}$ is the drug eutectic concentration in the absence of surfactant.[15] The eutectic dependence on pH and micellar solubilization, for an acidic coformer can be calculated according to

$$[HA]_{eu,T}=[HA]_{eu,aq}\left(1+\frac{K_a^{HA}}{[H^+]}+K_s^{HA}[M]\right) \quad (1.31)$$

where $[HA]_{eu,aq}$ is the unionized coformer concentration at the eutectic in the absence of surfactant. Figure 1.13 shows the drug and coformer eutectic concentration dependence on micellar solubilization, and the CSC determined by the intersection of the linear regression lines.

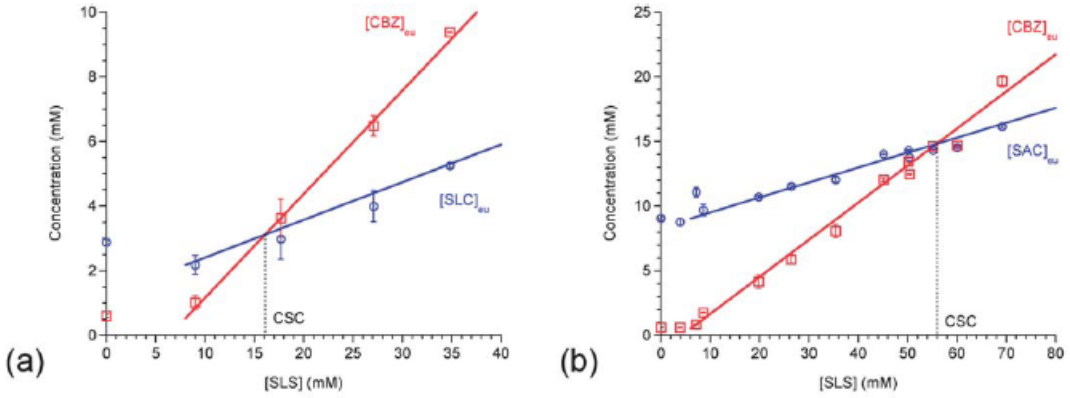

Figure 1.13 Drug and coformer eutectic concentration dependence on micellar solubilization. Solutions are in equilibrium with the solid drug and cocrystal, in aqueous solutions. (a) carbamazepine-salicylic (CBZ-SLC) pH 3.0 and (b) carbamazepine-saccharin (CBZ-SAC) pH 2.0. Lines represent linear regression analysis used to evaluate K_s^{drug} and $K_s^{coformer}$ from equations (1.30) and (1.31) respectively.[15]

Eutectic point measurements are valuable to characterize the equilibrium solubility behavior of cocrystals that are more soluble than the parent drug. Other methods of characterizing the solution behavior, such as dissolution, may grossly underestimate the true solubility when cocrystal converts to the less soluble drug, and are not easily extrapolated to other solution conditions. The solubility product and component ionization constants can be estimated from nonlinear regression analysis of the eutectic–pH dependence when the measurements are carried out in the pH range in which the components are ionized. Otherwise, component ionization constants are usually available in the literature. These parameters can be used to characterize the cocrystal solubility dependence on pH.

Pharmaceutically relevant surfactants

The most commonly used surfactants in pharmaceutical formulations are the nonionic surfactants due to their low toxicity, stability and ability to interact favorably with other surfactants.[49-51] Polysorbates (Tweens ®) are used to wet, solubilize, and stabilize drugs in oral, topical, ocular and parenteral formulations.[50,51] Polysorbate 20 and 80 can be used up to 10% in oral and topical formulations. Other nonionic surfactants commonly used in pharmaceutical applications include Myrj®, Brij® and the Pluronic® surfactants. Anionic surfactants are used to stabilize, solubilize and wet drugs during dissolution testing and in formulations. SLS and dioctyl sodium sulfosuccinate are examples of anionic surfactants that are used in oral formulations;[50] for example both are ingredients in carbamazepine extended release capsules.[52] SLS and Tween 80 are also commonly used in dissolution media to provide sink conditions.[49]

Polymeric surfactants are of interest as they have large solubilization capacities compared to the anionic and nonionic surfactants[53]. Pluronic® is a brand of triblock copolymers that have been observed to solubilize drugs such as carbamazepine and indomethacin.[54-56] They have also been used to encapsulate drugs such as paclitaxel for controlled release.[49] They are composed of a hydrophilic moiety, polyethylene oxide (POE) and a hydrophobic moiety, polypropylene oxide (PPO) in the form POE-PPO-POE. Pluronic® surfactants with higher POE content generally have higher solubilization capacities as they usually form larger micelles.[53] The structures of several pharmaceutically relevant synthetic surfactants are shown in Table 1.6.

Table 1.6. Chemical structures of synthetic surfactants

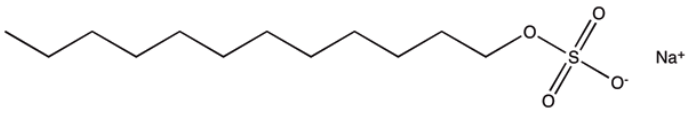

Sodium lauryl sulfate

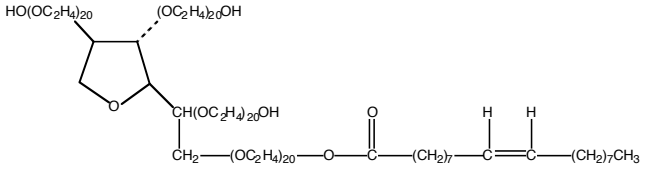

Tween 80

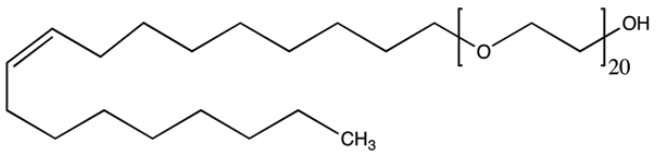

Brij 99

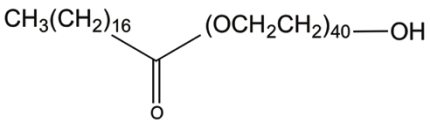

Myrj 52

Media proposed to simulate physiologically relevant solution conditions

The solubility of poorly soluble and highly permeable drugs is sensitive to solution conditions that affect the degree of ionization and micellar solubilization of the drug. It has been shown that selecting biorelevant conditions for in vitro evaluation of poorly soluble and highly permeable drugs (BCS class II) is essential to properly forecast the in vivo behavior.[57,58] Bile salts are natural surfactants present in the GI tract that have been shown to affect the bioavailability of poorly soluble drugs in the fed state through wetting and solubilizing effects.[59-63] The bile salt sodium taurocholate (NaTC) has been used alone or in combination with lecithin to simulate *in vivo* solution conditions of different regions of the GI tract as shown in Table 1.7.[60,62]

Table 1.7 Biorelevant media used for solubility profiling

GI segment	stomach	intestine				colon	
Media	FaSSGF[7]	FaSSIF	FaSSIF-V2[64]	FeSSIF	FeSSIF-V2[64e]	FaSSCOF[65]	FeSSCOF[65]
pH	1.6[a]	6.5[b]	6.5[c]	5[d]	5.8[c]	7.8[f]	6[f]
NaTC	0.08	3	3	15	10	1.5[g]	6[g]
Lecithin	0.02	0.75	0.2	3.75	2	3	5

(a) deionized water and HCl
(b) phosphate buffer
(c) maleate buffer
(d) acetate buffer
(e) oleate added to simulate lipolysis products present in the fed state
(f) tris/maleate buffer
(g) bile salt extract used in place of NaTC

NaTC is reported to make up (42%±17) of human bile in the duodenum to jejunum of healthy human subjects.[66] While there is some discrepancy as to which bile

salt is the most prevalent between sodium cholate (NaC) and NaTC in the duodenum, NaTC is used as the representative bile salt in the media presented in Table 1.7 due to its superior solubility in the entire physiologically relevant pH range;[64] it does not precipitate as the free acid even at pH 1.6 due to its low pKa (1.85).[67] In comparison, NaC precipitates as the free acid (cholic acid) at pH 6.5, [68] due to its pK_a (4.98-5.5).[69] Solubility studies conducted in FaSSIF and FeSSIF, which both contain only NaTC as the representative bile salt (and lecithin as the representative phospholipid) are reported to be in agreement with those conducted in human aspirates.[70]

The NaTC structure exhibits a hydrophobic side, a hydrophilic side and a hydrophilic tail as shown Figure 1.14. NaTC contains a cyclopentanophenanthrene structure with the A and B rings in a *cis* configuration relative to the B ring. NaTC contains three hydroxyl groups that reside on the alpha face resulting in a molecule with planar polarity. The flexibility of the side chain conjugated with taurine allows it to lie in the same plane as the hydroxyl groups, further contributing to the polarity of the alpha face.

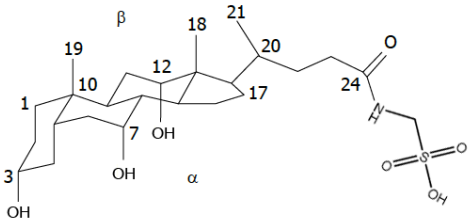

Figure 1.14. Structure of taurocholic acid showing the hydrophilic α side and the hydrophobic β side.

Due to their complex mechanism of aggregation, bile salts do not exhibit a distinct CMC and are characterized by a gradual increase in solubilization.[71,72] The solubilization achieved by bile salts can be analyzed based on the concentration range that exhibits a linear solubilization of the drug.[60,72] The CMC values of NaTC have been estimated despite their broad range; the CMC of NaTC is reported to occur at 3.3mM at 20 °C and 0.3 M NaCl and has an aggregation number of 6.[67] The CMC decreases with ionic strength and does not change significantly with temperature between 10-40°C, however the CMC increases as temperature increases beyond 40 °C.[67]

Lecithin, or phosphatidylcholine is a zwitterionic phospholipid that forms mixed micelles with NaTC. There are several proposed structures of the NaTC and lecithin

mixed micelles; a comparison of the structure proposed by Smalls versus the mixed disc model, proposed by Mazer, is shown in Figure 1.15.

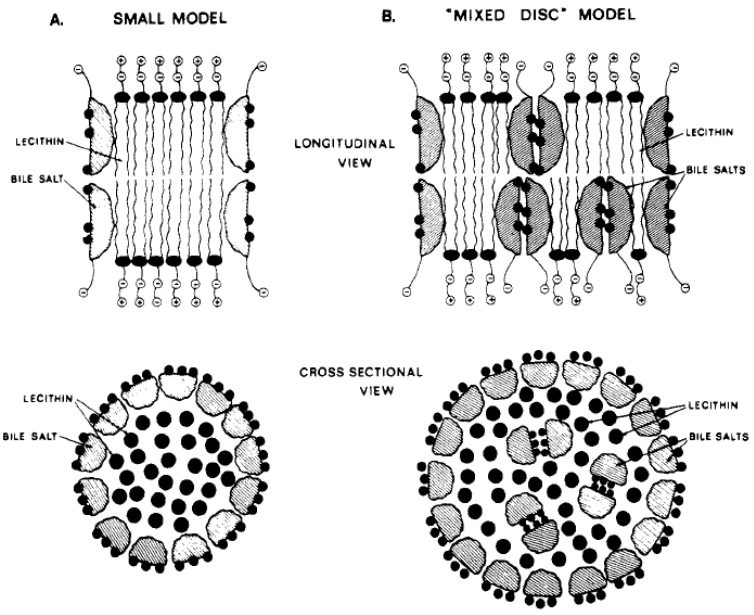

Figure 1.15. Proposed structure of the bile salt-lecithin mixed micelle, shown in longitudinal (cut through the disk diameter) and cross section (cut through the middle of the hydrocarbon steroid parts and fatty acid chains of bile salts and lecithin, respectively. The closed circles and ovals represent the nonionic polar groups of the molecules and the open circles with negative and positive signs represent the ionic polar parts of the molecules. (A)Small's mixed micellar. (B) Mazer's disk model.[73]

Lecithin has been observed to decrease the critical micelle concentration (CMC) of NaTC and enhance its solubilization capacity by mixed micelle formation.[59,60] The CMC of mixed micelles of NaTC and lecithin in a 6:1 to 3:1 ratio is 0.5 and 1 mM respectively at 20 °C.[67] NaTC and lecithin are in a 4:1 ratio in both FeSSIF and FaSSIF and both media contain the mixed micelle components well above the reported CMC.

The Effect of Temperature, pH and Ionic Strength on Micellar Solubilization

Micellar solubilization varies with temperature, pH and ionic strength; thus, K_s will vary with these parameters as well. Generally, solubilization by nonionic surfactants increases with increasing temperature; the micelle size increases and the CMC decreases with increasing temperature, resulting in an overall increase in micellar solubilization.[49,50,53] In contrast, the solubilization by of the ionic surfactants generally decreases with increasing temperature due to the disruption of water interactions with the hydrophobic groups which disrupts the micelle formation thereby increasing the

CMC.[49,50] The CMC of bile salts sodium taurocholate and sodium taurodeoxycholate are observed to increase with increasing temperature above 40°C with little change at lower temperatures.[50]

The effect of pH on the micellar solubilization by an ionic surfactant will depend on the pKa of the surfactant and the solubilizate as unionized solubilizates are expected to partition into the micelle more favorably than ionized species.[49,50] As the pH decreases towards the pKa of an ionic surfactant, it becomes less soluble resulting in a lowering of its CMC,[50] however the pKa of SLS is ~0 and the surfactant is ionized in the entire physiological pH range. However, the hydrolysis of SLS to lauryl alcohol and sodium bisulfate occurs faster in acidic solutions. Strong electrolytes have been observed to increase the solubilization capacity of both ionic and nonionic surfactants due to large decreases in the CMC. [49,50] Electrolytes also affect the micelle size of ionic surfactants by decreasing the repulsion between the polar head groups allowing for denser packing of the surfactant monomers. [50]

Statement of research

The purpose of this dissertation is to investigate the influence of solution chemistry on the solubility and thermodynamic stability of a cocrystal or cocrystalline salt relative to the parent drug or salt respectively. Due to the number of diverse crystalline forms that can be generated via cocrystallization, it is essential to establish robust methods to characterize cocrystal and cocrystalline salt solubility behavior in physiologically relevant environments and within pharmaceutical formulations. Knowledge of how the solution chemistry of a multicomponent system alters the observed supersaturation is critical to enable supersaturation *in vivo*. The solution chemistry of multicomponent systems is also important to design formulations and to protect against solution-mediated transformation during processing and manufacturing by careful selection of processing conditions.

Currently, cocrystal solution behavior is primarily evaluated using dissolution. While there is some understanding of how micellar solubilization and ionization affect cocrystal solubility and thermodynamic stability relative to the parent drug, this knowledge is seldom applied to select meaningful dissolution conditions or formulations additives. For example, there are several cases in which cocrystal solution behavior is

characterized by dissolution studies in fasted state intestinal fluid,[74-77] to evaluate solubility under "biorelevant" conditions, without consideration of how the pH and surfactant content of the media may affect cocrystal solubility, supersaturation and transformation kinetics.

There are several pharmacokinetic studies in which a cocrystal is suspended in an aqueous formulation prior to dosing with no mention of the cocrystal thermodynamic stability in the formulation.[2,19,20,74] The objective of this work is to evaluate the solution chemistry of a cocrystal (or cocrystalline salt) and derive mathematical models that predict the solubility behavior under a range of solution conditions to determine the key parameters necessary to characterize a cocrystal in a given aqueous system. These predictive tools will be used to rationally select surfactants to modulate cocrystal solubility and $S_{cocrystal}/S_{drug}$ based on the mathematical models that describe cocrystal solubility as a function of ionization and micellar solubilization. This information will be applied to understand the solution conditions under which cocrystal (or cocrystalline salt) is the stable phase relative to the drug (or parent salt).

Chapter 2 investigates the utility of mathematical solubility models to rationalize surfactant selection for the purpose of thermodynamically stabilizing cocrystals in suspension and reducing $S_{cocrystal}/S_{drug}$. There are a several examples in the literature of cocrystal dissolution being carried out in the presence of surfactants.[6,78] Based on previous work from our laboratory, this could lead to a dampening of the $S_{cocrystal}/S_{drug}$. Knowledge of the cocrystal solubility dependence on ionization and micellar solubilization would be useful to design suspensions in which cocrystal is thermodynamically stable relative to drug. This would also be advantageous to modulate $S_{cocrystal}/S_{drug}$ when the cocrystal is too soluble and transforms rapidly to the parent drug.

Mathematical models that describe cocrystal solubility dependence on ionization and micellar solubilization were used to predict cocrystal solubility in surfactant solutions based on the drug solubility dependence on micellar solubilization. These mathematical models were used to predict the surfactant concentration required to lower $S_{cocrystal}/S_{drug}$ to a target value or thermodynamically stabilize the cocrystal in aqueous media ($S_{cocrystal}/S_{drug}=1$).

Chapter 3 investigates the influence of biorelevant mixed micelles of NaTC and lecithin on the cocrystal equilibrium solubility, $S_{cocrystal}/S_{drug}$ and supersaturation generated during dissolution relative to buffer at the same pH. Fed state simulated intestinal fluid (FeSSIF) was selected for study as it contains the highest NaTC and lecithin concentrations and was therefore hypothesized to exhibit a larger micellar solubilization of the cocrystal components compared to media with lower concentrations. Mathematical models were derived to predict cocrystal solubility in a given biorelevant media based on the cocrystal aqueous solubility (K_{sp}), the component ionization and the component micellar solubilization. The mathematical models for ionization and micellar solubilization were used to predict cocrystal solubility and $S_{cocrystal}/S_{drug}$ in FeSSIF.

Chapter 4 considers the influence of solution chemistry on cocrystalline salt solubility relative to the parent salt. The objective of this chapter was to evaluate the cocrystalline salt solubility dependence on ionization, solution concentrations of counter-ion and coformer in addition to the cocrystalline salt stoichiometry. Mathematical equations are derived considering the equilibria for cocrystal dissociation and component ionization, to develop a theoretical framework to guide the solubility characterization of cocrystalline salts. These equations describe the solubility of a cocrystalline salt in terms of measureable thermodynamic parameters such as the cocrystalline salt K_{sp} and the coformer K_a. Salts that are cocrystallized with an ionizable component are hypothesized to exhibit different solubility-pH dependencies than the parent salt.

The solubility product behavior of cocrystalline salts is utilized to access the equilibrium solubility of supersaturating cocrystalline salts at a eutectic point between cocrystalline salt and salt. This methodology is similar to the analysis used to determine the equilibrium solubility of cocrystals, however, calculating the cocrystalline salt solubility in the absence of excess coformer is mathematically more complex due to the presence of a third component. Mathematical expressions to evaluate the stoichiometric and non-stoichiometric solubility (in excess chloride) were developed in this chapter to enable the evaluation of supersaturating cocrystalline salts. This chapter concludes with an analysis of the lattice and solvation contributions to the cocrystalline salt aqueous solubilities.

Chapter 5 describes the utility of eutectic point measurements in water and in a solution containing a given surfactant concentration to characterize the solution interactions between cocrystal components and a surfactant. This was demonstrated with two cocrystals of carbamazepine and two Pluronic® surfactants. The cocrystal component solubilization constants were evaluated from eutectic measurements and used to predict the effect of the Pluronic ® surfactants on the cocrystal solubility and $S_{cocrystal}/S_{drug.}$

Chapter 6 contains the conclusions of this dissertation and the future directions of the presented research. The chapters in this thesis focus primarily on the equilibrium solubility behavior of cocrystals and cocrystalline salts so that minimal solubility measurements can be used to predict the solubility behavior under a wide range of solution conditions using mathematical models derived from the solution chemistry of these multicomponent systems. Future challenges involve applying knowledge obtained from the equilibrium solubility studies to rationalize which kinetic solubility studies are meaningful to project the *in vivo* behavior of pharmaceutical cocrystals.

References

1. Basavoju S, Boström D, Velaga S 2008. Indomethacin–Saccharin Cocrystal: Design, Synthesis and Preliminary Pharmaceutical Characterization. Pharm Res 25(3):530-541.
2. Cheney ML, Weyna DR, Shan N, Hanna M, Wojtas L, Zaworotko MJ 2011. Coformer selection in pharmaceutical cocrystal development: A case study of a meloxicam aspirin cocrystal that exhibits enhanced solubility and pharmacokinetics. Journal of Pharmaceutical Sciences 100(6):2172-2181.
3. Gao Y, Zu H, Zhang J 2011. Enhanced dissolution and stability of adefovir dipivoxil by cocrystal formation. Journal of Pharmacy and Pharmacology 63(4):483-490.
4. Good DJ, Rodríguez-Hornedo Nr 2009. Solubility Advantage of Pharmaceutical Cocrystals. Cryst Growth Des 9(5):2252-2264.
5. Karki S, Friščić T, Fábián L, Laity PR, Day GM, Jones W 2009. Improving Mechanical Properties of Crystalline Solids by Cocrystal Formation: New Compressible Forms of Paracetamol. Advanced Materials 21(38-39):3905-3909.
6. Jung M-S, Kim J-S, Kim M-S, Alhalaweh A, Cho W, Hwang S-J, Velaga SP 2010. Bioavailability of indomethacin-saccharin cocrystals. Journal of Pharmacy and Pharmacology 62(11):1560-1568.
7. McNamara DP, Childs SL, Giordano J, Iarriccio A, Cassidy J, Shet MS, Mannion R, O'Donnell E, Park A 2006. Use of a glutaric acid cocrystal to improve oral bioavailability of a low solubility API. Pharm Res 23(8):1888-1897.
8. Remenar JF, Morissette SL, Peterson ML, Moulton B, MacPhee JM, Guzmán HR, Almarsson Ö 2003. Crystal Engineering of Novel Cocrystals of a Triazole Drug with 1,4-Dicarboxylic Acids. J Am Chem Soc 125(28):8456-8457.
9. Smith AJ, Kavuru P, Wojtas L, Zaworotko MJ, Shytle RD 2011. Cocrystals of Quercetin with Improved Solubility and Oral Bioavailability. Molecular Pharmaceutics 8(5):1867-1876.
10. Stanton MK, Kelly RC, Colletti A, Kiang YH, Langley M, Munson EJ, Peterson ML, Roberts J, Wells M 2010. Improved pharmacokinetics of AMG 517 through co-crystallization part 1: Comparison of two acids with corresponding amide co-crystals. Journal of Pharmaceutical Sciences 99(9):3769-3778.
11. Tsutsumi S, Iida M, Tada N, Kojima T, Ikeda Y, Moriwaki T, Higashi K, Moribe K, Yamamoto K 2011. Characterization and evaluation of miconazole salts and cocrystals for improved physicochemical properties. International Journal of Pharmaceutics 421(2):230-236.
12. Petruševski G, Naumov P, Jovanovski G, Ng SW 2008. Unprecedented sodium–oxygen clusters in the solid-state structure of trisodium hydrogentetravalproate monohydrate: A model for the physiological activity of the anticonvulsant drug Epilim®. Inorganic Chemistry Communications 11(1):81-84.
13. Schultheiss N, Newman A 2009. Pharmaceutical Cocrystals and Their Physicochemical Properties. Cryst Growth Des 9(6):2950-2967.
14. Bethune SJ, Huang N, Jayasankar A, Rodriguez-Hornedo N 2009. Understanding and Predicting the Effect of Cocrystal Components and pH on Cocrystal Solubility. Cryst Growth Des 9(9):3976-3988.

15. Huang N, Rodriguez-Hornedo N 2011. Engineering cocrystal thermodynamic stability and eutectic points by micellar solubilization and ionization. Crystengcomm 13(17):5409-5422.
16. Huang N, Rodríguez-Hornedo N 2011. Engineering cocrystal solubility, stability, and pHmax by micellar solubilization. Journal of Pharmaceutical Sciences 100(12):5219-5234.
17. Huang N, Rodríguez-Hornedo Nr 2010. Effect of Micellar Solubilization on Cocrystal Solubility and Stability. Cryst Growth Des 10(5):2050-2053.
18. Alhalaweh A, Roy L, Rodríguez-Hornedo N, Velaga SP 2012. pH-Dependent Solubility of Indomethacin–Saccharin and Carbamazepine–Saccharin Cocrystals in Aqueous Media. Molecular Pharmaceutics.
19. Weyna DR, Cheney ML, Shan N, Hanna M, Zaworotko MJ, Sava V, Song S, Sanchez-Ramos JR 2012. Improving Solubility and Pharmacokinetics of Meloxicam via Multiple-Component Crystal Formation. Molecular Pharmaceutics 9(7):2094-2102.
20. Cheney ML, Shan N, Healey ER, Hanna M, Wojtas L, Zaworotko MJ, Sava V, Song S, Sanchez-Ramos JR 2009. Effects of Crystal Form on Solubility and Pharmacokinetics: A Crystal Engineering Case Study of Lamotrigine. Cryst Growth Des 10(1):394-405.
21. Hickey MB, Peterson ML, Scoppettuolo LA, Morrisette SL, Vetter A, Guzmán H, Remenar JF, Zhang Z, Tawa MD, Haley S, Zaworotko MJ, Almarsson Ö 2007. Performance comparison of a co-crystal of carbamazepine with marketed product. European Journal of Pharmaceutics and Biopharmaceutics 67(1):112-119.
22. Etter MC 1991. Hydrogen bonds as design elements in organic chemistry. The Journal of Physical Chemistry 95(12):4601-4610.
23. Desiraju GR 1995. Supramolecular Synthons in Crystal Engineering—A New Organic Synthesis. Angewandte Chemie International Edition in English 34(21):2311-2327.
24. Etter MC 1990. Encoding and decoding hydrogen-bond patterns of organic compounds. Accounts of Chemical Research 23(4):120-126.
25. Donohue J 1952. The Hydrogen Bond in Organic Crystals. The Journal of Physical Chemistry 56(4):502-510.
26. Fleischman SG, Kuduva SS, McMahon JA, Moulton B, Bailey Walsh RD, Rodríguez-Hornedo N, Zaworotko MJ 2003. Crystal Engineering of the Composition of Pharmaceutical Phases: Multiple-Component Crystalline Solids Involving Carbamazepine. Cryst Growth Des 3(6):909-919.
27. Kitaigorodskii A 1965. The principle of close packing and the condition of thermodynamic stability of organic crystals. Acta Crystallographica 18(4):585-590.
28. Fábián Ls 2009. Cambridge Structural Database Analysis of Molecular Complementarity in Cocrystals. Cryst Growth Des 9(3):1436-1443.
29. Kojima T, Tsutsumi S, Yamamoto K, Ikeda Y, Moriwaki T 2010. High-throughput cocrystal slurry screening by use of in situ Raman microscopy and multi-well plate. International Journal of Pharmaceutics 399(1–2):52-59.
30. Childs SL, Rodriguez-Hornedo N, Reddy LS, Jayasankar A, Maheshwari C, McCausland L, Shipplett R, Stahly BC 2008. Screening strategies based on solubility and solution composition generate pharmaceutically acceptable cocrystals of carbamazepine. Crystengcomm 10(7):856-864.

31. Cheney ML, Weyna DR, Shan N, Hanna M, Wojtas L, Zaworotko MJ 2010. Supramolecular Architectures of Meloxicam Carboxylic Acid Cocrystals, a Crystal Engineering Case Study. Cryst Growth Des 10(10):4401-4413.
32. Childs SL, Hardcastle KI 2007. Cocrystals of Piroxicam with Carboxylic Acids. Cryst Growth Des 7(7):1291-1304.
33. Otte A, Boerrigter SX, Pinal R. 2012. Cocrystallization of Ketoconazole with Dicarboxylic Acids. AAPS, ed., Chicago, IL.
34. Sanphui P, Goud NR, Khandavilli UBR, Nangia A 2011. Fast Dissolving Curcumin Cocrystals. Cryst Growth Des 11(9):4135-4145.
35. Chadha R, Saini A, Arora P, Jain DS, Dasgupta A, Guru Row TN 2011. Multicomponent solids of lamotrigine with some selected coformers and their characterization by thermoanalytical, spectroscopic and X-ray diffraction methods. Crystengcomm 13(20):6271-6284.
36. Nehm SJ, Rodríguez-Spong B, Rodríguez-Hornedo N 2005. Phase Solubility Diagrams of Cocrystals Are Explained by Solubility Product and Solution Complexation. Cryst Growth Des 6(2):592-600.
37. Jayasankar A, Reddy LS, Bethune SJ, Rodríguez-Hornedo Nr 2009. Role of Cocrystal and Solution Chemistry on the Formation and Stability of Cocrystals with Different Stoichiometry. Cryst Growth Des 9(2):889-897.
38. Rodríguez-Hornedo N, Nehm SJ, Seefeldt KF, Pagán-Torres Y, Falkiewicz CJ 2006. Reaction Crystallization of Pharmaceutical Molecular Complexes. Molecular Pharmaceutics 3(3):362-367.
39. Maheshwari C, Jayasankar A, Khan NA, Amidon GE, Rodriguez-Hornedo N 2009. Factors that influence the spontaneous formation of pharmaceutical cocrystals by simply mixing solid reactants. Crystengcomm 11(3):493-500.
40. Jayasankar A, Good DJ, Rodríguez-Hornedo N 2007. Mechanisms by Which Moisture Generates Cocrystals. Molecular Pharmaceutics 4(3):360-372.
41. Stahl PH, Wermuth CG, International Union of P, Applied C. 2011. Handbook of pharmaceutical salts: properties, selection, and use. ed., Zürich: VHCA ; Weinheim : Wiley-VCH. p xvi, 446 p.
42. Kramer SF, Flynn GL 1972. Solubility of organic hydrochlorides. Journal of Pharmaceutical Sciences 61(12):1896-1904.
43. Chowhan ZT 1978. pH-solubility profiles of organic carboxylic acids and their salts. Journal of Pharmaceutical Sciences 67(9):1257-1260.
44. Bogardus JB, Blackwood RK 1979. Solubility of doxycycline in aqueous solution. Journal of Pharmaceutical Sciences 68(2):188-194.
45. Serajuddin A, Sheen PC, Augustine MA 1987. Common ion effect on solubility and dissolution rate of the sodium salt of an organic acid. Journal of Pharmacy and Pharmacology 39(8):587-591.
46. Babu NJ, Nangia A 2011. Solubility Advantage of Amorphous Drugs and Pharmaceutical Cocrystals. Cryst Growth Des 11(7):2662-2679.
47. Huang N. 2011. Engineering Cocrystal Solubility and Stability via Ionization and Micellar Solubilization. Pharmaceutical Sciences, ed., Ann Arbor, MI: University of Michigan.

48. Mooney KG, Mintun MA, Himmelstein KJ, Stella VJ 1981. Dissolution kinetics of carboxylic acids I: Effect of pH under unbuffered conditions. Journal of Pharmaceutical Sciences 70(1):13-22.
49. Liu R. 2008. Water-insoluble drug formulation. ed., Boca Raton, FL: CRC Press. p 669 p.
50. Yalkowsky SH. 1999. Solubility and solubilization in aqueous media. ed., Washington, D.C. : New York: American Chemical Society ; Oxford University Press. p xvi, 464 p.
51. Strickley R 2004. Solubilizing Excipients in Oral and Injectable Formulations. Pharm Res 21(2):201-230.
52. Niazi S. 2004. Handbook of pharmaceutical manufacturing formulations: Sterile Products. ed., Boca Raton: CRC Press. p 384.
53. Kadam Y, Yerramilli U, Bahadur A 2009. Solubilization of poorly water-soluble drug carbamezapine in Pluronic® micelles: Effect of molecular characteristics, temperature and added salt on the solubilizing capacity. Colloids and Surfaces B: Biointerfaces 72(1):141-147.
54. Najib NM, Suleiman MS 1985. The effect of hydrophilic polymers and surface active agents on the solubility of indomethacin. International Journal of Pharmaceutics 24(2–3):165-171.
55. El-Badry M, Fathy M, Abdel Mohsen M 2004. Solubilization of some non-steroidal anti-inflammatory drugs (NSAIDS) by Pluronic F-127 bloc copolymer Bulletin of Pharmaceutical Sciences 27(1):1-10.
56. Tian F, Zeitler JA, Strachan CJ, Saville DJ, Gordon KC, Rades T 2006. Characterizing the conversion kinetics of carbamazepine polymorphs to the dihydrate in aqueous suspension using Raman spectroscopy. Journal of Pharmaceutical and Biomedical Analysis 40(2):271-280.
57. Vertzoni M, Dressman J, Butler J, Hempenstall J, Reppas C 2005. Simulation of fasting gastric conditions and its importance for the in vivo dissolution of lipophilic compounds. European Journal of Pharmaceutics and Biopharmaceutics 60(3):413-417.
58. Klein S 2010. The Use of Biorelevant Dissolution Media to Forecast the <i>In Vivo Performance of a Drug. The AAPS Journal 12(3):397-406.
59. Hörter D, Dressman J 2001. Influence of physicochemical properties on dissolution of drugs in the gastrointestinal tract. Advanced Drug Delivery Reviews 46(1):75-87.
60. Naylor LJ, Bakatselou V, Dressman JB 1993. Comparison of the mechanism of dissolution of hydrocortisone in simple and mixed micelle systems. Pharm Res 10(6):865-870.
61. Charman WN, Porter CJH, Mithani S, Dressman JB 1997. Physicochemical and physiological mechanisms for the effects of food on drug absorption: the role of lipids and pH. Journal of Pharmaceutical Sciences 86(3):269-282.
62. Mithani SD, Bakatselou V, TenHoor CN, Dressman JB 1996. Estimation of the Increase in Solubility of Drugs as a Function of Bile Salt Concentration. Pharm Res 13(1):163-167.
63. Bakatselou V, Oppenheim RC, Dressman JB 1991. Solubilization and wetting effects of bile salts on the dissolution of steroids. Pharm Res 8(12):1461-1469.

64. Jantratid E, Janssen N, Reppas C, Dressman J 2008. Dissolution Media Simulating Conditions in the Proximal Human Gastrointestinal Tract: An Update. Pharm Res 25(7):1663-1676.
65. Vertzoni M, Diakidou A, Chatzilias M, Söderlind E, Abrahamsson B, Dressman J, Reppas C 2010. Biorelevant Media to Simulate Fluids in the Ascending Colon of Humans and Their Usefulness in Predicting Intracolonic Drug Solubility. Pharm Res 27(10):2187-2196.
66. Moreno MPdlC, Oth M, Deferme S, Lammert F, Tack J, Dressman J, Augustijns P 2006. Characterization of fasted-state human intestinal fluids collected from duodenum and jejunum. Journal of Pharmacy and Pharmacology 58(8):1079-1089.
67. Carey M.C. SDM 1972. Micelle formation by bile salts: Physical-chemical and thermodynamic considerations. Archives of Internal Medicine 130(4):506-527.
68. Dowling RH 1968. The effect of pH on the solubility of varying mixtures of free and conjugated bile salts in solution. Gastroenterology (New York, NY 1943) 54:1291.
69. Small DM. 1971. The physical chemistry of cholanic acids. The bile acids-Chemistry, physiology and metabolism, ed., New York: Plenum Publishing Co. p 274-354.
70. Kalantzi L, Persson E, Polentarutti B, Abrahamsson B, Goumas K, Dressman J, Reppas C 2006. Canine Intestinal Contents vs. Simulated Media for the Assessment of Solubility of Two Weak Bases in the Human Small Intestinal Contents. Pharm Res 23(6):1373-1381.
71. Ninomiya R, Matsuoka K, Moroi Y 2003. Micelle formation of sodium chenodeoxycholate and solubilization into the micelles: comparison with other unconjugated bile salts. Biochimica et Biophysica Acta (BBA)-Molecular and Cell Biology of Lipids 1634(3):116-125.
72. Samaha MW, Gadalla MAF 1987. The Solubilization of Carbamazepine by Different Classes of Nonionic Surfactants and a Bile Salt. Drug Development and Industrial Pharmacy 13(1):93-112.
73. Mazer NA, Benedek GB, Carey MC 1980. Quasielastic light-scattering studies of aqueous biliary lipid systems. Mixed micelle formation in bile salt-lecithin solutions. Biochemistry 19(4):601-615.
74. Bak A, Gore A, Yanez E, Stanton M, Tufekcic S, Syed R, Akrami A, Rose M, Surapaneni S, Bostick T, King A, Neervannan S, Ostovic D, Koparkar A 2008. The co-crystal approach to improve the exposure of a water-insoluble compound: AMG 517 sorbic acid co-crystal characterization and pharmacokinetics. Journal of Pharmaceutical Sciences 97(9):3942-3956.
75. Takata N, Takano R, Uekusa H, Hayashi Y, Terada K 2010. A Spironolactone−Saccharin 1:1 Cocrystal Hemihydrate. Cryst Growth Des 10(5):2116-2122.
76. Yadav AV, Dabke AP, Shete AS 2010. Crystal engineering to improve physicochemical properties of mefloquine hydrochloride. Drug Development and Industrial Pharmacy 36(9):1036-1045.
77. Shiraki K, Takata N, Takano R, Hayashi Y, Terada K 2008. Dissolution Improvement and the Mechanism of the Improvement from Cocrystallization of Poorly Water-soluble Compounds. Pharm Res 25(11):2581-2592.

78. Remenar JF, Peterson ML, Stephens PW, Zhang Z, Zimenkov Y, Hickey MB 2007. Celecoxib:Nicotinamide Dissociation: Using Excipients To Capture the Cocrystal's Potential. Molecular Pharmaceutics 4(3):386-400.

Chapter 2

Rational surfactant selection to control cocrystal solubility and stabilize against solution-mediated transformation

Introduction

Cocrystal formation has been successfully used to increase drug solubility,[4,30] dissolution,[1,8,34,78,79] and bioavailability.[2,6,7,9,74] However, evaluation, selection and formulation of these high-energy multi-component systems is often empirically based. Cocrystal supersaturation is frequently evaluated by kinetic dissolution prior to knowledge of its equilibrium solubility. It has been shown that cocrystal solubility behavior is dependent on component solution interactions, and can be different from that of the parent drug.[14,16,37] There are reported mathematical models that describe cocrystal solubility dependence on pH, coformer and surfactant concentration for cocrystals of varying ionization behaviors.[14,15,17,36] Using these models, cocrystal solubility product, component ionization and component micellar solubilization, are all that is required to calculate cocrystal solution behavior under a wide range of pH and surfactant conditions. Yet, these concepts have not been applied to rationalize cocrystal evaluation or formulation.

High solubility cocrystals that undergo solution-mediated phase transformation are vulnerable in aqueous environments. Conversion to the more stable (less soluble) form may prevent sustained supersaturation and therefore may not provide a solubility advantage relative to the drug. Knowledge of the mechanisms that control cocrystal solubility and supersaturation would be useful to guide efforts to evaluate and formulate cocrystals. Recently cocrystals of carbamazepine, observed to transform to the parent drug in aqueous solutions, were reported to be the thermodynamically stable form in aqueous solutions containing sodium lauryl sulfate (SLS) above a critical stabilization concentration (CSC) at a defined pH.[15-17,47]

At the CSC, cocrystal solubility and drug solubility were equal,[16] and this solution behavior was explained by the preferential solubilization of the hydrophobic drug relative to the hydrophilic coformer.[16] Cocrystals of carbamazepine with a monoprotic acidic coformer, a diprotic acidic coformer and an amphoteric coformer, that were 3-4 times more soluble than the drug under the pH conditions studied achieved a CSC in SLS. The solubility dependence on micellar solubilization of these cocrystals was well described by mathematical models that consider the equilibria for cocrystal dissociation, component ionization and component micellar solubilization. The effect of micellar solubilization on cocrystal solubility has not been studied for cocrystals containing different drugs, and the hydrophobicity and ionization properties of the drug may affect the preferential solubilization of the drug relative to the coformer.

Higher octanol/water partition coefficients (log P), a measure of the hydrophobicity of a drug, are correlated with higher micellar solubilization constants in a variety of synthetic and biologically relevant surfactants.[60,62,80] Therefore, drugs that are more hydrophobic than carbamazepine may exhibit a greater preferential solubilization; indomethacin (IND) an acidic drug that forms cocrystals, is more hydrophobic (log P = 4.4)[81] than carbamazepine (log P = 2.5),[82] and therefore was selected to study the ability to control cocrystal solubility and $S_{cocrystal}/S_{drug}$ using micellar solubilization.

IND forms a cocrystal with the weakly acidic coformer saccharin (IND-SAC), which we have reported to be 13-65 times more soluble than the parent drug in a pH range of 1-3. Therefore either a higher concentration of surfactant is required to achieve a CSC, or a surfactant with a greater solubilization power, may be required to stabilize the IND-SAC cocrystal against transformation. There are several pharmaceutically relevant surfactants, but currently, there are no guidelines to select surfactants to stabilize cocrystals against solution mediated phase transformations. In addition, there is little information regarding the characterization of surfactant interactions with cocrystal components, which is shown to impact cocrystal solubility and thermodynamic stability in aqueous solutions.

Indomethacin solubility in surfactant solutions has been reported for a wide range of surfactants such as Tweens®, Myrjs®, SLS, Pluronics®, and Brijs®, which can be used to characterize the micellar solubilization of indomethacin in each surfactant. The

published mathematical models and the reported micellar solubilization of indomethacin were used to rationalize surfactant selection to increase cocrystal solubility, decrease $S_{cocrystal}/S_{drug}$ and achieve CSC. The objective of this work is to predict and measure the cocrystal solubility dependence on surfactant concentration for the IND-SAC cocrystal. A variety of surfactants are evaluated based on their ability to modulate IND-SAC solubility relative to the drug and to achieve a CSC. Surfactants were selected for study based on reported or measured indomethacin solubilization.[54,83-85] Cocrystal solubility dependence on micellar solubilization and ionization is evaluated in four surfactants: SLS, Tween 80, Myrj 52, and Brij 99. We show for the first time that the cocrystal solubility increases with a square-root dependence on micellar concentrations of Tween 80, Myrj 52, Brij 99, and SLS. All surfactants exhibit a CSC in a defined pH range and can be used stabilize cocrystal against solution-mediated transformation. All surfactants studied solubilized the coformer to a small extent, and an accurate prediction of the cocrystal solubility dependence on micellar solubilization and CSC from the reported mathematical models requires knowledge of both the solubilization of the drug and coformer.

Theoretical Section

Cocrystal solubility dependence on pH and surfactant concentration is well described by mathematical models that consider cocrystal dissociation, component ionization and component micellar solubilization.[14,16] This work expands upon the previously derived mathematical models that describe cocrystal solubility dependence on micellar solubilization, and develops criteria to rationalize surfactant selection to modulate $S_{cocrystal}$, cocrystal solubility advantage relative to drug ($S_{cocrystal}/S_{drug}$) and CSC. Mathematical relationships describing $S_{cocrystal}$ and $S_{cocrystal}/S_{drug}$ dependence on micellar solubilization are derived for a cocrystal HDHA composed of an acidic drug (HD) and acidic coformer (HA).

The relevant equilibria that describes the HDHA cocrystal solubility dependence on ionization and micellar solubilization in an aqueous solution containing [M], moles/kg, of surfactant includes cocrystal dissociation:

$$HDHA \overset{Ksp}{\longleftrightarrow} HD_{aq}+HA_{aq} \quad (2.1)$$

ionization of the cocrystal components:

$$HD_{aq} \overset{K_a^{HD}}{\longleftrightarrow} D^-_{aq}+H^+_{aq} \quad (2.2)$$

$$HA_{aq} \overset{K_a^{HA}}{\longleftrightarrow} A^-_{aq}+H^+_{aq} \quad (2.3)$$

and micellar solubilization of the cocrystal components

$$HD_{aq}+M \overset{K_s^{HD}}{\longleftrightarrow} HD_m \quad (2.4)$$

$$D^-_{aq}+M \overset{K_s^{D^-}}{\longleftrightarrow} D^-_m \quad (2.5)$$

$$HA_{aq}+M \overset{K_s^{HA}}{\longleftrightarrow} HA_m \quad (2.6)$$

$$A^-_{aq}+M \overset{K_s^{A^-}}{\longleftrightarrow} A^-_m \quad (2.7)$$

where subscripts aq and m refer to components in the aqueous phase or the micellar phase respectively. Above its critical micellar concentration (CMC), a surfactant forms micelles, which solubilize hydrophobic components. Thus, all equations describing micellar solubilization are expressed in terms of micellar surfactant concentration M where

$$M=[Surfactant]_{total}-CMC \quad (2.8)$$

Cocrystal solubility in micellar solutions has been predicted from the cocrystal solubility product and the solubilization and ionization constants of the drug and coformer.[15-17] The solubility product is defined by the equilibria in equation (2.1) and is calculated from the nonionized solutions concentrations of the cocrystal components according to

$$K_{sp}=[HD]_{aq}[HA]_{aq} \quad (2.9)$$

The solubility product has been evaluated by nonlinear and linear regression analysis of the coformer eutectic dependence on pH.[14,18] Drug and coformer ionize based on the solution concentration of $[H^+]$ and the respective equilibrium ionization constants described by:

$$K_a^{HD}=\frac{[D^-]_{aq}[H^+]_{aq}}{[HD]_{aq}} \tag{2.10}$$

$$K_a^{HA}=\frac{[A^-]_{aq}[H^+]_{aq}}{[HA]_{aq}} \tag{2.11}$$

The micellar solubilization for each component is described by the following equilibrium constants:

$$K_s^{D-}=\frac{[HD]_m}{[HD]_{aq}[M]} \tag{2.12}$$

$$K_s^{D-}=\frac{[D^-]_m}{[D^-]_{aq}[M]} \tag{2.13}$$

$$K_s^{A-}=\frac{[HA]_m}{[HA]_{aq}[M]} \tag{2.14}$$

$$K_s^{A-}=\frac{[A^-]_m}{[A^-]_{aq}[M]} \tag{2.15}$$

The mass balance for a weakly acidic drug in an aqueous micellar solution is:

$$S_T^{HD}=S_{aq}^{HD}+S_{aq}^{D-}+S_m^{HD}+S_m^{D-} \tag{2.16}$$

The solubility dependence on ionization and micellar solubilization for a weakly acidic drug is then:

$$S_T^{HD}=S_{aq}^{HD}\left(1+\frac{K_a^{HD}}{[H^+]}+\left(K_s^{HD}+\frac{K_a^{HD}}{[H^+]}K_s^{D-}\right)[M]\right) \tag{2.17}$$

by substituting the equilibrium constants into equation (2.16). The micellar equilibrium solubilization constants for a weakly acidic component (K_s^{HD} and K_s^{D-}) have been calculated using either nonlinear or linear regression of measured drug solubilities, at different values of $[H^+]$ and micellar surfactant concentrations, [M], according to equation (2.17).[86,87]

At a given pH, the total micellar solubilization constant, K_s^{HDT}, is equal to

$$K_s^{HD,T}=K_s^{HD}+\frac{K_a^{HD}}{[H^+]}K_s^{D-} \tag{2.18}$$

Based on the method of *Grbic et al.*, two values of K_s^{HDT} , are required to determine K_s^{HD} and K_s^{D-} from linear regression analysis according to (2.18);[87] K_s^{HDT} under pH conditions where drug is mostly unionized and K_s^{HDT} evaluated under pH conditions where the drug is mostly ionized. Under nonionizing conditions $K_s^{HDT} = K_s^{HD}$. The K_s^{HDT} is evaluated from the drug solubility dependence, S_T^{HD}, on [M], holding pH constant according to

$$S_T^{HD}=S_{aq}^{HD}\left(1+\frac{K_a^{HD}}{[H^+]}+K_s^{HD,T}[M]\right) \tag{2.19}$$

which is obtained by substituting equation (2.18) into equation (2.17). Equations (2.16)-(2.19) apply to the acidic coformer, by substituting the relevant HD parameters with those of HA.

Prediction and evaluation of $S_{cocrystal}$, $S_{cocrystal}/S_{drug}$ and CSC dependence on micellar solubilization

Cocrystal solubility, S_T^{HDHA}, under stoichiometric conditions is equal to the total concentration of each cocrystal component in equilibrium with the solution, $S_T^{HDHA}= [HD]_T=[HA]_T$. The solubility of a cocrystal of two weakly acidic components, HDHA, in a micellar solution is equal to the sum of the following species:

$$\begin{aligned} S_T^{HDHA}&=[HD]_{aq}+[D^-]_{aq}+[HD]_m+[D^-]_m \\ &=[HA]_{aq}+[A^-]_{aq}+[HA]_m+[A^-]_m \end{aligned} \tag{2.20}$$

The cocrystal solubility dependence on micellar solubilization is described at a given $[H^+]$ using K_s^{HAT} and K_s^{HDT} evaluated at a given $[H^+]$ according to

$$S_T^{HDHA}=\sqrt{K_{sp}\left(1+\frac{K_a^{HD}}{[H^+]}+K_s^{HD,T}[M]\right)\left(1+\frac{K_a^{HA}}{[H^+]}+K_s^{HA,T}[M]\right)} \tag{2.21}$$

The above expression was obtained by combining equation (2.20) with the equilibrium constant equations (2.9)-(2.15).[16] The superscript HD refers to the weakly acidic drug and HA the weakly acidic coformer. The equilibrium constants are expressed in terms of concentrations with the understanding that they approximate activities under dilute solution conditions.

Figure 2.1 shows the HDHA cocrystal solubility increases with surfactant concentration according to equation (2.21). When $K_s^{coformer} << K_s^{drug}$, the cocrystal exhibits a weaker solubility dependence on micellar solubilization compared to the parent

drug resulting in an intersection of the cocrystal and drug solubility curves at the CSC. Often, high solubility cocrystals of poorly soluble, hydrophobic drugs are formed using hydrophilic coformers.[7,11,13,29] The hydrophobic drug is hypothesized to have a higher micellar solubilization constant relative to that of the hydrophilic coformer as micellar solubilization is correlated with the hydrophobicity of a molecule.[62,80]

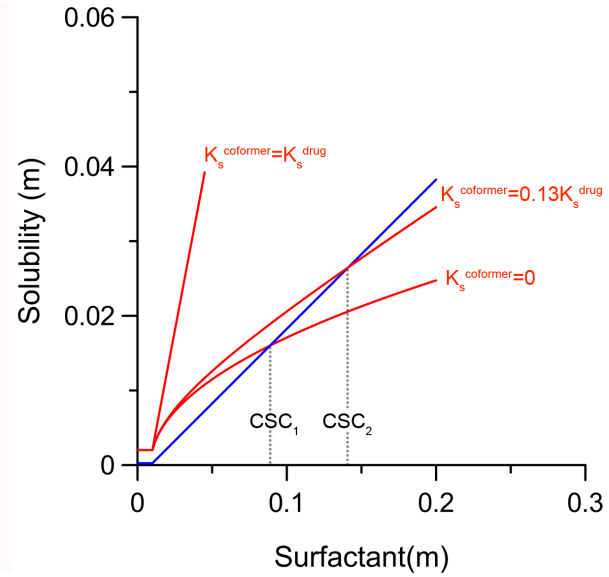

Figure 2.1. The influence of micellar solubilization on cocrystal solubility and CSC at pH 2.0. The solubility of cocrystal (——) and drug (——) were calculated from equation (2.21) and (2.19) respectively using K_{sp} = 2.0 x10 $^{-6}$ m^2, pK_a^{HD} =4.0, pK_a^{HA} =2.0, $K_s^{HD,TpH2.1}$ = 800 $m^{-1,}$ $K_s^{HA,T}$=0 and S_{aq}^{HD} = 2.5 x 10^{-4} m. The influence of coformer solubilization is represented by the dotted line red line, where $K_s^{HA,T\ pH2}$ = 10 m^{-1}.

Cocrystal solubility is predicted to exhibit a square-root dependence on surfactant concentration based on equation (2.21), while the drug is predicted to exhibit a linear dependence on surfactant concentration according to equation (2.19). Therefore for cocrystals that exhibit $S_{cocrystal}>S_{drug}$ in solutions containing no surfactant, there exists an intersection of the cocrystal and drug solubility curves that is defined by a CSC of surfactant at a specified [H^+] when drug is preferentially solubilized.[15-17] As shown in Figure 2.1, in a given surfactant solution, cocrystal solubility and the CSC are higher when K_s^{HAT} = 0.013K_s^{HDT} compared to when the coformer is not solubilized (K_s^{HAT} =0). The CSC is increased 1.7 fold when the coformer is solubilized such that, K_s^{HAT} = 0.013K_s^{HDT} relative to when K_s^{HAT} = 0. If the coformer is solubilized to the same extent as the drug (K_s^{HAT}=K_s^{HDT}) the cocrystal and drug solubility curves do not intersect and CSC cannot be achieved. The cocrystal solubility and the CSC increase due to coformer

solubilization, even when the coformer is solubilized to a small extent relative to drug ($K_s^{HAT} << K_s^{HDT}$).

The drug and cocrystal solubility are equal at the CSC, therefore the cocrystal is thermodynamically stable in solutions containing surfactant concentrations ≥ CSC. The CSC in a solution at a given $[H^+]$ is predicted according to:

$$CSC = \frac{\frac{Ksp}{(S_{aq}^{HD})^2}\left(1+\frac{K_a^{HA}}{[H^+]}\right) - \left(1+\frac{K_a^{HD}}{[H^+]}\right)}{K_s^{HDT} - \frac{Ksp}{(S_{aq}^{HD})^2}K_s^{HAT}} + CMC \quad (2.22)$$

This equation is obtained by setting equation (2.19) equal to equation (2.21) and solving for the micellar surfactant concentration [M]. According to the denominator in equation (2.22), the CSC is achieved by surfactants that solubilize the drug preferentially to the coformer such that

$$K_s^{HD,T} > \frac{K_{sp}}{(S_{aq}^{HD})^2}K_s^{HA,T} \quad (2.23)$$

Equation (2.22) predicts that the CSC decreases as K_s^{HDT} increases and as K_s^{HAT} decreases. Therefore, surfactants can be rationally selected to stabilize a cocrystal against transformation (achieve CSC) based on their relative K_s^{HDT} values and $K_s^{HDT} >> K_s^{HAT}$. Surfactants that achieve a CSC reduce the cocrystal solubility advantage relative to drug ($S_{cocrystal}/S_{drug}$). The $S_{cocrystal}/S_{drug}$ dependence on micellar solubilization is described according to

$$\frac{S_T^{HDHA}}{S_T^{HD}} = \frac{\sqrt{K_{sp}\left(1+\frac{K_a^{HD}}{[H^+]}+K_s^{HDT}[M]\right)\left(1+\frac{K_a^{HA}}{[H^+]}+K_s^{HAT}[M]\right)}}{S_{aq}^{HD}\left(1+\frac{K_a^{HD}}{[H^+]}+K_s^{HDT}[M]\right)} \quad (2.24)$$

This equation is obtained by dividing equation (2.21) by equation (2.19). Figure 2.2. shows the cocrystal solubility advantage ($S_{cocrystal}/S_{drug}$) dependence on micellar solubilization according to equation (2.24). $S_{cocrystal}/S_{drug} = 1$ at the CSC which is shown by the intersection of $S_{cocrystal}/S_{drug}$ with the dashed line. Below the CSC, and above the surfactant CMC, $S_{cocrystal}/S_{drug}$ is reduced by micellar solubilization when the drug is preferentially solubilized.

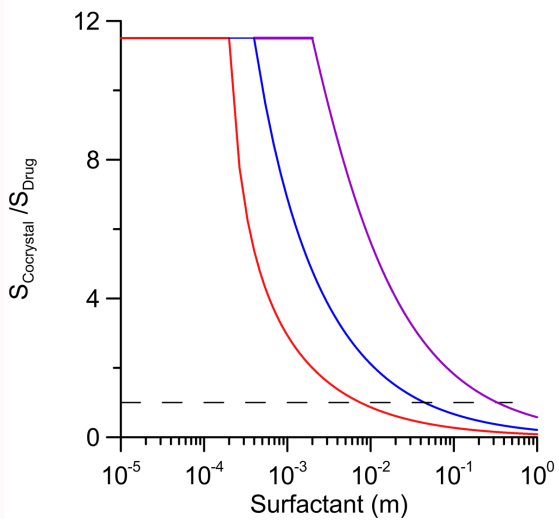

Figure 2.2. Influence of K_s^{HDT} and CMC on the $S_{cocrystal}/S_{drug}$ and CSC dependence. $S_{cocrystal}/S_{drug}$ was calculated from equation (2.24) in surfactant solutions described by K_s^{HDT}= 400 m^{-1}, CMC = 2 x 10^{-3} m (——), K_s^{HDT}= 3000 m^{-1}, CMC = 4 x 10^{-4} m (——), and K_s^{HDT} =18000 m^{-1} CMC= 2 x10^{-4} m (——), for a cocrystal described by S_{aq}^{drug} = 2.5x10^{-4} m K_{sp} = 2.0 x10^{-6} m^2, pK_a^{HD} = 4.0, pK_a^{HA} = 1.5.

The power of a given surfactant to reduce $S_{cocrystal}/S_{drug}$ to half its value in aqueous media correlates to the magnitude of K_s^{HDT} and the CMC of the surfactant. As shown by a plot of $S_{cocrystal}/S_{drug}$ as a function of [M], the higher the K_s^{HDT}, and the lower the CMC, the less surfactant is required to decrease the $S_{cocrystal}/S_{drug}$ by half. The hypothetical case considered in Figure 2.2 shows the effect of micellar solubilization on a cocrystal that exhibits $S_{cocrystal}/S_{drug}$ = 11.5 in the absence of surfactant. The $S_{cocrystal}/S_{drug}$ ranges from 11.5-1in the surfactant concentration range of CMC-CSC; micellar solubilization can be used to control, or engineer the cocrystal solubility relative to a drug. A target $S_{cocrystal}/S_{drug}$ can be achieved using equation (2.24) to calculate the surfactant concentration required to lower the solubility advantage of the cocrystal to a desired value.

Prediction and evaluation of CSC dependence on pH

Figure 2.3 shows the cocrystal and drug solubility dependence on micellar solubilization and ionization for a cocrystal HDHA in which $pK_a^{HD} > pK_a^{HA}$. This plot shows that both cocrystal and drug solubility increase with increasing pH and surfactant concentration according to equations (2.21) and (2.17). The intersection of the two surfaces is the CSC, which increases with pH as shown in Figure 2.3. The CSC increases

with $S_{cocrystal}/S_{drug}$; for a cocrystal composed of an acidic drug and an acidic coformer, $S_{cocrystal}/S_{drug}$ increases with pH due to the ionization of the components, therefore the cocrystal CSC will also increase with increasing pH.

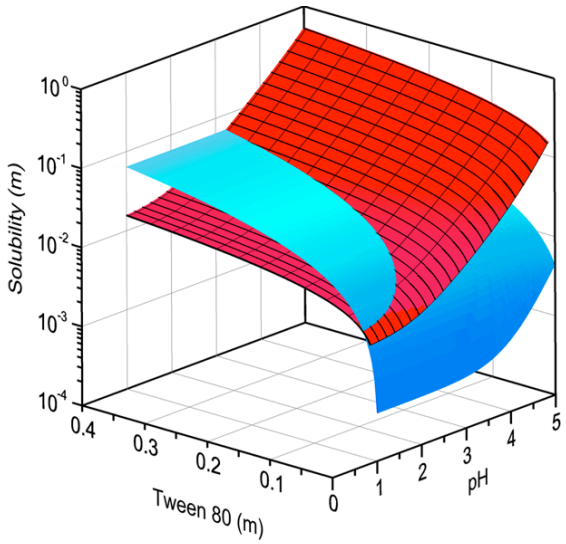

Figure 2.3. Cocrystal and drug solubility dependence on surfactant concentration and pH. HDHA (red surface) drug HD (blue surface). Drug and cocrystal solubility were calculated from equations (2.19) and (2.21), respectively, substituting equation (2.18) to describe the pH dependence of the micellar solubilization using K_{sp} = 1.4 x10^{-6} m^2, S_{aq}^{HD} = 4 x10^{-4} m, pK_a^{HA}= 2.0, pK_a^{HD}= 4.0, K_s^{HD}= 400 m^{-1}, K_s^{D-} =10 m^{-1}, and K_s^{HA} =K_s^{A-} = 0 m^{-1}.

Figure 2.3 shows that for a pH range of 1-3.25 the CSC increases from 0.021 m to 0.41 m. The effect of the component ionization on the CSC determines the pH range in which the CSC is achievable. The $[H^+]$ dependence of the CSC equation is given by

$$CSC=\frac{\frac{Ksp}{(S_{aq}^{HD})^2}\left(1+\frac{K_a^{HA}}{[H^+]}\right)-\left(1+\frac{K_a^{HD}}{[H^+]}\right)}{\left(K_s^{HD}+K_s^{D-}\frac{K_a^{HD}}{[H^+]}\right)-\frac{Ksp}{(S_{aq}^{HD})^2}\left(K_s^{HA}+K_s^{A-}\frac{K_a^{HA}}{[H^+]}\right)}+CMC \qquad (2.25)$$

which is obtained by substituting equation (2.18) into equation (2.22). The CSC is predicted to increase as coformer ionization increases relative to the drug ionization ($K_a^{HA} > K_a^{HD}$, $pK_a^{HA} < pK_a^{HD}$), and decrease as drug ionization increases relative to coformer ionization ($K_a^{HA} < K_a^{HD}$, $pK_a^{HA} > pK_a^{HD}$) based on the numerator of equation (2.25). The CSC of the hypothetical cocrystal shown in Figure 2.3 is 0.02 m at 1 pH unit below pK_a^{HA}, and doubles to 0.04 m at pH = pK_a^{HA}. The CSC increases to 0.23 m at 1 pH unit above pK_a^{HA}. At 2 pH units above the pK_a^{HA}, the CSC is 2.15 m, which is not a

reasonable surfactant concentration for pharmaceutical applications.[50] The pH range in which the CSC is achievable is dependent on the coformer ionization when $pK_a^{HA} < pK_a^{HD}$ and, can be modulated by selection of the cocrystal coformers based on pK_a^{HA}.

The concepts outlined in this section provide a theoretical framework that can be applied to control the solubility and $S_{cocrystal}/S_{drug}$ of pharmaceutical cocrystals utilizing micellar solubilization as well as ionization. The cocrystal solubility advantage will be reduced in micellar solutions that preferentially solubilize the drug. This may be useful to mitigate unnecessarily high cocrystal solubility, thus if there exists only one cocrystal of a drug and its solubility is too high, micellar solubilization can be used to lower $S_{cocrystal}/S_{drug}$ to the required value. Often cocrystals are dosed in aqueous suspensions without consideration of their possible transformation. Solution-mediated transformation of a cocrystal that exhibits $S_{cocrystal}>S_{drug}$, can avoided in an aqueous suspension that contains $[M] \geq CSC$ because the cocrystal is thermodynamically stable under these solution conditions. The cocrystal solubility advantage relative to the drug can be restored by either dilution of the suspension so that $[M] < CSC$ or by modulation of the solution pH to increase $S_{cocrystal}/S_{drug}$.

Determination of equilibrium solubilization constants from eutectic point measurements

The equilibria at the eutectic point between solid cocrystal, solid drug, and the solution is described by

$$HDHA_{solid}+HD_{solid} \leftrightarrow HD_{aq}+HA_{aq} \tag{2.26}$$

The analytical concentration of acidic drug concentration at the eutectic point, $[HD]_{eu,T}$, is

$$[HD]_{eu,T}=[HD]_{eu,un}\left(1+\frac{K_a^{HD}}{[H^+]}+K_s^{HD,T}[M]\right) \tag{2.27}$$

where $[HD]_{eu,un}$ is the unionized drug in equilibrium at the eutectic. Equation (2.27) also applies to the acidic coformer. The analytical concentration of acidic coformer $[HA]_{eu,T}$ is obtained by replacing the terms of HD in equation (2.27) with those pertaining to HA, therefore both the drug and coformer concentrations in equilibrium at the eutectic point have a linear dependence on the micellar surfactant concentration at a given $[H^+]$.[15]

The drug concentration at the eutectic point is equal to the drug solubility under the same conditions assuming that the coformer is not affecting the drug solubility or the

micellar solubilization of the drug. The analytical drug concentration at the eutectic is the drug solubility determined in the presence of coformer in solution,[4] and a comparison of the drug eutectic concentration, $[HD]_{T,eu}$ and the drug solubility, S_T^{HD}, in a micellar solution allows for evaluation of the influence of coformer on the drug solubilization. The coformer is not affecting the drug solubilization by the micelle if $[HD]_{T,eu} = S_T^{HD}$ under the same conditions of $[H^+]$ and [M].

Materials and Methods

Materials

Indomethacin γ-form (IND γ), saccharin and sodium lauryl sulfate were purchased from Sigma Chemical Company (St. Louis, MO). Brij 99, Myrj 52 and Tween 80 were received as gifts from Sigma Chemical Company (St. Louis, MO). All materials were used as received. X-ray powder diffraction (XRPD) and differential scanning calorimetry (DSC) were used to characterize the materials prior to use. HPLC grade acetonitrile was purchased from Fisher. Water used in this study was filtered through a double deionized purification system (MilliQ Plus Water System from Millipore Co., Bedford, MA).

Media preparation

Phosphate buffer was prepared at pH 2.1 by mixing 1.3 g NaH_2PO_4 and 0.68 mL of 85% phosphoric acid (H_3PO_4) with deionized water to prepare a 100 mL of 0.2 M buffer. Brij 99, Tween 80,SLS or Myrj 52 was dissolved in the buffer.

Cocrystal synthesis

The indomethacin-saccharin cocrystal was prepared by slurry suspension. 1.1985 g of IND γ and 0.6181 g SAC were added to 10 ml of 0.05 m SAC solution in ethyl acetate. Solid phases were characterized by XRPD and full conversion to cocrystal was achieved in 24 hrs.

Drug solubility measurement

Drug solubility was measured by adding excess IND γ (50 mg) to a screw-capped vial containing 2 ml of pH 2.1 phosphate buffer with a known amount of surfactant. This was repeated in solutions varying surfactant concentration. Micellar solubilization constants (K_s) of the drug in each surfactant were determined by linear regression analysis of the

measured drug solubilities at 25±0.1°C as a function of micellar surfactant concentration according to equation (2.19) using S_0^{IND}=2.85x10^{-6} m.[48]

$S_{cocrystal}$ dependence on micellar solubilization and CSC

Calculated from the intersection of $S_{cocrystal}$ and S_{drug} (Method 1)

$S_{cocrystal}$ dependence on [M] and CSC were calculated from equations (2.19) and (2.21) using K_{sp} =1.38 x10^{-9}m^2,[18] pKa^{SAC}=1.6,[18] pKa^{IND}=4.2,[88] and the $K_s^{IND,T}$ values in Table 2.4. $K_s^{SAC,T}$=0 was assumed for initial calculations; K_s^{SACT} was evaluated and included in the model to determine its influence on the calculated $S_{cocrystal}$ and CSC. Cocrystal aqueous solubility was determined by measuring eutectic concentrations of the drug and the coformer in pH 2.1 phosphate buffer at 25±0.1°C. Cocrystal (50-100 mg) and drug (25–50 mg) were suspended in 3 mL of media up to 4 days. The pH at equilibrium was measured. Cocrystal aqueous solubility was calculated according to $S_T^{HDHA} = \sqrt{[HD]_{T,eu}[HA]_{T,eu}}$ where HD is the drug (IND) and HA is the coformer (SAC). At the eutectic or transition point, the solution is saturated with respect to two solid phases, in this case, cocrystal (IND-SAC) and drug (IND). This method allows for cocrystal solubility measurement under thermodynamic equilibrium that may not otherwise be accessible due to transformation to the less soluble phase. Drug and coformer concentrations were analyzed by high-performance liquid chromatography (HPLC). Solid phases at equilibrium were confirmed by XRPD.

Evaluated from measured eutectic points (Method 2)

Cocrystal solubilities were obtained by measuring eutectic concentrations of drug and coformer in buffered surfactant solutions (pH 2.1). $S_{cocrystal}$ was evaluated as a function of surfactant concentration in water at 25±0.1°C. Cocrystal (50–100 mg) and drug (25–50 mg) were suspended in 3 mL of solution up to 3 days and the pH at equilibrium was measured. The cocrystal eutectic concentrations were used to evaluate cocrystal solubility, and CSC. Cocrystal solubilities were determined according to $S_T^{HDHA} = \sqrt{[HD]_{T,eu}[HA]_{T,eu}}$. This equation considers ionization and micellar solubilization of cocrystal components and assumes that no solution complexation is taking place. The range of the observed CSC was established based on the observed component concentrations at the eutectic point measured in a solution containing [M]

surfactant: when $[HD]_{T,eu}<[HA]_{T,eu}$, [M]<CSC because drug is the stable phase, when $HD]_{T,eu}=[HA]_{T,eu}$, [M]=CSC because $S_{cocrystal}=S_{drug}$ and when $[HD]_{T,eu}>[HA]_{T,eu}$, [M]> CSC because cocrystal is the stable phase.

Calculated from the intersection of $[drug]_{eu}$ and $[coformer]_{eu}$ dependence on [M](Method 3)

Drug and coformer eutectic concentrations increase linearly with surfactant concentration and intersect at the CSC.[15] Linear regression analysis was used to obtain the respective K_s values from the measured drug and coformer eutectic concentration dependence on [M] according to equation (2.27). The CSC was calculated from the intersection of the drug and coformer lines generated from the linear regression analysis. The cocrystal solubility dependence on [M] was calculated from equation (2.21) using $K_{sp}=1.38x10^{-9}$ m^2,[18] $pK_a^{SAC}=1.6$, $pK_a^{IND}=4.2$,[88] and the drug and coformer K_s values that were determined from the linear regression analysis.

Cocrystal dissolution studies

50 mg of sieved IND-SAC (45-106 μm) was suspended in 9 mL 0.2m phosphate buffer with and without $7.65x10^{-4}$m Tween 80 at 25 ± 0.1°C. The resulting slurry was stirred at 600 rpm by magnetic stirring. Aliquots were withdrawn at predetermined time points and filtered through a 0.45 μm PVDF syringe filter. Solution concentrations were analyzed by HPLC. Final solid phases were characterized by XRPD and DSC.

High-Performance Liquid Chromatography

The solution concentrations of IND and SAC were analyzed by a Waters HPLC (Milford, MA), equipped with an ultraviolet-visible spectrometer detector. A C18 Thermo Electron Corporation (Quebec, Canada) column (5μm, 250 x 4.6 mm) at ambient temperature was used. The mobile phase composed of 70% acetonitrile and 30% water with 0.1% trifluoroacetic acid. The injection sample volume was 20 or 40 μl and the retention times were 3.5 and 6.1 minutes for SAC and IND respectively. Absorbance was monitored at 265 nm. Waters' operation software, Empower 2, was used to collect and process the data. All concentrations are reported in molality (moles solute/kilogram solvent) unless otherwise indicated.

X-ray Powder Diffraction

X-ray powder diffraction diffractograms of solid phases were collected with a benchtop Rigaku Miniflex X-ray diffractometer (Rigaku, Danverse, MA) using Cu Kα radiation (λ= 1.54Å), a tube voltage if 30 kV, and a tube current of 15 mA. Data were collected from 5 to 40° at a continuous scan rate of 2.5°/min.

Thermal Analysis

Solid phases collected from the slurry studies were dried and analyzed by differential scanning calorimetry (DSC) using a TA instrument (Newark, DE) 2910MDSC system equipped with a refrigerated cooling unit. DSC experiments were performed by heating the samples at a rate of 10 K/min under a dry nitrogen atmosphere. Temperature and enthalpy calibration of the instruments was achieved using a high purity indium standard. Standard aluminum sample pans were used for all measurements.

Results

We have previously reported that the indomethacin-saccharin cocrystal (IND-SAC) is more soluble than IND γ in the entire pH range.[18] The solubility of IND-SAC is 13, 26, and 65 times higher than the parent drug at pH 1.4, 2.1, and 3, respectively. In pH 2.1 phosphate buffer, IND-SAC was observed to achieve a maximum supersaturation of 7.5 after 2 minutes and subsequently transforms to parent drug as shown by a drop in solution concentration after 2 minutes (supplemental information). At pH 2.1, IND-SAC does not achieve its true solubility advantage of 26 and cannot maintain a supersaturation of 7.5 due to solution-mediated transformation. Surfactants may be useful to reduce $S_{cocrystal}/S_{drug}$ to modulate supersaturation during dissolution or, to achieve a CSC in an aqueous solution to protect IND-SAC against solution-mediated transformation in a suspension.

Rational Surfactant Selection to Modulate $S_{cocrystal}$ based on drug solubilization, $K_s^{IND,T}$

The thermodynamic equilibrium constants required to predict the cocrystal solubility, $S_{cocrystal}/S_{drug}$ and CSC using the equations described in the theoretical section, have been reported previously and are shown in Table 2.1. The minimum $K_s^{IND,T}$ required to achieve a CSC of 0.1 to 0.4 m for the IND-SAC cocrystal at pH 2.1 and 25 °C was calculated from equation (2.22) assuming, $K_s^{SAC,T}=0$. A surfactant with a $K_s^{IND,T}$ =

6450 m^{-1} is required to achieve a CSC = 0.1 m, and a surfactant with a $K_s^{IND,T}$ = 1620 m^{-1} is required to achieve a CSC = 0.4 m. Surfactants were rationally selected to reduce the $S_{cocrystal}/S_{drug}$ of IND-SAC based on their observed drug solubilization ($K_s^{IND,T}$).

Table 2.1 K_{sp} and component K_a values 25 °C

Equilibrium constant	Reported Value	Reference
K_{sp}	(1.38±0.09)x10^{-9} m^2	18
pK_a^{SAC}	1.6	89
pK_a^{IND}	4.17	88

Equilibrium micellar solubilization constants for IND were calculated from reported solubilities in solutions of varying surfactant concentration using equation (2.19).[54,83-85] K_s^{IND} and K_s^{IND-} were not separately determined, instead the $K_s^{IND,T}$ was determined and the pH of the experiment is indicated in Table 2.2 when reported. The $K_s^{IND,T}$ values range from 22600-36200 m^{-1} in several types of nonionic surfactants at pH 3. Myrj 52 and Tween 80 have the highest solubilization constants relative to the other surfactants at pH 3. In several cases the IND solubility was measured in water without indication of equilibrium solution pH. $K_s^{IND,T}$ ranges from 6900-240,000 (nonionic surfactants and SLS) in water (pH not reported). The $K_s^{IND,T}$ of Myrj 52 and Tween 80 were observed to increase with pH indicating that the micellar solubilization by these surfactants is pH dependent (K_s^{IND-} is not zero).

Table 2.2 Calculated $K_s^{IND,T}$ from reported IND solubility in surfactant solutions

Surfactant	Type	pH	$K_s^{IND,T}$ [a]	Reference
Myrj 49	nonionic	3 (0.001N H_2SO_4)	26900 ± 900	Krasowska
Myrj 51	nonionic	3 (0.001N H_2SO_4)	33000 ± 400	Krasowska
Myrj 52	nonionic	1.2 (buffer)	26500±2000	Valizadeh
Myrj 52	nonionic	3 (0.001N H_2SO_4)	36200 ± 300	Krasowska
Myrj 52	nonionic	7.2 (buffer)	150000 ±10000	Valizadeh
Tween 20	nonionic	3 (0.001N H_2SO_4)	22600 ± 300	Krasowska
Tween 40	nonionic	3 (0.001N H_2SO_4)	26800 ± 100	Krasowska
Tween 60	nonionic	3 (0.001N H_2SO_4)	26800 ± 700	Krasowska
Tween 80	nonionic	3 (0.001N H_2SO_4)	28600 ± 200	Krasowska
Tween 80	nonionic	pH 5.7 (water)[b]	240000±4000	Najib
F108	nonionic	(water)[c]	145000 ± 6000	Lin & Kawashima
SLS	ionic	(water) [c]	75016± 600	Najib
F-88	nonionic	(water) [c]	11400 ± 300	Lin & Kawashima
F-68	nonionic	(water) [c]	6900 ± 300	Lin & Kawashima

(a) Calculated from reported IND solubilities at 25 °C, according to equation (2.17) using S_{aq}^{IND}=2.85x10^{-6} m and pKa^{IND}=4.2.

(b) pH not reported, the pH of solutions of IND, deionized water and Tween 0-10%w/w were measured in this work (pH=5.7).
(c) pH not reported.

Based on the $K_s^{IND,T}$ values obtained from measurements in water (pH not reported) IND solubilization by Tween 80 was highest followed by F-108, SLS, F-88, and F-68 respectively. Brij 99 is reported to solubilize IND to a similar extent as Tween 80, but the $K_s^{IND,T}$ could not be calculated based on the reported solubility data.[85] Thus, Tween 80, SLS, Myrj 52, and Brij 99 were selected for study based on their solubilization power ($K_s^{IND,T}$) and utility as pharmaceutical excipients.[49,50] Three methods were used to evaluate the cocrystal solubility dependence on [M] and CSC in the different surfactants:

(1) By calculation of the intersection of $S_{cocrystal}$ and S_{drug} as a function of surfactant concentration according to equation (2.22) using cocrystal K_{sp}, cocrystal component ionization (K_a), micellar solubilization (K_s), surfactant CMC, and solution [H^+].

(2) By measurement of cocrystal eutectic point as a function of [M].

(3) By calculation of the intersection of $[drug]_{eu}$ and $[coformer]_{eu}$ as function of surfactant concentration according to equation (2.27).

$S_{cocrystal}$ and CSC calculated from intersection of $S_{cocrystal}$ and S_{drug} (Method 1, assuming $K_s^{SACT}=0$)

The $S_{cocrystal}$ and CSC dependence on micellar solubilization were calculated from equation (2.21) from the cocrystal K_{sp}, the intrinsic drug solubility and the drug micellar solubilization constant K_s^{IND}. The IND γ and the IND-SAC solubilities were measured in pH 2.1 phosphate buffer without surfactant and confirm that the cocrystal is 26 times more soluble as shown in Table 2.3

Table 2.3.Cocrystal and drug solubility in water at pH 2.1 and 25 °C

Solid Phase	Aqueous Solubility
IND-SAC	(7.2±0.2) x10^{-5} m
IND γ	(2.8±0.1) x10^{-6} m

The measured IND solubilities in pH 2.1 phosphate buffer solutions of varying surfactant concentration, shown in Figure 2.4, were used to calculated $K_s^{IND,T}$ from equation

(2.19).[54,83-85] This pH was chosen to study IND-SAC at the lowest $S_{cocrystal}/S_{drug}$, while operating under pH conditions in which the surfactants were chemically stable.[90]

The resulting $K_s^{IND,T}$ values for SLS, Tween 80, Myrj 52 and Brij 99 are shown in Table 2.4. Based on the $K_s^{IND,T}$, Myrj 52 is the surfactant with the highest solubilization power. The nonionic surfactants had higher $K_s^{IND,T}$ relative to the anionic surfactant SLS and are expected to be more effective in reducing $S_{cocrystal}/S_{drug}$ and achieve lower CSC values. The CSC for each surfactant was predicted using equation (2.22) from $K_s^{IND,T}$ values in Table 2.4, K_a values in Table 2.1, and assuming the $K_s^{SAC,T}=0$. All of the surfactants studied exhibited a CSC and are capable of protecting cocrystal against solution-mediated transformation.

Table 2.4. $K_s^{IND,T}$ and CSC at pH 2.1, 25°C.

Surfactant	$K_s^{IND,T}$ (m^{-1})[a]	CSC (m)[b]
SLS	6300 ± 300	0.11 ± 0.01
Tween 80	23540 ± 20	0.029 ± 0.003
Brij 99	26700 ± 900	0.026 ± 0.003
Myrj 52	32700 ± 400	0.022 ± 0.003

(a) Calculated from the analytical drug solubility dependence on [M] according to equation (2.19) using $S_0^{IND}= 2.85\times10^{-6}$ m

(b) Calculated from equation (2.22) using $K_{sp}= 1.38\times10^{-9}$ m, $K_s^{IND,T}$ in this table and assuming $K_s^{SACT}=0$.

Figure 2.2 shows the cocrystal solubility and drug solubility dependence on micellar solubilization in SLS, Tween 80, Brij 99, and Myrj 52, calculated from cocrystal K_{sp} and $K_s^{IND,T}$. The cocrystal solubility increase due to micellar solubilization is weaker than that of the drug which leads to an intersection of the $S_{cocrystal}$ and S_{drug} curves at the CSC. This intersection occurs because $S_{cocrystal}$ has a square-root dependence on surfactant concentration ($\sqrt{M}$), wheras S_{drug} has a linear dependence. Below the CSC $S_{cocrystal}>S_{drug}$, at the CSC $S_{cocrystal}=S_{drug}$, and above the CSC $S_{cocrystal}<S_{drug}$, for a 1:1 cocrystal. According to this behavior, a thermodynamically stable aqueous suspension of a cocrystal with $S_{cocrystal}>S_{drug}$ can be prepared in solutions containing [M]≥CSC.

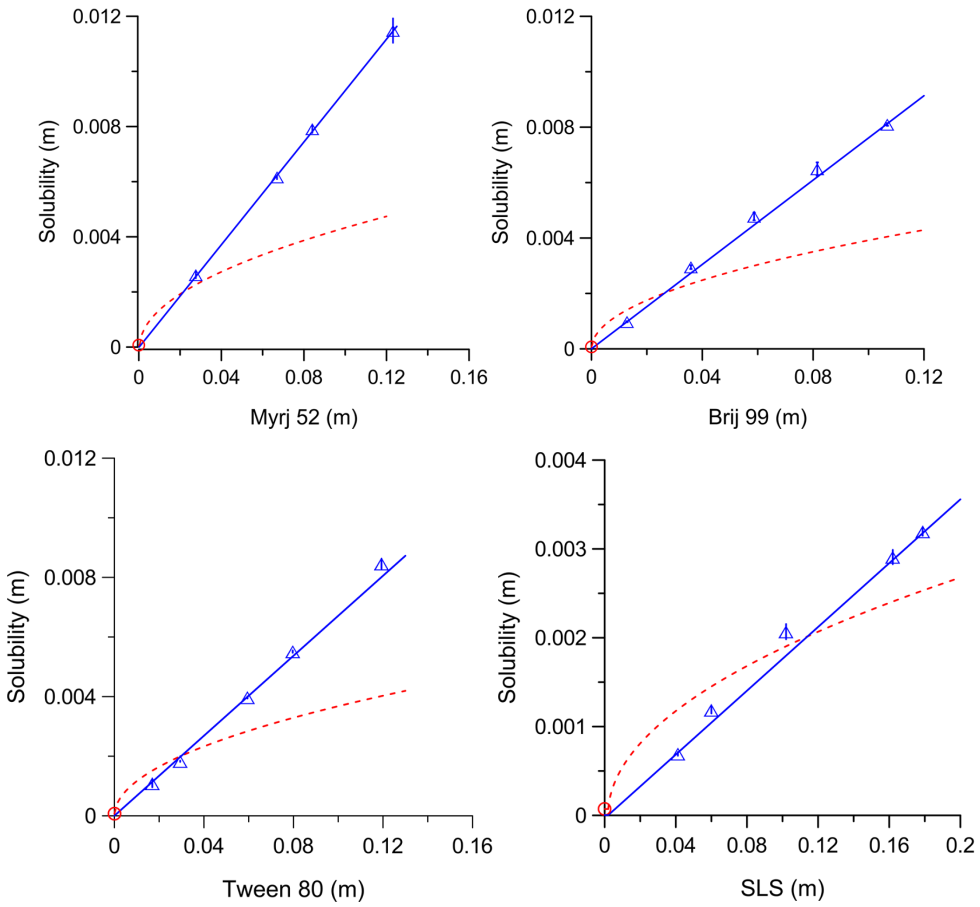

Figure 2.4. Cocrystal solubility (·····) dependence on [M] was calculated from equation (2.21) using K_{sp}=1.38x10^{-9} m^2, pK_a^{SAC}=1.6, pK_a^{IND}=4.2, and the $K_s^{IND,T}$ values in Table 2.4, according to Method 1, assuming K_s^{SACT}=0. $K_s^{IND,T}$ was evaluated for each surfactant by linear regression analysis of the measured drug solubility (Δ) in surfactant solutions. The measured cocrystal solubility in the absence of surfactant at pH 2.1 and 25 °C was (7.2±0.2)x10^{-5} m, shown by (○). The surfactants studied include Myrj 52, Brij 99, Tween 80, and SLS. The drug solubility is described by equation (2.17) at pH 2.1 using S_{aq}^{IND}=2.85x10^{-6} m, pK_a^{IND}=4.2 and $K_s^{IND,T}$ values in Table 2.4. The CSC was calculated from equation (2.25), which is the intersection of the drug and cocrystal solubility curves.

CSC measured from $S_{cocrystal}$ in surfactant solutions determined at the eutectic point (Method 2)

Cocrystal solubilities were measured in equilibrium at the eutectic point between drug and cocrystal solid phases. Figure 2.5 shows the solution concentrations of drug and coformer in equilibrium at the eutectic point; at lower surfactant concentrations, $[coformer]_{eu}$>$[drug]_{eu}$ and at higher surfactant concentrations there is a reversal of the relative drug and coformer eutectic concentrations such that $[coformer]_{eu}$<$[drug]_{eu}$. The component eutectic concentrations of a 1:1 cocrystal are a function of $S_{cocrystal}/S_{drug}$ according to

$$\frac{[\text{coformer}]_{eu}}{[\text{drug}]_{eu}} = \left(\frac{S_{cocrystal}}{S_{drug}}\right)^2 \quad (2.28)$$

This relationship has been derived and shown in our previous publications.[4,18] According to equation (2.28), when $[\text{coformer}]_{eu}=[\text{drug}]_{eu}$ the cocrystal and drug solubilities are equal, thus the surfactant concentration range in which the CSC occurs can be determined from the measured eutectic concentrations.

Saccharin-rich solutions in equilibrium at the eutectic point indicate the surfactant concentration range in which drug is the stable phase ($[\text{drug}]_{eu}<[\text{coformer}]_{eu}$). While the surfactant concentration range in which cocrystal is the stable phase is indicated by the drug-rich solution concentrations at the eutectic point ($[\text{drug}]_{eu} > [\text{coformer}]_{eu}$).[15] The hydrophobic drug, IND, is preferentially solubilized compared to the hydrophilic coformer, SAC, as shown by the reversal in the measured drug concentrations in equilibrium at the eutectic point compared to coformer (bar charts in Figure 2.5).

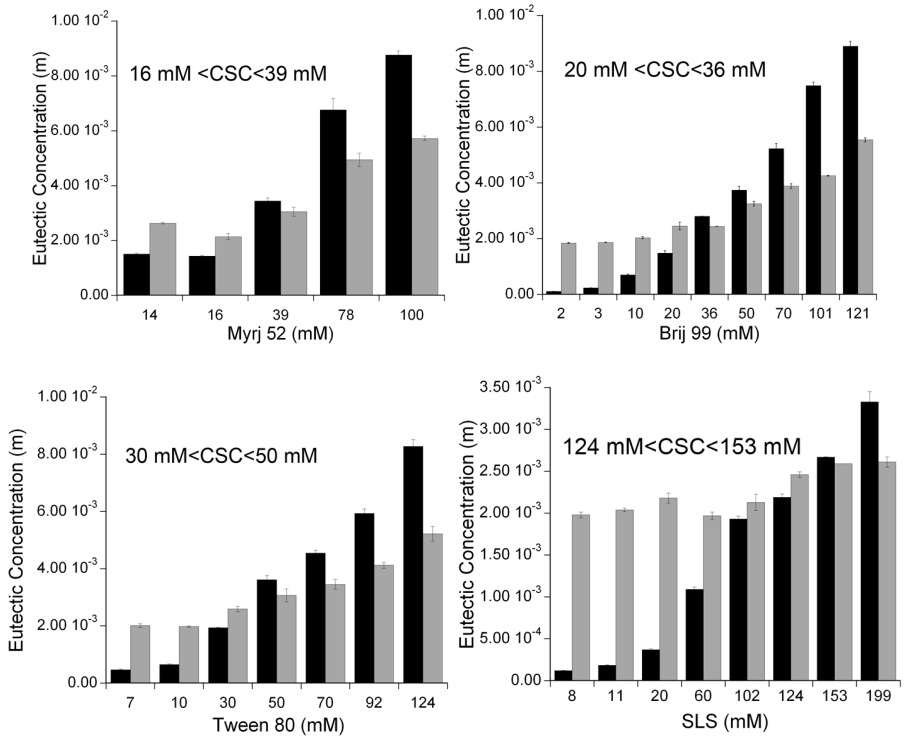

Figure 2.5. Range of CSC based on eutectic concentration dependence on surfactant concentration. Eutectic concentrations of drug (black bar) and coformer (grey bar) in buffer solutions containing different concentrations of surfactant at pH 2.1, 25 °C.

The measured eutectic concentrations reveal that the equilibrium saccharin solution concentrations in equilibrium at the eutectic point (cocrystal solubility measurement)

increase with increasing surfactant concentration and suggest that the coformer is being solubilized.

$K_s^{IND,T}$, $K_s^{SAC,T}$ and CSC from the linear relationship of the measured component eutectic concentration dependence on surfactant concentration (Method 3)

The eutectic concentration dependence on micellar solubilization was used to evaluate the CSC and component K_s values.[15] The measured drug and coformer concentrations in equilibrium at the eutectic point increased linearly with increasing surfactant concentration for all the surfactants studied as shown in Figure 2.6. The $[drug]_{eu}$ exhibits a steeper slope than the $[coformer]_{eu}$ indicting that the drug is preferentially solubilized relative to the coformer. Due to the severe asymmetric solubilization of the cocrystal components, the regression lines of the $[drug]_{eu}$ and $[coformer]_{eu}$ intersect at the CSC. Similar behavior has been reported for cocrystals of carbamazepine in sodium lauryl sulfate.[15]

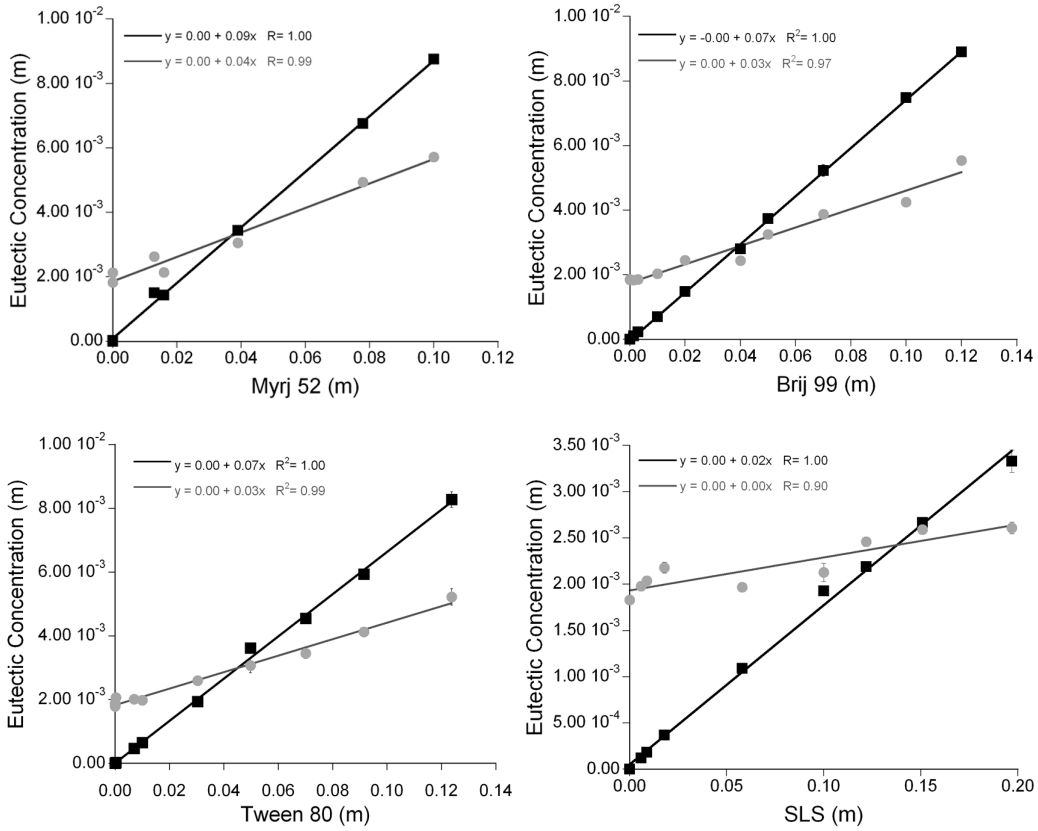

Figure 2.6. Evaluation of micellar solubilization constants (K_s) and CSC from eutectic point measurement dependence on surfactant concentration. Measured equilibrium concentrations of drug (■) and coformer (●) at the eutectic point in solutions of varying surfactant concentrations at pH 2.1. The surfactant concentration plotted is micellar

concentration (total-CMC). Lines represent linear regressions of eutectic concentrations used to calculate K_s for each component according to equation (2.27).

The $K_s^{IND,T}$ and $K_s^{SAC,T}$ were determined from linear regression analysis according to equation (2.27) and are shown in Table 2.5 for each surfactant. As hypothesized, the drug was solubilized to a greater extent than the coformer, as evidenced by its higher K_s value. The $K_s^{IND,T}$ determined from the $[drug]_{eu}$ dependence on [M] was not significantly different than the $K_s^{IND,T}$ values in Table 2.4, which were determined from drug solubility dependence on [M] in the same concentration range ($p<0.05$). Therefore, the presence of coformer at the eutectic point does not effect the solubilization of IND.

Table 2.5. K_s values determined from linear regression of eutectic concentration dependence on [M] at pH 2.1.

Surfactant	$K_s^{IND,T}$ (m^{-1})	$K_s^{SAC,T}$ (m^{-1})	CSC[a](m)	CMC (m)
Myrj 52	30900±500	83 ± 7	37 ± 8	1.5×10^{-4} m [b]
Brij 99	26500 ± 200	58 ± 4	39 ± 5	2.65×10^{-4} [c]
Tween 80	23700 ± 600	59 ± 3	45 ± 5	1×10^{-5} [c]
SLS	6100 ± 100	8 ± 2	140 ± 20	0.005-0.008 [d]

(a) Calculated intersection of linear regressions of measured component dependence on surfactant at the eutectic point.
(b) From reference [91]
(c) From reference [92]
(d) From reference [93,94]

$S_{cocrystal}$ and CSC calculated from cocrystal K_{sp}, $K_s^{IND,T}$ and $K_s^{SAC,T}$ (Method 1) compared to $S_{cocrystal}$ evaluated by eutectic measurements (Method 2)

The drug and coformer solution concentrations in equilibrium at the eutectic point were used to evaluate the stoichiometric cocrystal solubility according to

$$S_T^{HDHA} = \sqrt{[HD]_{T,eu}[HA]_{T,eu}} \qquad (2.29)$$

This equation applies to a 1:1 cocrystal, and includes contributions of ionization and micellar solubilization. Figure 2.7 shows the experimentally determined cocrystal solubility increased with surfactant concentration, and was higher than that predicted from equation (2.21) assuming $K_s^{SAC,T}=0$. The experimental cocrystal solubility increases in the presence of SLS as well as the nonionic surfactants, and the cocrystal is observed to be less soluble than the drug above the CSC. The measured cocrystal solubilities are in excellent agreement with the solubility calculated from equation (2.21) when saccharin solubilization ($K_s^{SAC,T}$) was included in the mathematical model.

Even though $K_s^{IND,T}$ was 600-1000 times greater than $K_s^{SAC,T}$ for the surfactants studied, the cocrystal solubility predicted using the measured $K_s^{SAC,T}$ was 4-70% higher than that predicted assuming $K_s^{SAC,T}=0$. The difference between the predicted and measured $S_{cocrystal}$ increased with surfactant concentration above the CMC. Micellar solubilization of the coformer increases $S_{cocrystal}$ and can be easily monitored using eutectic point measurements. The cocrystal solubility was lower than that of the drug above 0.05 m (50 mM) for the nonionic surfactants and above 0.15 m (150 mM) for SLS. The cocrystal solubility and CSC were under predicted when the assumption that $K_s^{SAC}=0$ was made for all the surfactants studied.

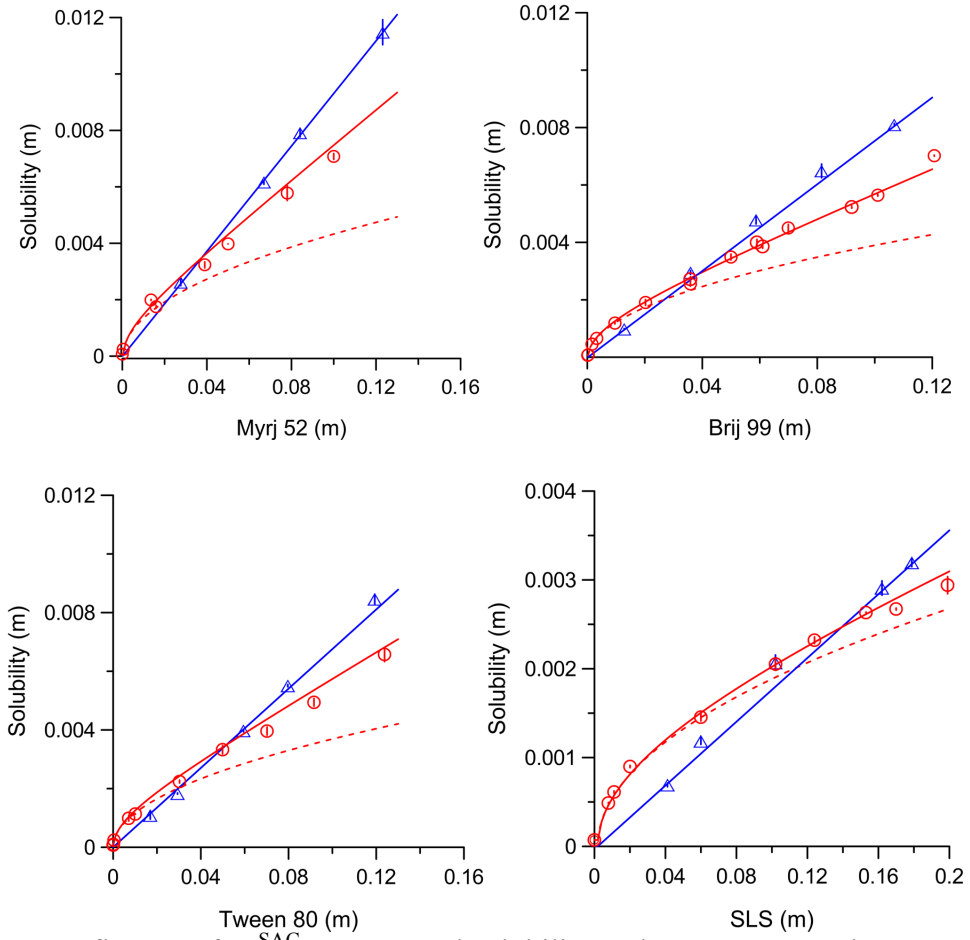

Figure 2.7. Influence of K_s^{SAC} on cocrystal solubility and CSC. Measured cocrystal solubility dependence on total surfactant concentration for Myrj 52, Brij 99, Tween 80, and SLS (○). Cocrystal solubility was predicted using equation (2.21) using a K_{sp} = 1.38 x10^{-9} m^2, SAC pK_a = 1.6 and assuming $K_s^{SAC,T}=0$ (——) or using measured $K_s^{SAC,T}$ (·····) from Table 2.5. The measured drug solubility is represented by (Δ). Theoretical drug solubility (——) dependence on surfactant concentration was calculated from equation (2.19) using a S_0 of 2.85x10^{-6} m, IND pK_a = 4.2 and $K_s^{IND,T}$ values in Table 2.4.

Higher surfactant concentrations are required to stabilize cocrystal when the coformer is solubilized. The CSC calculated assuming $K_s^{SAC,T}=0$ is compared to the CSC calculated using the evaluated K_s^{SAC} in Table 2.5. The CSC calculated using the measured $K_s^{SAC,T}$ is ~1.5 times larger than the CSC calculated assuming $K_s^{SAC,T}=0$ for all surfactants studied. However, the CSC evaluated assuming $K_s^{SAC,T}=0$ served as lower limit approximation that may be useful when the $K_s^{SAC,T}$ is unknown. The component concentrations at the eutectic point were useful for determining whether SAC solubilization was occurring.

$S_{cocrystal}/S_{drug}$ dependence on micellar solubilization

It is essential to identify the lowest surfactant concentration that increases the drug solubility to accurately predict $S_{cocrystal}/S_{drug}$ below the CSC at the low surfactant concentrations where $S_{cocrystal}/S_{drug}$ exhibits the highest rate of change. The observed $[drug]_{eu}$ in solutions containing surfactant concentrations close to, or at the CMC of Tween 80 and SLS, indicate deviations from their reported CMC values. The reported CMC of Tween 80 is $1x10^{-5}$ m,[92] yet $[drug]_{eu}$ was not enhanced in a solution containing $4.95x10^{-5}$ m Tween 80, while $[drug]_{eu}$ was increased 2- fold in the presence of $9.96x10^{-5}$ m Tween 80; the CMC of Tween 80 appears to be higher than the reported value based on this data. $[drug]_{eu}$ was increased 43-fold in the presence of 0.008 m SLS, and while this is within the published range of the CMC (0.005-0.008 m)[93] the large solubility increase at this value indicates that the CMC is lower than 0.008 m.

The CMC was estimated by performing linear regression analysis of the measured $[IND]_{T,eu}$ dependence on surfactant concentrations at surfactant concentrations approaching the reported CMC. The intersection of the linear regression with the IND solubility in buffer with surfactant is approximated as the CMC (supplemental information). The estimated CMC values of SLS and Tween 80 were used to accurately predict the $S_{cocrystal}$ and $S_{cocrystal}/S_{drug}$ dependence on [M] at lower surfactant concentrations. The prediction is less sensitive to deviations of the CMC at higher surfactant concentrations.

The $S_{cocrystal}/S_{drug}$ dependence on micellar solubilization is shown in Figure 2.8. K_s values evaluated from the eutectic measurements were used to predict $S_{cocrystal}/S_{drug}$ according to equation (2.24). The experimental $S_{cocrystal}/S_{drug}$ was determined from each

eutectic measurement according to the following equation, which applies to a 1:1 cocrystal (and includes contributions of ionization and micellar solubilization):[95]

$$\frac{S_{cocrystal}}{S_{drug}} = \sqrt{\frac{[coformer]_{eu}}{[drug]_{eu}}} \qquad (2.30)$$

The measured and calculated $S_{cocrystal}/S_{drug}$ dependence on surfactant concentration is shown in Figure 2.8. $S_{cocrystal}/S_{drug}$ =1 is shown by the dotted line and indicates the concentration required to reach the CSC.

Interestingly, very small concentrations of surfactant can decrease the $S_{cocrystal}/S_{drug}$; $S_{cocrystal}/S_{drug}$ is reduced by half in the presence of 0.14 mM Tween 80, 0.25 mM Myrj 52, 0.39 mM Brij 99, and 2.12 mM SLS. The surfactant concentration required to reduce $S_{cocrystal}/S_{drug}$ in half is directly related to the surfactant CMC; the lower the CMC, the lower the surfactant concentration that is required to reduce $S_{cocrystal}/S_{drug}$.

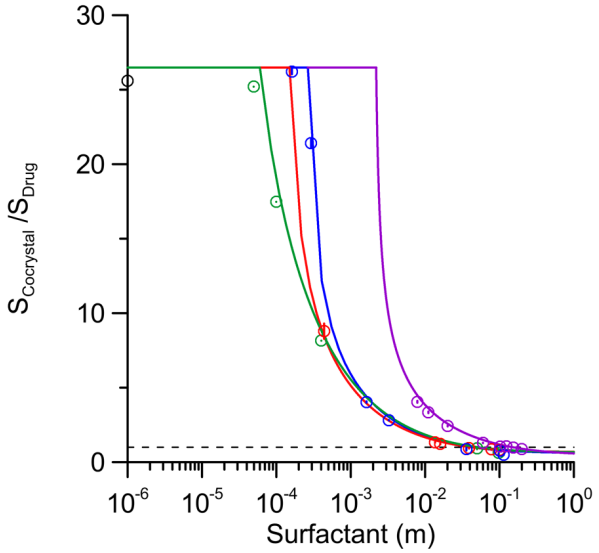

Figure 2.8. Measured (O) and predicted cocrystal solubility advantage ($S_{cocrystal}/S_{drug}$) dependence on total surfactant concentration at pH 2.1 for (—) Myrj 52, (—) Brij 99, (—) Tween 80, and (—) SLS at 25°C. $S_{cocrystal}/S_{drug}$ was predicted from equation (2.24) and was determined from the eutectic measurement according to equation (2.30).

The measured cocrystal solubility advantage is in excellent agreement with the predicted values. Based on these findings, adding surfactant to a dissolution medium may decrease the $S_{cocrytal}/S_{drug}$ of the cocrystal if the drug is preferentially solubilized by the surfactant. Therefore if IND-SAC solubility is compared that that of the drug in solutions containing surfactant concentrations above the CSC, no solubility advantage will be seen because

$S_{cocrystal}/S_{drug} < 1$. Cocrystals that are more soluble than the drug under aqueous conditions may appear to be as soluble, or less soluble than the drug in solutions containing surfactant above the CSC. If a cocrystal is to achieve a solubility advantage over the drug, it is essential to know the CSC of a surfactant to avoid reducing $S_{cocrystal}/S_{drug}$.

Table 2.6 summarizes the results of different methods used to evaluate CSC. The methods used to calculate the CSC (Method 1 and 3) provide a range of CSC values based on the error associated with linear regression analysis. Linear regression analysis of the cocrystal component concentrations is used to obtain the K_s values used in Method 1. Method 3 relies on linear regression analysis of the drug and coformer eutectic dependence on surfactant concentration to determined the CSC at the intersection of the regression lines. Both of these methods are in good agreement with the measured CSC, despite the error associated with the linear regression analysis. The average measured CSC range for the surfactants studied is 22 mM, which is higher than the error associated with the calculated CSC (Method 1 and 3). The magnitude of the CSC range determined by the cocrystal solubility from eutectic measurements is dependent on the number of measurements carried out. For example, the widest range was observed for SLS. This range can be decrease by performing experiments below 153 mM and above 124 mM. Regardless, Method 1 requires the least amount of experiments to obtain a CSC range, the eutectic measurements can then be used to confirm the range.

Table 2.6 CSC values at pH 2.1 obtained by three different methods

	CSC (mM)			
	Intersection of $S_{cocrystal}$ and S_{drug} (Method 1)		Measured from eutectic concentrations (Method 2) [c]	Intersection of $[drug]_{eu}$ and $[coformer]_{eu}$ (Method 3) [d]
Surfactant (CMC)	Calculated using K_{sp}, K_s^{INDa}, $K_s^{SAC}=0$	Calculated using K_{sp}, K_s^{IND}, K_s^{SAC} [b]		
Myrj 52 (1.5×10^{-4}m)[a]	22 ±3	42 ± 7	16 < CSC < 39	37 ± 8
Brij 99 (2.65×10^{-4}) [a]	26±3	42± 5	20 < CSC < 36	39 ± 5
Tween 80 (6×10^{-5}) [b]	29±3	52± 7	30 < CSC < 50	45 ± 5
SLS (2×10^{-3}) [b]	110 ± 10	150 ± 20	124 < CSC < 153	140 ± 20

(a) Calculated from equation (2.22) using $K_s^{IND,T}$ from Table 2.4, assuming $K_s^{SAC}=0$
(b) Calculated from equation (2.22) using $K_s^{IND,T}$, $K_s^{SAC,T}$ values shown in Table 2.5
(c) CSC range from measured component concentrations at eutectic: $[drug]_{eu} < [coformer]_{eu}$ is below CSC and $[drug]_{eu} > [coformer]_{eu}$ is above CSC
(d) Calculated intersection of linear regressions of measured $[component]_{eu}$ dependence on [M] at the.

The nonionic surfactants achieved CSC < 50 mM, while CSC of SLS was at least 3 times higher (140-150 mM). A CSC of 20 and 40 mM was achieved for 1:1 carbamazepine cocrystals that were 2 and 4 times more soluble than the drug respectively. While the K_s^{CBZ} (600 m^{-1}) is an order of magnitude lower than that of $K_s^{IND,T}$, the $S_{cocrystal}/S_{drug}$ of IND-SAC is a magnitude higher than the CBZ cocrystals. Ultimately, the higher $S_{cocrystal}/S_{drug}$ requires more surfactant to achieve CSC. As expected, cocrystal solution concentrations were maintained for 96 hours in suspensions containing [M] ≥ CSC for all surfactants studied. Thus, it is possible to create a stable suspension of cocrystal that would otherwise transform using surfactant concentrations above the CSC. Based on these results, ignoring the solubilization of saccharin results in an under predicted CSC.

Critical stabilization concentration dependence on pH

The cocrystal solubility dependence on pH relative to the drug must be considered in order to evaluate the effect of pH on the CSC. The solubilities of the IND-SAC cocrystal and the parent drug IND are both reported to increase with pH.[18] However, in the pH range of 1 to 3 the cocrystal solubility increases from 4.71×10^{-5} m at pH 1 to 2.34×10^{-4} m at pH 3 (5.2 fold increase in solubility) while the parent drug does not appreciably increase (2.85×10^{-6} to 3.03×10^{-6} m) in the same pH range. In this pH range, the percent of IND ionized increases from 0.17% to 6%, while the percent of SAC ionized increases from 40% to 96%, the IND-SAC cocrystal solubility increases from 13 to 64 times higher than the parent drug in the pH range of 1 to 3 due to coformer ionization.[18] The $S_{cocrystal}/S_{drug}$ increases with pH because the ionized fraction of SAC (pK_a= 1.6) is increasing with pH relative to the drug due to the lower pK_a of SAC as shown in Figure 2.9.

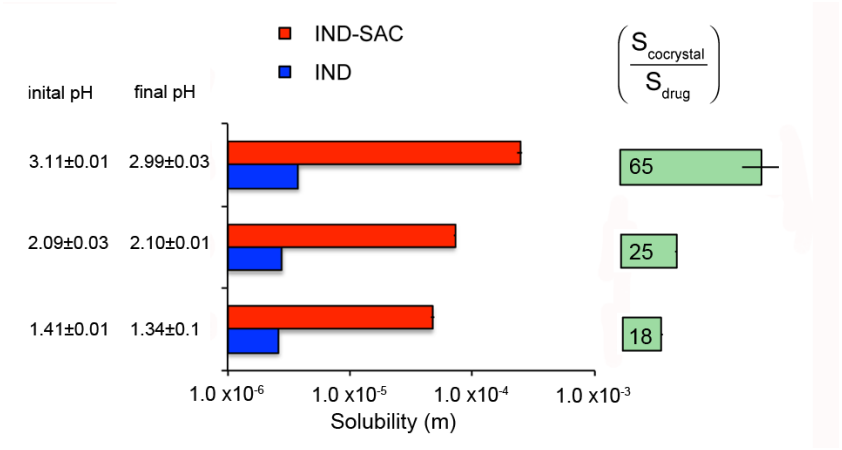

Figure 2.9. Comparison of cocrystal (IND-SAC) and drug (INDγ) solubility-pH dependence in buffered solutions without surfactant at 25°C.[18]

An increase in pH of 0.5 units above the coformer pK_a lead to an increase of $S_{cocrystal}/S_{drug}$ from 18 to 25 and an increase in pH of 1.5 units above the coformer pK_a lead to an increase of $S_{cocrystal}/S_{drug}$ from 18 to 64. The magnitude of $S_{cocrystal}/S_{drug}$ has been associated with higher CSC values,[15-17] therefore the CSC-pH dependence of IND-SAC was evaluated.[16] IND exhibits pH-dependent micellar solubilization as the reported K_s values increase with pH as shown in Table 2.2; therefore K_s^{IND} and K_s^{IND-} are required to evaluate the CSC dependence on $[H^+]$ according to equation (2.22). Due to the availability of reported IND solubilities under ionized conditions in Tween 80, which is necessary to evaluate K_s^{IND-}, the CSC dependence of Tween 80 on $[H^+]$ was investigated. Tween 80 was also selected to further investigate because it exhibits a lower CSC than SLS at pH 2.1, and is commonly used as an excipient and as a dissolution additive during drug evaluation.[49,50]

The K_s values used to predict the CSC dependence on $[H^+]$ for Tween 80 are shown in Table 2.7. The K_s^{IND} and K_s^{IND-} were determined from the $K_s^{IND,T}$ at pH 2.1 and the $K_s^{IND,T}$ at pH 5.7 according to the method by *Grbic et al*. Based on this method, $K_s^{IND,T}$ values were determined from the linear IND solubility dependence on surfactant concentration according to equation (2.19) at pH 2.1 (drug mostly unionized) and pH 5.7 (drug mostly ionized). The values of $K_s^{IND,T}$ at pH 2.1 and pH 5.7 were used to solve for the two unknowns, K_s^{IND} and K_s^{IND-}, according to equation (2.18). The $K_s^{IND,T}$ at pH 5.7 was determined from the reported solubility dependence of IND in aqueous Tween 80 solutions, [54] which in this work was found to equilibrate to pH 5.7

Table 2.7. Influence of pH on K_s values of IND

pH	$K_s^{IND,T}$ (m^{-1})	K_s^{IND} (m^{-1}) [b]	K_s^{IND-} (m^{-1}) [b]	fraction IND^-
2.1	23540 ± 20	23540 ± 20		0.008
5.7[a]	240000 ± 4000		6900 ± 500	0.969

(a) Calculated from reported solubility of IND in aqueous solutions containing Tween 80 (0-10% w/w), pH was not modified and was not measured.[54] The pH of Tween 80 aqueous solutions was measured in the present work (0.1-10%w/w).
(b) Calculated according to the method reported by Grbric et al..[87]

The CSC of Tween 80 was predicted from equation (2.22) using the K_s^{IND} and K_s^{IND-} from Table 2.7 and K_s^{SACT} in Tween 80 from Table 2.5 (Method 1). Figure 2.10 shows that the CSC increases exponentially with pH; the CSC is 15.6 mM at pH 1 and increases by1.6 fold to 25 mM at pH 1.6(the coformer pKa). Increasing the solution pH to one unit above the pKa increases the CSC by 5.5 fold to 136 mM. At values above the coformer pKa the CSC increases exponentially. The coformer ionization increases from 40% to 96% in the pH range of 1 to 3 while the drug is primarily unionized (<6% ionized). To achieve the CSC, the surfactant must increase the drug solubility relative to the cocrystal solubility to reduce the $S_{cocrystal}/S_{drug}$ to 1. As $S_{cocrystal}/S_{drug}$ increases, the weaker the effectiveness of the surfactant in reducing $S_{cocrystal}/S_{drug}$ and the greater the surfactant concentration required to reach the CSC. Beyond pH 3, the cocrystal solubility increases relative to drug due to the ionization of coformer.

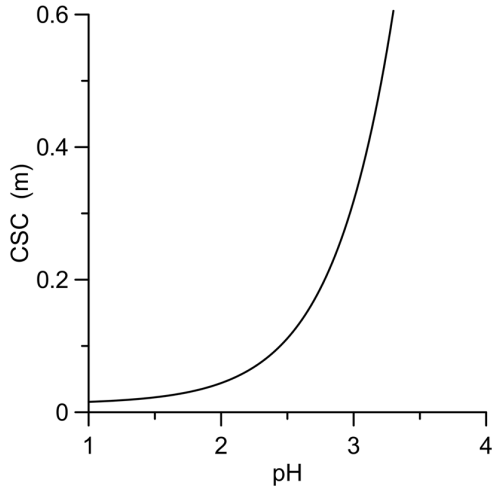

Figure 2.10. CSC dependence on pH for the IND-SAC cocrystal at 25°C in Tween 80. Curve was generated from equation (2.22) using the K_s^{IND} = 23540 m^{-1}, K_s^{IND-}= 6800 m^{-1}, K_s^{SACT}=59 m^{-1}, and the CMC values in Table 2.6 according to Method 1.

Above pH 3, micellar solubilization of the drug, which increases S_{drug} relative to $S_{cocrystal}$, can no longer compete with the ionization of saccharin, which increases $S_{cocrystal}$

relative to S_{drug}. At pH 3, saccharin is ~96% ionized, thus the ionization of saccharin overwhelms the contribution of preferential micellar solubilization of the drug to the $S_{cocrystal}/S_{drug}$. A surfactant with a K_s^{IND} that is 10^4 times higher than K_s^{IND} of Tween 80 would achieve a CSC between pH 1-7. However, no surfactants are reported to solubilize IND to such an extent. An IND cocrystal with a coformer pK_a that is higher than the pK_a of SAC would increase the pH range of the CSC according to equation (2.25). Any solution mechanism that increases the cocrystal solubility relative to drug is expected to increase the CSC.

Table 2.8 shows the measured eutectic concentrations in surfactant solutions close to the calculated CSC. The surfactant concentrations were selected based on the CSC calculated from equation (2.25) at each pH value. The final solution pH at the eutectic point was less than the initial pH during the measurements without surfactant as shown in Figure 2.10. Therefore the eutectic point was measured in solutions containing surfactant slightly above and slightly below the predicted CSC in anticipation of possible changes between initial and final pH. $S_{cocrystal}/S_{drug} <1$ was observed by eutectic measurements at pH 1.4 and 2.1 and $S_{cocrystal}/S_{drug}=1$ was observed at pH 3. The CSC dependence on $[H^+]$ predicted from equation (2.25) was therefore useful to identify the surfactant concentration necessary to stabilize the cocrystal against transformation by achieving $S_{cocrystal}/S_{drug}\leq 1$. It should be noted that if cocrystal transformation is to be avoided, it is advisable to use [M]>CSC.

Table 2.8. Measured eutectic concentrations and $S_{cocrystal}/S_{drug}$ in solutions containing [M] Tween 80.

pH initial	pH final	[M] (mM)	$[IND]_{eu}$ (mM)	$[SAC]_{eu}$ (mM)	$S_{cocrystal}/S_{drug}$
1.41±0.01	1.33±0.06	19	1.01±0.01	0.79±0.01	0.89±0.01
		24	1.30±0.01	0.849±0.003	0.81±0.01
2.09±0.04	2.09±0.03	30	1.94±0.01	2.6±0.1	1.16±0.02
		50	3.6±0.2	3.1±0.2	0.92±0.05
3.13±0.02	2.74±0.01	240	14.1±0.4	16.8±0.3	1.09±0.01
		320	19.7±0.1	19.7±0.3	1.00±0.01

The component eutectic concentrations from Table 2.8 is shown in Figure 2.11 and shows that the surfactant concentration required to achieve $[drug]_{eu} > [coformer]_{eu}$ increases with pH. IND-SAC exhibited $[drug]_{eu} > [coformer]_{eu}$ in 19 mM of Tween 80 at pH 1 indicating that $S_{cocrystal}<S_{drug}$ and CSC<19 mM. At pH 2, 50 mM of Tween 80 was

required to achieve $[drug]_{eu}>[coformer]_{eu}$, and at pH 3, 320 mM of Tween 80 was required to achieve $[drug]_{eu}=[coformer]_{eu}$.

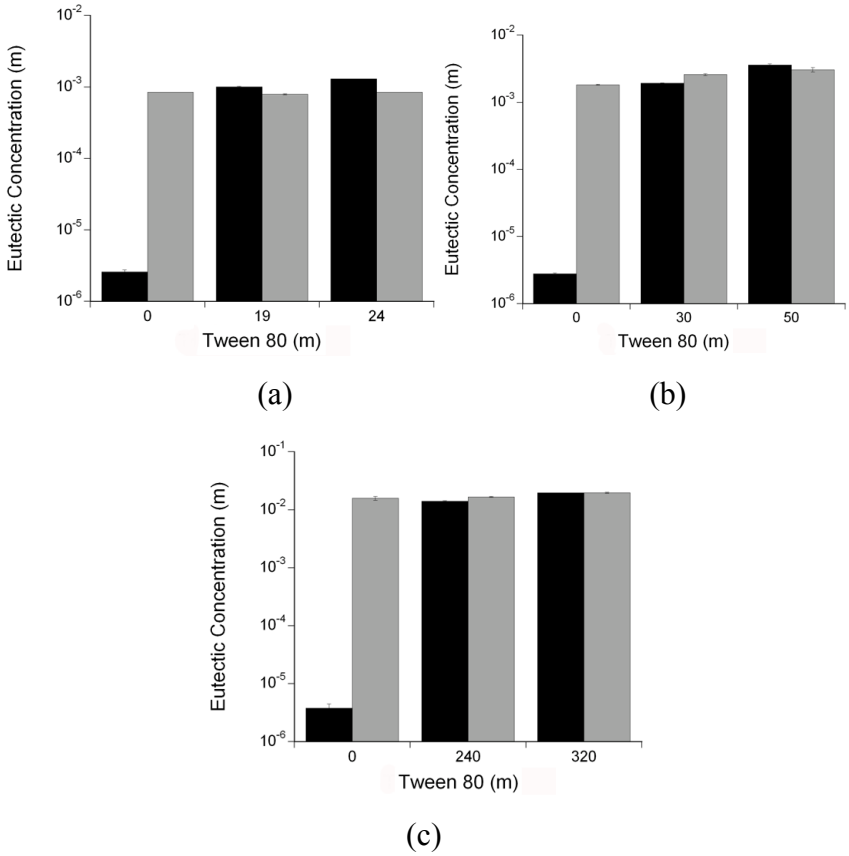

Figure 2.11. CSC range based on measured eutectic concentration dependence on surfactant concentration in solution. Eutectic concentrations of drug (black bar) and coformer (grey bar) in buffer solutions containing different concentrations of surfactant at 25 °C and (a) pH 1.3 (b) pH 2.1 and (c), pH 2.74.

The eutectic point measurements were carried out in solutions with an initial pH of 1.4, 2.1, and 3.13, however the solutions equilibrated to a pH of 1.34, 2.09, and 2.74, respectively. As solution pH increases, cocrystal solubility increases, as does the SAC concentration in equilibrium in the suspension which lowers the pH back down thereby having a self-buffering effect. The equilibrium pH values of the pH 1.40 and pH 2.10 suspensions were within 0.05 pH units of the initial value, while the equilibrium pH value of the pH 3.11 suspension was 0.30 units lower than the initial value at equilibrium due to the buffering effects of SAC. This behavior was also observed during the solubility-pH measurements of IND-SAC.[18]

The CSC determined by the measured cocrystal eutectic point dependence on micellar solubilization (method 2), is in excellent agreement with the predicted CSC values (method 1), thus equation (2.25) is useful to predict the amount of surfactant required to achieve CSC. Equation (2.25) is also useful to determine the pH limitations of the CSC based on the ionization properties of the coformer and drug. Table 2.9 compares the CSC determined by the two methods; prediction by equation (2.25) and measurement of the eutectic point concentrations (i.e. $S_{cocrystal}<S_{drug}$ when $[drug]_{eu} > [coformer]_{eu}$) in surfactant solutions. The prediction by equation (2.25) assumes that only ionization and micellar solubilization are taking place (no complexation, aggregation or hydrotropy are occurring).

Table 2.9. Summary of predicted and measured CSC dependence on pH

Initial pH	Final pH	CSC (m)		
		Calculated intersection of $S_{cocrystal}$ and S_{drug} (Method 1) [a]		Measured from eutectic point in surfactant solutions (Method 2)[b]
		at initial pH	at final pH	
1.41±0.01	1.34±0.01	21 ± 3	19 ± 3	0 < CSC < 19
2.09±0.03	2.09±0.03	51± 7	51± 7	30 < CSC < 50
3.13 ± 0.02	2.74 ± 0.03	420 ± 50	180 ± 20	CSC = 320

(a) Calculated from equation (2.22) using $K_{sp} = (1.38±0.09)x10^{-9}$ m^2, K_s^{IND}=23540±20 m^{-1}, K_s^{IND-}=6900±500 m^{-1}, K_s^{SACT}= 59±3 m^{-1}

(b) CSC range from measured component concentrations at the eutectic point in surfactant solutions: $[drug]_{eu} = [coformer]_{eu}$ at the CSC, $[drug]_{eu} < [coformer]_{eu}$ is below CSC and $[drug]_{eu} > [coformer]_{eu}$ is above CSC

Enabling cocrystal dissolution via Thermodynamic Control of Supersaturation

Micellar solubilization decreases $S_{cocrystal}/S_{drug}$, therefore it should also decrease the supersaturation generated by a cocrystal, resulting in a decrease in the driving force for transformation. The cocrystal dissolution was performed in the presence of Tween 80 to decrease the cocrystal supersaturation in an attempt to prevent the solution-mediated transformation. Solution-mediated transformation has been mitigated by inhibiting nucleation of the stable form, or by reducing the supersaturation of the metastable phase relative to the drug.[56,78] The IND-SACcocrystal was observed to reach a maximum concentration of 2.14 x10^{-5} m with a supersaturation of 7.5 after 2 minutes prior to solution-mediated transformation. Equation (2.24) was used to calculate the surfactant concentration required to reduce $S_{cocrystal}/S_{drug} < 7.5$.

As a first attempt, $S_{cocrystal}/S_{drug}$ was reduced to 6 by adding $7.65x10^{-4}$ m (0.1 w/w%) of Tween 80 to a pH 2.1 aqueous solution, according to equation (2.24). Figure 2.12(a) shows that IND-SAC transforms at pH 2.1 (no surfactant),with IND solution concentrations decreasing after 2 minutes, generating a maximum supersaturation ($[IND]_T/S_T^{drug}$) of 7.5 relative to drug which is lower than the $S_{cocrystal}/S_{drug}$=26 determined from the eutectic point measurement at pH 2.1. IND-SAC dissolution in 0.1% Tween 80 ($7.7x10^{-4}$ m) in pH 2.1 phosphate buffer resulted in higher drug solution concentrations up to 2.18 $x10^{-4}$ m, that were maintained for 15 minutes prior to a drop in solution concentrations, signifying transformation, as shown in Figure 2.12(a).

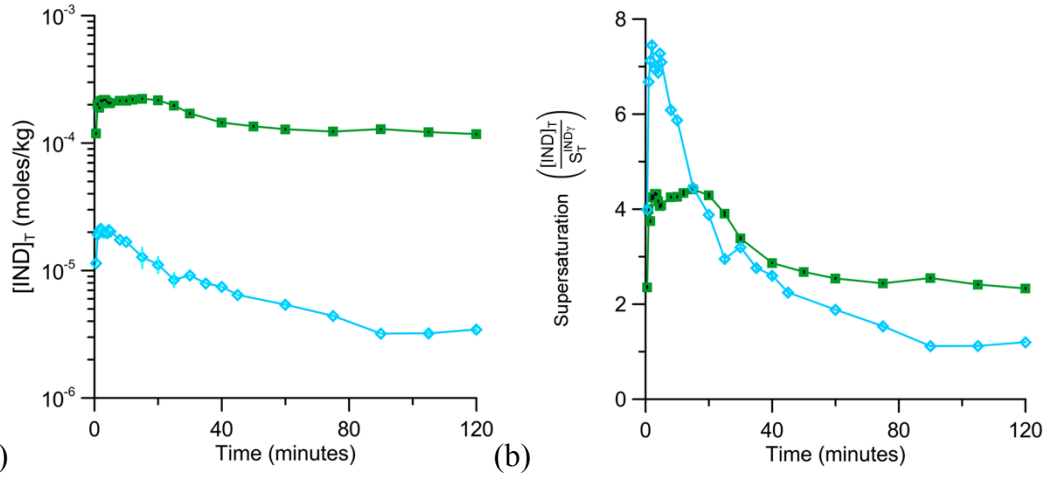

Figure 2.12. IND-SAC dissolution and supersaturation relative to the parent drug ($[IND]_T/S_T^{IND\gamma}$) in Tween 80 ($7.7x10^{-4}$ m, 0.1% w/w) (■) pH 2.1 buffer (◇). Supersaturation was calculated by dividing each IND concentration time point by S_T^{IND}. $S_T^{IND\gamma}$ (pH 2.1 buffer)=(2.85 ±0.03) $x10^{-6}$ m. $S_T^{IND\gamma}$ (0.1% tween 80 in buffer) = (5.05±0.05) $x10^{-5}$ m.

The reduction in $S_{cocrystal}/S_{drug}$ due to the presence of 0.1% Tween 80 corresponded to a reduction in supersaturation from 7 to 4 as shown by Figure 2.12b. The supersaturation generated by the cocrystal in 0.1% Tween 80 was 1.8 times lower than that observed in buffer alone; however the cocrystal maintained a supersaturation of 2 after 2 hours in 0.1% Tween 80. In comparison, the cocrystal exhibited no supersaturation in buffer after 90 minutes and the solution conceentrations approached the solubility of IND γ at pH 2.1 ($2.85x10^{-6}$ m).[18,88] The increased solution concentrations and maintainance of supersaturation during the dissolution of the IND-SAC cocrystal were improved in the presence of 0.1% Tween 80, which is under the CSC.

While amorphous IND achieves a higher peak solution concentration and supersaturation than the INDS-SAC cocrystal at pH 2, it does not dissolve as quickly. Amorphous IND is reported to achieve a peak drug concentration of 4.2 $x10^{-5}$ m with a supersaturation of 14 at pH 2 after 25 minutes.[96] It takes 4.4 minutes to achieve a solution concentration of $1.65x10^{-5}$ m while the cocrystal achieves a concentration of $2.15x10^{-5}$ after 2 minutes. According to previous studies with IND-SAC, a supersaturation of 3 in pH 7.4 phosphate buffer without surfactant can be sustained for 15 minutes which then drops to 2 which is maintained for 2 hours. [1] This is comparable to the supersaturation we achieved with the use of surfactants. The work presented here suggests that surfactants may be very useful to target a desired supersaturation and cocrystal solubility. It is possible to increase $S_{cocrystal}$ and decrease $S_{cocrystal}/S_{drug}$ using the mechanism of preferential micellar solubilization of the drug component.

Conditions under which cocrystal has a solubility advantage or is thermodynamically stable (less soluble than drug) can be anticipated from the presented mathematical models. Small amounts (40-50 mM) of nonionic surfactant can stabilize the IND-SAC cocrystal against transformation. This has important implications for the evaluation of cocrystals, as their solution behavior is often evaluated by dissolution in the presence of a surfactant.[6,11,74] SLS and Tween 80 are examples of surfactants that are used during dissolution to aid in the wetting process and allow for sink conditions. If IND-SAC were evaluated in a solution containing 5% w/w Tween 80 (0.40 m) the cocrystal would be only 1.1 times more soluble than the drug. This information could also be used to strategically design a suspension containing surfactant in which cocrystal is thermodynamically stable. Upon dosing the suspension, surfactant is diluted to allow for a predetermined solubility advantage relative to the drug. The eutectic measurement is useful to evaluate the cocrystal solubility, and $S_{cocrystal}/S_{drug}$ at any surfactant concentration as well to estimate the cocrystal component equilibrium solubilization constants and the CSC.

Conclusions

The work presented here shows that cocrystal solubility and $S_{cocrystal}/S_{drug}$ can be fine-tuned to achieve a target value using micellar solubilization and ionization. IND-SAC solubility has a weaker dependence on micellar solubilization than the parent drug

due to the preferential solubilization of the drug relative to the coformer. For the first time, mathematical models that describe cocrystal solubility dependence on pH and surfactant concentration are used to rationalize surfactant selection to modulate cocrystal solubility and $S_{cocrystal}/S_{drug}$. Measured IND-SAC cocrystal solubilities were in excellent agreement with the predicted values in all surfactants studied when micellar solubilization of both drug and coformer were used in the solubility calculation. The surfactants studied were useful to increase $S_{cocrystal}$ and lower $S_{cocrystal}/S_{drug}$. Therefore the use of surfactants during the evaluation of cocrystals during dissolution should be carefully considered, and perhaps avoided until the cocrystal is confirmed to undergo solution-mediated transformation within a time frame that would be detrimental to the exposure of the drug. The presented mathematical models offer insight as to how any surfactant could potentially affect a given cocrystal using knowledge of the component solubilization constants, which can be approximated by a eutectic measurement in water and a eutectic measurement in a surfactant solution.

Supplemental Information

Solution-mediated transformation of IND-SAC during powder dissolution.

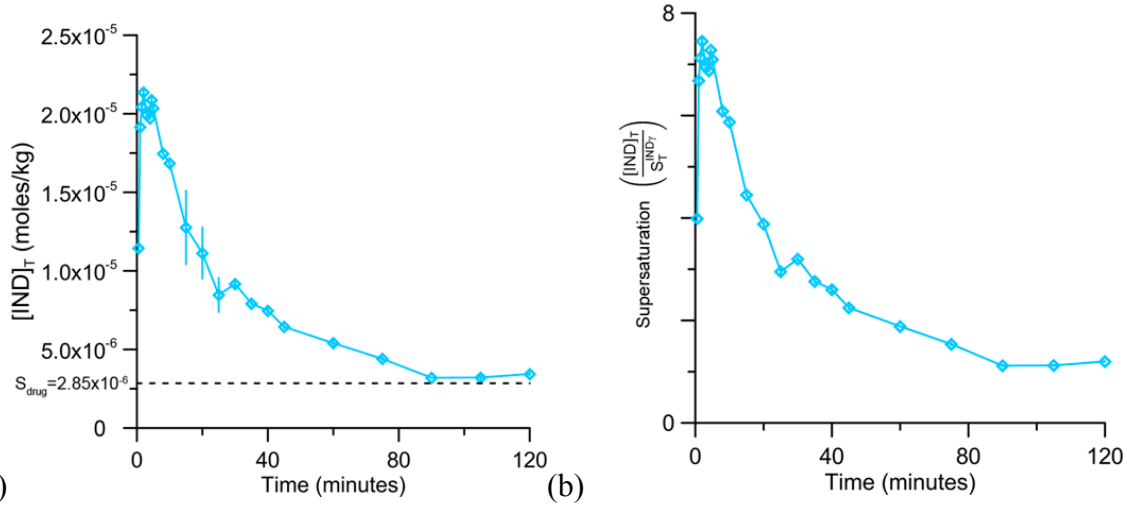

Figure 2.13. Powder dissolution of 50 mg of sieved IND-SAC (45-106 μm) in 9 mL of pH 2.1 phosphate buffer at 25 ± 0.1°C. (a) $[IND]_T$ measured as a function of time (b) supersaturation as a function of time determined as $[IND]_T$ divided by the solubility of IND γ in pH 2.1 phosphate buffer ($S_T^{IND\gamma}$=2.85x10^{-6} m).[18]

Calculation of the CMC of Tween 80 and SLS in the presence of IND and SAC

The CMC in the presence of the eutectic (IND-SAC/IND) was calculated from the intersection between the drug solubility $[IND]_{T,eu}=2.85x10^{-6}$ and the linear regression of the measured $[IND]_{T,eu}$ as a function of total surfactant concentration. Indomethacin was not solubilized at concentrations of Tween 80 that were above reported the CMC ($1x10^{-6}$ m);[92] IND solubility was not enhanced in a solution containing $4.95x10^{-5}$ m Tween 80 and was increased 2- fold in the presence of $9.96x10^{-5}$ m Tween 80. The CMC was calculated to obtain the most accurate predictions of $S_{cocrystal}$ and $S_{cocrystal}/S_{drug}$ as a function of surfactant concentration.

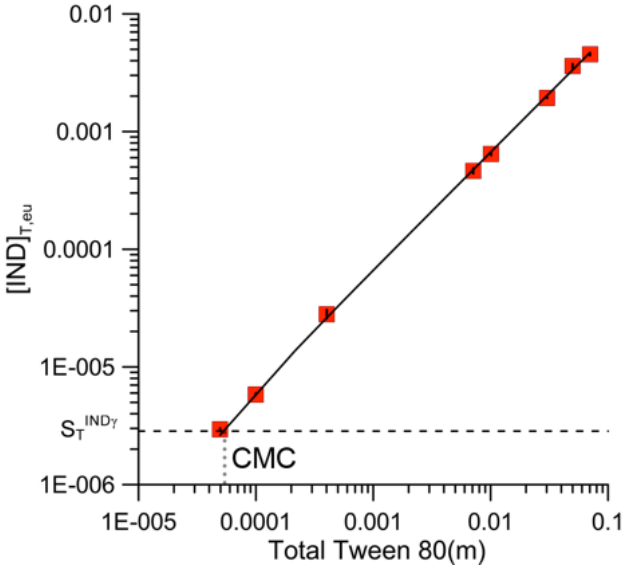

Figure 2.14. Calculated CMC of Tween 80 occurs at $5.26x10^{-6}$ m. CMC calculated from intersection between $[IND]_{T,eu}=2.85x10^{-6}$ and the linear regression of the measured $[IND]_{Teu}$ as a function of total concentration of Tween 80. The resulting equation from the linear regression is: $y=6.7x\ 10^{-2}X-6.7x10^{-7}$

IND solubility was increased 43 fold in the presence of 0.008 m SLS even though the published range of the CMC is 0.005-0.008 m,[93] indicating that the CMC is lower than 0.008m.

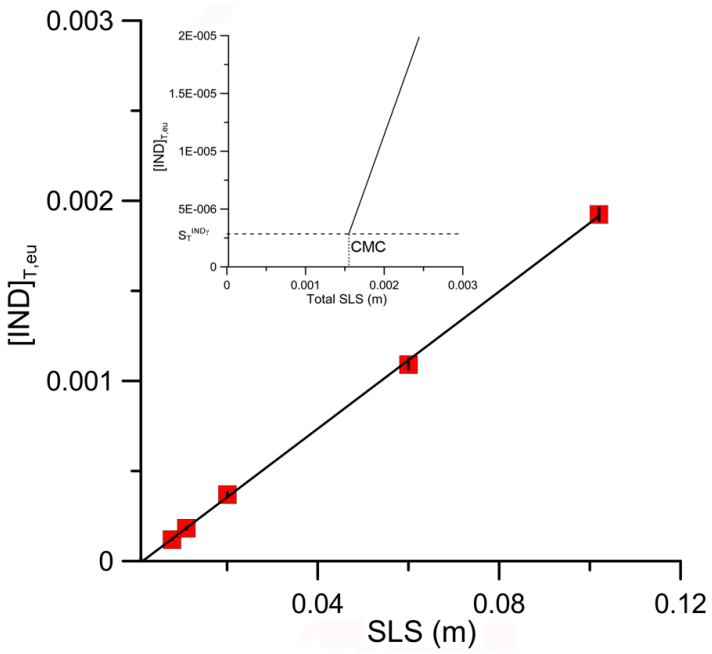

Figure 2.15 The estimated CMC of SLS occurs at 0.0016 m. The measured $[IND]_{T,eu}$ increases linearly with increasing SLS in solution. Linear regression analysis was performed resulting in the solid line described by $y=0.019X-2.67x10^{-5}$ m. The intersection of this line with $[IND]_{T,eu}=2.85x10^{-6}$ is the estimated CMC. The region in which the CMC occurs is magnified to show the intersection of the two lines.

References

1. Basavoju S, Boström D, Velaga S 2008. Indomethacin–Saccharin Cocrystal: Design, Synthesis and Preliminary Pharmaceutical Characterization. Pharm Res 25(3):530-541.
2. Cheney ML, Weyna DR, Shan N, Hanna M, Wojtas L, Zaworotko MJ 2011. Coformer selection in pharmaceutical cocrystal development: A case study of a meloxicam aspirin cocrystal that exhibits enhanced solubility and pharmacokinetics. Journal of Pharmaceutical Sciences 100(6):2172-2181.
4. Good DJ, Rodríguez-Hornedo Nr 2009. Solubility Advantage of Pharmaceutical Cocrystals. Cryst Growth Des 9(5):2252-2264.
6. Jung M-S, Kim J-S, Kim M-S, Alhalaweh A, Cho W, Hwang S-J, Velaga SP 2010. Bioavailability of indomethacin-saccharin cocrystals. Journal of Pharmacy and Pharmacology 62(11):1560-1568.
7. McNamara DP, Childs SL, Giordano J, Iarriccio A, Cassidy J, Shet MS, Mannion R, O'Donnell E, Park A 2006. Use of a glutaric acid cocrystal to improve oral bioavailability of a low solubility API. Pharm Res 23(8):1888-1897.
8. Remenar JF, Morissette SL, Peterson ML, Moulton B, MacPhee JM, Guzmán HR, Almarsson Ö 2003. Crystal Engineering of Novel Cocrystals of a Triazole Drug with 1,4-Dicarboxylic Acids. J Am Chem Soc 125(28):8456-8457.
9. Smith AJ, Kavuru P, Wojtas L, Zaworotko MJ, Shytle RD 2011. Cocrystals of Quercetin with Improved Solubility and Oral Bioavailability. Molecular Pharmaceutics 8(5):1867-1876.
11. Tsutsumi S, Iida M, Tada N, Kojima T, Ikeda Y, Moriwaki T, Higashi K, Moribe K, Yamamoto K 2011. Characterization and evaluation of miconazole salts and cocrystals for improved physicochemical properties. International Journal of Pharmaceutics 421(2):230-236.
13. Schultheiss N, Newman A 2009. Pharmaceutical Cocrystals and Their Physicochemical Properties. Cryst Growth Des 9(6):2950-2967.
14. Bethune SJ, Huang N, Jayasankar A, Rodriguez-Hornedo N 2009. Understanding and Predicting the Effect of Cocrystal Components and pH on Cocrystal Solubility. Cryst Growth Des 9(9):3976-3988.
15. Huang N, Rodriguez-Hornedo N 2011. Engineering cocrystal thermodynamic stability and eutectic points by micellar solubilization and ionization. Crystengcomm 13(17):5409-5422.
16. Huang N, Rodríguez-Hornedo N 2011. Engineering cocrystal solubility, stability, and pHmax by micellar solubilization. Journal of Pharmaceutical Sciences 100(12):5219-5234.
17. Huang N, Rodríguez-Hornedo Nr 2010. Effect of Micellar Solubilization on Cocrystal Solubility and Stability. Cryst Growth Des 10(5):2050-2053.
18. Alhalaweh A, Roy L, Rodríguez-Hornedo N, Velaga SP 2012. pH-Dependent Solubility of Indomethacin–Saccharin and Carbamazepine–Saccharin Cocrystals in Aqueous Media. Molecular Pharmaceutics.
29. Kojima T, Tsutsumi S, Yamamoto K, Ikeda Y, Moriwaki T 2010. High-throughput cocrystal slurry screening by use of in situ Raman microscopy and multi-well plate. International Journal of Pharmaceutics 399(1–2):52-59.

30. Childs SL, Rodriguez-Hornedo N, Reddy LS, Jayasankar A, Maheshwari C, McCausland L, Shipplett R, Stahly BC 2008. Screening strategies based on solubility and solution composition generate pharmaceutically acceptable cocrystals of carbamazepine. Crystengcomm 10(7):856-864.
34. Sanphui P, Goud NR, Khandavilli UBR, Nangia A 2011. Fast Dissolving Curcumin Cocrystals. Cryst Growth Des 11(9):4135-4145.
36. Nehm SJ, Rodríguez-Spong B, Rodríguez-Hornedo N 2005. Phase Solubility Diagrams of Cocrystals Are Explained by Solubility Product and Solution Complexation. Cryst Growth Des 6(2):592-600.
37. Jayasankar A, Reddy LS, Bethune SJ, Rodríguez-Hornedo Nr 2009. Role of Cocrystal and Solution Chemistry on the Formation and Stability of Cocrystals with Different Stoichiometry. Cryst Growth Des 9(2):889-897.
47. Huang N. 2011. Engineering Cocrystal Solubility and Stability via Ionization and Micellar Solubilization. Pharmaceutical Sciences, ed., Ann Arbor, MI: University of Michigan.
48. Mooney KG, Mintun MA, Himmelstein KJ, Stella VJ 1981. Dissolution kinetics of carboxylic acids I: Effect of pH under unbuffered conditions. Journal of Pharmaceutical Sciences 70(1):13-22.
49. Liu R. 2008. Water-insoluble drug formulation. ed., Boca Raton, FL: CRC Press. p 669 p.
50. Yalkowsky SH. 1999. Solubility and solubilization in aqueous media. ed., Washington, D.C. : New York: American Chemical Society ; Oxford University Press. p xvi, 464 p.
54. Najib NM, Suleiman MS 1985. The effect of hydrophilic polymers and surface active agents on the solubility of indomethacin. International Journal of Pharmaceutics 24(2–3):165-171.
56. Tian F, Zeitler JA, Strachan CJ, Saville DJ, Gordon KC, Rades T 2006. Characterizing the conversion kinetics of carbamazepine polymorphs to the dihydrate in aqueous suspension using Raman spectroscopy. Journal of Pharmaceutical and Biomedical Analysis 40(2):271-280.
60. Naylor LJ, Bakatselou V, Dressman JB 1993. Comparison of the mechanism of dissolution of hydrocortisone in simple and mixed micelle systems. Pharm Res 10(6):865-870.
62. Mithani SD, Bakatselou V, TenHoor CN, Dressman JB 1996. Estimation of the Increase in Solubility of Drugs as a Function of Bile Salt Concentration. Pharm Res 13(1):163-167.
74. Bak A, Gore A, Yanez E, Stanton M, Tufekcic S, Syed R, Akrami A, Rose M, Surapaneni S, Bostick T, King A, Neervannan S, Ostovic D, Koparkar A 2008. The co-crystal approach to improve the exposure of a water-insoluble compound: AMG 517 sorbic acid co-crystal characterization and pharmacokinetics. Journal of Pharmaceutical Sciences 97(9):3942-3956.
78. Remenar JF, Peterson ML, Stephens PW, Zhang Z, Zimenkov Y, Hickey MB 2007. Celecoxib:Nicotinamide Dissociation: Using Excipients To Capture the Cocrystal's Potential. Molecular Pharmaceutics 4(3):386-400.
79. Childs SL, Chyall LJ, Dunlap JT, Smolenskaya VN, Stahly BC, Stahly GP 2004. Crystal engineering approach to forming cocrystals of amine hydrochlorides with organic

acids. Molecular complexes of fluoxetine hydrochloride with benzoic, succinic, and fumaric acids. J Am Chem Soc 126(41):13335-13342.
80. Alvarez-Núñez FA, Yalkowsky SH 2000. Relationship between Polysorbate 80 solubilization descriptors and octanol–water partition coefficients of drugs. International Journal of Pharmaceutics 200(2):217-222.
81. Muramatsu Tea 1981. Mechanism of Indomethacin Partition Between Normal-Octanol and Water. Chemical & pharmaceutical bulletin 29(8):2330-2337.
82. Fourie L, Breytenbach JC, Du Plessis J, Goosen C, Swart H, Hadgraft J 2004. Percutaneous delivery of carbamazepine and selected N-alkyl and N-hydroxyalkyl analogues. International Journal of Pharmaceutics 279(1–2):59-66.
83. Krasowska H 1976. Solubilization of indomethacin and cinmatacin by non-ionic surfactants of the polyoxyethylene type. Il Farmaco 31(9):463-472.
84. Valizadeh H, Nokhodchi A, Qarakhani N, Zakeri‐Milani P, Azarmi S, Hassanzadeh D, Löbenberg R 2004. Physicochemical Characterization of Solid Dispersions of Indomethacin with PEG 6000, Myrj 52, Lactose, Sorbitol, Dextrin, and Eudragit® E100. Drug Development and Industrial Pharmacy 30(3):303-317.
85. El-Sabbagh H 1978. Solubilization of indometacin. Pharmazie 33(8):529-531.
86. Sheng JJ, Kasim NA, Chandrasekharan R, Amidon GL 2006. Solubilization and dissolution of insoluble weak acid, ketoprofen: Effects of pH combined with surfactant. European Journal of Pharmaceutical Sciences 29(3–4):306-314.
87. Grbic S, Parojcic J, Djuric Z, Ibric S 2009. Mathematical modeling of pH-surfactant-mediated solubilization of nimesulide. Drug Development and Industrial Pharmacy 35(7):852-856.
88. KG Mooney MMHK, Stella VJ 1981. Dissolution kinetics of carboxylic acids I:effect of pH under unbuffered condtions. J Pharm Sci 70:13-22.
89. Kluza RB, Newton DW 1978. pKa values of Medicinal Compounds in Pharmacy Practice. Drug Intelligence & Clinical Pharmacy 12(9):546-554.
90. Rowe RC, Sheskey PJ, Owen SC editors. 2006. Handbook of Pharmaceutical Excipients. 5th ed., Washington, DC: Pharmaceutical press.
91. Walters KA, Dugard PH, Florence AT 1981. Non-ionic surfactants and gastric mucosal transport of paraquat1. Journal of Pharmacy and Pharmacology 33(1):207-213.
92. Hait S, Moulik S 2001. Determination of critical micelle concentration (CMC) of nonionic surfactants by donor-acceptor interaction with Iodine and correlation of CMC with hydrophile-lipophile balance and other parameters of the surfactants. Journal of Surfactants and Detergents 4(3):303-309.
93. Williams R, Phillips J, Mysels K 1955. The critical micelle concentration of sodium lauryl sulphate at 25 C. Transactions of the Faraday Society 51:728-737.
94. Rodríguez-Hornedo N, Murphy D 2004. Surfactant-facilitated crystallization of dihydrate carbamazepine during dissolution of anhydrous polymorph. Journal of Pharmaceutical Sciences 93(2):449-460.
95. Good DJ, Rodríguez-Hornedo Nr 2010. Cocrystal Eutectic Constants and Prediction of Solubility Behavior. Cryst Growth Des 10(3):1028-1032.
96. Alonzo D, Zhang G, Zhou D, Gao Y, Taylor L 2010. Understanding the Behavior of Amorphous Pharmaceutical Systems during Dissolution. Pharm Res 27(4):608-618.

Chapter 3

Mechanisms of Cocrystal Solubilization in Biorelevant Media

Introduction

Cocrystals are of increasing interest lately because of their ability to enhance and fine-tune the aqueous solubility of inherently insoluble drugs that are otherwise difficult to develop. Pharmaceutical cocrystals enhance solubility by several orders of magnitude,[4,7,74,95] and in some cases achieve dissolution levels as high or higher than the amorphous solid.[1,8,97] Demonstration of improved bioavailability of cocrystals *in vivo* is scarce,[6,7,19,21,74] in part due to poor formulations and lack of understanding of cocrystal behavior under biorelevant conditions.

Cocrystal solubility and $S_{cocrystal}/S_{drug}$ is highly dependent on the solution interactions of the cocrystal components such as ionization and micellar solubilization.[14-17,47] We have recently shown that cocrystal solubility increases with the concentration of sodium lauryl sulfate (SLS) in solution, while $S_{cocrystal}/S_{drug}$ decreases with increasing SLS.[15-17,47] When $S_{cocrystal}/S_{drug} = 1$ the critical stabilization concentration (CSC) of SLS is achieved. Above the CSC, the cocrystal is thermodynamically stable relative to the parent drug.[15-17] Four different cocrystals of carbamazepine were found to be thermodynamically stable in solutions containing SLS above the CSC.[16]

The bile salt sodium taurocholate (NaTC) and the phospholipid lecithin, found in simulated intestinal fluid, are reported to form mixed micelles.[67] The aim of this work was to evaluate how these physiologically relevant mixed micelles influence $S_{cocrystal}/S_{drug}$ and whether they are capable of stabilizing cocrystals. Among the commonly used biorelevant media, the highest concentration of NaTC and lecithin is found in Fed State Simulated Intestinal Fluid version 1 (FeSSIF).[98] While there is an updated version (FESSIF-V2),[64] it contains a lower concentration of NaTC and lecithin and was therefore not used for this study.

Drugs that are hydrophobic and highly permeable (BCS class II) often exhibit higher solubilities in FeSSIF compared to aqueous buffers at the same pH.[62,99-101] The BCS class II drugs IND and CBZ are reported to be 7 and 1.8 times more soluble in FeSSIF compared to acetate buffer (FeSSIF without surfactant) due to micellar solubilization.[101,102] These drugs were selected because they form cocrystals and exhibit different hydrophobicities. IND (log P=4.4)[81] is more hydrophobic than CBZ (log P = 2.7).[82] As a result, the solubility increase due to micellar solubilization is higher for IND relative to CBZ. Cocrystals of both drugs are reported in the literature and their solubility-pH dependence has been evaluated.[14,18]

Knowledge of the cocrystal equilibrium solubility in FeSSIF and acetate buffer provides the opportunity to anticipate the influence of mixed micelles on $S_{cocrystal}/S_{drug}$ and is useful to predict the initial supersaturation with respect to drug that a cocrystal may attain. Is it possible that under fed state conditions a cocrystal may be less soluble than the drug? Will a cocrystal that transforms quickly in aqueous media have a slower conversion time in FeSSIF due to a decrease in $S_{cocrystal}/S_{drug}$? Cocrystal powder dissolution is routinely assessed in biorelevant media without knowledge of the effects of the ingredients on the cocrystal solution chemistry.[10,74,76] Knowledge of cocrystal equilibrium solubility in biorelevant media is necessary to examine the mechanisms by which cocrystal solubility is influenced. The ability to predict the influence of solution conditions on cocrystal solubility would provide a useful tool to guide the evaluation and development of cocrystals.

The work presented here shows for the first time the mechanisms that influence the equilibrium solubility of cocrystals in FeSSIF compared to acetate buffer. Mathematical models describing cocrystal solubility dependence on ionization and micellar solubilization have been reported in the literature for cocrystals of a wide variety of ionization properties and stoichiometries in buffered and nonbuffered aqueous systems.[15-17] These reported mathematical models were used to predict the contributions of micellar solubilization and ionization to overall cocrystal solubility in FeSSIF based on the solubility of the cocrystal components in FeSSIF and acetate buffer. The predicted solubilities were compared to the stoichiometric cocrystal solubility determined from eutectic measurement. The solution-mediated transformation of cocrystal to parent drug

was evaluated in FeSSIF and acetate buffer when $S_{cocrystal}/S_{drug}$ was found to be significantly lower in FeSSIF relative to acetate buffer.

The cocrystals selected for this study make up both 1:1 and 2:1 cocrystal stoichiometries, and contain components of various hydrophobicities and ionization behavior. The cocrystals studied include: 1:1 carbamazepine-saccharin (CBZ-SAC), 1:1 carbamazepine-salicylic acid (CBZ-SLC), 2:1 carbamazepine 4-aminobenzoic acid hydrate, (CBZ-4ABA (H)) and 1:1 indomethacin-saccharin (IND-SAC). SAC (pKa 1.6-2.2),[89] SLC (pKa 3.0)[103,104] and IND (pKa 4.2)[48] are monoprotic acids. 4ABA (pKa 2.6 and 4.8)[105] is amphoteric and CBZ is nonionizable. All cocrystals studied have reported solubility products in aqueous media. Under nonionizing conditions, the CBZ cocrystals are 2.4-2.5 times more soluble than the parent drug and undergo solution-mediated transformation to CBZ (H) in water.[14,18] IND-SAC is reported to be 13 times more soluble than IND under nonionizing conditions and also undergoes solution–mediated transformation in water.[18] The IND-SAC and CBZ cocrystals become increasingly more soluble than the parent drug as pH increases.

Materials and Methods

Materials

Anhydrous monoclinic form III carbamazepine (CBZ (III)) and anhydrous form γ indomethacin (IND) were purchased from Sigma Chemical Company (St. Louis, MO) and used as received. Carbamazepine dihydrate (CBZ (H)) was prepared by slurrying CBZ (III) in water for at least 24 h. The cocrystal coformers saccharin (SAC), 4-aminobenzoic acid (4ABA), and salicylic acid (SLC), were purchased from Sigma Chemical Company (St. Louis, MO) and used as received. All crystalline drugs and coformers were characterized by X-ray power diffraction (XRPD) and differential scanning calorimetry (DSC) before carrying out experiments.

FeSSIF was prepared using sodium taurocholate (NaTC) purchased from Sigma Chemical Company (St. Louis, MO), lecithin purchased from Fisher Scientific (Pittsburgh, PA), sodium hydroxide (NaOH) purchased from J.T. Baker (Philipsburg, NJ), and acetic acid and potassium chloride (KCl) purchased from Acros (Pittsburgh, PA). Ethyl acetate, ethanol and potassium chloride were purchased from Acros (Pittsburgh, PA) and used as received, and HPLC grade methanol and acetonitrile were

purchased from Fisher Scientific (Pittsburgh, PA). Water used in this study was filtered through a double deionized purification system (Milli Q Plus Water System) from Millipore Co. (Bedford, MA).

Cocrystal Synthesis

Cocrystals were prepared by slurry suspension. The indomethacin-saccharin (IND-SAC) cocrystal was synthesized by adding 1.1985 g of IND γ and 0.6181 g SAC (cocrystal components in a 1:1 molar ratio) to 10 ml of 0.05 m SAC solution in ethyl acetate. The carbamazepine saccharin cocrystal (CBZ-SAC) was prepared by adding 1.12 g of CBZA and 0.87 g SAC to 10 ml of 0.05 m SAC solution in ethanol. The carbamazepine-salicylic acid cocrystal (CBZ-SLC) was prepared by adding 1.26 g CBZA and 0.40 g of SLC to a 10 ml solution of 0.01 m SLC solution in acetonitrile. The carbamazepine-4-aminobenzoic acid monohydrate cocrystal (CBZ-4ABA (H)) was prepared by suspending 1.50 g CBZA and 0.44 g 4ABA in a 0.01 m 4ABA aqueous solution at pH 3.9. Solid phases were characterized by XRPD and full conversion to cocrystal was achieved in 24 hrs.

Solubility Studies

Solubility studies were performed at 25 ± 0.1°C with the pure drug and the selected cocrystals. Solubilities were measured in Fed State Intestinal Fluid (FeSSIF) and acetate buffer (FeSSIF without NaTC and lecithin) which both exhibit a pH of 5. FeSSIF and acetate buffer were prepared in accordance to the protocol of Galia and coworkers.[58,98] Fresh FeSSIF was prepared by dissolving 0.41 g sodium taurocholate in 12.5 mL of pH 5 acetate buffer. 0.148 g lecithin was added with magnetic stirring at 37 °C until dissolved. The volume was adjusted to exactly 50 mL with acetate buffer. Acetate buffer was prepared as a stock solution at room temperature by dissolving 8.08 g NaOH (pellets), 17.3 g glacial acetic acid and 23.748 g NaCl in 2 L of purified water. The pH was adjusted to 5.00 with 1 N NaOH and 1N HCl.

Cocrystal equilibrium solubility was evaluated at the eutectic point, where drug and cocrystal solid phases are in equilibrium with solution. The eutectic point between cocrystal and drug was approached by cocrystal dissolution (suspending solid cocrystal (100 mg) and drug (50 mg) in 3 mL of media) and by cocrystal precipitation (suspending solid cocrystal (50 mg) and drug (100 mg) in 3 mL of media saturated with coformer).

Vials were maintained with magnetic stirring at 25 ± 0.1°C for up to 96 h. A detailed discussion of eutectic point measurements has been presented elsewhere.[4,95] All studies were conducted at 25 ± 0.1°C by keeping vials in a temperature controlled water bath. At 24 hour time intervals solution pH was measured and 0.25 mL of samples were collected and filtered through 0.45 mm membrane, and diluted with mobile phase. Drug and coformer concentrations were analyzed by HPLC. The final solid phases were characterized by XRPD and DSC.

The solubilities of the cocrystal components were determined by adding excess solid to 3 mL of media. Solutions were magnetically stirred and maintained at 25 ± 0.1°C using a water bath for up to 96 h. At 24 hour time intervals solution pH was measured and 0.25 mL of samples were collected and filtered through 0.45 mm membrane, and diluted with mobile phase. Solution concentrations were analyzed by HPLC. The final solid phase was characterized by XRPD and DSC.

Cocrystal dissolution studies

250 mg of sieved cocrystal fraction (45-106 μm) was suspended in 30 mL of FeSSIF or acetate buffer at 25 ± 0.1°C. The resulting slurry was stirred at 150 rpm using an overhead stirrer. Aliquots were withdrawn and filtered through a 0.45 μm PVDF syringe filter. Solution concentrations were analyzed by HPLC. Final solid phases were characterized by XRPD and DSC.

High-Performance Liquid Chromatography

The solution concentrations were analyzed by Waters HPLC (Milford, MA) equipped with an ultraviolet-visible spectrometer detector. A C18 Thermo Electron Corporation (Quebec, Canada) column (5μm, 250 x 4.6 mm) at ambient temperature was used. The injection sample volume was 20 μl and the IND-SAC cocrystal was analyzed using an isocratic method with a mobile phase composed of 70% acetonitrile and 30% water with 0.1% trifluoroacetic acid and a flow rate of 1 ml/min. Absorbance of IND and SAC were monitored at 265 nm. The carbamazepine cocrystals were analyzed using an isocratic method with a mobile phase composed of 55% methanol and 45% water with 0.1% trifluoroacetic acid and a flow rate of 1 mL/min. Absorbance was monitored as follows: CBZ and 4ABA at 284, IND and SAC at 265 and SLC at 303. Waters' operation

software, Empower 2, was used to collect and process the data. All concentrations are reported in molality (moles solute/kilogram solvent) unless otherwise indicated.

X-ray Powder Diffraction

X-ray powder diffraction diffractograms of solid phases were collected with a benchtop Rigaku Miniflex X-ray diffractometer (Rigaku, Danverse, MA) using Cu Kα radiation (λ= 1.54Å), a tube voltage if 30 kV, and a tube current of 15 mA. Data were collected from 5 to 40° at a continuous scan rate of 2.5°/min.

Thermal Analysis

Solid phases collected from the slurry studies were dried and analyzed by differential scanning calorimetry (DSC) using a TA instrument (Newark, DE) 2910MDSC system equipped with a refrigerated cooling unit. DSC experiments were performed by heating the samples at a rate of 10 °C/min under a dry nitrogen atmosphere. Temperature and enthalpy calibration of the instruments was achieved using a high purity indium standard. Standard aluminum sample pans were used for all measurements.

Results

Prediction of cocrystal solubilization from drug solubilization in FeSSIF

The solubility of a cocrystal of general stoichiometry, A_xB_y, composed of drug A and coformer B in surfactant solution has been derived previously by considering the following equilibria and equilibrium constants for cocrystal dissociation

$$A_xB_{ysolid} \leftrightarrow xA+yB$$

$$K_{sp}=[A]^x[B]^y$$

and cocrystal component micellar solubilization

$$A_{solid}+M \leftrightarrow A_m$$

$$K_s^A=\frac{[A]_m}{[A]_{aq}[M]}$$

$$B_{solid}+M \leftrightarrow B_m$$

$$K_s^A=\frac{[B]_m}{[B]_{aq}[M]}$$

The cocrystal solubility enhancement due to micellar solubilization is reported to relate to the drug solubility enhancement according to

$$\frac{S_{A_xB_y,T}}{S_{A_xB_y,aq}} = \left(\frac{S_{A,T}}{S_{A,aq}}\right)^{\frac{x}{x+y}} \quad (3.1)$$

Equation (3.1) assumes that the coformer is not solubilized, that there is no solution complexation or self association affecting the solubility of the cocrystal components and that the increase in drug solubility is due to micellar solubilization only.[16] According to equation (3.1), the cocrystal solubility enhancement is less than that of the drug. This relationship was observed for cocrystals of carbamazepine in solutions of SLS, and is now being evaluated for the cocrystal solubility enhancement by physiologically relevant mixed micelles of NaTC and lecithin. The solubility enhancement of the cocrystal is predicted to be higher than that calculated by equation (3.1) when the coformer is solubilized.

The equilibrium solubilities of IND-γ and CBZ (H) in FeSSIF and buffer at 25°C are shown in Table 3.1. Results show that the drug solubilities are higher in FeSSIF relative to acetate buffer. The increase in solubility in FeSSIF relative to buffer has been shown to correlate with the hydrophobicity of a drug as measured by log P.[62,100,101] The solubility of CBZ (H) (log P =2.7) is 1.8 times higher in FeSSIF relative to buffer while IND γ (log P=4.4) is 16 times higher. Thus the more hydrophobic drug, IND γ, has a higher solubility increase in FeSSIF. These results are in agreement with the solubilities reported in the literature at 25°C.[99,100]

Table 3.1. Measured drug solubility in pH 5 FeSSIF and acetate buffer used to predict S_{FeSSIF}/S_{buffer} of 1:1 and 2:1 cocrystal.

	IND γ (m) (pH)	CBZ (H) (m)
Intrinsic (S_{un})[a]	(2.85±0.03) x10^{-6}	(4.6±0.07) x10^{-4}
S_{buffer}[b]	(2.3±0.1) x10^{-5} (4.95±0.01)	(4.2±0.2) x10^{-4}
S_{FeSSIF}[b]	(3.7±0.2)x10^{-4} (4.97±0.06)	(7.5±0.2) x10^{-4}
$\left(\frac{S_{FeSSIF}}{S_{buffer}}\right)_{drug,\ expt}$	16±1	1.8±0.1
$\left(\frac{S_{FeSSIF}}{S_{buffer}}\right)_{cocrystal\ (1:1),\ pred}$	4.0±0.1	1.34±0.04

$\left(\frac{S_{FeSSIF}}{S_{buffer}}\right)_{cocrystal\ (2:1),pred}$	6.4±0.3	1.5±0.1

(a) Reported in literature for IND[18,48,106] and CBZ[94]
(b) Values are in agreement with reported solubilities in FeSSIF and buffer.

While IND solubility is 16 times higher in FeSSIF than buffer, a 1:1 cocrystal of IND is predicted to be only 4 times higher and a 2:1 cocrystal is predicted to be only 6.4 times higher. Carbamazepine exhibits a solubility increase of 1.8-fold in FeSSIF relative to buffer, whereas a 1:1 cocrystal of CBZ is predicted to increase by 1.3 fold and a 2:1 cocrystal is expected to increase by 1.5 fold. The solubilities of cocrystals of CBZ and IND were measured in FeSSIF and buffer to compare with the predicted behavior. The solubility dependence of CBZ-SAC, CBZ-SLC, CBZ-4ABA (H) and IND-SAC on $[H^+]$ have been evaluated and successfully predicted by mathematical models derived from the equilibria for cocrystal dissociation and ionization of the components.[14,18] The solubility dependence of a 1:1 cocrystal RHA (nonionizable drug R, and acidic coformer HA) such as CBZ-SAC and CBZ-SLC on $[H^+]$ can be calculated from

$$S_T^{RHA} = \sqrt{K_{sp}^{RHA}\left(1+\frac{K_a^{HA}}{[H^+]}\right)} \tag{3.2}$$

where K_{sp} is the solubility product of the cocrystal, K_a^{HA} is the ionization constant of the acidic coformer and $[H^+]$ is a measure of the solution acidity with is related to the solution pH according $-\log[H^+]$.

The reported solubility dependence of a 1:1 cocrystal HDHA (acidic drug HD, and coformer HA) on $[H^+]$, such as IND-SAC is described by

$$S_T^{HDHA} = \sqrt{K_{sp}^{HDHA}\left(1+\frac{K_a^{HD}}{[H^+]}\right)\left(1+\frac{K_a^{HA}}{[H^+]}\right)} \tag{3.3}$$

where K_a^{HD} is the ionization constant of the drug and K_a^{HA} is the ionization constant of the coformer. The reported solubility dependence of the 2:1 cocrystal R_2HAB on $[H^+]$, such as CBZ-4ABA (H) is

$$S_T^{R_2HAB} = \sqrt[3]{K_{sp}^{R_2HAB}\left(1+\frac{K_a^{-AB}}{[H^+]}+\frac{[H^+]}{K_a^{HABH^+}}\right)} \quad (3.4)$$

where the K_a^{-AB} and K_a^{HABH+} are the ionization constants of the amphoteric coformer.

Table 3.2 shows the reported K_{sp} values that were used to calculate $S_{cocrystal}$ from equations (3.2)-(3.4). $S_{cocrystal}/S_{drug}$ was also calculated at pH 5 by dividing the calculated $S_{cocrystal}$ by the measured S_{drug} at pH 5. The CBZ cocrystals are 4.4 to 120 times more soluble than the parent drug and the IND-SAC cocrystal is 220 times more soluble than the parent drug at pH 5. All of the cocrystals in this study are more soluble than the parent drug, and therefore the cocrystal equilibrium solubility was evaluated from the component solution concentrations in equilibrium at the eutectic point between cocrystal and drug.[4,14,95]

Table 3.2. Cocrystal solubility and $S_{cocrystal}/S_{drug}$ at pH 5 calculated from K_{sp}

Cocrystal	K_{sp} [a]	$S_{cocrystal}$ (m) [b]	$S_{cocrystal}/S_{drug}$ [c]	Reference
IND-SAC	$(1.38\pm0.09)\times10^{-9}$ m^2	$(5.0\pm0.8)\times10^{-3}$	220 ± 40	18
CBZ-SAC	$(1.00\pm0.05)\times10^{-6}$ m^2	$(5.0\pm0.6)\times10^{-2}$	120 ± 30	18
CBZ-SLC	$(1.13\pm0.05)\times10^{-6}$ m^2	$(1.0\pm0.3)\times10^{-2}$	25 ± 6	14
CBZ-4ABA (H)	$(1.2\pm0.2)\times10^{-9}$ m^3	$(1.8\pm0.1)\times10^{-3}$	4.4 ± 0.3	14

(a) Reported K_{sp} of CBZ-SAC and IND-SAC evaluated from nonlinear regression of coformer eutectic dependence on pH (pH 1-3, 25 °C).[18] Reported K_{sp} of CBZ-SLC and CBZ-4ABA (H) evaluated from linear regression of coformer eutectic dependence on pH (water pH 1-4, and water pH 1-5 respectively, 25°C).[14]
(b) Calculated from equation (3.2) for CBZ-SAC and CBZ-SLC, equation (3.3) for IND-SAC and equation (3.4) for CBZ-4ABA-HYD using Ksp and the following pKa values: SAC 1.6,[89] IND 4.2,[48] SLC 3.0,[103,104] and 4-ABA 2.6 and 4.8.[105]
(c) Ratio of calculated $S_{cocrystal}$ over the measured drug solubility in Table 3.1.

Evaluation of cocrystal solubility in FeSSIF and buffer

Equilibrium cocrystal solubilities were measured at the eutectic points where solid drug and cocrystal are in equilibrium with the solution phase. The measured component concentrations at the eutectic and the stoichiometric cocrystal solubility in FeSSIF and buffer are shown in Table 3.3. For all the cocrystals studied, the $[coformer]_{eu}>[drug]_{eu}$,

Table 3.3. Cocrystal stoichiometric solubility in FeSSIF and buffer determined from solution concentrations in equilibrium at the eutectic point with cocrystal and drug.

Media	Cocrystal	$[drug]_{eu}$ (mM)	$[coformer]_{eu}$ (mM)	$S_{cocrystal}$ (mM)[a]	$\frac{S_{cocrystal}b}{S_{drug}}$	pH
	IND-SAC	0.15±0.02	87±4	3.6±0.2	24 ± 1	3.65±0.05

FeSSIF	CBZ-SAC	1.07±0.03	95.9±0.3	10.1±0.1	9.5±0.1	3.11±0.02
	CBZ-SLC	0.91±0.02	49.9±0.6	6.71±0.09	7.4±0.1	4.29±0.02
	CBZ-4ABA (H)	0.74±0.03	15.6±0.4	2.57±0.05	3.5±0.1	4.94±0.02
buffer	IND-SAC	0.006±0.0003	104±10	0.79±0.03	132 ± 4	3.66±0.02
	CBZ-SAC	0.78±0.05	124±20	9.8±0.3	12.6 ± 0.4	3.08±0.03
	CBZ-SLC	0.51±0.02	50±1	5.1±0.1	9.9±0.2	4.29±0.02
	CBZ-4ABA (H)	0.44±0.02	13.1±0.4	1.73±0.06	3.9±0.1	4.84±0.03

(a) Calculated from equation (2.10) for a 1:1 cocrystal and equation (3.6) for a 2:1 cocrystal.
(b) Calculated from $S_{cocrystal}/[drug]_{eu}$

which means that $S_{cocrystal}>S_{drug}$.[4,95] Cocrystals that exhibit $S_{cocrystal}=S_{drug}$ exhibit $[coformer]_{eu}/[drug]_{eu}$ equal to 1 for a 1:1 and equal to 0.5 for a 2:1 cocrystal which requires that $[coformer]_{eu} \leq [drug]_{eu}$. The CBZ cocrystals exhibited $[coformer]_{eu}$ that was 21-90 times higher than the $[drug]_{eu}$ in FeSSIF and 30-158 times higher than the $[drug]_{eu}$ in buffer. The IND-SAC cocrystal exhibits the largest $[coformer]_{eu}/[drug]_{eu}$ compared to the other cocrystals; the $[coformer]_{eu}$ is $1.7x10^4$ times higher than the $[drug]_{eu}$ in buffer and is only $5.9\ x10^2$ times higher in FeSSIF. This indicates that $S_{cocrystal}/S_{drug}$ is higher in buffer relative to FeSSIF.

Stoichiometric cocrystal solubilities were determined from the drug and coformer solution concentrations in equilibrium at the eutectic point,[16] according to

$$S_T^{1:1\ cocrystal}=\sqrt{[drug]_{T,eu}\,[coformer]_{T,eu}} \tag{3.5}$$

for a 1:1 cocrystal, and

$$S_T^{2:1\ cocrystal}=2\left(\sqrt[3]{\frac{[drug]_{T,eu}^2\,[coformer]_{T,eu}}{4}}\right) \tag{3.6}$$

for a 2:1 cocrystal.

The stoichiometric cocrystal solubilities in buffer at pH 5 determined by eutectic point measurement were lower than that predicted in Table 3.2 for all cocrystals except CBZ-4ABA (H). The eutectic point measurements of cocrystals containing acidic coformers equilibrated at a solution pH lower than 5, which explains why the experimental solubilities are lower than the predicted solubilities at pH 5. CBZ-4ABA (H) was the only cocrystal that equilibrated to pH 5 during the eutectic point measurement. The

experimental solubility of CBZ-4ABA shown in Table 3.3 is in excellent agreement with that predicted in Table 3.2.

Figure 3.1 shows that all of the CBZ cocrystals have a higher solubility compared to CBZ (H) in both media. The CBZ-SAC cocrystal had the highest solubility relative to CBZ (H) in both media. The CBZ (H) and CBZ cocrystals studied have a higher solubility in FeSSIF compared to buffer, except for CBZ-SAC. The S_{FeSSIF}/S_{buffer} is shown next to the solubility bars to quantify the solubility enhancement due to micellar solubilization for each drug and cocrystal. CBZ (H) solubility was found to be 1.8 times higher in FeSSIF compared to buffer. The experimental cocrystal solubility was found to be 1.3 and 1.5 times higher in FeSSIF compared to buffer for CBZ-SLC (1:1) and CBZ-4-ABA (H) (2:1) respectively which is in agreement with the findings from equation (3.1) shown in Table 3.1.[16]

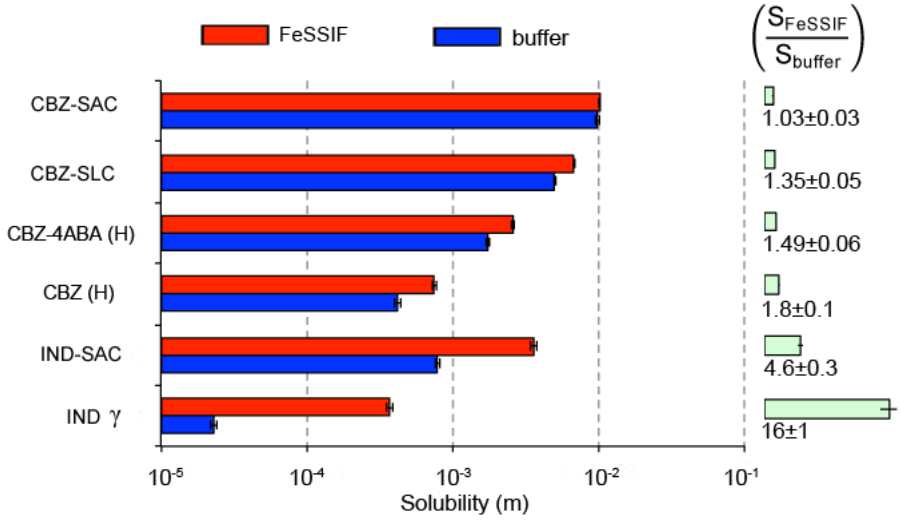

Figure 3.1.Drug and cocrystal solubilities evaluated in FeSSIF and buffer at 25 °C. The stoichiometric cocrystal solubilities were calculated from measured pH and component concentrations at the eutectic point (Table 3.3) using equation (3.5) for 1:1 cocrystals and equation (3.6) for the 2:1 cocrystal as described in the methods section. The final pH of the cocrystal solubility measurement was lower than the initial pH 5 of FeSSIF: CBZ-4ABA (H) (4.89±0.06), CBZ-SLC (4.32±0.04), CBZ-SAC (3.09±0.01) and IND-SAC (3.65±0.04). The final pH of the drug solubility measurements was 5.

The IND-SAC cocrystal was more soluble than its parent drug in both FeSSIF and buffer. The solubility increase of both IND and IND-SAC in FeSSIF compared to buffer was more than that observed for CBZ (H). IND solubility is 16 times higher in FeSSIF relative to buffer. The experimental IND-SAC cocrystal solubility was 4.6 times higher in

FeSSIF relative to buffer. This is in agreement with the predicted cocrystal solubility enhancement based on equation (3.1), which is shown in Table 3.1. Therefore cocrystal solubility enhancement due to micellar solubilization compared to buffer of both ionizable and nonionizable cocrystals can be estimated by equation (3.1) based on the observed solubility enhancement of the parent drug assuming the two media equilibrate to the same pH.

Prediction of cocrystal solubility in FeSSIF from cocrystal K_{sp} and K_s^{drugT}

We have derived mathematical models that describe the contributions of micellar solubilization and ionization of the cocrystal components to the cocrystal solubility in previous publications.[16,17] Table 3.4 summarizes the equations that describe cocrystal solubility for the 1:1 RHA, 1:1 HDHA and 2:1 R_2HAB cocrystals. These equations assume the drug solubility increases linearly with increasing

Table 3.4. Equations that describe cocrystal solubility in FeSSIF

Cocrystal	Solubility Equation	
CBZ-SAC CBZ-SLC	$S_T^{RHA}=\sqrt{K_{sp}^{RHA}\left(1+K_s^R[M]\right)\left(1+\frac{K_a^{HA}}{[H^+]}+K_s^{HA,T}[M]\right)}$	(3.7)
IND-SAC	$S_T^{HDHA}=\sqrt{K_{sp}^{HDHA}\left(1+\frac{K_a^{HD}}{[H^+]}+K_s^{HD,T}[M]\right)\left(1+\frac{K_a^{HA}}{[H^+]}+K_s^{HA,T}[M]\right)}$	(3.8)
CBZ-4ABA (H)	$S_T^{R_2HAB}=2x\sqrt[3]{\frac{K_{sp}^{R_2HAB}}{4}\left(1+K_s^R[M]\right)^2\left(1+\frac{K_a^{-AB}}{[H^+]}+\frac{[H^+]}{K_a^{HABH^+}}+K_s^{HAB,T}[M]\right)}$	(3.9)

NaTC and lecithin maintaining a 4:1 ratio of NaTC to lecithin, which is the ratio utilized to make FeSSIF.[58] This assumption was made based on the observed drug solubilization by NaTC and lecithin in a 4:1 ratio reported in the literature. For example, the solubility of halofantrine increases linearly in a range of 3.75-30 mM NaTC maintaining a 4:1 ratio of NaTC:lecithin.[107] and the solubility of hydrocortisone also increases linearly in a range of 3.72-15 mM of NaTC containing lecithin in a 4:1 ratio.[60] FeSSIF contains 15 mM of NaTC, thus this concentration is in the linear range of 4:1 NaTC:lecithin mixed micelles.

Table 3.5 shows the predicted cocrystal solubilities compared to the experimental cocrystal solubilities in FeSSIF and buffer. Equations (3.7), (3.8), and (3.9) were used to predict the cocrystal solubility in FeSSIF from the K_{sp} and component K_a values (Table

3.2) and the drug K_s values (Table 3.6). The cocrystal solubility was predicted at the equilibrium eutectic pH (Table 3.3) for the sake of comparison to the solubility evaluated from the eutectic point measurements. The equilibrium pH at the eutectic point was lower than the initial media (pH 5) for cocrystals containing acidic coformers. These coformers have pK_a values that are 2 or more pH units lower than pH 5 (SAC pKa=1.6,[18] SLC pKa= 3.0). The predicted cocrystal solubilities are in good agreement with the observed values in both FeSSIF and buffer.

Table 3.5. Comparison of predicted and experimental cocrystal solubilities in FeSSIF

	$S_{cocrystal,FeSSIF}$ (mM)		Eutectic pH	$S_{cocrystal,buffer}$(mM)		Eutectic pH
Cocrystal	predicted	experimental		predicted	experimental	
IND-SAC	2.88	3.6±0.2	3.65±0.05	0.48	0.79±0.02	3.66±0.02
CBZ-SAC	7.53	10.1±0.1	3.11±0.02	5.59	9.8±0.3	3.08 ±0.03
CBZ-SLC	6.28	6.71±0.09	4.29±0.02	5.26	5.0±0.1	4.37±0.02
CBZ-4ABA(H)	2.63	2.57±0.05	4.94±0.02	1.84	1.73±0.06	4.84±0.03

The predicted cocrystal solubilities in FeSSIF and buffer are plotted against the observed solubility in Figure 3.2 and compared to the dotted line representing the function y=x. Data points that fall above the dotted line indicate that the solubility is over predicted while those that fall below are under predicted. The solubilities of CBZ-SLC and CBZ-4ABA (H) are very close to the line while the solubilities of the SAC cocrystals were under predicted. The predicted SAC cocrystal solubilities in buffer were less accurate than those in FeSSIF and the higher the $[coformer]_{eu}$ the less accurate the prediction. The SAC cocrystals exhibited $[coformer]_{eu}$ ranging from 86-124 mM, shown in Table 3.3. CBZ-SLC and CBZ-4ABA (H) had lower $[coformer]_{eu}$ values ranging from 50-51 mM and 13-15mM respectively(Table 3.3).

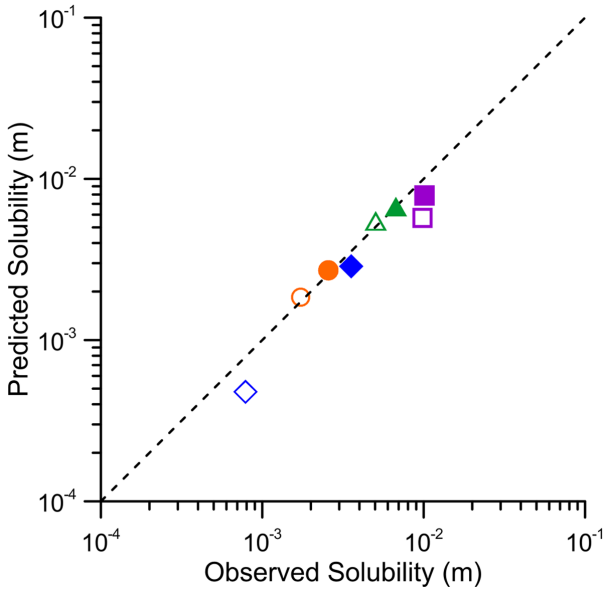

Figure 3.2. Comparison of predicted and observed cocrystal solubility in FeSSIF (closed symbols) and buffer (open symbols) at the equilibrium eutectic pH for IND-SAC (◆) CBZ-SAC (■) CBZ-SLC (▲) and CBZ-4-ABA(H) (●). Errors associated with measured solubilities range from 1-6% of the measured value.

Coformer concentrations much higher than the stoichiometric coformer concentration can lead to errors due to non-ideal behavior during the $S_{cocrystal}$ evaluation. Consideration of solution complexation, component activities, hydrotropy or other solution interactions may need to be considered to obtain a more accurate prediction.[4,95] Other cocrystals reported to have a $[coformer]_{eu}$ in this range are CBZ-NCT and CBZ-GTA, both of which are under predicted by solubility models due to non-ideal behaviors. Drug solubility may be affected at high coformer concentrations, which can be identified by the eutectic measurement when $[drug]_{eu}>S_{drug}$. This may also occur due to supersaturation generated when approaching the eutectic point from cocrystal dissolution and drug precipitation. Approaching the eutectic from cocrystal precipitation and drug dissolution should avoid generating supersaturation with respect to drug. According to Table 3.3, the $[drug]_{eu} >S_{drug}$ at the eutectic point measurements for both of the SAC cocrystals which may contribute to the difference between the predicted and the experimental $S_{cocrystal}$.

The micellar solubilization constants, K_s values, were needed in order to predict the cocrystal solubilities in FeSSIF. The K_s values, were calculated from the measured component solubilities in FeSSIF and buffer, which are plotted in Figure 3.3. The coformer solubilities were not statistically different in FeSSIF compared to buffer

($p<0.05$) and therefore $K_s=0$ for SAC, SLC and 4-ABA in FeSSIF. The hydrophobic drugs were solubilized by the mixed micelles in FeSSIF while the hydrophilic coformers were not. Similar behavior has been reported for CBZ cocrystal components in solutions of SLS.[15-17,47]

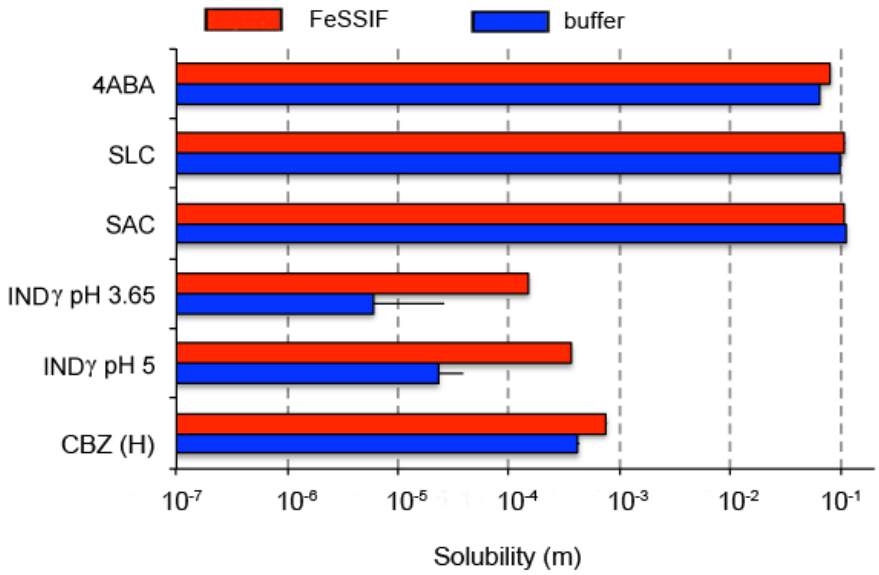

Figure 3.3. Component solubilities in FeSSIF, buffer at 25 °C. The final pH of the coformer solubility measurement was lower than the initial pH 5 of FeSSIF: 4-ABA (4.6±0.1), SLC (3.7±0.1), and SAC (2.60±0.01). The final pH of the drug solubility measurements were 5.

The solubility enhancement of CBZ (H) and IND γ in FeSSIF relative to buffer due to micellar solubilization was quantified based on reported mathematical models.[16] The micellar solubilization of a nonionizable drug like CBZ (H) is described by the following equilibria and equilibrium constant:

$$R_{solid} \overset{S_{R,aq}}{\longleftrightarrow} R_{aq} \tag{3.10}$$

$$R_{aq}+M \overset{K_S}{\leftrightarrow} R_m \tag{3.11}$$

$$K_s^R=\frac{[R]_m}{[R]_{aq}[M]} \tag{3.12}$$

The drug solubility in FeSSIF is described by

$$S_R = S_{R,aq}(1+K_s^R[M]) \quad (3.13)$$

The K_s of CBZ (H) is assumed to be pH independent as CBZ (H) is nonionizable. The solubility of a monoprotic acidic drug in an aqueous surfactant solution is affected by the following equilibria and equilibrium constants.[86,87]

$$HD \leftrightarrow H^+_{aq} + D^-_{aq} \quad (3.14)$$

$$K_a^{HD} = \frac{[H^+][D\text{-}]}{[HD]} \quad (3.15)$$

$$HD_{aq} + M \leftrightarrow HD_m \quad (3.16)$$

$$K_s^{HA} = \frac{[HD]_m}{[HD]_{aq}[M]} \quad (3.17)$$

$$D^-_{aq} + M \leftrightarrow A^-_m \quad (3.18)$$

$$K_s^{D-} = \frac{[D^-]_m}{[D^-]_{aq}[M]} \quad (3.19)$$

The ionization and micellar contributions to the monoprotic acidic drug solubility in a surfactant solution is thus described by[87]

$$S_T^{HD} = S_{aq}^{HD}\left(1 + \frac{K_a^{HD}}{[H^+]} + \left(K_s^{HD} + \frac{K_a^{HD}}{[H^+]}K_s^{D-}\right)[M]\right) \quad (3.20)$$

$$K_s^{HDT} = K_s^{HD} + \frac{K_a^{HD}}{[H^+]}K_s^{D-} \quad (3.21)$$

The total micellar solubilization constant of IND, K_s^{HDT}, exhibits a pH dependence when K_s^{D-} is not zero according to equation (3.20). In this study, the K_s^{HDT} of IND was quantified from the drug solubility in FeSSIF and buffer, at pH 5, and at the equilibrium pH observed at the eutectic, as shown in Table 3.6. K_s^{HDT} can be determined at a given $[H^+]$, without solving for the individual K_s^{HD} and K_s^{D-}. When the total solubility (S_T^{HD}) unionized solubility (S_{aq}^{HD}), K_a, [M] and $[H^+]$ are known, the K_s^{HDT} can be solved according to

$$K_s^{HD,T} = \frac{\frac{S_T^{HD}}{S_{aq}^{HA}} - 1 - \frac{K_a^{HD}}{[H^+]}}{[M]} \quad (3.22)$$

Equation (3.22) was obtained by substituting equation (3.21) into equation (3.20) and solving for K_s^{HDT}.

The cocrystal component solubilities shown in Table 3.6 were used to calculate the K_s for each component. K_s values of CBZ (H) and IND γ were calculated using equation (3.13) and (3.22) respectively. While the coformers in this study were not solubilized by the components of FeSSIF and K_s=0, this may not always be the case. The appendix outlines the equations necessary to calculate the K_s of acidic, and amphoteric

Table 3.6. Cocrystal component solubilities and pK_a values used to calculated K_s.

Component	S_{FeSSIF} (mM) Final pH	S_{buffer} (m) Final pH	pKa	K_s (m^{-1}) [a]
CBZ(H)	0.75±0.02) 4.86±0.05	(4.20±0.2) x10^{-4} 4.95±0.01	---	53 ± 5b
IND γ	0.37±0.02 4.97±0.06	(2.3±0.1) x10^{-5} 4.96±0.03	4.2[b]	6700 ± 600[c]
IND γ	0.15± 0.02 3.65±0.05	(6.0± 0.3) x10^{-6} 3.66±0.02		3300 ±300[c]
SAC	105.3±0.5 2.60±0.02	110±1 2.58±0.02	1.6[b]	0[d]
SLC	108.2±0.9 3.78±0.03	97±1 3.58±0.06	3.0[b]	0[d]
4-ABA	80.0±0.9 4.72±0.02	64.4±0.8 4.57±0.04	2.6,4.8[b]	0[d]

(a) K_s^R was evaluated according to equation (3.13) for CBZ, where S_R,aq is the solubility in buffer and $K_s^{HD,T}$ according to equation (3.19) for IND where S_{aq}^{HD} is the reported unionized solubility (2.85x10^{-6} m).[18,48]
(b) References for pKa values:
(c) Statistically significant difference in solubilities in FeSSIF compared to buffer, $p < 0.05$
(d) Statistically insignificant difference in solubilities in FeSSIF compared to buffer, $p > 0.05$

coformers for the interested reader. The measured K_s of CBZ (H) in FeSSIF is 9.8 times lower than in SLS.[15,16] The K_s^{HDT} for IND was evaluated at pH 5 as well as pH 3.65 (pH of eutectic measurement) to examine whether the solubilization was pH-dependent. Under both pH conditions IND has a much higher K_s than CBZ(H) because it is solubilized to a greater extent by NaTC and lecithin micelles. As shown in Table 3.6, The K_s^{HDT} (pH 5) >K_s^{HDT} (pH 3.65), therefore the micellar solubilization of IND by NaTC and lecithin is pH-dependent.

Relationship between the eutectic constant, K_{eu}, and $S_{cocrystal}/S_{drug}$

The eutectic constant, K_{eu}, is a parameter that can be evaluated directly from the measured cocrystal component concentrations at the eutectic point for a 1:1 cocrystal and a 2:1 cocrystal according to

$$K_{eu}=\frac{[\text{coformer}]_{eu}}{[\text{drug}]_{eu}} \tag{3.23}$$

We have shown in previous publications that the eutectic constant is a function of $S_{cocrystal}/S_{drug}$.[95] For a cocrystal A_yB_z, composed of drug A and coformer B, with y and z indicating the stoichiometry, the general equation relating K_{eu} to $S_{cocrystal}/S_{drug}$ is

$$K_{eu}=zy^{y/z}\left(\frac{S_{cocrystal}}{S_{drug}}\right)^{\frac{(y+z)}{z}} \tag{3.24}$$

Thus for a 1:1 cocrystal AB

$$K_{eu}=\left(\frac{S_{cocrystal}}{S_{drug}}\right)^{2} \tag{3.25}$$

The K_{eu} values of the 1:1 cocrystals are plotted against the predicted $S_{cocrystal}/S_{drug}$. $S_{cocrystal}/S_{drug}$ can be calculated from

$$\left(\frac{S_{cocrystal}}{S_{drug}}\right)^{RHA}=\frac{\sqrt{K_{sp}^{RHA}\left(1+K_s^R[M]\right)\left(1+\frac{K_a^{HA}}{[H^+]}+K_s^{HAT}[M]\right)}}{S_{R,aq}\left(1+K_s^R[M]\right)} \tag{3.26}$$

for a 1:1 cocrystal RHA, such as CBZ-SAC and CBZ-SLC. The $S_{cocrystal}/S_{drug}$ of a 1:1 cocrystal HDHA is

$$\left(\frac{S_{cocrystal}}{S_{drug}}\right)^{HDHA}=\frac{\sqrt{K_{sp}^{HDHA}\left(1+\frac{K_a^{HD}}{[H^+]}+K_s^{HDT}[M]\right)\left(1+\frac{K_a^{HA}}{[H^+]}+K_s^{HAT}[M]\right)}}{S_{HA,aq}\left(1+\frac{K_a^{HD}}{[H^+]}+K_s^{HDT}[M]\right)} \tag{3.27}$$

which applies to the IND-SAC cocrystal and the $S_{cocrystal}/S_{drug}$ for the 2:1 cocrystal R_2HAB is

$$\left(\frac{S_{cocrystal}}{S_{drug}}\right)^{R_2HAB}=\frac{2x\sqrt[3]{\frac{K_{sp}^{R_2HAB}}{4}\left(1+K_s^R[M]\right)^2\left(1+\frac{K_a^{-AB}}{[H^+]}+\frac{[H^+]}{K_a^{HABH^+}}\right)}}{S_{R,aq}\left(1+K_s^R[M]\right)} \tag{3.28}$$

which applies to CBZ-4ABA (H).

Figure 3.4 shows the observed K_{eu} for the 1:1 cocrystals studied, plotted against $S_{cocrystal}/S_{drug}$. K_{eu} is calculated from the eutectic concentrations according to equation (3.23), and $S_{cocrystal}/S_{drug}$ is calculated from equation (3.26) for a 1:1 RHA cocrystal and (3.27) for a 1:1 HDHA cocrystal. The slope of the linear regression of $S_{cocrystal}/S_{drug}$ versus K_{eu} on a log-log plot is 2, which confirms equation (3.25) and that the experimental component concentrations at the eutectic can be used to characterize the cocrystal solubility advantage ($S_{cocrystal}/S_{drug}$) in a given media.

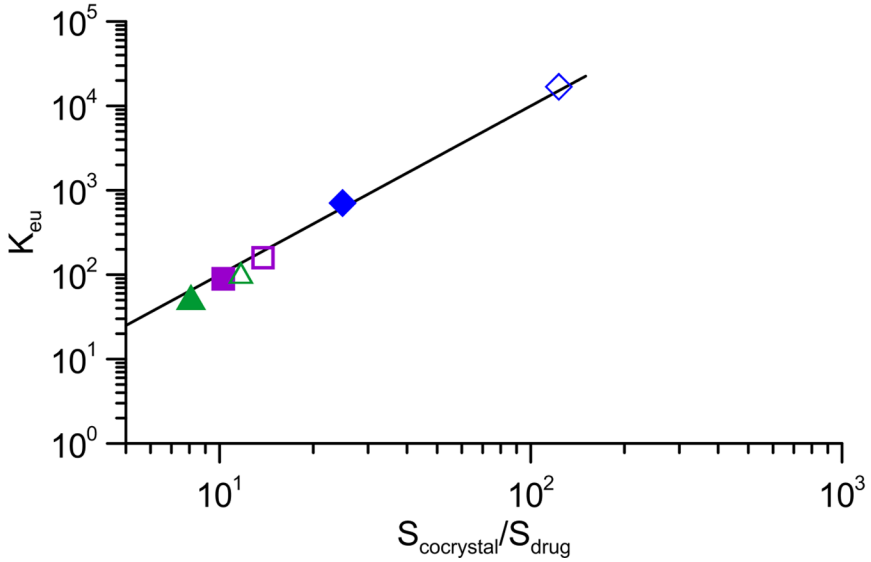

Figure 3.4. K_{eu} dependence on $S_{cocrystal}/S_{drug}$ for IND-SAC (◆), CBZ-SAC (■), and CBZ-SLC (▲)in buffer (open symbols) and FeSSIF (closed symbols). $S_{cocrystal}/S_{drug}$ is calculated at the eutectic pH shown in Table 3.3. The line corresponds to $K_{eu}=(S_{cocrystal}/S_{drug})^2$. Errors associated with measured solubilities range from 1-6% of the measured value.

The relationship between the eutectic constant and $S_{cocrystal}/S_{drug}$ for a 2:1 cocrystal is

$$K_{eu}=4\left(\frac{S_{cocrystal}}{S_{drug}}\right)^3 \qquad (3.29)$$

The $S_{cocrystal}/S_{drug}$ is calculated from solubility in molarity where moles are expressed in terms of drug moles. As shown in Table 3.7, the eutectic constant, K_{eu}, is useful to determine $S_{cocrystal}/S_{drug}$ directly from the cocrystal component concentrations in equilibrium with the eutectic point using equation (3.25) for a 1:1 cocrystal and equation (3.29) for a 2:1 cocrystal.

Table 3.7. K_{eu} and $S_{cocrystal}/S_{drug}$ from measured eutectic point compared to predicted $S_{cocrystal}/S_{drug}$ at the eutectic pH

Media	Cocrystal (stoichiometry)	K_{eu}[a]	$\frac{S_{cocrystal}}{S_{drug}} = f(K_{eu})$	$\frac{S_{cocrystal}}{S_{drug}}$[c]	pH
buffer	IND-SAC (1:1)	(1.7±0.1)x10^4	132 ± 4	123.2	3.66±0.02
FeSSIF		710±80	24 ± 1	24.9	3.65±0.05
buffer	CBZ-SAC (1:1)	160±10	12.6 ± 0.4	13.8	3.08±0.03
FeSSIF		90 ±2	9.5±0.1	10.3	3.11±0.02
buffer	CBZ-SLC (1:1)	97±5	9.9±0.2	11.7	4.29±0.02
FeSSIF		55 ± 1	7.4±0.1	8.1	4.37±0.02
buffer	CBZ-4ABA (H) (2:1)	21	3.5	3.5	4.94±0.02
FeSSIF		29	3.9	4.1	4.84±0.03

(a) Calculated from eutectic concentrations in Table 3.3 according to equation (3.23).

(b) Calculated from Keu according to $\frac{S_{cocrystal}}{S_{drug}} = \sqrt[2]{K_{eu}}$ for a 1:1 cocrystal and to $\frac{S_{cocrystal}}{S_{drug}} = 2\left(\frac{K_{eu}}{4}\right)^{(\frac{1}{3})}$ for a 2:1 cocrystal.

(c) Calculated using K_{sp} values from Table 3.2, pKa 4ABA: 2.6, 4.8,[105] and K_s^R in Table 3.6 according to equation (3.28).

The drug and cocrystal solubility are equal at the critical stabilization concentration, CSC, of a given surfactant; an equation for CSC can be obtained by setting the equations for drug and cocrystal solubility equal and solving for the concentration [M]. The CSC equations in Table 3.8 were used to determine the concentration of NaTC and lecithin required to thermodynamically stabilize the cocrystals studied. According to Table 3.8, none of the cocrystals studied achieve a CSC in a 4:1 NaTC and lecithin mixed micelle solution. The K_s values observed for CBZ and IND are not high enough to allow for the thermodynamic stabilization of the cocrystal relative to the drug. However, the preferential solubilization of IND γ was found to lower the $S_{cocrystal}/S_{drug}$ of the IND-SAC cocrystal (Table 3.3).

Table 3.8. CSC values estimated from cocrystal K_{sp}, component K_a and drug K_s

Cocrystal	CSC	Equation	NaTC (mM) [a]	Lecithin (mM) [b]
CBZ-SAC	$CSC=\frac{\frac{K_{sp}}{(S_{R,aq})^2}\left(1+\frac{K_a^{HA}}{[H^+]}\right)}{\left(K_s^R\right)}+CMC$	(3.30)	35.7	8.9
CBZ-SLC		(3.31)	24.7	6.2
IND-SAC	$CSC=\frac{\frac{Ksp}{(HD_{aq})^2}\left(1+\frac{K_a^{HA}}{[H^+]}\right)-\left(1+\frac{K_a^{HD}}{[H^+]}\right)}{\left(K_s^{HD,T}\right)}+CMC$	(3.32)	28.9	7.2
CBZ-4ABA (H)	$CSC=\frac{\frac{2K_{sp}}{(S_{R,aq})^3}\left(1+\frac{K_a^{-AB}}{[H^+]}+\frac{[H^+]}{K_a^{HABH^+}}\right)-1}{\left(K_s^R\right)}+CMC$	(3.33)	14.6	3.7

(a) Calculated from the K_{sp} and K_a values in Table 3.2,the drug K_s values in Table 3.6 at the eutectic pH shown in Table 3.3.

(b) The lecithin required to achieve CSC is equal ¼ of the NaTC CSC to maintain a 4 to 1 ratio of NaTC to lecithin.

$S_{cocrystal}$ and $S_{cocrystal}/S_{drug}$ as indicators of relative drug concentration and supersaturation

Figure 3.5 shows the solubilities of cocrystal and drug at pH 5 in FeSSIF and buffer. The drug solubilities are the measured values in FeSSIF and buffer while the cocrystal solubilities had to be calculated from equations (3.7), (3.8), and (3.9). According to these results, cocrystals are more soluble than the parent drug in both FeSSIF and buffer at pH 5. The cocrystals are also predicted to have a higher solubility in FeSSIF than in buffer at pH 5. The S_{FeSSIF}/S_{buffer} ratio of IND (16) is the highest followed by IND-SAC (3.8).

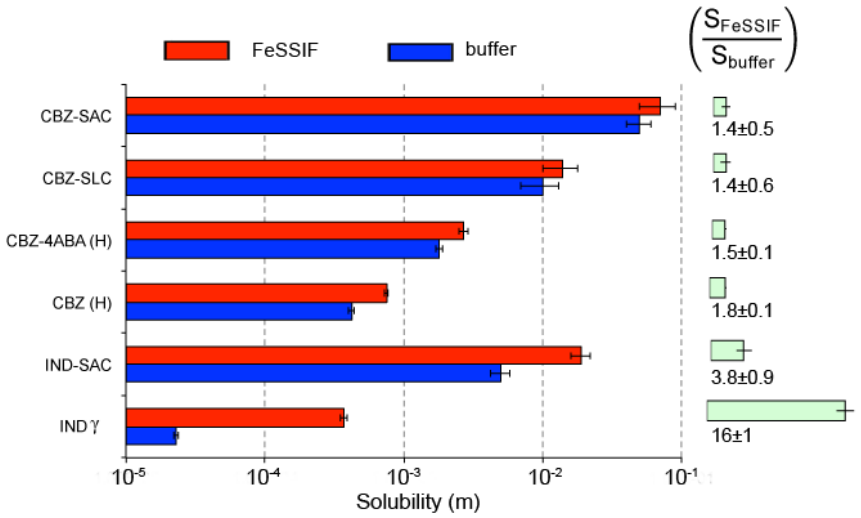

Figure 3.5. Comparison of drug and cocrystal solubility in FeSSIF and buffer at pH 5. Cocrystal solubility was predicted using the K_{sp} and pKa values in Table 3.2 and K_s values in Table 3.6 and the equations presented in Table 3.4. Drug solubilities plotted are from Table 3.1.

Table 3.9 shows the calculated values of $S_{cocrystal}$ in FeSSIF and in buffer at pH 5; this could not be experimentally determined because all of the cocrystals studied equilibrated to a lower pH during the eutectic point measurement, except CBZ-4ABA (H). The cocrystal solubility at pH 5 is useful to anticipate the upper limit of the drug concentrations the cocrystal could achieve during dissolution when there is no excess coformer and no solution-mediated transformation. For example, IND-SAC could achieve a solution concentration of 19 mM in FeSSIF, and a solution concentration of 5 mM in buffer if the cocrystal does not transform to the lower solubility drug.

Table 3.9. Cocrystal solubility in FeSSIF and buffer at pH 5

Cocrystal	$S_{cocrystal}$ (mM) FeSSIF[a]	S_{drug} (mM) FeSSIF[b]	$\left(\frac{S_{cocrystal}}{S_{drug}}\right)_{FeSSIF}$	$S_{cocrystal}$ (mM) buffer[a]	S_{drug}(mM) buffer[b]	$\left(\frac{S_{cocrystal}}{S_{drug}}\right)_{buffer}$
IND-SAC	19±3	0.37±0.02	53 ± 7	5.0±0.8	0.023±0.001	220 ± 40
CBZ-SAC	70±20	0.75±0.02	90 ± 20	50±10	0.42±0.02	120 ± 30
CBZ-SLC	14±4		19 ± 5	11±3		25 ± 6
CBZ-4ABA (H)	2.7±0.2		3.6 ± 0.25	1.8±0.1		4.4 ± 0.3

(a) Calculated using the K_{sp} values in Table 3.2, K_s values in Table 3.6 and the following pKa values: SAC 1.6,[89] IND 4.2,[48] SLC 3.0,[103,104] and 4-ABA 2.6 and 4.8.[105] using equations (3.7) to (3.9).
(b) Taken from Table 3.1.

Even though cocrystals have higher solubilities in FeSSIF, the difference between the cocrystal and drug solubility ($S_{cocrystal}/S_{drug}$) is higher in buffer. The driving force for

transformation depends on the drug supersaturation generated during cocrystal dissolution. The higher the cocrystal solubility is relative to the drug in a given media, the greater the driving force for transformation. $S_{cocrystal}/S_{drug}$ was used to quantify the potential supersaturation that could be generated for each cocrystal in FeSSIF and buffer at pH 5 if the cocrystal did not undergo solution-mediated transformation and is shown in Table 3.9. Equations (3.26) to (3.28) were used to calculate $S_{cocrystal}/S_{drug}$ at pH 5 in FeSSIF and buffer. The IND-SAC cocrystal is predicted to be 220 times more soluble than IND in buffer and only 53 times more soluble than IND in FeSSIF at pH 5. Thus IND-SAC exhibits a considerably lower $S_{cocrystal}/S_{drug}$ in FeSSIF relative to buffer. The $S_{cocrystal}/S_{drug}$ of the CBZ cocrystals were not significantly different in FeSSIF relative to buffer ($p<0.05$).

The greater the solubilization of the drug by a given surfactant (higher K_s) relative to the coformer, the larger the decrease in $S_{cocrystal}/S_{drug}$ in a surfactant solution compared to blank media.[108] The $S_{cocrystal}/S_{drug}$ is lower in FeSSIF relative to buffer because the cocrystal solubility has a weaker dependency on the concentration of NaTC and lecithin than the parent drug. We have shown in previous work that preferential micellar solubilization of the drug by the synthetic surfactant SLS decreases the $S_{cocrystal}/S_{drug}$. Similar to SLS, preferential micellar solubilization of IND by NaTC and lecithin reduces $S_{cocrystal}/S_{drug}$. We show for the first time that preferential micellar solubilization of IND by mixed micelles of NaTC and lecithin results in an increase in cocrystal solubility and a decrease in $S_{cocrystal}/S_{drug}$ compared to buffer.

The $S_{cocrystal}$ and $S_{cocrystal}/S_{drug}$ have important implications on the concentration and supersaturation achieved and the kinetics of transformation during dissolution. $S_{cocrystal}$ indicates the maximum concentration that can be achieved in a given media while $S_{cocrystal}/S_{drug}$ indicates the maximum supersaturation that can be achieved in a given media and may be useful to assess the relative driving forces for transformation between a variety of media. The powder dissolution of IND-SAC was performed in FeSSIF and buffer to evaluate the transformation kinetics and supersaturation generated relative to drug. This behavior was compared to the measured $S_{cocrystal}$ and $S_{cocrystal}/S_{drug}$. Dissolution studies were not pursued for the CBZ cocrystals because there was not a significant difference in $S_{cocrystal}/S_{drug}$ in FeSSIF compared to buffer ($P<0.05$). The driving force for

transformation and the supersaturation achieved is predicted to be lower in FeSSIF relative to buffer because $S_{cocrystal}/S_{drug}$ is lower in FeSSIF relative to buffer. The solution concentrations achieved during dissolution are predicted to be the highest in FeSSIF as $S_{cocrystal}$ is the highest in FeSSIF. Overall, IND-SAC is expected to achieve higher solution concentrations for a longer period of time in FeSSIF relative to buffer based on $S_{cocrystal}$ and $S_{cocrystal}/S_{drug}$.

As predicted, IND-SAC achieves and maintains higher drug solution concentrations in FeSSIF relative to the buffer as shown in Figure 3.6a. IND-SAC reaches a peak concentration of 0.36 mM at 10 minutes in buffer. This concentration is 15 times higher than the equilibrium IND solubility in buffer (Figure 3.1). The drug solution concentrations decrease thereafter, indicating that a solution-mediated transformation is occurring. The final solid phase at 4 hours was a mixed phase containing both IND-SAC and IND γ form as determined by XRPD analysis. SAC concentrations during cocrystal dissolution in buffer increased with time and lowered the bulk pH from pH 5 to 4.7.

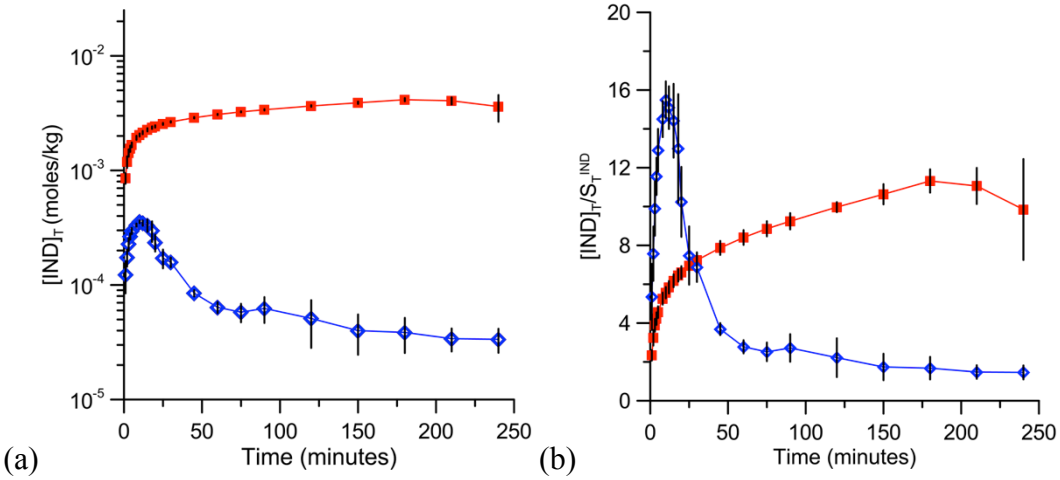

Figure 3.6. IND-SAC dissolution in FeSSIF (■) and buffer (●) 25 °C. (a) Concentration-time profile of $[IND]_T$ (b) Supersaturation generated by IND-SAC ($[IND]_T/S_T^{IND}$). Courtesy of Maya Lipert, University of Michigan.

IND-SAC dissolution in FeSSIF reached IND concentrations of 2.00 mM at 10 minutes and continued to increase to 4.14 mM at 3 hours (Figure 3.6). This concentration is lower than the predicted cocrystal solubility in FeSSIF (19±3 mM, pH 5). No excess SAC was observed to dissolve from the cocrystal, thus the bulk pH during dissolution in FeSSIF remained unchanged. IND-SAC generates concentrations that are 5.8 to 11 times

higher than the IND solubility in FeSSIF (Figure 3.6b). The final solid phase at 4 hours was IND-SAC cocrystal. The IND-SAC cocrystal achieved higher solution concentrations in FeSSIF than in buffer, which is in agreement with the equilibrium solubility measurements and the predicted solubility shown in Table 3.9. The supersaturation increased slowly over 3 hours. The lower supersaturation achieved in FeSSIF relative to buffer indicates that the driving force for transformation was indeed lower in FeSSIF as predicted by $S_{cocrystal}/S_{drug}$. As hypothesized, the lower $S_{cocrystal}/S_{drug}$ of IND-SAC in FeSSIF correlates with a lower supersaturation and a decrease in the driving force for solution-mediated transformation.

Previous reports of IND-SAC dissolution at pH 7.4 achieved a supersaturation of 3-4, with the higher supersaturation occurring in media containing a higher buffer concentration (60 vs. 200 mM phosphate buffer).[1] A supersaturation of 14 (pH 2)[96] and 12 (pH 7)[97] have been observed during the dissolution of the amorphous form of IND. The supersaturation generated by the amorphous form was hindered due to solution-mediated transformation, which was reported to occur between 10-20 minutes at pH 7.[97] The IND-SAC cocrystal generates supersaturation similar to that of the amorphous form. Due to the solution chemistry of the multicomponent solid, it is possible to optimize the transformation kinetics of IND-SAC using the mechanism of preferential micellar solubilization of the drug component.

Because cocrystal solubility and $S_{cocrystal}/S_{drug}$ governs cocrystal dissolution behavior, using mathematical models that predict these parameters under a wide variety of solution conditions is essential to design meaningful dissolution studies. These mathematical models are useful to confirm mechanisms that may modulate cocrystal solution chemistry *in vivo*. For example, if a cocrystal has improved dissolution and solubility in FeSSIF, will dosing a cocrystal in the fed state lead to superior performance relative to the fasted state?

In vivo performance of high solubility cocrystals can potentially be hindered if the cocrystal under goes solution-mediated transformation to a less soluble form before it can be absorbed. The propensity of a cocrystal to transform among different media can be indicated by the magnitude of $S_{cocrystal}/S_{drug}$. Additives that differentially modify the cocrystal component solubilities can be used to optimize $S_{cocrystal}/S_{drug,}$ which will affect

the transformation kinetics as well. Identifying other cocrystals that exhibit a lower $S_{cocrystal}/S_{drug}$ in FeSSIF compared to buffer may be useful to guide *in vivo* studies.

Conclusions

Cocrystals exhibit a weaker solubility dependence on micellar concentrations of solutions of NaTC and lecithin. This behavior is in agreement with the reported cocrystal solubility dependence on the synthetic surfactant SLS. Similar to SLS, mixed micelles of lecithin and NaTC preferentially solubilize the parent drug resulting in an increase in cocrystal solubility and a decrease in $S_{cocrystal}/S_{drug}$ relative to buffer. Knowledge of the component ionization and drug micellar solubilization in FeSSIF was useful to predict cocrystal solubility and determine the ionization and micellar solubilization contributions to solubility.

The reported mathematical models describing cocrystal solubility dependence on ionization and micellar solubilization were useful to identify IND-SAC as a cocrystal that exhibits a lower $S_{cocrystal}/S_{drug}$ in FeSSIF relative to buffer due to preferential micellar solubilization of the drug. The cocrystal solubility measurements confirmed IND-SAC has a lower $S_{cocrystal}/S_{drug}$ in FeSSIF relative to buffer. IND-SAC undergoes solution-mediated transformation to the parent drug in buffer after 10 minutes. As predicted by the lower $S_{cocrystal}/S_{drug}$ and the higher $S_{cocrystal}$ in FeSSIF relative to buffer, IND-SAC achieved higher solution concentrations of drug and was protected against solution-mediated transformation for 4 hours in FeSSIF. Solubility studies often require less material than dissolution studies and are useful to indicate which cocrystals may have improved transformation kinetics in FeSSIF versus buffer. The presented equations can be applied to a variety of biorelevant media, with K_s specific to each media and pH condition.

Appendix

The derivations of the equations from Table 3.4 in the manuscript are presented in this appendix. These derivations consider the component ionization and drug micellar solubilization contributions to cocrystal solubility in biorelevant media. Activity contributions, solution complexation and aggregation are not considered. All equilibria and concentrations without subscripts refer to the solution phase.

1:1 cocrystal with nonionizable drug and acidic coformer.

Cocrystal dissociation

$$RHA_{solid} \leftrightarrow R_{aq}+HA_{aq}$$

$$K_{sp}=[R][HA] \quad (A1)$$

Coformer ionization

$$HA \leftrightarrow H^{+}_{aq}+A^{-}_{aq}$$

$$K_a^{HA}=\frac{[H^+][A-]}{[HA]} \quad (A2)$$

Drug micellar solubilization

$$R_{aq}+M \leftrightarrow R_m$$

$$K_s^R=\frac{[R]_m}{[R]_{aq}[M]} \quad (A3)$$

the total drug in the micellar solution is then:

$$S_R=[R]_T=[R]_{aq}+[R]_m \quad (A4)$$

substituting equation (A3) into (A4) the solubility dependence on micellar solubilization for a nonionizable drug becomes

$$S_R=[R]_{aq}\left(1+K_s^R[M]\right) \quad (A5)$$

Coformer micellar solubilization

$$HA_{aq}+M \leftrightarrow HA_m$$

$$K_s^{HA}=\frac{[HA]_m}{[HA]_{aq}[M]} \quad (A6)$$

$$A^-_{aq}+M \leftrightarrow A^-_m$$

$$K_s^{A-}=\frac{[A^-]_m}{[A]_{aq}[M]} \quad (A7)$$

the total coformer in the micellar solution is then:

$$S_{HA}=[HA]_T=[HA]_{aq}+[A^-]_{aq}+[HA]_m+[A^-]_m \quad (A8)$$

Substituting equation (A2), (A6), (A7), into equation (A8) the solubility dependence on micellar solubilization for an acidic coformer becomes

$$S_{HA}=[HA]_{aq}\left(1+\frac{K_a^{HA}}{[H^+]}+K_s^{HA}[M]+\frac{K_a^{HA}}{[H^+]}K_s^{A^-}[M]\right) \quad (A9)$$

The total solubilization of the acidic coformer ($K_s^{HA,T}$) is described as

$$K_s^{HA,T}=K_s^{HA}+\frac{K_a^{HA}}{[H^+]}K_s^{A^-} \quad (A10)$$

Substituting equation (A10) into equation (A9) resulting in the final expression for coformer solubility in biorelevant media

$$S_T^{HA}=[HA]_{aq}\left(1+\frac{K_a^{HA}}{[H^+]}+K_s^{HA,T}[M]\right) \quad (A11)$$

The $K_s^{HA,T}$ can be calculated from a solubility measurement in a micellar solution (S_T^{HA}) and a solubility measurement in an aqueous solution in the absence of micellar components when K_a^{HA} is known using equation (A11).

Mass balance of cocrystal components

$$S_T^{RHA}=[R]_{aq}+[R]_m$$

$$=[HA]_{aq}+[A^-]_{aq}+[HA]_m+[A^-]_m \quad (A12)$$

Inserting equations (A1)-(A3), (A6) and (A7)into equation (A12), the cocrystal solubility dependence on micellar solubilization described for a 1:1 cocrystal RHA is

$$S_T^{RHA}=\sqrt{K_{sp}^{RHA}\left(1+K_s^R[M]\right)\left(1+\frac{K_a^{HA}}{[H^+]}+K_s^{HA,T}[M]\right)} \quad (A13)$$

2:1 cocrystal with nonionizable drug and amphoteric coformer:

Cocrystal dissociation:

$$R_2HAB \overset{Ksp}{\leftrightarrow} R_{aq}+HAB_{aq}$$

$$K_{sp}=[R]^2[HAB] \quad (A14)$$

Coformer Ionization:

$$HAB \leftrightarrow {}^-AB_{aq}+H^+$$

$$K_{a1}^{-AB}=\frac{[H^+][{}^-AB]}{[HAB]} \quad (A15)$$

$$HABH^+ \leftrightarrow HAB_{aq}+H^+$$

$$K_{a2}^{HAB}=\frac{[H^+][HAB]}{[HABH^+]} \quad (A16)$$

Micellar solubilization of the drug:

$$R_{aq}+M \leftrightarrow R_m$$

$$K_s^R=\frac{[R]_m}{[R]_{aq}[M]} \quad (A17)$$

Micellar solubilization of the coformer

$$HABH_{aq}^+ + M \leftrightarrow HABH_m^+$$

$$K_s^{HABH^+}=\frac{[HABH^+]_m}{[HABH^+]_{aq}[M]} \quad (A18)$$

$$HAB_{aq}+M \leftrightarrow HA_m$$

$$K_s^{HAB}=\frac{[HAB]_m}{[HAB]_{aq}[M]} \quad (A19)$$

$$^-AB_{aq}+M \leftrightarrow {}^-AB_m$$

$$K_s^{^-AB}=\frac{[^-AB]_m}{[^-AB]_{aq}[M]} \quad (A20)$$

the total coformer in the micellar solution is then:

$$S_T^{HAB} = [HAB]_{aq}+[^-AB]_{aq}+[HABH^+]_{aq} + [HAB]_m+[^-AB]_m+[HABH^+]_m \quad (A21)$$

Substituting equations(A15), (A16), and (A18)-(A20) into equation (A21) results in the final expression for coformer solubility in biorelevant media

$$S_T^{HAB}=[HAB]_{aq}\left(1+\frac{K_a^{^-AB}}{[H^+]}+\frac{[H^+]}{K_a^{HABH^+}}+[M]\left(K_s^{HAB}+\frac{K_a^{^-AB}}{[H^+]}K_s^{^-AB}+\frac{[H^+]}{K_a^{HABH^+}}K_s^{HABH^+}\right)\right) \quad (A22)$$

The total solubilization of the amphoteric coformer ($K_s^{HAB,T}$) is described as

$$K_s^{HAB,T} = K_s^{HAB}+\frac{K_a^{^-AB}}{[H^+]}K_s^{^-AB}+\frac{[H^+]}{K_a^{HABH^+}}K_s^{HABH^+} \quad (A23)$$

Substituting equation (A23) into equation (A22) results in the final expression for coformer solubility in biorelevant media

$$S_T^{HAB}=[HAB]_{aq}\left(1+\frac{K_a^{-AB}}{[H^+]}+\frac{[H^+]}{K_a^{HABH^+}}+K_s^{HAB,T}[M]\right) \quad (A24)$$

The $K_s^{HAB,T}$ can be calculated from a solubility measurement in a micellar solution (S_T^{HAB}) and a solubility measurement in an aqueous solution in the absence of micellar components when K_a^{-AB} and K_a^{HABH+} is known using equation (A24).

Mass balance of cocrystal components

$$S_T^{R_2HAB}=[R]_{aq}+[R]_m$$

$$=[HAB]_{aq}+[^-AB]_{aq}+[HABH^+]_{aq}+[HAB]_m+[^-AB]_m+[HABH^+]_m \quad (A25)$$

For a 2:1 $S_T^{cocrystal}=[A]_T=1/2[R]_T$ and inserting equations (A14)-(A20)into equation (A25), the cocrystal solubility dependence on micellar solubilization and ionization for a 2:1 cocrystal R_2HAB is

$$S_T^{R_2HAB}=\sqrt[3]{\frac{K_{sp}^{R_2HAB}}{4}\left(1+K_s^R[M]\right)^2\left(1+\frac{K_a^{-AB}}{[H^+]}+\frac{[H^+]}{K_a^{HABH^+}}+K_s^{HAB,T}[M]\right)} \quad (A26)$$

1:1 cocrystal with acidic drug (HD) and acidic coformer (HA).

Cocrystal dissociation:

$$HDHA \overset{Ksp}{\leftrightarrow} HD_{aq}+HA_{aq}$$

$$K_{sp}=[HD][HA] \quad (A27)$$

The micellar solubilization and ionization of an acidic drug is described by the following equilibria:

$$HD \leftrightarrow H_{aq}^+ + D_{aq}^-$$

$$K_a^{HD}=\frac{[H^+][D-]}{[HD]} \quad (A28)$$

$$HD_{aq}+M \leftrightarrow HD_m$$

$$K_s^{HD}=\frac{[HD]_m}{[HD]_{aq}[M]} \quad (A29)$$

$D^-_{aq}+M \leftrightarrow D^-_m$

$$K_s^{D-}=\frac{[D^-]_m}{[D^-]_{aq}[M]} \quad (A30)$$

the total drug in the micellar solution is then:

$$S_{HD}=[HD]_T=[HD]_{aq}+[D^-]_{aq}+[HD]_m+[D^-]_m \quad (A31)$$

Substituting equation (A28),(A29), and (A30) into equation (A31) the solubility dependence on micellar solubilization for an acidic drug becomes

$$S_{HD}=[HD]_{aq}\left(1+\frac{K_a^{HD}}{[H^+]}+K_s^{HD}[M]+\frac{K_a^{HD}}{[H^+]}K_s^{D-}[M]\right) \quad (A32)$$

The total solubilization of the acidic drug ($K_s^{HD,T}$) is described as

$$K_s^{HD,T}=K_s^{HD}+\frac{K_a^{HD}}{[H^+]}K_s^{D-} \quad (A33)$$

Substituting equation (A33) results in the final expression for drug solubility in biorelevant media

$$S_{HD}=[HD]\left(1+\frac{K_a^{HD}}{[H^+]}+K_s^{HD,T}[M]\right) \quad (A34)$$

where $K_s^{HD,T}$ must be defined at a given pH unless K_s^{D-} is not zero.

Mass balance:

$$S_T^{HDHA}=[HD]_{aq}+[D^-]_{aq}+[HD]_m+[D^-]_m$$

$$=[HA]_{aq}+[A^-]_{aq}+[HD]_m+[D^-]_m \quad (A35)$$

inserting equations (A2), (A28), (A29), into equation(A35) results in the equation describing cocrystal solubility for a 1:1 cocrystal HDHA

$$S_T^{HDHA}=\sqrt{K_{sp}\left(1+\frac{K_a^{HD}}{[H^+]}+K_s^{HD,T}\right)\left(1+\frac{K_a^{HA}}{[H^+]}+K_s^{HA,T}\right)} \quad (A36)$$

References

1. Basavoju S, Boström D, Velaga S 2008. Indomethacin–Saccharin Cocrystal: Design, Synthesis and Preliminary Pharmaceutical Characterization. Pharm Res 25(3):530-541.

4. Good DJ, Rodríguez-Hornedo Nr 2009. Solubility Advantage of Pharmaceutical Cocrystals. Cryst Growth Des 9(5):2252-2264.

6. Jung M-S, Kim J-S, Kim M-S, Alhalaweh A, Cho W, Hwang S-J, Velaga SP 2010. Bioavailability of indomethacin-saccharin cocrystals. Journal of Pharmacy and Pharmacology 62(11):1560-1568.

7. McNamara DP, Childs SL, Giordano J, Iarriccio A, Cassidy J, Shet MS, Mannion R, O'Donnell E, Park A 2006. Use of a glutaric acid cocrystal to improve oral bioavailability of a low solubility API. Pharm Res 23(8):1888-1897.

8. Remenar JF, Morissette SL, Peterson ML, Moulton B, MacPhee JM, Guzmán HR, Almarsson Ö 2003. Crystal Engineering of Novel Cocrystals of a Triazole Drug with 1,4-Dicarboxylic Acids. J Am Chem Soc 125(28):8456-8457.

10. Stanton MK, Kelly RC, Colletti A, Kiang YH, Langley M, Munson EJ, Peterson ML, Roberts J, Wells M 2010. Improved pharmacokinetics of AMG 517 through co-crystallization part 1: Comparison of two acids with corresponding amide co-crystals. Journal of Pharmaceutical Sciences 99(9):3769-3778.

14. Bethune SJ, Huang N, Jayasankar A, Rodriguez-Hornedo N 2009. Understanding and Predicting the Effect of Cocrystal Components and pH on Cocrystal Solubility. Cryst Growth Des 9(9):3976-3988.

15. Huang N, Rodriguez-Hornedo N 2011. Engineering cocrystal thermodynamic stability and eutectic points by micellar solubilization and ionization. Crystengcomm 13(17):5409-5422.

16. Huang N, Rodríguez-Hornedo N 2011. Engineering cocrystal solubility, stability, and pHmax by micellar solubilization. Journal of Pharmaceutical Sciences 100(12):5219-5234.

17. Huang N, Rodríguez-Hornedo Nr 2010. Effect of Micellar Solubilization on Cocrystal Solubility and Stability. Cryst Growth Des 10(5):2050-2053.

18. Alhalaweh A, Roy L, Rodríguez-Hornedo N, Velaga SP 2012. pH-Dependent Solubility of Indomethacin–Saccharin and Carbamazepine–Saccharin Cocrystals in Aqueous Media. Molecular Pharmaceutics.

19. Weyna DR, Cheney ML, Shan N, Hanna M, Zaworotko MJ, Sava V, Song S, Sanchez-Ramos JR 2012. Improving Solubility and Pharmacokinetics of Meloxicam via Multiple-Component Crystal Formation. Molecular Pharmaceutics 9(7):2094-2102.

21. Hickey MB, Peterson ML, Scoppettuolo LA, Morrisette SL, Vetter A, Guzmán H, Remenar JF, Zhang Z, Tawa MD, Haley S, Zaworotko MJ, Almarsson Ö 2007. Performance comparison of a co-crystal of carbamazepine with marketed product. European Journal of Pharmaceutics and Biopharmaceutics 67(1):112-119.

47. Huang N. 2011. Engineering Cocrystal Solubility and Stability via Ionization and Micellar Solubilization. Pharmaceutical Sciences, ed., Ann Arbor, MI: University of Michigan.

48. Mooney KG, Mintun MA, Himmelstein KJ, Stella VJ 1981. Dissolution kinetics of carboxylic acids I: Effect of pH under unbuffered conditions. Journal of Pharmaceutical Sciences 70(1):13-22.

58. Klein S 2010. The Use of Biorelevant Dissolution Media to Forecast the <i>In Vivo Performance of a Drug. The AAPS Journal 12(3):397-406.
60. Naylor LJ, Bakatselou V, Dressman JB 1993. Comparison of the mechanism of dissolution of hydrocortisone in simple and mixed micelle systems. Pharm Res 10(6):865-870.
62. Mithani SD, Bakatselou V, TenHoor CN, Dressman JB 1996. Estimation of the Increase in Solubility of Drugs as a Function of Bile Salt Concentration. Pharm Res 13(1):163-167.
64. Jantratid E, Janssen N, Reppas C, Dressman J 2008. Dissolution Media Simulating Conditions in the Proximal Human Gastrointestinal Tract: An Update. Pharm Res 25(7):1663-1676.
67. Carey M.C. SDM 1972. Micelle formation by bile salts: Physical-chemical and thermodynamic considerations. Archives of Internal Medicine 130(4):506-527.
74. Bak A, Gore A, Yanez E, Stanton M, Tufekcic S, Syed R, Akrami A, Rose M, Surapaneni S, Bostick T, King A, Neervannan S, Ostovic D, Koparkar A 2008. The co-crystal approach to improve the exposure of a water-insoluble compound: AMG 517 sorbic acid co-crystal characterization and pharmacokinetics. Journal of Pharmaceutical Sciences 97(9):3942-3956.
76. Yadav AV, Dabke AP, Shete AS 2010. Crystal engineering to improve physicochemical properties of mefloquine hydrochloride. Drug Development and Industrial Pharmacy 36(9):1036-1045.
81. Muramatsu Tea 1981. Mechanism of Indomethacin Partition Between Normal-Octanol and Water. Chemical & pharmaceutical bulletin 29(8):2330-2337.
82. Fourie L, Breytenbach JC, Du Plessis J, Goosen C, Swart H, Hadgraft J 2004. Percutaneous delivery of carbamazepine and selected N-alkyl and N-hydroxyalkyl analogues. International Journal of Pharmaceutics 279(1–2):59-66.
86. Sheng JJ, Kasim NA, Chandrasekharan R, Amidon GL 2006. Solubilization and dissolution of insoluble weak acid, ketoprofen: Effects of pH combined with surfactant. European Journal of Pharmaceutical Sciences 29(3–4):306-314.
87. Grbic S, Parojcic J, Djuric Z, Ibric S 2009. Mathematical modeling of pH-surfactant-mediated solubilization of nimesulide. Drug Development and Industrial Pharmacy 35(7):852-856.
89. Kluza RB, Newton DW 1978. pKa values of Medicinal Compounds in Pharmacy Practice. Drug Intelligence & Clinical Pharmacy 12(9):546-554.
94. Rodríguez-Hornedo N, Murphy D 2004. Surfactant-facilitated crystallization of dihydrate carbamazepine during dissolution of anhydrous polymorph. Journal of Pharmaceutical Sciences 93(2):449-460.
95. Good DJ, Rodríguez-Hornedo Nr 2010. Cocrystal Eutectic Constants and Prediction of Solubility Behavior. Cryst Growth Des 10(3):1028-1032.
96. Alonzo D, Zhang G, Zhou D, Gao Y, Taylor L 2010. Understanding the Behavior of Amorphous Pharmaceutical Systems during Dissolution. Pharm Res 27(4):608-618.
97. Hancock BC, Parks M 2000. What is the True Solubility Advantage for Amorphous Pharmaceuticals? Pharm Res 17(4):397-404.
98. Galia E, Nicolaides E, Hörter D, Löbenberg R, Reppas C, Dressman JB 1998. Evaluation of Various Dissolution Media for Predicting In Vivo Performance of Class I and II Drugs. Pharm Res 15(5):698-705.

99. Yazdanian M, Briggs K, Jankovsky C, Hawi A 2004. The "High Solubility" Definition of the Current FDA Guidance on Biopharmaceutical Classification System May Be Too Strict for Acidic Drugs. Pharm Res 21(2):293-299.
100. Bard B, Martel S, Carrupt P-A 2008. High throughput UV method for the estimation of thermodynamic solubility and the determination of the solubility in biorelevant media. European Journal of Pharmaceutical Sciences 33(3):230-240.
101. Fagerberg JH, Tsinman O, Sun N, Tsinman K, Avdeef A, Bergström CAS 2010. Dissolution Rate and Apparent Solubility of Poorly Soluble Drugs in Biorelevant Dissolution Media. Molecular Pharmaceutics 7(5):1419-1430.
102. Ottaviani G, Gosling DJ, Patissier C, Rodde S, Zhou L, Faller B 2010. What is modulating solubility in simulated intestinal fluids? European Journal of Pharmaceutical Sciences 41(3–4):452-457.
103. Geiser L, Henchoz Y, Galland A, Carrupt P-A, Veuthey J-L 2005. Determination of pKa values by capillary zone electrophoresis with a dynamic coating procedure. Journal of Separation Science 28(17):2374-2380.
104. Aydin R, Ozer, U 1997. Potentiometric and Spectroscopic Determination of Acid Dissociation Constants of Some Phenols and Salicylic Acids. Turkish Journal of Chemistry 21:428-436.
105. Robinson RA 1957. The ionization constants of p-Aminobenzoic Acid in Aqueous solution at 25°C. Australian journal of chemistry 10(2):128.
106. Patel DD, Joguparthi V, Wang Z, Anderson BD 2011. Maintenance of supersaturation I: Indomethacin crystal growth kinetic modeling using an online second-derivative ultraviolet spectroscopic method. Journal of Pharmaceutical Sciences 100(7):2623-2641.
107. Humberstone AJ, Porter CJH, Charman WN 1996. A physicochemical basis for the effect of food on the absolute oral bioavailability of halofantrine. Journal of Pharmaceutical Sciences 85(5):525-529.
108. Roy L, Rodríguez-Hornedo N. 2010. A rational Approach for Surfactant Selection to Modulate Cocrystal Solubility and Stability. AAPS Annual Meeting and Exposition, ed., New Orlean, LA: AAPS Journal.

Chapter 4

Modifying solubility-pH dependence and common-ion effect of a pharmaceutical salt via cocrystallization.

Introduction

Many pharmaceutical compounds in development fail to exhibit adequate solubility, which can negatively impact drug dissolution and bioavailability. Polymorphs, salts, cocrystals or amorphous forms of a drug may improve solubility by altering lattice energy. The solubility of a hydrophobic drug is highly influenced by the solvation energy required to dissolve the drug. Both salts and cocrystals can alter the solvation properties of the drug in addition to altering the crystal lattice. For example, cocrystals and salts have different solubility-pH dependencies than the parent drug due to their ionizable constituents.[14,18,42,43] Cocrystals of pharmaceutical salts (cocrystalline salts) provide yet another solid form modification to alter the physicochemical properties of a drug.

Mathematical models describing the solubility-pH dependence of both salts and cocrystals are well documented and reported in the literature.[14,41-44,109,110] Cocrystal and salt solubility is highly dependent on solution composition,[36,44] and both solid forms exhibit lower solubilities in solutions containing components in stoichiometric excess.[4,41,45,109] Cocrystalline salts of fluoxetine HCl are reported to alter the melting point, concentration-time profiles and dissolution rate relative to the parent salt.[79] Similar to cocrystals and salts, it is hypothesized that cocrystalline salts will alter solubility by both lattice energy and solution chemistry.[18,109,111] Through careful selection of coformers, cocrystalline salts may be useful to increase solubility relative to the free drug and parent salt.

Currently, there is no knowledge of the cocrystalline salt solubility dependence on pH, or the common-ion effect. Mathematical models that predict the cocrystalline salt solubility behavior would be useful to assess their solubility-pH dependence and common-ion effect relative to the parent salt. The majority of the reported cocrystalline salts contain only two components (drug and an acid) with the acid existing in multiple

ionization states in the crystal lattice.[12,112-115] The fluoxetine HCl cocrystalline salts are some of the few examples of cocrystalline salts that are composed of more than two components.[79] While cocrystalline salts of mefloquine HCl are reported,[76] their crystal structures have not been determined, and therefore the reported stoichiometries cannot be confirmed. The fluoxetine HCl cocrystals were chosen to evaluate the solubility behavior of cocrystalline salts because they represent a range of stoichiometries and ionization behaviors and their stoichiometries have been determined by single-crystal x-ray analysis.

In this study, mathematical models are derived that describe cocrystalline salt solubility dependence on solution pH, counter-ion and coformer. These models predict the cocrystalline salt solubility and thermodynamic stability regions from a minimal set of equilibrium solubility measurements. The presented mathematical models predict cocrystal solubility behavior in terms of experimentally accessible thermodynamic parameters such as coformer ionization constants, K_a, and cocrystalline salt solubility product, K_{sp}. The predictive power of the mathematical models was evaluated by measuring the influence of ionization and excess chloride on the solubility of cocrystalline salts for cocrystals of a chloride salt containing a hydrophobic basic salt (fluoxetine HCl) with acidic coformers. The cocrystalline salts studied include: 1:1 fluoxetine HCl benzoic acid (FH^+Cl^-BA), 2:1 fluoxetine HCl fumaric acid ($(FH^+Cl^-)_2FA$) and 2:1 fluoxetine HCl succinic acid ($(FH^+Cl^-)_2SA$). These cocrystals represent high and low solubility cocrystalline salts (relative to the parent salt) as demonstrated by powder dissolution in water.[79]

For the first time, the equilibrium solubility of metastable cocrystalline salts were measured at the eutectic point between cocrystalline salt and salt. Measured aqueous solubilities were compared to the reported apparent solubilities in water. Phase diagrams are developed from derived mathematical models and measured solubilities. These diagrams were useful to determine stability regions between the cocrystalline salt and the parent salt. The main findings from our work are that the cocrystallization of salts can be used to alter the intrinsic solubility, the solubility-pH dependence and the common-ion effect relative to the parent salt. A single solubility or eutectic point measurement in conjunction with the proposed models was shown to successfully predict the solubility-

pH dependence, the counter-ion dependence and the coformer dependence of a cocrystalline salt; this can save both time and material during solubility characterization. The outlined relationships apply to cocrystalline salts with a range of stoichiometries and coformer ionization properties.

Theoretical Considerations

Cocrystalline salt solubility dependence on pH

The aim of this work is to provide a theoretical framework to guide the solubility characterization of a cocrystalline salt by careful analysis of the solution equilibria that govern the molecular associations between the cocrystalline salt components in solution. Cocrystal and salt-solution equilibria follow solubility product behavior whereby increasing the solution concentration of one component, results in the decrease of the other. Mathematical models derived from cocrystal dissociation and component ionization describe the cocrystal solubility-pH dependence from knowledge of the solubility product and component ionization constants. Similarly, the relevant solution equilibria describing the solubility of a cocrystalline salt are the dissociation of the cocrystalline salt and ionization of the components.

The cocrystalline salt solubility of a 1:1 cocrystalline salt (salt/coformer) BH^+Cl^- HA where the chloride salt is BH^+Cl^- and the coformer is HA, a monoprotic acid, is described by the following equilibrium reactions:

$$(BH^+Cl^-)HA_{solid} \overset{Ksp}{\leftrightarrow} BH^+_{aq} + Cl^-_{aq} + HA_{aq}$$

$$K_{sp}^{1:1cc} = [BH^+][Cl^-][HA] \quad (4.1)$$

$$HA_{aq} \leftrightarrow A^-_{aq} + H^+_{aq}$$

$$K_a^{HA} = \frac{[A^-][H^+]}{[HA]} \quad (4.2)$$

where $K_{sp}^{1:1cc}$ is the solubility product of the cocrystalline salt, and K_a^{HA} is the ionization constant of the coformer. The presented derivation applies to a chloride salt, but could be applied to a salt with other counter-ions as well. Species without subscripts refer to the solution phase and the terms in brackets refer to the component solution concentrations, which approximate component activities under dilute solution conditions. In order to

establish the key parameters affecting cocrystalline salt solubility, non-idealities due to solution complexation are ignored and will need to be considered as appropriate.

The cocrystalline salt is composed of the ionized drug and ionized chloride ion, therefore the total analytical concentrations of drug, $[B]_T$, and chloride, $[Cl]_T$ under solution conditions where the salt is the stable form relative to the free drug (i.e. below pH_{max}) are described by

$$[B]_T = [BH^+] \tag{4.3}$$

$$[Cl]_T = [Cl^-] \tag{4.4}$$

while the analytical concentration of the acid is the sum of the ionized and nonionized species, given by

$$[HA]_T = [HA] + [A^-] \tag{4.5}$$

The analytical drug concentrations in equilibrium with the 1:1 cocrystalline salt can be expressed in terms of $[HA]_T$, $[Cl]_T$, $K_{sp}^{1:1cc}$, K_a and $[H^+]$ by substituting equations (4.1) and (4.2) into equation (4.5) and rearranging to give

$$[B]_T = \frac{K_{sp}^{1:1cc}}{[HA]_T[Cl]_T}\left(1 + \frac{K_a^{HA}}{[H^+]}\right) \tag{4.6}$$

The cocrystalline salt solubility is highly dependent on the solution composition, similar to cocrystals and salts based on equation (4.6). According to this equation, increasing the solution concentrations of one component will result in the decrease of the other components assuming solubility product behavior.

Cocrystalline salt solubility products can be evaluated from the measured component solution concentrations in equilibrium with the cocrystalline salt according to equation (4.6) when the cocrystalline salt is the thermodynamically stable phase. The cocrystalline salt solubility, $S_T^{1:1cc}$, under stoichiometric conditions, is equal to the total concentration of each component of the cocrystalline salt according to

$$S_T^{1:1cc} = [B]_T = [Cl]_T = [HA]_T \tag{4.7}$$

An expression for the cocrystalline salt solubility dependence on $[H^+]$ in terms of experimentally accessible thermodynamic equilibrium constants is obtained below by substituting equation (4.7) into equation (4.6).

$$S_T^{1:1cc} = \sqrt[3]{K_{sp}^{1:1cc}\left(1 + \frac{K_a^{HA}}{[H^+]}\right)} \tag{4.8}$$

Under these conditions, the solubility is the stoichiometric solubility, or cocrystalline salt solubility in the absence of excess components.

The cocrystalline salt solubility is dependent on the cocrystalline salt solubility product $K_{sp}^{1:1cc}$, the ionization constant, K_a of the coformer and the solution $[H^+]$. Equation (4.8) predicts that the solubility of cocrystalline salt BH^+Cl^-HA will increase with pH (decreasing $[H^+]$). At pH<<coformer pK_a, or $[H^+]>>K_a$, cocrystalline salt solubility approaches its intrinsic solubility, $S_0^{1:1cc}=\sqrt[3]{K_{sp}^{1:1cc}}$. At pH = coformer pK_a, or $[H^+]=K_a$, the cocrystal solubility is $\sqrt[3]{2}$ or 1.25 times higher than the intrinsic cocrystal solubility. As pH increases beyond the coformer pK_a ($[H^+]<<K_a$) cocrystalline salt solubility increases exponentially. The parent salt exhibits a solubility plateau region which is its intrinsic solubility, $S_0^{salt}=\sqrt{K_{sp}^{salt}}$, below the pH_{max} (salt / free drug) in the absence of excess chloride where the salt solubility product, K_{sp}^{salt}, is defined by

$$K_{sp}^{salt}=[BH^+][Cl^-] \tag{4.9}$$

Figure 4.1 shows the stoichiometric solubility-pH dependence of the cocrystalline salt relative to the parent salt when $S_0^{1:1cc}<S_0^{salt}$. The cocrystalline salt exhibits a plateau region under solution conditions in which the coformer is unionized which is the intrinsic solubility, $S_0^{1:1cc}$. The cocrystalline salt solubility increases with increasing pH due to the ionization of the acidic coformer. This phase solubility diagram dictates the solution

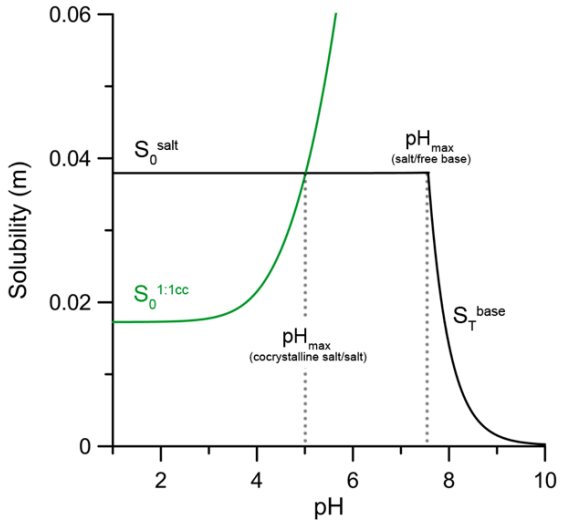

Figure 4.1. Cocrystalline salt solubility dependence on pH according to equation (4.8) for a hypothetical cocrystalline salt. There exists a pH_{max} where the cocrystalline salt and

parent salt solubilities are equal. S_0^{salt}=3.8x10^{-2} m, $K_{sp}^{1:1cc}$ = 5.0x10^{-6} m^3, coformer pK_a = 4.0

conditions under which the cocrystalline salt is the stable phase. The cocrystalline salt is the stable phase when pH < pH_{max} (cocrystalline salt/salt) assuming that there is enough coformer in solution to be saturated with respect to cocrystalline salt, $[HA]_T \geq S_T^{1:1cc}$. The salt will be the stable phase if there is not enough coformer present to saturate the system with the respect to the cocrystalline salt. If the parent salt was added to a solution under these conditions, cocrystalline salt may precipitate from solution, as it is the thermodynamically stable phase under these conditions.

As shown in Figure 4.1, a cocrystalline salt that exhibits a $S_0^{1:1cc} < S_0^{salt}$ is predicted to have a pH_{max} at which the cocrystalline salt and parent salt have equal solubilities. The pH_{max} between the 1:1 cocrystalline salt and the parent salt is described by

$$pH_{max} = \frac{3}{2}\log_{10} K_{sp}^{salt} - \log_{10} K_{sp}^{1:1cc} + pK_a^{HA} \quad (4.10)$$

assuming the pH_{max} between the cocrystalline salt and the parent salt occurs below the pH_{max} between the salt and free base. Based on this equation, the pH_{max} for a 1:1 cocrystalline salt depends on the cocrystalline salt solubility product, $K_{sp}^{1:1cc}$, the salt solubility product, K_{sp}^{salt}, and the ionization constant of the coformer, pK_a^{HA}. As shown in Figure 4.2, the following relationships exist between the cocrystalline salt pH_{max} and these 3 parameters:

(1) the pH_{max} will increase by 1 unit for every unit increase in coformer pK_a
(2) the pH_{max} will decrease by 1 unit with an increase in magnitude of the $K_{sp}^{l:1cc}$
(3) the pH_{max} will increase by 1.5 units with an increase in magnitude of the K_{sp}^{salt}

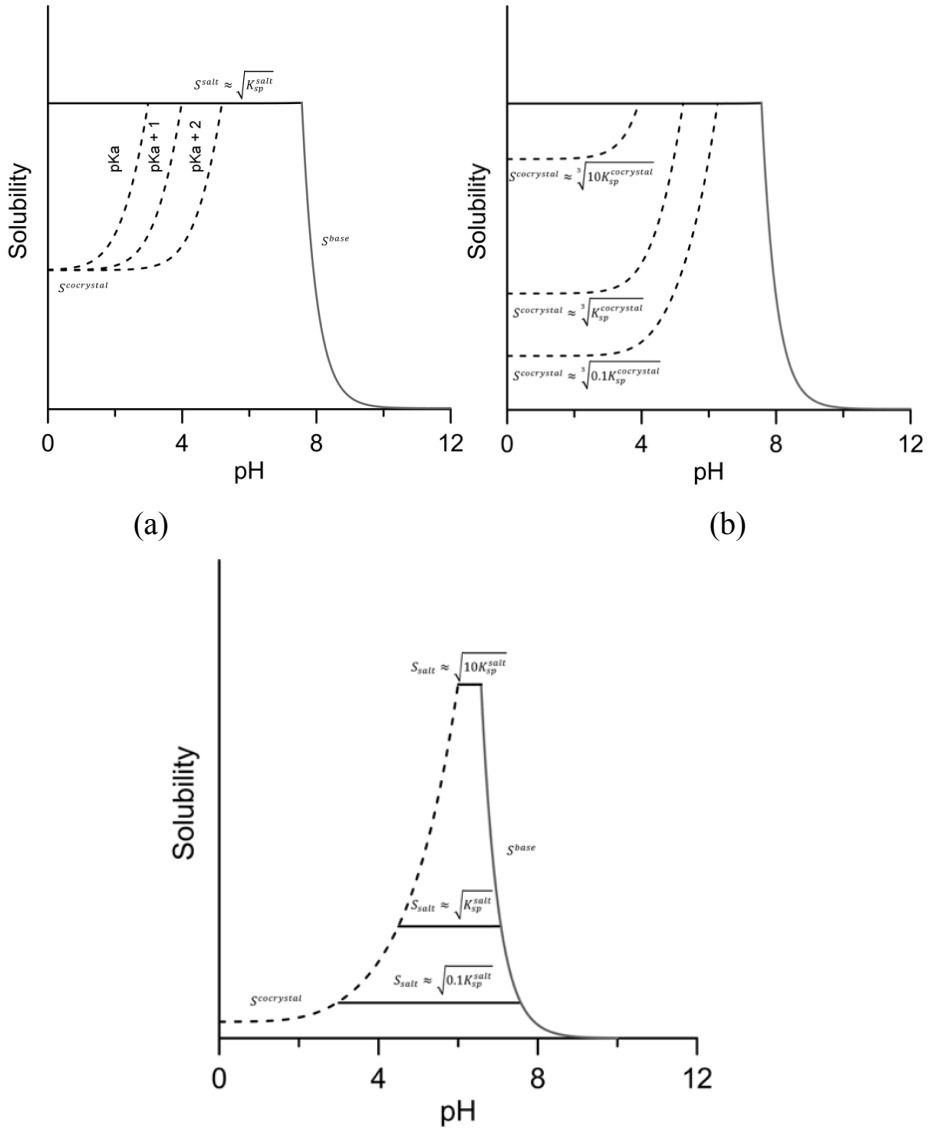

Figure 4.2. Salt/cocrystalline salt pH_{max} dependence on (a) coformer pK_a (b) $K_{sp}^{1:1cc}$ and (c) K_{sp}^{salt}.

It is possible to design the cocrystalline salt pH_{max} with salt based on the relationship between pH_{max} and K_{sp}^{salt}, $K_{sp}^{1:1cc}$ and pK_a coformer. pH_{max} between cocrystalline salt and salt characterizes the solution conditions required to achieve the desired solid phase (cocrystalline salt or salt) in solution.

The cocrystalline salt solubility advantage relative to the parent salt increases with decreasing $[H^+]$ (increasing pH) according to

$$\frac{S_T^{1:1cc}}{S_T^{salt}} = \frac{\sqrt{K_{sp}^{1:1cc}\left(1 + \frac{K_a^{HA}}{[H^+]}\right)}}{\sqrt{K_{sp}^{salt}}} \tag{4.11}$$

which is obtained by dividing equation (4.8) by the intrinsic salt solubility. A cocrystalline salt that exhibits a lower S_0 compared to the parent salt is hypothesized to be more soluble relative to the parent salt above pH_{max}. Depending on the kinetics of transformation, cocrystalline salts may be useful as supersaturating drug delivery systems.

The common-ion effect on cocrystalline salt solubility relative to parent salt solubility

The salt solubility dependence on chloride concentration is described by

$$S_{T,Cl}^{salt} = [B]_T = \frac{K_{sp}^{salt}}{[Cl]_T} \tag{4.12}$$

in solutions in which $pH < pH_{max}$ (salt / free drug).[41,45] Equation (4.12) describes the solubility product behavior or common-ion effect of the salt whereby salt solubility decreases as solution concentrations of chloride increase. Similarly the 1:1 and 2:1 cocrystalline salt solubility dependence on chloride concentration in solution can be described considering equations (4.6) and (4.29). An expression describing the 1:1 cocrystalline salt solubility dependence on the chloride concentration in solution is derived from equation (4.6), assuming the coformer is unionized. As solution concentrations of chloride increase, the drug and coformer concentrations will decrease, maintaining solution concentrations such that $[B]_T=[HA]_T$ which describes the stoichiometry between drug and coformer within the cocrystalline salt. This results in the following expression

$$S_{T,Cl}^{1:1cc} = [B]_T = \sqrt{\frac{K_{sp}^{1:1cc}}{[Cl]_T}} \tag{4.13}$$

which applies under solution conditions where $pH < pH_{max}$ (salt/free drug) and the coformer is unionized ($pH << pK_a$ coformer).

The 1:1 cocrystalline salt solubility will decrease with increasing solution concentrations of chloride according to an inverse square-root dependence. Equation

(4.13) indicates that the solubility of a 1:1 cocrystalline salt has a weaker dependence on chloride compared to the parent salt. Figure 4.3 shows the calculated cocrystalline salt solubility dependence on chloride for a cocrystalline salt system which exhibits $S_0^{1:1cc} < S_0^{salt}$. Figure 4.3 shows that there is a chloride concentration at which the theoretical solubility curves of the cocrystalline salt and the parent salt intersect and therefore both solid phases are thermodynamically stable at a chloride concentration, $[Cl^-]_{max}$.

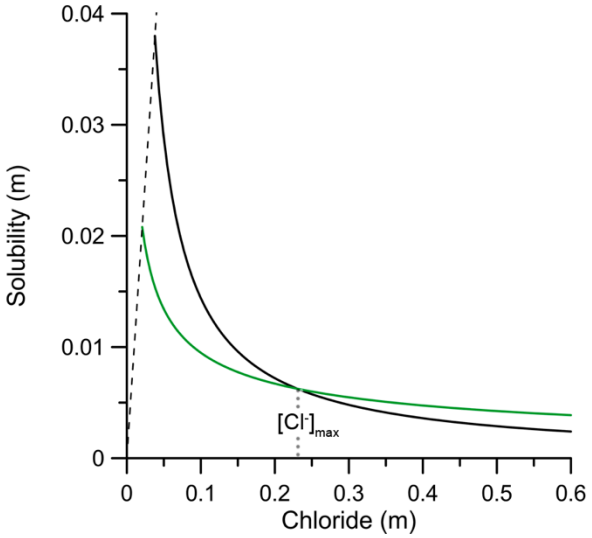

Figure 4.3 Common-ion effect on the solubility of a 1:1 cocrystalline salt (——) compared to its parent salt according to equations (4.12) and (4.13). There exists a chloride concentration at which both cocrystalline salt and salt are simultaneously saturated, $[Cl^-]_{max}$, assuming $[HA]_T=S_T^{1:1cc}$. Theoretical solubility lines were generated using $K_{sp}^{salt}=1.44x10^{-3}$ m^2, $K_{sp}^{1:1cc}=2x10^{-5}$ m^3. According to this graph $[Cl^-]_{max}=0.23$ m and solid salt and cocrystalline salt are in equilibrium when $[HA]_T=S_{T,Cl}^{1:1cc}$.

A cocrystalline salt that is less soluble than the parent salt becomes more soluble due to the different solubility dependencies on chloride. The cocrystalline salt will be the stable solid form in solutions with $[Cl]_T \leq [Cl^-]_{max}$ containing $[HA]_T = S_T^{1:1CC}$. The solubility of the 1:1 cocrystalline salt decreases as the solution concentration of chloride increases as predicted by equation (4.13).

The solubility advantage of the cocrystalline salt ($S_{T,Cl}^{1:1cc}/S_{T,Cl}^{salt}$) relative to the parent salt as a function of chloride is

$$\frac{S_{T,Cl}^{1:1cc}}{S_{T,Cl}^{salt}} = \frac{\sqrt{K_{sp}^{1:1cc}}}{K_{sp}^{salt}} \sqrt{[Cl]_T} \tag{4.14}$$

which is obtained by dividing equation (4.13) by equation (4.12). Because the cocrystalline salt solubility dependence on chloride is weaker than the parent salt, the $S_{T,Cl}^{1:1cc}/S_{T,Cl}^{salt}$ increases with chloride. When $S_0^{1:1cc}<S_0^{salt}$ there exists a $[Cl^-]_{max}$ or chloride concentration at which $S_T^{1:1cc}=S_T^{salt}$. $[Cl^-]_{max}$ is determined according to

$$[Cl^-]_{max} = \frac{\left(K_{sp}^{salt}\right)^2}{K_{sp}^{1:1cc}} \tag{4.15}$$

obtained from setting equation(4.12) equal to equation(4.13). Above $[Cl^-]_{max}$, $S_T^{1:1cc} > S_T^{salt}$ and salt is the thermodynamically stable phase.

1:1 cocrystalline salt solubility dependence on ionization and the common-ion effect

The cocrystalline salt solubility dependence on counter-ion concentration and ionization is derived from equation (4.6). As solution concentrations of chloride is increased, the drug and coformer will decrease maintaining solution concentrations such that $[B]_T = [HA]_T$, according to the cocrystalline salt stoichiometry of the drug and coformer. This analysis results in the following expression

$$S_{T,Cl}^{1:1cc} = \sqrt{\frac{K_{sp}^{1:1cc}}{[Cl]_T}\left(1 + \frac{K_a^{HA}}{[H^+]}\right)} \tag{4.16}$$

which applies under solution conditions where pH $<pH_{max}$ (salt/free drug). Figure 4.4 shows the 1:1 cocrystalline salt solubility, and $S_{T,Cl}^{1:1cc}/S_{T,Cl}^{salt}$ are predicted to increase with pH and increasing counter-ion.

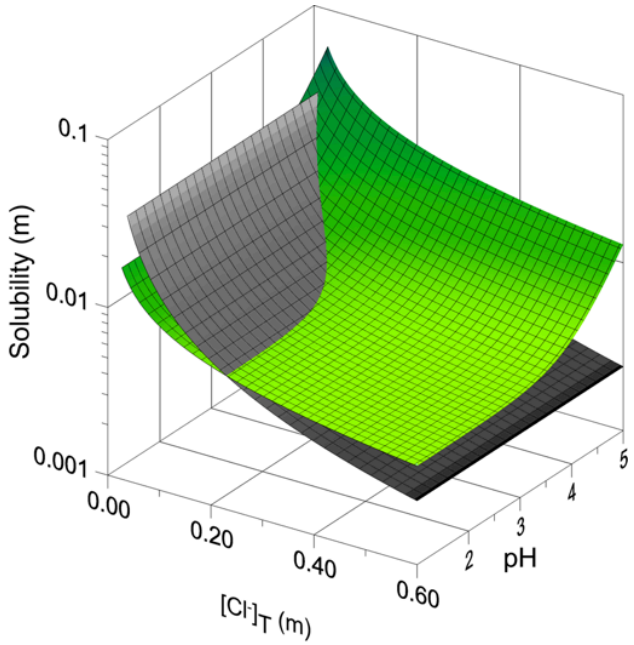

Figure 4.4. Theoretical 1:1 cocrystalline salt solubility (green surface) dependence on $[Cl^-]_T$ and $[H^+]$ compared to its parent salt (grey surface) according to equations (4.16) and (4.12) respectively. Theoretical curves were generated using $K_{sp}^{1:1cc} = 9 \times 10^{-6}$ m^3, $K_{sp}^{salt} = 1.44 \times 10^{-3}$ m^2 and coformer pKa= 4.0.

The $S_{T,Cl}^{1:1cc}/S_{T,Cl}^{salt}$ increases with $[Cl]_T$ and $[H^+]$ in solution according to

$$\frac{S_{T,Cl}^{1:1cc}}{S_{T,Cl}^{salt}} = \frac{\sqrt{K_{sp}^{1:1cc}\left(1+\frac{K_a^{HA}}{[H^+]}\right)}}{K_{sp}^{salt}}\sqrt{[Cl^-]_T} \qquad (4.17)$$

which is obtained by dividing equation (4.16) by equation (4.12). According to this relationship, the $S_{T,Cl}^{1:1cc}/S_{T,Cl}^{salt}$ increases as excess chloride is introduced into solution. There may be an advantage to using a cocrystalline salt when $S_0^{1:1cc} \geq S_0^{salt}$ under gastric conditions to mitigate the common-ion effect. The cocrystalline salt could generate supersaturation under gastric conditions to improve the bioavailability of a chloride salt.

Measuring the equilibrium solubility of a metastable cocrystalline salt.

The cocrystalline salt may transform to the parent salt during equilibrium solubility determinations when $S_T^{1:1cc} \geq S_T^{salt}$ resulting in an underestimation of the cocrystalline salt solubility. The equilibrium solubility of cocrystals that are more soluble than the parent drug have been determined from eutectic point measurements.[4,95] This measurement takes advantage of the solubility product behavior whereby the addition of coformer in excess of the cocrystal stoichiometry lowers the cocrystal solubility.

Eutectic measurements can be used to evaluate the equilibrium solubility of metastable cocrystalline salts.

The 1:1 cocrystalline salt solubility dependence on $[HA]_T$ is derived by rearranging equation (4.6) in terms of $[B]_T$ assuming the solution concentrations of drug and chloride will both decrease with increasing coformer maintaining $[B]_T=[Cl]_T$ according to the cocrystal stoichiometry. The resulting expression

$$S_{T,HA}^{1:1cc} = \sqrt{\frac{K_{sp}^{1:1cc}}{[HA]_T}\left(1+\frac{K_a^{HA}}{[H^+]}\right)} \qquad (4.18)$$

shows that cocrystal solubility will decrease with increasing coformer in solution. This expression applies to solutions in which the $pH<pH_{max}$ (salt/drug). According to equation (4.18) the solubility curve of a cocrystalline salt that is more soluble than the parent salt will intersect the salt solubility curve as shown in Figure 4.5.

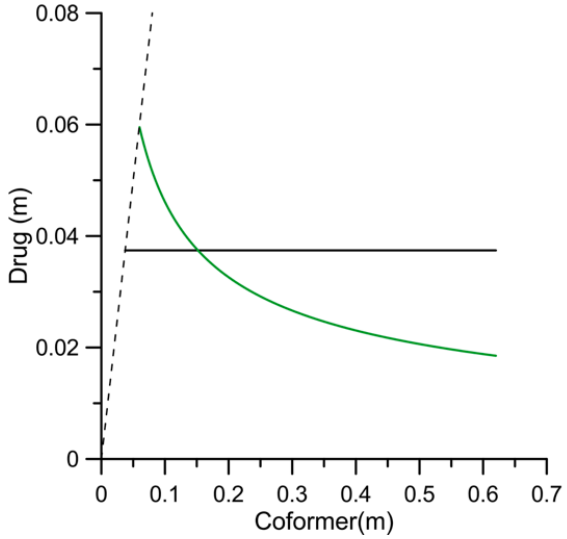

Figure 4.5. The theoretical solubility dependence of a 1:1 cocrystalline salt on coformer solution concentration, according to equation (4.18). Theoretical curves were generated using $K_{sp}^{1:1cc} = 2 \times 10^{-4}$ m^3, $S_0^{salt} = 3.74 \times 10^{-2}$ m^2 and coformer $pK_a = 4.4$.The cocrystalline salt and drug saturation curves intersect at the eutectic point, which is invariant when solid salt (BH^+Cl^-) and cocrystalline salt (BH^+Cl^-HA) are in equilibrium with the liquid phase at a given temperature and pH.

This intersection is the eutectic point between cocrystalline salt and salt, and the solution concentrations in equilibrium with the solid phases are invariant. The solubility of the salt and 1:1 cocrystalline salt can be determined at the eutectic point under equilibrium conditions. At the eutectic point of the 1:1 cocrystalline salt and parent salt,

$[F]_T = S_0^{salt}$ when chloride is not added to the solution in excess of the cocrystalline salt stoichiometry. $K_{sp}^{1:1cc}$ can be calculated from the analytical solution concentrations in equilibrium with the eutectic point between cocrystalline salt and salt according to equation (4.6) or (4.29) for a 1:1 cocrystalline salt and a 2:1 cocrystalline salt respectively.

1:1 cocrystalline salt stoichiometric solubility-pH dependence at the eutectic point

The thermodynamic equilibrium solubility of the 1:1 cocrystalline salt can be determined at the eutectic point. Combining and rearranging equation (4.6) and (4.8), the stoichiometric solubility of the 1:1 cocrystalline salt is related to the solution components according to:

$$\left(S_T^{1:1cc}\right)^3 = [B]_T[Cl]_T[HA]_T = K_{sp}^{1:1cc}\left(1+\frac{K_a^{HA}}{[H^+]}\right) \tag{4.19}$$

Therefore the stoichiometric solubility of the cocrystalline salt can be obtained from the equilibrium analytical component concentrations according to

$$S_T^{1:1cc} = \sqrt[3]{[B]_T[Cl]_T[HA]_T} \tag{4.20}$$

Equation (4.20) is useful to determine the stoichiometric solubility from a solution in equilibrium with cocrystalline salt, such as the eutectic point, and is analogous to the eutectic point analysis in the cocrystal literature.[4,15,16,95]

1:1 cocrystalline salt solubility dependence on chloride at the eutectic point

The cocrystalline salt solubility dependence on chloride is related to the drug and coformer analytical solution concentration according to

$$S_{T,Cl}^{1:1cc} = [B]_T = [HA]_T = \frac{K_{sp}^{1:1cc}}{[Cl]_T}\left(1+\frac{K_a^{HA}}{[H^+]}\right) \tag{4.21}$$

by rearranging equation (4.13). The cocrystalline salt solubility dependence on chloride can be evaluated according to

$$S_{T,Cl}^{1:1cc} = \sqrt{[B]_T[HA]_T} \tag{4.22}$$

As excess coformer is added to solution, the equilibrium drug concentration will decrease due to solubility product behavior such that equation (4.22) equals the cocrystalline salt solubility in the absence of excess coformer.

Analytical considerations for a 2:1 cocrystalline salt

Equations that describe the 2:1 cocrystalline salt solubility dependence on $[H^+]$, $K_{sp}^{2:1cc}$, $K_a^{coformer}$, and $[Cl]_T$ can be derived by considering cocrystal dissociation and component ionization. The cocrystalline salt solubility of a 2:1 cocrystalline salt, $(BH^+Cl^-)_2H_2A$ where the chloride salt is BH^+Cl^- and the coformer is a diprotic acid, H_2A, is described by the following equilibrium reactions:

$$(BH^+Cl^-)_2H_2A_{solid} \overset{Ksp}{\leftrightarrow} BH^+_{aq} + Cl^-_{aq} + H_2A_{aq}$$

$$K_{sp}^{(BH^+Cl^-)_2H_2A} = [BH^+]^2[Cl^-]^2[H_2A] \quad (4.23)$$

$$H_2A_{aq} \leftrightarrow HA^-_{aq} + H^+_{aq}$$

$$K_{a,1}^{H_2A} = \frac{[HA^-][H^+]}{[H_2A]} \quad (4.24)$$

$$HA^-_{aq} \leftrightarrow A^{2-}_{aq} + H^+_{aq}$$

$$K_{a,2}^{HA-} = \frac{[A^-][H^+]}{[HA^-]} \quad (4.25)$$

The total analytical concentrations of drug and counter-ion under solution conditions where the salt is the stable form relative to the free drug (i.e. below pH_{max}) are described by

$$[B]_T = [BH^+] \quad (4.26)$$

$$[Cl]_T = [Cl^-] \quad (4.27)$$

while the analytical concentration of the acid, the sum of the ionized and nonionized species, is given by

$$[H_2A]_T = [H_2A] + [HA^-] + [A^{2-}] \quad (4.28)$$

The analytical drug concentration in equilibrium with the 2:1 cocrystalline salt can be expressed in terms of $[H_2A]_T$, $[Cl]_T$, $K_{sp}^{2:1cc}$, K_a and $[H^+]$ by substituting $[H_2A]$, $[HA^-]$ and $[A^{2-}]$ from equations (4.23)-(4.25) into equation (4.28) and rearranging to give

$$[H_2A]_T = \frac{K_{sp}^{2:1cc}}{[B]_T^2[Cl]_T^2}\left(1 + \frac{K_{a,1}^{H_2A}}{[H^+]} + \frac{K_{a,1}^{H_2A}K_{a,2}^{HA-}}{[H^+]^2}\right) \quad (4.29)$$

which applies to solutions in which the pH <<pH_{max} (salt/free base). Equation (4.29) is in terms of component concentrations, understanding that they approximate component activities under dilute conditions.The solubility product can be determined from the analytical $[H_2A]_T$, $[Cl]_T$ and $[B]_T$ concentrations and $[H^+]$ in equilibrium with a solution that is saturated with the cocrystalline salt. This is achieved in solutions containing stoichiometric solution concentrations when $S_0^{2:1cc} < S_0^{salt}$ or at the eutectic point between 2:1 cocrystalline salt and salt.

2:1 Cocrystalline salt solubility-pH dependence

The cocrystalline salt solubility, $S_T^{2:1cc}$ is equal to the total concentration of each component of the cocrystalline salt under stoichiometric solution conditions according to

$$S_T^{2:1cc} = \frac{1}{2}[B]_T = \frac{1}{2}[Cl]_T = [H_2A]_T \quad (4.30)$$

An equation for the cocrystalline salt solubility-pH dependence in terms of experimentally accessible thermodynamic equilibrium constants is obtained by substituting equation (4.30) into equation (4.29) and multiplying the final equation by two; the equation is in terms of moles drug/kg solvent.

$$S_T^{2:1cc} = 2x\left(\sqrt[5]{\frac{K_{sp}^{2:1cc}}{16}\left(1 + \frac{K_{a,1}^{H_2A}}{[H^+]} + \frac{K_{a,1}^{H_2A}K_{a,2}^{HA-}}{[H^+]^2}\right)}\right) \quad (4.31)$$

Under these conditions, the solubility is the stoichiometric solubility, or cocrystalline salt solubility in the absence of excess components.

The cocrystalline salt solubility is dependent on its solubility product $K_{sp}^{2:1cc}$, the ionization constants K_a^{H2A} and K_a^{HA-} of the coformer, and the solution $[H^+]$. According to equation (4.31), the solubility of cocrystalline salt $(BH^+Cl^-)_2H_2A$ will decrease with $[H^+]$ (increase with pH). At pH << coformer pK_a^{H2A}, or $[H^+]>>K_a^{H2A}$, cocrystalline salt

solubility approaches its intrinsic solubility, $S_0^{2:1cc} = 2x\sqrt[5]{\frac{K_{sp}^{2:1cc}}{16}}$. At pH = coformer pK_a^{H2A}, or $[H^+]=K_a^{H2A}$, the cocrystal solubility is $\sqrt[5]{2}$ or 1.15 times $S_0^{2:1cc}$. As pH increases beyond the first coformer pKa^{H2A} ($[H^+]<<K_a^{H2A}$) the cocrystalline salt solubility increases exponentially.

2:1 Cocrystalline salt solubility dependence on $[H^+]$ and $[Cl^-]$

As chloride solution concentrations increase, the drug and coformer in equilibrium with the 2:1 cocrystalline salt decrease due to solubility product behavior, maintaining solution concentrations such that

$$S_{T,Cl}^{2:1cc} = \frac{1}{2}[B]_T = [H_2A]_T \quad (4.32)$$

according to the 2:1 cocrystalline salt stoichiometry. The 2:1 cocrystalline salt solubility dependence on $[Cl]_T$ and $[H^+]$ is derived by combining equation (4.29) and (4.32) and solving in terms of $S_{T,Cl}^{2:1cc}$ resulting in the following equation

$$S_{T,Cl}^{2:1cc} = 2x\sqrt[3]{\frac{K_{sp}^{2:1cc}}{4[Cl]_T^2}\left(1 + \frac{K_{a,1}^{H_2A}}{[H^+]} + \frac{K_{a,1}^{H_2A}K_{a,2}^{HA-}}{[H^+]^2}\right)} \quad (4.33)$$

Equation (4.33) applies under solution conditions where pH < pH_{max} (salt/free drug). The 2:1 cocrystalline salt solubility will decrease with increasing $[Cl]_T$ of chloride according to equation (4.33). The 1:1 cocrystalline salt exhibits the weakest chloride dependence, followed by the 2:1 cocrystalline salt followed by the parent salt based on equations (4.12), (4.16) and (4.33).

2:1 cocrystalline salt stoichiometric solubility-pH dependence at the eutectic point

The 2:1 cocrystalline salt solubility dependence on $[H_2A]_T$ is derived by assuming the solution concentrations of drug and chloride will both decrease with increasing coformer concentration in solution maintaining that

$$S_T^{2:1cc} = \frac{1}{2}[B]_T = \frac{1}{2}[Cl]_T \quad (4.34)$$

according to the stoichiometry of the 2:1 cocrystalline salt. The cocrystalline salt solubility dependence on $[H_2A]_T$ is obtained by combining and rearranging equations (4.29) and (4.34) resulting in the following equation

$$S_{T,H2A}^{2:1cc} = 2x\sqrt[4]{\frac{K_{sp}^{2:1cc}}{16[H_2A]_T}\left(1+\frac{K_{a,1}^{H_2A}}{[H^+]}+\frac{K_{a,1}^{H_2A}K_{a,2}^{HA-}}{[H^+]^2}\right)} \quad (4.35)$$

According to equation (4.35), the cocrystalline salt solubility will decrease with increasing coformer in solution. This expression applies to solutions in which the pH<pH_{max} (salt/drug). According to equation (4.35), the solubility curve of a cocrystalline salt that is more soluble than the parent salt will intersect the salt solubility curve.

The thermodynamic equilibrium solubility of the 2:1 cocrystalline salt can be determined at the eutectic point between cocrystalline salt and salt. Combining and rearranging equation (4.29) and (4.33) the stoichiometric solubility of the 2:1 cocrystalline salt is related to the solution components according to:

$$16x\left(\frac{S_T^{2:1cc}}{2}\right)^5 = [B]_T^2[Cl]_T^2[H_2A]_T = K_{sp}^{2:1}\left(1+\frac{K_{a,1}^{H_2A}}{[H^+]}+\frac{K_{a,1}^{H_2A}K_{a,2}^{HA-}}{[H^+]^2}\right) \quad (4.36)$$

therefore the stoichiometric solubility of the cocrystalline salt can be obtained from the equilibrium analytical component concentrations according to

$$S_T^{2:1cc} = 2x\sqrt[5]{\frac{[B]_T^2[Cl]_T^2[H_2A]_T}{16}} \quad (4.37)$$

regardless of the presence of excess coformer or chloride due to solubility product behavior. Equation (4.37) is useful to determine the cocrystalline salt stoichiometric solubility from the eutectic point measurement and is analogous to the eutectic point analysis in the cocrystal literature.[15,16,18,47] The cocrystalline salt solubility dependence on chloride cannot be determined from equation (4.37).

2:1 cocrystalline salt solubility dependence on chloride at the eutectic point

The thermodynamic equilibrium solubility of the 2:1 cocrystalline salt in solutions containing excess chloride can be determined at the eutectic point. The 2:1 cocrystalline salt solubility dependence on chloride is related to the drug and coformer analytical solution concentration according to

$$4(2S_T^{2:1})^3 = [B]_T^2[H_2A]_T = \frac{K_{sp}^{2:1}}{[Cl]_T^2}\left(1 + \frac{K_{a,1}^{H_2A}}{[H^+]} + \frac{K_{a,1}^{H_2A}K_{a,2}^{HA-}}{[H^+]^2}\right) \quad (4.38)$$

This equation is obtained by combining and rearranging equations (4.29) and(4.33). The cocrystalline salt solubility dependence on chloride can be evaluated according to

$$S_{T,cl}^{2:1cc} = 2x\sqrt[3]{\frac{[B]_T^2[H_2A]_T}{4}} \quad (4.39)$$

This equation can be used to determine the cocrystalline salt solubility in chloride solutions from eutectic point measurements. As excess coformer is added to solution, the equilibrium drug concentrations decrease due to solubility product behavior such that equation (4.39) equals the cocrystalline salt solubility in the absence of excess coformer.

For the first time mathematical models that describe cocrystalline salt solubility are derived for the solubility dependence on $[H^+]$, coformer, and counter-ion for a 1:1 cocrystal with a monoprotic acidic coformer and a 2:1 cocrystal with a diprotic acidic coformer. HCl salts that exhibit unfavorable solubility under gastric conditions due to the common-ion effect may benefit from cocrystal formation which mitigates the common-ion effect.[116,117] Cocrystallization of pharmaceutical HCl salts can reduce the common-ion effect, and may increase the intrinsic solubility. Cocrystallization of a salt may also be useful to customize the solubility-pH dependence of the parent salt in addition to S_0. The cocrystalline salt solubility at the plateau (S_0) is characterized by the $K_{sp}^{1:1cc}$ while the pH-solubility profile depends on the ionization properties of the coformer.

Materials and Methods

Materials

Fluoxetine hydrochloride (FH^+Cl^-) was purchased from Jai Radhe Sales (Ahmedabad, India) and was used as received. Benzoic acid (BA) was purchased from Acros (Pittsburgh, PA) and fumaric acid (FA) and succinic acid (SA) were purchased from Sigma Chemical Company (St. Louis, MO). All crystalline solids were characterized by X-ray power diffraction (XRPD) and differential scanning calorimetry (DSC) before carrying out experiments. HPLC grade acetonitrile was purchased from Fisher Scientific (Pittsburgh, PA). Water used in this study was filtered through a double deionized purification system (Milli Q Plus Water System) from Millipore Co. (Bedford, MA).

Cocrystal Synthesis

Cocrystalline salts were prepared at ambient temperature. Salt and coformer were added in their stoichiometric ratio (1:1 for BA, and 2:1 for FA and SA) to an aqueous solution saturated with coformer. The solution pH during synthesis was 3.2 for BA and 2.2 for SA and FA. The solid phase was characterized by XRPD and DSC.

Solubility Measurements

Fluoxetine HCl (FH^+Cl^-), fluoxetine HCl benzoic acid (FH^+Cl^-BA) and fluoxetine HCl fumaric acid ($(FH^+Cl^-)_2FA$) were measured as a function of solution pH and $[Cl]_T$. Fluoxetine HCl succinic acid ($(FH^+Cl^-)_2SA$) was measured as a function of SA. FH^+Cl^-, FH^+Cl^-BA were measured by traditional phase solubility techniques.[118] 50-100 mg of solid (salt or cocrystal) was added to 3 mL of water or aqueous solutions (varying pH or $[Cl]_T$) at 25±0.1°C. $(FH^+Cl^-)_2SA$ solubility was measured in aqueous SA solutions in which cocrystalline salt was the stable phase. $(FH^+Cl^-)_2FA$ was characterized from eutectic point measurements as outlined in the theoretical section. Solubilities were determined from measured solution concentrations in equilibrium at the eutectic point between cocrystalline salt and salt.

The eutectic point was evaluated by suspending cocrystalline salt (100 mg) and salt (50 mg) in 3 mL of water or aqueous solutions (varying pH or $[Cl^-]_T$). pH was modified by dropwise addition of either 1M HCl or 1M NaOH. NaCl was dissolved in water to vary $[Cl]_T$ prior to suspending solid phase(s). Solubility experiments were maintained with magnetic stirring at 25 ± 0.1°C using a water bath. The solution phase was analyzed at 24 hour time intervals, for 72-96 hours. Solution pH was measured and 0.3 mL of sample was collected and filtered through 0.45 mm membrane, and diluted with water or mobile phase. Drug and coformer concentrations were analyzed by HPLC. Chloride concentrations were analyzed by ICP-HRMS. The recovered solid phase(s) were characterized by XRPD and DSC.

As outlined in the theoretical section, the $(FH^+Cl^-)_2FA$ solubilities were determined from the analytical solution concentrations from eutectic point measurements according to equation (4.37):

$$S_T^{2:1cc} = 2x\sqrt[5]{\frac{([F]_T)^2([Cl]_T)^2[H_2A]_T}{16}}$$

in water or when pH was modified. The cocrystalline salt solubilities were determined from the eutectic point measurement according to equation (4.38):

$$S_T^{2:1cocrystal} = 2x\sqrt[3]{\frac{([F]_T)^2[H_2A]_T}{4}}$$

in solutions containing excess chloride.

Cocrystal transformation study in water and pH 7 buffer

200 mg of cocrystalline salt was suspended in 3 mL of deionized water of pH 7 buffer and stirred at 250 rpm at 25 ± 0.1°C. An aliquot were withdrawn after 24 hours and filtered through a 0.45 μm PVDF syringe filter. Solution concentrations of $[F]_T$ and $[H_2A]_T$ were analyzed by HPLC. Recovered solid phases were characterized by XRPD and DSC.

High-Performance Liquid Chromatography

The drug and coformer concentrations were analyzed by a Waters HPLC (Milford, MA) equipped with an ultraviolet-visible spectrometer detector. A C18 Thermo Electron Corporation (Quebec, Canada) column (5μm, 250 x 4.6 mm) at ambient temperature was used. The injection sample volume was 20 μl and an isocratic method with a mobile phase composed of 50% acetonitrile and 50% water with 0.1% trifluoroacetic acid and a flow rate of 1 ml/min was used. Absorbance of all components were monitored at 228 nm. Waters' operation software, Empower 2, was used to collect and process the data. All concentrations are reported in molality (moles solute/kilogram solvent) unless otherwise indicated.

X-ray Powder Diffraction

X-ray powder diffraction diffractograms of solid phases were collected with a benchtop Rigaku Miniflex X-ray diffractometer (Rigaku, Danverse, MA) using Cu Kα radiation (λ= 1.54Å), a tube voltage if 30 kV, and a tube current of 15 mA. Data were collected from 5 to 40° at a continuous scan rate of 2.5°/min.

Thermal Analysis

Solid phases collected from the slurry studies were dried and analyzed by differential scanning calorimetry (DSC) using a TA instrument (Newark, DE) 2910MDSC system equipped with a refrigerated cooling unit. DSC experiments were performed by heating the samples at a rate of 10 K/min under a dry nitrogen atmosphere. Temperature and enthalpy calibration of the instruments was achieved using a high purity indium standard. Standard aluminum sample pans were used for all measurements.

Inductively coupled plasma-high resolution mass spectrometer.

We thank Ted Huston in the W. M. Keck Elemental Geochemistry Laboratory, within the Department of Earth and Environmental Sciences, at the University of Michigan for the ICP analyses. The chloride concentrations were analyzed using a Thermo Scientific Element Inductively Coupled Plasma-High Resolution Mass Spectrometer (ICP-HRMS). The aqueous samples were diluted nominally 10-fold with HNO_3, containing 1ng/g (ppb) Indium (In), to normalize the matrix and better match calibration standards. The In signal was not used as an internal standard, but to monitor instrumental matrix effects and drift. Other instrumental parameters: 1400W forward power; sample uptake ~0.3mL/min by peristaltic pump to a MicroMist nebulizer and Scott double-pass spray chamber; scanning in medium resolution ($m/\Delta m > 4000$); system optimized daily for stability and sensitivity (~1.2Mcps/ppb In); isotopes used, ^{35}Cl, ^{115}In. The calibration was from 0 to 25µg/g, with blank and linearity checks; independent calibration check was included with each batch using NIST1640 (not certified for Cl, but found to contain 19.0 +/- 0.6µg/g Cl); samples were at least an order of magnitude above batch method detection limits, which was typically better than 0.07µg/g Cl; spike recovery was tested for the initial batch with results within 90-110%.

Results

The derived equations presented in the theoretical section describe the solubility behavior of a cocrystalline salt based on the cocrystal solubility product (K_{sp}^{cc}) and coformer ionization (K_a). The salt plateau (pH-independent) region is modified by cocrystallization with a coformer that has a pK_a that falls within the salt plateau region, which occurs below pH_{max} between the salt and free base. According to the equations derived in the theoretical section, the cocrystalline salt solubility dependence on $[H^+]$ and

counter-ion concentration, $[Cl]_T$ can be *a priori* predicted from knowledge of the K_{sp}^{cc}, and coformer K_a. Assuming that cocrystalline salts follow solubility product behavior, the equilibrium solubility of metastable cocrystalline salts can be determined from equilibrium component solution concentrations at the eutectic between the cocrystalline salt and salt solid phases.

To evaluate the predictive power of the proposed models, the solubility of fluoxetine hydrochloride (FH^+Cl^-) cocrystalline salts with 1:1 and 2:1 stoichiometries, containing coformers of different ionization properties were investigated as a function of $[H^+]$ and $[Cl]_T$. These include a 1:1 cocrystalline salt with benzoic acid (monoprotic acid) (FH^+Cl^-BA), and the 2:1 cocrystalline salts with diprotic acidic coformers, fumaric acid, $(FH^+Cl^-)_2FA$, and succinic acid, $(FH^+Cl^-)_2SA$. Fluoxetine HCl solubility is pH independent below $pH_{max,}$ which is pH 7.6 according to the equation for the pH_{max} of a monoprotic base:[44]

$$pH_{max} = pK_a^{FH+} + log\left(\frac{S_{un}^F}{\sqrt{K_{sp}^{FH^+Cl^-}}}\right) \quad (4.40)$$

The pH_{max} of fluoxetine HCl was calculated from the thermodynamic parameters (intrinsic solubility of the free base, the salt K_{sp}, and the pK_a of fluoxetine) that are listed in Table 4.1. The coformers BA, FA, and SA all have pK_a values that are lower than the pH_{max} of fluoxetine HCl, and they are all expected to modify the plateau region of the salt. The cocrystalline salt solubilities are studied under solution conditions such that pH << pH_{max} (salt/free drug) following the assumption used to derive the solubility equations in the theoretical section

Table 4.1 Solubilities in the plateau region (S_0) and ionization constants of the cocrystal components 25°C

Solid	S_0 (m)	pK_a
fluoxetine	1.24×10^{-4} [a]	10.05[b]
fluoxetine-HCl	3.31x10-2[c]	
benzoic acid[d]	2.60×10^{-2}	4.2
fumaric acid[e]	4.48×10^{-2}	3.0,4.4
succinic acid	0.64	4.1, 5.6

(a) fluoxetine free base precipitated as an oil
(b) Calculated using AMD labs
(c) Ref[48]
(d) Ref[88]
(e) Ref[119]

$(FH^+Cl^-)_2FA$ exhibits a higher solubility than the parent salt,[79] therefore the solubility of $(FH^+Cl^-)_2FA$ was evaluated by eutectic point measurement to avoid solution transformation to salt during equilibration as discussed in the theoretical section. FH^+Cl^- and FH^+Cl^-BA solubilities were determined by traditional equilibrium solubility methods. The phase solubility behavior of $(FH^+Cl^-)_2SA$ is presented in the last section, as considerations of solution complexation were required to determine the cocrystalline salt and salt solubility dependence on $[SA]_T$.

The salt and cocrystalline salt solubilities and the corresponding solution pH were measured in deionized water and the equilibrium solution concentrations are shown in Table 4.2. The stoichiometric solubilities of 1:1 FH^+Cl^-BA and 2:1 $(FH^+Cl^-)_2FA$ were determined according to equations (4.20) and (4.37) respectively. Preliminary solubility experiments of $(FH^+Cl^-)_2FA$ in water indicate solution transformation of the cocrystalline salt by solution phase analysis ($1/2[F]_T < [H_2A]_T$) even though there was no solid phase transformation detected by XRPD or DSC. The $(FH^+Cl^-)_2FA$ solubility was determined by eutectic point measurement because the cocrystalline salt exhibited higher solution concentrations during dissolution in water relative to the parent salt.[79] The measured $[F]_{T,eu}=[Cl]_{T,eu}$ (the values are not significantly different ($p<0.05$)) which confirms the assumption required to obtain equation (4.37).

Cocrystalline salt equilibrium solubilities in deionized water are in agreement with the apparent solubilities reported by *Childs et al.*[79] The salt solubility equilibrated to a pH of 7.14±0.03, which is lower than the predicted pH_{max} (salt/free base). The solution pH values of the cocrystalline salt solubility studies were much lower than the salt studies; FH^+Cl^-BA equilibrated to a pH of 3.14, and $(FH^+Cl^-)_2FA$ equilibrated to pH 2.39±0.04. Thus, cocrystalline salts may be useful to control the solution-pH of the dissolving solid in the boundary layer, especially for salts that exhibit narrow pH ranges of stability.

Table 4.2. Cocrystalline salt and salt solubility in water and K_{sp} 25°C

Solid	pH	$[F]_T$ (mM)	$[Cl]_T$ (mM)	$[coformer]_T$ (mM)	S_{water} (mM)	K_{sp}
FH^+Cl^-	7.14±0.03	32.7±0.3	42.1±0.1		37.7±0.6	(1.42±0.05) x10^{-3} m^2
FH^+Cl^-BA[a]	3.14±0.02	18.9±0.2	19.3±0.3	16.3±0.7	17.2±0.1	(4.7±0.1) x10^{-6} m^3
$(FH^+Cl^-)_2FA$[ab]	2.39±0.04	37±2	42±2	23.0±0.3	40.6±0.6	(4.4±0.4) x10^{-8} m^5

(a) $[FH]_T=[Cl]_T$ ($p<0.05$)

(b) Determined by eutectic point measurement

As shown in Table 4.2, $[F]_{T,eu}=[Cl^-]_{T,eu}$ at the eutectic point between FH^+Cl^- and $(FH^+Cl^-)_2FA$(the values are not significantly different ($p<0.05$)) which confirms the assumption that both drug and chloride concentrations are equal and decrease as coformer increases in solution, while maintaining their stoichiometric ratio; this assumption was required to obtain equation (4.34). The measured equilibrium component concentrations (Table 4.2) were used to calculate the solubility product of the salt FH^+Cl^-, 1:1 FH^+Cl^-BA and $(FH^+Cl^-)_2FA$ using equations (4.12), (4.6) , and (4.29) respectively. The K_{sp} values in Table 4.2 and the component ionization constants in Table 4.1 were used to predict salt and cocrystalline salt solubility dependence on $[H^+]$ and $[Cl]_T$ as outlined in the theoretical section.

The common-ion effect on cocrystalline salts and K_{sp} evaluation

The salt solubility dependence on chloride solution concentrations is predicted to be pH-independent below the salt pH_{max} with the free base (pH_{max}=7.6). The salt solubility was measured as a function of the chloride concentration in solution at pH 2 and in water (pH 6-7) to confirm this behavior prior to carrying out solubility-pH studies with cocrystalline salts. The solubility of FH^+Cl^- decreases as the analytical chloride increases in solution as shown in Figure 4.6, and the solubility dependence on chloride at pH 2 is in agreement with that determined in water (pH 6-7).

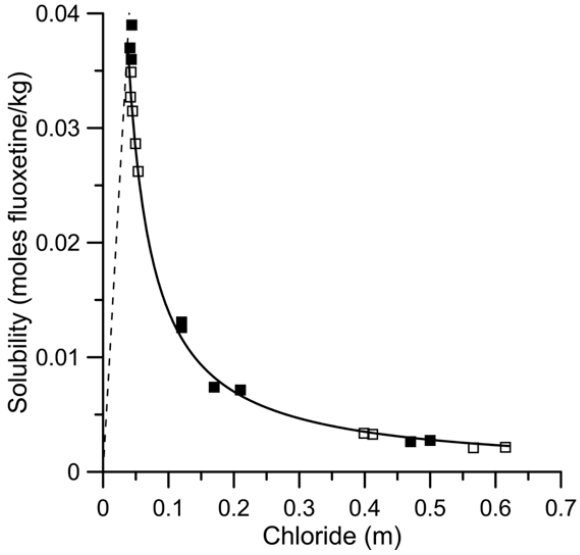

Figure 4.6. The solubility of Fluoxetine HCl decreases due to common ion effect at pH 2 (■) and in water, pH 6-7, (□) at 25 °C. The predicted salt solubility (——) and $K_{sp,}$

(1.40±0.03[a]) x10^{-3} $m^{2,}$ were determined by nonlinear regression analysis of the data according to equation (4.12).

The measured salt solubility $[F]_T$, decreased with increasing $[Cl]_T$. The salt solubility dependence on $[Cl_T$ at pH 2 and pH 6-7 was described well by equation (4.12) according to non-linear regression analysis (R_{sq}=0.98 ,P <0.0001). The salt K_{sp} evaluated from nonlinear regression analysis (K_{sp} =(1.40±0.03) x10^{-3} m^2) is in agreement with that determined from the single solubility measurement in water (K_{sp} =(1.42±0.05) x10^{-3} m^2). The analytical concentrations of the salt components are shown in Table 4.3. The salt solubility is equal to the analytical drug concentration, S_{salt} =$[F]_T$.

Table 4.3. Equilibrium FH^+Cl^- component concentrations in aqueous chloride solution, pH 2-2.4 at 25°C.

pH	$[Cl^-]_T$(mM)	$[FH^+]_T$ (mM)
2.06±0.02	43±2	34.9±0.7
2.35±0.03	44±2	39±1
2.39±0.01	41±2	37±7
2.43±0.01	43±2	36±1
2.37±0.01	120±10	13.1±0.1
2.36±0.03	120 ± 10	12.6±0.1
2.33±0.01	170± 10	7.41±0.01
2.37±0.02	210 ± 10	7.16±0.01
2.35±0.01	470± 20	2.65±0.01
2.35±0.01	500± 30	2.77±0.02
7.07±0.03	42±2	32.7±0.3
7.36±0.05	45±2	32±2
7.25±0.05	50±3	28.6±0.4
7.49±0.03	54±3	26.2±0.7
6.98±0.06	400 ± 20	33.5±0.01
6.4±0.01	410 ± 20	3.28±0.02
6.72±0.08	570 ± 30	2.10±0.02
6.04±0.03	620 ± 30	2.14±0.01

The 1:1 and 2:1 cocrystalline salts are predicted to exhibit a weaker dependence on chloride relative to the parent salt. The FH^+Cl^-BA and $(FH^+Cl^-)_2$FA solubility dependence on solution concentrations of chloride was measured to evaluate the predictive power of equations (4.16) and (4.37) respectively. These experiments were

carried out in deionized water and pH was not independently modified. The measured solution pH and equilibrium concentrations of the components of FH^+Cl^-BA in solutions containing various chloride concentrations are shown in Table 4.4. The equilibrium solution pH ranged between 3.14-3.40 for the FH^+Cl^-BA solubility experiments. As the chloride concentration is increased from 19 to 155 mM, the analytical concentrations of drug and coformer decrease such that $[BA]_T = [F]_T$ ($p<0.05$) which is in agreement with the assumption required to obtain equation (4.13).

Table 4.4. Equilibrium FH^+Cl^-BA component concentrations in aqueous chloride solutions at pH 2-2.4 at 25°C.

pH	$[Cl]_T$ (mM)	$[BA]_T$ (mM) [a]	$[F]_T$ (mM) [a]	$S_{T,Cl}^{1:1}$ [b] (mM)
3.14±0.02	19.3±0.3	16.3±0.7	18.9±0.2	17.2±0.1
3.16±0.02	44±1	11.2±0.1	11.9±0.2	11.6±0.1
3.17±0.01	85±1	8.6±0.2	8.3±0.1	8.45±0.01
3.25±0.03	155±3	6.2±0.1	6.55±0.01	6.37±0.05
3.40±0.01	400±9	4.16±0.01	3.82±0.05[c]	3.99±0.03
3.35±0.03	586±6	4.00±0.03	2.31±0.01[c]	3.04±0.01

(a) The value of the solution concentrations of BA and F are not significantly different ($p<0.05$) as determined by a paired sample t-Test

(b) $S_T^{1:1cc}$ was calculated from equation (4.22) using the measured solution concentrations of cocrystalline salt components in this table.

(c) $[F]_T < [BA]_T$ indicating solution phase transformation, no conversion was detected by solid phase analysis

The FH^+Cl^-BA solubility dependence on chloride is compared to that of the parent salt in Figure 4.7. The measured FH^+Cl^-BA solubility decreases with increasing chloride in solution. Non-linear regression analysis shows that the measured solubilities are well described by equation (4.13) (R_{sq} =0.99, $P<0.004$).). The coformer pK_a from nonlinear regression analysis (4.4±0.9) is in agreement with value (4.03) reported by Mooney *et. al.*. [88] The FH^+Cl^-BA $K_{sp}^{1:1cc}$ was determined to be (K_{sp} =(5.61±0.07)x10^{-6} m^3) from nonlinear regression analysis. Based on the solubility products of the cocrystalline salt and the salt, the $[Cl^-]_{max}$ =0.35 m according to equation (4.15). Above $[Cl^-]_{max}$, the cocrystalline salt is predicted to be more soluble than the parent salt. While FH^+Cl^-BA was 2.2 times less soluble than the parent salt under solution conditions without stoichiometric excess of chloride, in solutions containing 0.4m and 0.586 m chloride, the solubility of FH^+Cl^-BA appears to be equal to the parent salt.

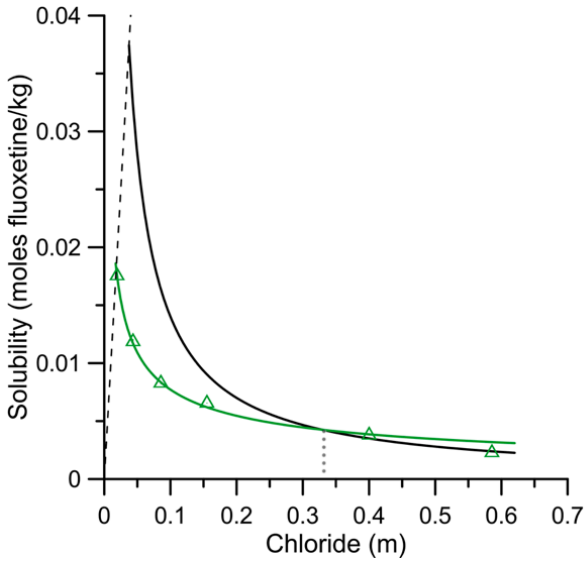

Figure 4.7. The measured solubility of FH^+Cl^-BA (Δ) decreases with increasing chloride in solution. The predicted FH^+Cl^-BA solubility (——), $K_{sp,}$ (5.61±0.7) x10^{-6} m^3, and coformer pK_a = 4.4±0.9, were evaluated by nonlinear regression of the data according to equation (4.16). The predicted salt solubility (——), according to equation (4.12) and K_{sp}^{salt} =(1.40±0.03) x10^{-3} $m^{2,}$ intersects the FH^+Cl^-BA solubility curve at $[Cl^-]_{max}$= 0.35, according to equation (4.15).

Interestingly in the solutions containing 400 and 586 mM chloride, $[F]_T < [BA]_T$, indicating phase transformation of the cocrystalline salt to the parent salt. Cocrystals that transform to the parent drug generally exhibit a decrease in drug solution concentrations paired with an increase in coformer concentrations.[47,120] Even though solid phase analysis of the recovered solids is FH^+Cl^-BA, the solution concentrations indicate transformation of the cocrystalline salt to the parent salt.

The solubility of $(FH^+Cl^-)_2FA$ solubility is predicted to decrease with increasing solution concentrations of chloride according to (4.33). Due to the weaker dependence of $(FH^+Cl^-)_2FA$ on chloride relative to the parent salt, the $S_{T,Cl}^{2:1cc}/S_{T,Cl}^{salt}$ is predicted to increase with increasing solution concentrations of chloride according to equations (4.12) and (4.33). The $(FH^+Cl^-)_2FA$ solubility was determined from the eutectic point between cocrystalline salt and salt to avoid transformation to the parent salt. The component solution concentrations of $[F]_T$, $[Cl]_T$ and $[H_2A]_T$ in equilibrium at the eutectic point between salt and $(FH^+Cl^-)_2FA$ are shown in Table 4.5

$(FH^+Cl^-)_2FA$ is increasingly more soluble relative to the parent salt in solutions containing excess chloride confirming that it does have a weaker dependence on chloride,

as shown in Table 4.5. The equilibrium drug concentration at the eutectic is equal to the salt solubility, $S_T^{salt}=[F]_{T,eu}$. The 2:1 cocrystalline salt, $(FH^+Cl^-)_2FA$, which has the same intrinsic solubility as the parent salt becomes increasingly more soluble relative to the parent salt as excess chloride in solution increases (Table 4.5). For example, $(FH^+Cl^-)_2FA$ is 2.9 times more soluble than the salt in 0.6 m chloride.

Table 4.5. $(FH^+Cl^-)_2FA$ component concentrations in equilibrium at the eutectic point in aqueous chloride solutions, pH 2-2.4 at 25°C.

pH	$[Cl]_{T,eu}$ (mM)	$[FA]_{T,eu}$ (mM)	$[F]_{T,eu}$ (mM)	$S_T^{2:1cc}$ (mM) [a]	$S_{cocrystal}/S_{Salt}$
2.35±0.03	44±2	22.9±0.6	39±1	41.1±0.8	1.05±0.03
2.39±0.01	41±20	22.8±0.6	37.0±0.7	39.7±0.6	1.07±0.03
2.43±0.01	43±2	23.4±0.9	36±1	39.3±0.9	1.09±0.04
2.37±0.01	120±10	21.1±0.1	13.1±0.1	19.4±0.3	1.48±0.03
2.36±0.03	120±10	20.9±0.1	12.6±0.1	18.7±0.1	1.48±0.01
2.33±0.01	170±10	21.1±0.1	7.41±0.01	13.2±0.1	1.78±0.01
2.37±0.02	210±10	20.5±0.1	7.16±0.01	12.9±0.1	1.80±0.01
2.35±0.01	470±20	18.5±0.1	2.65±0.01	6.38±0.02	2.41±0.01
2.35±0.01	500±30	19.8±0.1	2.77±0.02	6.72±0.03	2.43±0.02

(a) $S_T^{2:1}$ was calculated from equation (4.39) using the measured solution concentrations of cocrystal components

Equation (4.39) was used to determine the solubility dependence of $(FH^+Cl^-)_2FA$ on $[Cl]_T$ in the absence of excess coformer, $S_{T,Cl}^{2:1cc}$, which is plotted in Figure 4.8. As shown in Figure 4.8, the solubility of $(FH^+Cl^-)_2FA$ decreases with increasing chloride in solution, with a weaker dependence than that of the parent salt, which is agreement with the solubility curve predicted by equations (4.12), and (4.33). Non-linear regression analysis shows that the measured solubilities of $(FH^+Cl^-)_2FA$ are well described by equation (4.33) (R_{sq} =0.98, P<0.0001).). The coformer pK_a from nonlinear regression analysis (2.6±0.3) is in excellent agreement with reported value (3.0)[88] The $(FH^+Cl^-)_2FA$ $K_{sp}^{1:1cc}$ was determined to be ($K_{sp,}$ (3.4±0.3)x10^{-8} m^5) from nonlinear regression analysis.

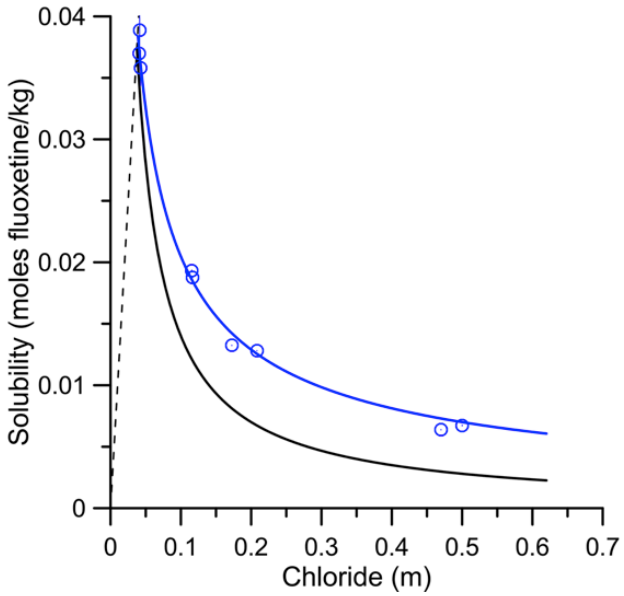

Figure 4.8. Measured solubility of $(FH^+Cl^-)_2FA$ (○) decreases with increasing chloride in solution. The predicted $(FH^+Cl^-)_2FA$ solubility (——), $K_{sp,}$ (3.4±0.3)x10^{-8} m^5, and coformer pK_{a1}=2.6±0.3 were determined by nonlinear regression analysis of the data according to equation (4.33). pK_{a2} could not be determined from the data due to the low pH range (pH 1.4 - 2.88) of the solubility measurements. The salt solubility (——) was predicted according to equation (4.12) using K_{sp}^{salt} (1.40±0.03) x10^{-3} $m^{2.}$ The second pK_a of FA is reported: pK_{a2}=4.4.[119]

A summary of the solubility products evaluated from the nonlinear regression analysis of the measured chloride dependence of FH^+Cl^-, FH^+Cl^-BA and $(FH^+Cl^-)_2FA$ is shown in Table 4.6. The K_{sp} values are in agreement with those determined from the single water measurement shown in Table 4.2 and the pK_a values determined using the nonlinear regression analysis are in agreement with the reported values as shown in Table 4.1. Only the first ionization constant of FA could be determined from the measured solubility data due to the pH range of the solubility measurements.

Table 4.6. K_{sp} determined from nonlinear regression of chloride dependence.

Solid	K_{sp}	S_0 (mM)	$pK_{a1}^{coformer}$	$pK_{a2}^{coformer}$	R_{sq}
FH^+Cl^-	(1.40±0.03)x10^{-3} $m^{2\ d\ a}$	37.4±0.4			0.99
FH^+Cl^-BA	(5.6±0.7)x10^{-6} $m^{3\ a}$	17.8±0.7	4.4±0.9 [b]		0.99
$(FH^+Cl^-)_2FA$	(3.4±0.3) x10^{-8} $m^{5\ c}$	36.9±0.7	2.6±0.3[b]	4.4[d]	0.98

(a) Statistically significant, p< 0.004.
(b) Statistically significant p<0.01 and in agreement with reported values
(c) Statistically significant p<0.0001
(d) Reported pKa values[119]

Cocrystallization of a pharmaceutical salt could potentially mitigate the common-ion effect. For example, there may be an advantage to using a cocrystal of a HCl salt in

cases in which the salt exhibits too low of a solubility under gastric conditions where excess chloride is present.[116] The solubility order of the salt and its cocrystals in solutions containing physiologically relevant concentrations of chloride (100mM)[121] is : $(FH^+Cl^-)_2FA > FH^+Cl^- > FH^+Cl^-BA$. Based on our experimental measurements, $(FH^+Cl^-)_2FA$ is almost 1.5 times more soluble than the parent salt at 100 mM chloride, and pH 2.3 according to equations (4.33) and (4.12).

Cocrystalline salt-pH dependence

The solubility products and ionization constants evaluated in Table 4.6 were used to generate solubility-pH profiles of FH^+Cl^-, FH^+Cl^-BA and $(FH^+Cl^-)_2FA$. Figure 4.9 shows the predicted cocrystalline salt solubility curves exhibit a plateau under pH conditions in which the coformer is unionized. The salt exhibits a plateau below pH_{max} (pH_{max}=7.6). The FH^+Cl^-BA exhibits a plateau below pH 3.44, and $(FH^+Cl^-)_2FA$ exhibits a plateau below pH 1.4. The aqueous equilibrium solubilities of FH^+Cl^- and FH^+Cl^-BA (Table 4.2) equilibrated to solution pH values in the solubility plateau region, which is the intrinsic solubility (S_0). The $S_0^{1:1cc}$ of FH^+Cl^-BA is 2.2 times lower than the S_0^{salt}. However the FH^+Cl^-BA solubility is predicted to increases with pH due to the ionization of BA resulting in a pH_{max}=5.2 between FH^+Cl^-BA and FH^+Cl^- based on equation (4.10). Above the pH_{max}, FH^+Cl^-BA is predicted to have a higher solubility than the salt. The S_0 of $(FH^+Cl^-)_2$ FA is not significantly higher than that of the parent salt ($p<0.05$). However, the cocrystalline salt solubility is predicted to increase relative to the parent salt as FA ionizes. The cocrystalline salt solubilities were measured at higher pH values to evaluate their solubility-pH dependence.

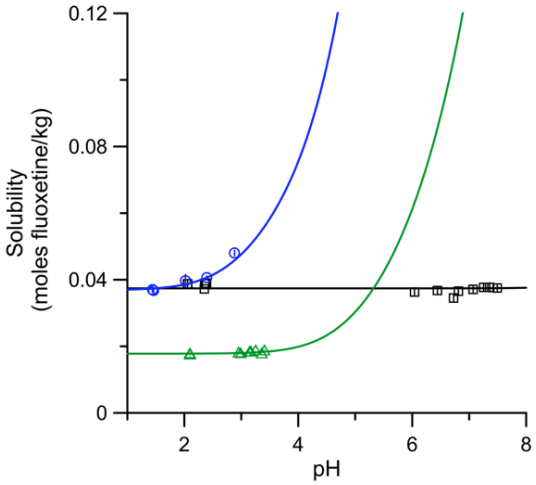

Figure 4.9. Predicted (——) solubility-pH dependence compared to measured solubilities of FH^+Cl^- (□), FH^+Cl^-BA (Δ) and $(FH^+Cl^-)_2FA$ cocrystal (○) at 25°C. All solubilities are expressed in terms of FH^+Cl^- molal concentrations. Cocrystalline salt solubilities were predicted from equations (4.8) and (4.31) using the K_{sp} values in Table 4.6, BA pK_a=4.4, and FA pK_a=2.6, 4.4.

The predicted and measured cocrystalline salt and salt solubilities were in excellent agreement in the pH range examined as shown by Figure 4.9. The salt solubility was measured at pH 2 and pH 6-7.3. FH^+Cl^-BA solubility was only accessible in the plateau region of the curve (pH 2.1 to 3.5). Solubility measurements for FH^+Cl^-BA were approached from above and below the predicted pH_{max} and both attempts resulted in a final solution pH of 3.5. The solubility of $(FH^+Cl^-)_2FA$ was measured between 1.4-2.8. Above pH 2.8 the solution pH could not be independently modified. FH^+Cl^-BA and $(FH^+Cl^-)_2FA$ exhibited degradation in 0.1 m solutions of H_2SO_4, at pH 1. FH^+Cl^-BA also exhibited degradation in a pH 1.4 solution. Degradation was visually observed as suspended solid transformed to oil-like droplets.

The narrow pH region of the FH^+Cl^-BA solubility measurements may be attributed to the self-buffering effects of BA. *Serajuddin et al.* reported difficulty in altering the bulk solution pH of acids such as salicylic acid and BA due to self-buffering effects in the boundary layer.[122] The boundary layer pH of FH^+Cl^-BA salt can be approximated as the equilibrium pH during the solubility measurements (pH 2.1-3.5).[122] $(FH^+Cl^-)_2FA$ solubility measurements also exhibited a narrow pH range. FA is used as a pH modifier to lower the micro-environmental pH of weak bases in pharmaceutical formulations.[123] Due to the excess FA required for the eutectic point measurement, the

pH of the $(FH^+Cl^-)_2FA$ at the eutectic is not representative of the boundary layer pH during dissolution.

The solubility of $(FH^+Cl^-)_2FA$ was determined from the measured component solution concentration in equilibrium at the eutectic between cocrystalline salt and salt to avoid solution-mediated transformation to the parent salt. The solution concentrations used to determine the cocrystalline salt solubility-pH dependence are shown in Table 4.7. The stoichiometric solubility of $(FH^+Cl^-)_2FA$ was determined from the equilibrium component concentrations according to equation (4.36). The stoichiometric solubility is plotted versus solution pH in Figure 4.9.

Table 4.7. $(FH^+Cl^-)_2H_2A$ equilibrium eutectic concentrations of the drug, coformer and chloride in water at various pH values.

pH	$[H_2A]_{T,eu}$ (mM)	$[Cl]_{T,eu}$ (mM)	$[F]_{T,eu}$ (mM)	$S_T^{2:1cc\ b}$ (mM)
1.45±0.01	16.5±0.1	51.4±0.1	27.9±0.2	37±0.2
2.02±0.05	19.6±0.8	44.5±0.6	36±3	40±2
2.39±0.04[a]	23.0±0.3	42±1	37.0±0.2	40.6±0.6
2.88±0.02	36±3	53.3±0.6	35±1	45.5±0.8

(a) Eutectic measured in water

(b) Determined from eutectic component concentrations according to equation (4.37).

The coformer concentration in equilibrium at the eutectic for $(FH^+Cl^-)_2FA$ is predicted to increase with pH according to equation (4.30). As the cocrystalline salt solubility increases with pH, more coformer is required to lower the cocrystalline salt solubility to that of the parent salt via solubility product behavior. The measured coformer eutectic concentrations were found to increase with pH as shown in Figure 4.10, which is in excellent agreement with equation (4.30). The coformer eutectic concentrations of reported cocrystals containing acidic components have also been found to increase with pH as this increases the cocrystal solubility.

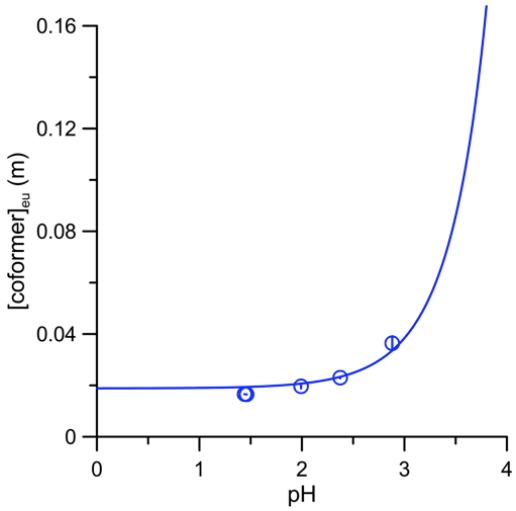

Figure 4.10. Measured $(FH^+Cl^-)_2FA$ (○) coformer eutectic concentration pH dependence at 25°C compared to the (——) predicted eutectic concentration pH according to equation (4.29)

pH dependent supersaturation of the $(FH^+Cl^-)_2FA$ cocrystalline salt

The apparent solution concentration of drug during suspension of $(FH^+Cl^-)_2FA$ in a pH 7 phosphate buffer was evaluated to determine whether cocrystalline salt would generate supersaturation at higher pH conditions. This was done because the pH of a solution in equilibrium with the eutectic point of $(FH^+Cl^-)_2FA$ and FH^+Cl^- could not be independently modified in the region in which the cocrystalline salt exhibits an increased solubility advantage relative to the parent salt (above pH 3). As shown in Figure 4.11(a), $(FH^+Cl^-)_2FA$ does not offer a solubility advantage relative to the parent salt in water, however this may be due to the resulting pH at equilibrium (2.4); the solubility of $(FH^+Cl^-)_2FA$ is not significantly different than that of the salt under these conditions ($p<0.05$ value). When $(FH^+Cl^-)_2FA$ is suspended in pH 7 buffer, the resulting solution concentration of fluoxetine after 24 hours was 2 times higher than the equilibrium solubility of the parent salt, even though $(FH^+Cl^-)_2FA$ transformed to the parent salt, as shown by the XRPD in Figure 4.11(b). The $(FH^+Cl^-)_2FA$ cocrystal did not convert to salt in deionized water as determined by XRPD analysis of the solid phase.

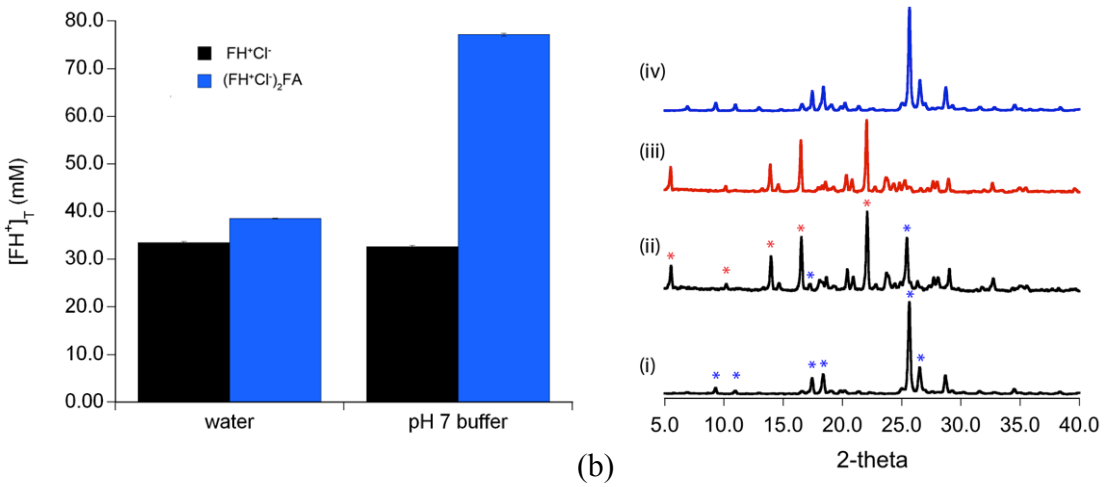

Figure 4.11. Supersaturation generated by $(FH^+Cl^-)_2FA$ relative to parent salt in water and pH 7 buffer. (a) Solution concentrations of $[F]_T$ measured after suspending $(FH^+Cl^-)_2FA$ or salt in water compared to pH 7 buffer. Concentrations were analyzed after suspending solids for 24 hours. (b) XRPD of recovered solid phases after suspending $(FH^+Cl^-)_2FA$ in water (i), and in pH 7 buffer (ii) for 24 hours, compared to the reference diffraction patterns of (iii) salt and (iv) $(FH^+Cl^-)_2FA$.

According to the cocrystalline salt solubility-pH dependence predicted by equation (4.31), $(FH^+Cl^-)_2FA$ is 20 times more soluble than the parent salt at pH 7. The solution concentration of $[F]_T$=77.2 mM generated by $(FH^+Cl^-)_2FA$ is 2 times S_0^{salt} and the final solution pH is 3.2. FA decreases the pH of the solution significantly. At pH 3.2, $(FH^+Cl^-)_2FA$ is predicted to be 1.2 times more soluble than the parent salt. The $(FH^+Cl^-)_2FA$ generated a higher $[F]_T$ in phosphate buffer than that reported for the $(FH^+Cl^-)_2SA$ (58.4 mM) in water. The $(FH^+Cl^-)_2FA$ can sustain a supersaturation of 2 after 24 hours, while the $(FH^+Cl^-)_2SA$ reaches the maximum $[F]_T$ at 1 min followed by a decrease in solution concentration such that $[F]_T=S_0^{salt}$ after only 2 hrs.

Cocrystalline salt and salt solubility when coformer complexes with drug

The solubility of FH^+Cl^- was observed to increase linearly with $[SA]_T$ as shown in Figure 4.12. The linear increase of FH^+Cl^- solubility indicates that the complex formed is first order with respect to SA (FH^+ SA, FH^+_2SA,FH^+_3SA,…,FH^+_MSA).[118,124] The slope of the line was less than unity, thus an apparent complexation constant was determined assuming 1:1 complex formation (FH^+SA). The complexation constant was evaluated from linear regression analysis of the data in Figure 4.12 using equation (4.41) which is

based on reported mathematical models describing 1:1 solution complexation as a first approximation.[118,124]

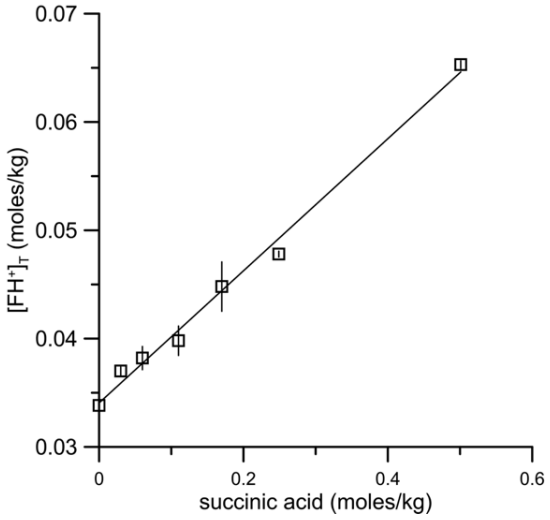

Figure 4.12. FH^+Cl^- solubility as a function of SA concentration in deionized water at 25 °C. Symbols represent experimental data and the line (——) is a result of linear regression of the data (y= 0.0341(±0.0005) + (0.061±0.002)x) used to obtain the apparent complexation constant from equation (4.42), K_{11}=1.9±0.07 m^{-1}.

Both $[F]_T$ and $[Cl]_T$ were observed to increase with $[SA]_T$ from 0.03-0.1m as shown in Table 4.8. The rest of complexation studies were carried out without chloride analysis assuming that $[F]_T = [Cl]_T$.

Table 4.8 Component concentrations in equilibrium with FH^+Cl^- in SA solutions, 25°C

pH	$[SA]_T$ (mM)	$[FH^+]_T$ (mM)	$[Cl^-]_T$ (mM)	S_T^{salt} (mM)
2.90±0.02	29 ± 1	36.9±0.4	39 ± 2	37.9 ± 0.2
2.73±0.02	57 ± 1	38 ± 1	40 ± 2	39 ± 1
2.59±0.02	111 ± 2	39 ± 1	42 ± 2	40.9±0.7

As a first approximation, it was assumed that the ionized base was the species complexing with SA. The unbound, ionized base, $[FH^+]$ was assumed to be the salt solubility in the absence of SA (S_0^{salt}). The following equation has been used to model 1:1 solution complexation:[118]

$$[F]_T = [FH^+] + \frac{K_{11}[FH^+][SA]_T}{1+K_{11}[FH^+]} \qquad (4.41)$$

A linear regression was performed on the experimental salt solubility as a function of $[SA]_T$. Based on equation (4.41), the unbound ionized base can be determined from the y-

intercept of the linear regression and used to obtain the apparent complexation constant (K_{11}) from the slope according to

$$slope = \frac{K_{11}[FH^+]}{1+K_{11}[FH^+]} \quad (4.42)$$

Salt solubility experiments were conducted in deionized water that equilibrated between pH 2 to pH 3. Under these conditions, SA is completely unionized and $[FH^+]$ is completely ionized.

Table 4.9. S_0^{salt} and K_{11} determined from linear regression analysis

Equation of the line	y= 0.0341(±0.0005) + (0.061±0.002)x
K_{11} (m^{-1})	1.91 ±0.07
$S_0^{salt}=[FH^+]$ (m)	0.0341(±0.0005)

The $(FH^+Cl^-)_2SA$ cocrystalline salt has the highest apparent solubility (58.5mM)[79] compared to the other cocrystalline salts of FH^+Cl^-. However, $(FH^+Cl^-)_2SA$ underwent solution-mediated transformation after 1 min in water. In the present study the $(FH^+Cl^-)_2SA$ underwent solution-mediated transformation in solutions containing [SA] ≤0.35 m but did not transform to parent drug in 0.56 m SA after 48 hours (Figure 4.13). The solid phase stability studies indicate that the coformer eutectic is between 0.35 m and 0.56 m (0.56 m> $[coformer]_{eu}$ >0.35 m).

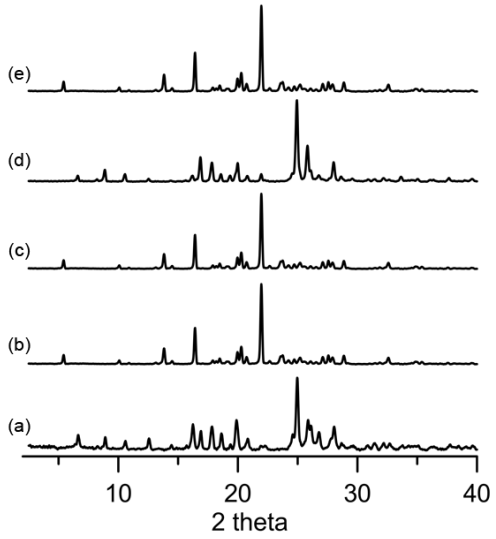

Figure 4.13. XRPD patterns indicating phase stability of 2:1 cocrystal $(FH^+Cl^-)_2SA$ transformation in aqueous solutions of succinic acid; 2:1 cocrystal $(FH^+Cl^-)_2SA$ (a) before slurrying, and (b) after slurrying in 0.22 M SA, and (c) after slurrying in 0.35 m SA and (d) after slurrying in 0.56 m SA; (e) reference pattern of FH^+Cl^- salt.

The solubility of a 2:1 cocrystalline salt in which the coformer solubilizes the parent salt was derived considering cocrystal dissociation and solution complexation under conditions in which the coformer ionization is negligible. The equilibrium reactions and the associated equilibrium constants for cocrystalline salt dissociation in solution and solution complexation are

$$(FH^+Cl^-)_2H_2A_{solid} \overset{Ksp}{\leftrightarrow} FH^+_{aq} + Cl^-_{aq} + H_2A_{aq}$$

$$K_{sp}^{2:1} = [FH^+]^2[Cl^-]^2[H_2A] \quad (4.43)$$

$$FH^+_{aq} + H_2A_{aq} \overset{K11}{\leftrightarrow} FH^+H_2A_{aq}$$

$$K_{11}^{HA} = \frac{[FH^+H_2A]}{[H_2A]} \quad (4.44)$$

Mass balance for the concentration of the drug, coformer and chloride in solution are

$$[F]_T = [FH^+] + [FH^+H_2A_{aq}] \quad (4.45)$$

$$[A]_T = [H_2A] + [FH^+H_2A_{aq}] \quad (4.46)$$

$$[Cl]_T = [Cl^-] \quad (4.47)$$

Substituting $K_{sp}^{2:1cc}$ and K_{11} (equations (4.43) and (4.44)) for $[FH^+]$ and $[FH^+H_2A]$ in equations (4.45) and (4.46) gives

$$[F]_T = \frac{1}{[Cl]_T}\sqrt{\frac{K_{sp}^{2:1}}{[H_2A]}} + \frac{K_{11}}{[Cl]_T}\sqrt{K_{sp}^{2:1}[H_2A]} \quad (4.48)$$

$$[A]_T = [H_2A](1 + K_{11}[FH^+]) \quad (4.49)$$

Re-arranging equation (4.48)

$$[F]_T[Cl]_T = \sqrt{\frac{K_{sp}^{2:1}}{[H_2A]}} + K_{11}\sqrt{K_{sp}^{2:1}[H_2A]} \quad (4.50)$$

Because SA is observed to have high solution concentration above the eutectic, the free $[H_2A]=[H_2A]_T$ as a first approximation. Assuming $[FH^+H_2A]_T << [H_2A]$ because of the high concentration of SA required to reach the eutectic between cocrystalline salt and salt:

$$[H_2A]_T = [H_2A] \quad (4.51)$$

Therefore

$$[F]_T = [FH^+](1 + K_{11}[H_2A]_T) \quad (4.52)$$

Squaring both sides of equation(4.50) and inserting (4.51) results in

$$([F]_T[Cl]_T)^2 = \frac{K_{sp}^{2:1}}{[H_2A]} + 2K_{11}K_{sp}^{2:1} + {K_{11}}^2K_{sp}^{2:1}[H_2A]_T \quad (4.53)$$

The cocrystalline salt solubility in solutions containing excess coformer is determined from equation (4.53) assuming $[F]_T=[Cl]_T=2S_T^{2:1cc}$. The following expression is in terms of moles of drug:

$$S_T^{2:1cc} = 2x\sqrt[4]{\frac{1}{16}\left(\frac{K_{sp}^{2:1cc}}{[H_2A]_T} + 2K_{11}K_{sp}^{2:1cc} + {K_{11}}^2K_{sp}^{2:1cc}[H_2A]_T\right)} \quad (4.54)$$

Table 4.10 shows the measured component solution concentrations in equilibrium with $(FH^+Cl^-)_2SA$. According to the phase stability studies the cocrystalline salt is the thermodynamically stable phase when suspended in $[SA]_T \geq 0.56$ m. The $(FH^+Cl^-)_2SA$ K_{sp} was evaluated from measured component solution concentrations under solution conditions in which the cocrystalline salt is the thermodynamically stable phase (in aqueous solutions above $[coformer]_{eu}$)).

Table 4.10. Component solution concentrations in equilibrium with $(FH^+Cl^-)_2SA$

pH_{water}	$[F]_T$ (mM)	$[SA]_T$ (mM)	$[FH^+]^a$ (mM)	$[Cl^-]^b$ (mM)	$S_0^{2:1cc}$ (mM)	$K_{sp}{}^c$
2.22±0.04	61.7±0.1	540±2	30.3±0.1	61.7±0.1	82.4 ± 0.8	(1.89±0.08)x10^{-7} m^5
1.99±0.01	60.3±0.3	650±20	26.9±0.7	60.3±0.3	80.7 ± 0.1	(1.7±0.2) x10^{-7} m^5

(a) Calculated according to equation (4.57)
(b) Calculated according to equation (4.55)
(c) Calculated from $[FH^+]$, $[Cl^-]$ and $[H_2A]$ according to equation (4.43).

The measured component solution concentrations were used to determine the K_{sp} from the unbound solution concentrations of the cocrystalline salt component. The unbound concentrations were determined according to

$$[Cl^-] = [Cl\ \ ]_T = [F]_T \quad (4.55)$$

$$[H_2A] = [H_2A]_T \quad (4.56)$$

$$[FH^+] = \frac{[F]_T}{(1 + K_{11}[H_2A]_T)} \quad (4.57)$$

which were obtained from equation (4.51) and(4.52). The average K_{sp} determined at 0.54m and 0.65 m SA is $K_{sp}^{2:1cc}$=(1.8±0.1) x10^{-7} m^5. This was used to generate a phase

solubility diagram of $(FH^+Cl^-)_2SA$ and FH^+Cl^- using equations (4.54) and (4.52) respectively.

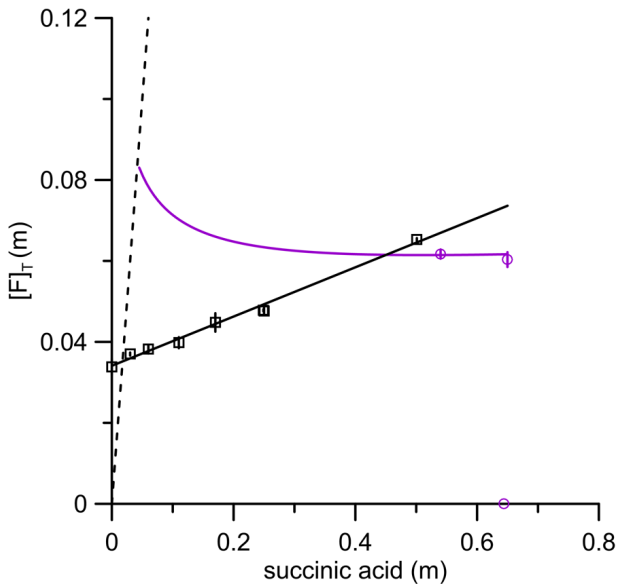

Figure 4.14. Predicted effect of 1:1 complexation on the solubility of a 2:1 cocrystalline salt (—) and its (—) parent salt as a function of $[SA]_T$ compared to the measured cocrystalline salt (○) and salt (□). The predicted cocrystalline salt solubility and salt solubility curves were generated from equations (4.54) and (4.41) using, $K_{sp}^{2:1cc}$=(1.8±0.1) x10^{-7} m^5, K_{11}=1.91±0.07 m^{-1}, and K_{sp}^{salt}=(1.40±0.03) x10^{-3} m^2.

$(FH^+Cl^-)_2SA$ is predicted to decrease with increasing $[SA]_T$. However, the solubility curve exhibits the highest rate of change under solution conditions in which the cocrystalline salt is not the thermodynamically stable phase. Above $[coformer]_{eu}$, the cocrystalline salt solubility is not predicted to change significantly, which was confirmed by the solubility studies in Table 4.10. The stoichiometric solubility in the absence of excess coformer was calculated to be 82 mM, which is 1.4 times higher than the apparent solubility.[79]

Lattice and Solvation Contributions to Cocrystalline Salt aqueous solubility.

Salt and cocrystalline salt melting temperature, T_m, and melting enthalpy, ΔH_m, were obtained from analysis of the DSC thermographs shown in (4.15). T_m and ΔH_m measured in this study are in agreement with the values reported by *Childs et al*.[79] The cocrystalline salts exhibit unique melting properties relative to the parent salt. The ideal solubilities of the cocrystalline salts and the parent salt were calculated from T_m and ΔH_m to determine the lattice energy contributions to solubility. The ideal solubility quantifies the lattice energy contribution to the solubility and is solvent independent. The measured

solubility of a solid depends on the release of solute molecules from the crystal lattice (lattice energy) and the solvation of the released solute molecules (solvation energy). The free energy of solution considering lattice and solvation energy contributions is described by the following equation:

$$\Delta G_{solution} = \Delta G_{lattice} + \Delta G_{solvation} \quad (4.58)$$

The free energy of solution can be reduced by lowering the $\Delta G_{lattice}$ and/or by lowering the $\Delta G_{solvation}$. Cocrystallization and salt formation of a drug affects both lattice and solvation energies.

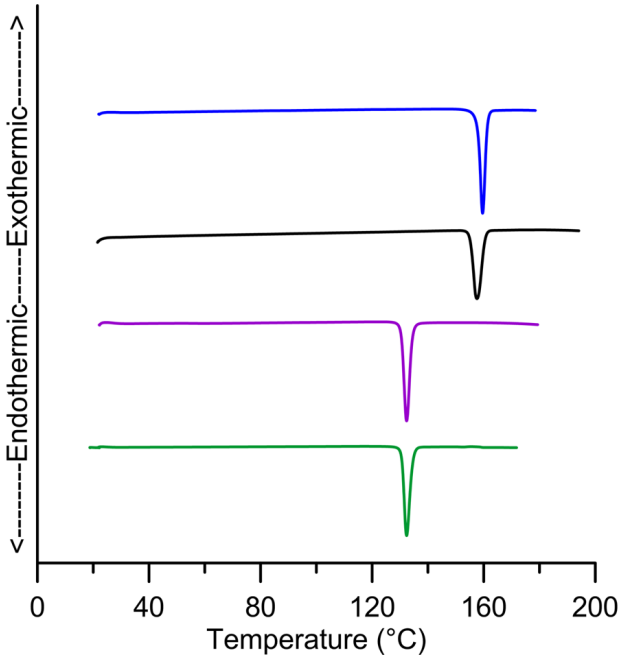

Figure 4.15 DSC for $(FH^+Cl^-)_2FA$ (——), FH^+Cl^- (——), $(FH^+Cl^-)_2SA$ (——) and FH^+Cl^-BA (——).

The ideal mole fraction solubility (X_{ideal}) was calculated from the following equation assuming that the heat capacity change upon melting is zero and the enthalpy of the solution (ΔH_{Sideal}) is equal to the enthalpy of melting (ΔH_m):

$$\log_{10} X_{ideal} = \frac{-\Delta H_m}{2.303R}\left(\frac{T_m - T}{T_m T}\right) \quad (4.59)$$

where T is the solution temperature (298K), T_m is the melting temperature (in Kelvin) and R is the gas constant. The enthalpy of melting, ΔH_m listed in Table 4.11, was normalized by the cocrystalline salt or salt stoichiometry.[4,111] This method is analogous to

what has been done to obtain ideal solubility values of cocrystal and salt forms, wherein the melting enthalpy is normalized per mole of constituent ions.[111]

Table 4.11 Ideal and Measured Aqueous Solubilities of Salt and Cocrystalline Salts

crystalline phase	Solubility (m)		T_m (°C)	ΔH_m [c] (kj/mol)
	Ideal [a]	Experimental (S_0)[b]		
FH^+Cl^-	5.8	$3.7x10^{-2}$	157.7	18.9
FH^+Cl^-BA	9.4	$1.8x10^{-2}$	131.6	18.2
$(FH^+Cl^-)_2FA$	11.8	$3.7x10^{-2}$	160.2	19.2
$(FH^+Cl^-)_2SA$	16.3	$8.2x10^{-2}$	132.6	18.6

(a) Ideal solubilities were calculated using equation (4.59). Mole fraction cocrystal was converted to moles drug/ kg solvent.
(b) Experimental intrinsic solubility (when coformer is unionized) from Table 4.6 (FH^+Cl^-, FH^+Cl^-BA and $(FH^+Cl^-)_2FA$) and Table 4.9 ($(FH^+Cl^-)_2SA$) in moles drug/kg
(c) Measured heats of fusion were normalized by moles of component constituents (i.e. 2 for the 1:1 salt, 3 for the cocrystal of a 1:1 salt and 5 for the 2:1 cocrystal of a 1:1 salt).

Based on the results in Table 4.11, the aqueous solubilities are 10^2 times lower than the ideal solubilities indicating that solvation of the hydrophobic drug is the main barrier for both salt and cocrystalline salt solubilization in water. The ideal solubilities were compared to the measured solubilities to determine the contributions of lattice versus solvation energy. The solvation contribution (γ) was evaluated from the measured aqueous solubility under nonionizing conditions and the calculated ideal solubility (X_{ideal}) according to the following equation:

$$\log_{10} X = \log_{10} X_{ideal} - \log_{10} \gamma \qquad (4.60)$$

Figure 4.16 plots the $\log_{10} X_{ideal}$ and the $-\log_{10} \gamma$ based on the methods described by *Pinal et al.*[125] The lattice contribution to the solubility is not sufficient for predicting the cocrystalline salt solubility relative to the parent salt.

While the ideal solubility of FH^+Cl^-BA is 1.6 times higher than that of the parent salt, the measured solubility is 2 times lower. $(FH^+Cl^-)_2FA$ and $(FH^+Cl^-)_2SA$ lower the solvation energy compared to the parent salt. The magnitude of the lattice contribution is much smaller than the solvation contributions for both cocrystalline salts and the parent salt. These results indicate that parameters associated with crystal lattice energy, such as T_m and ΔH_m are not sufficient for predicting cocrystalline salt solubility relative to the parent salt. The solution chemistry of the salt and its cocrystalline salts appear to be critical for describing their solubility behavior.

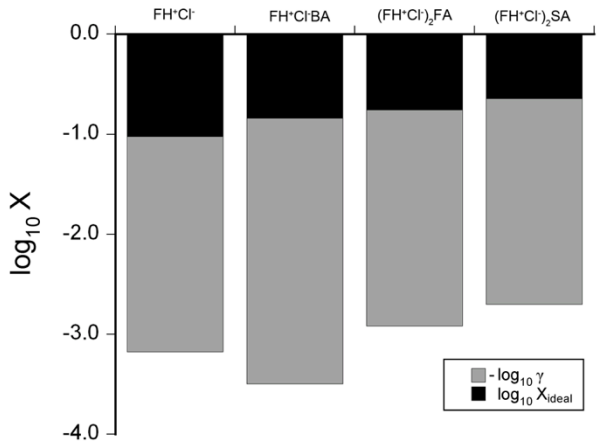

Figure 4.16. Lattice energy ($\log_{10}X_{ideal}$) and solvation energy (plotted as $-\log_{10}\gamma$) contributions to the measured aqueous solubilities of FH^+Cl^-, FH^+Cl^-BA, $(FH^+Cl^-)_2FA$, $(FH^+Cl^-)_2SA$. The black area of the bars represents $\log_{10} X_{ideal}$ calculated from equation (4.59). The grey area represents $-\log_{10}\gamma$ calculated from equation (4.60).

Conclusions

In this work, novel mathematical models are presented that explain the solubility behavior of 1:1 and 2:1 cocrystalline salts as a function of component concentrations in solution and the ionization of the cocrystalline salt components. For the first time we are able to predict cocrystalline salt solubility under a variety of conditions from a single water solubility measurement and the derived mathematical models presented in this chapter. These models are useful to define the parameters and minimum experiments required to properly assess and characterize the solubility behavior of cocrystalline salts. These models can also guide coformer selection to achieve a desired solubility-pH profile. The solubility-pH profile is dependent on the ionization behavior of the coformer when the coformer ionizes at a lower pH than the pH_{max} of the salt. The eutectic point between the cocrystalline salt and salt was useful to access the equliibrium solubility of a metastable cocrystalline salt. As predicted, the measured equilibrium coformer eutectic concentrations were dependent on the solution pH. Cocrystalline salt solubility-$[H^+]$ dependence can be calculated from knowledge of the cocrystalline salt solubility product (K_{sp}) and its component ionization constants (K_a) based on the equations presented in the theoretical section. The solubility product can be obtained from a single solubility measurement of cocrystalline salt, therefore the cocrystalline salt solubility can be predicted in the entire pH range from a single solubility measurement.

References

4. Good DJ, Rodríguez-Hornedo Nr 2009. Solubility Advantage of Pharmaceutical Cocrystals. Cryst Growth Des 9(5):2252-2264.

12. Petruševski G, Naumov P, Jovanovski G, Ng SW 2008. Unprecedented sodium–oxygen clusters in the solid-state structure of trisodium hydrogentetravalproate monohydrate: A model for the physiological activity of the anticonvulsant drug Epilim®. Inorganic Chemistry Communications 11(1):81-84.

14. Bethune SJ, Huang N, Jayasankar A, Rodriguez-Hornedo N 2009. Understanding and Predicting the Effect of Cocrystal Components and pH on Cocrystal Solubility. Cryst Growth Des 9(9):3976-3988.

15. Huang N, Rodriguez-Hornedo N 2011. Engineering cocrystal thermodynamic stability and eutectic points by micellar solubilization and ionization. Crystengcomm 13(17):5409-5422.

16. Huang N, Rodríguez-Hornedo N 2011. Engineering cocrystal solubility, stability, and pHmax by micellar solubilization. Journal of Pharmaceutical Sciences 100(12):5219-5234.

18. Alhalaweh A, Roy L, Rodríguez-Hornedo N, Velaga SP 2012. pH-Dependent Solubility of Indomethacin–Saccharin and Carbamazepine–Saccharin Cocrystals in Aqueous Media. Molecular Pharmaceutics.

36. Nehm SJ, Rodríguez-Spong B, Rodríguez-Hornedo N 2005. Phase Solubility Diagrams of Cocrystals Are Explained by Solubility Product and Solution Complexation. Cryst Growth Des 6(2):592-600.

41. Stahl PH, Wermuth CG, International Union of P, Applied C. 2011. Handbook of pharmaceutical salts: properties, selection, and use. ed., Zürich: VHCA ; Weinheim : Wiley-VCH. p xvi, 446 p.

42. Kramer SF, Flynn GL 1972. Solubility of organic hydrochlorides. Journal of Pharmaceutical Sciences 61(12):1896-1904.

43. Chowhan ZT 1978. pH-solubility profiles of organic carboxylic acids and their salts. Journal of Pharmaceutical Sciences 67(9):1257-1260.

44. Bogardus JB, Blackwood RK 1979. Solubility of doxycycline in aqueous solution. Journal of Pharmaceutical Sciences 68(2):188-194.

45. Serajuddin A, Sheen PC, Augustine MA 1987. Common ion effect on solubility and dissolution rate of the sodium salt of an organic acid. Journal of Pharmacy and Pharmacology 39(8):587-591.

47. Huang N. 2011. Engineering Cocrystal Solubility and Stability via Ionization and Micellar Solubilization. Pharmaceutical Sciences, ed., Ann Arbor, MI: University of Michigan.

48. Mooney KG, Mintun MA, Himmelstein KJ, Stella VJ 1981. Dissolution kinetics of carboxylic acids I: Effect of pH under unbuffered conditions. Journal of Pharmaceutical Sciences 70(1):13-22.

76. Yadav AV, Dabke AP, Shete AS 2010. Crystal engineering to improve physicochemical properties of mefloquine hydrochloride. Drug Development and Industrial Pharmacy 36(9):1036-1045.

79. Childs SL, Chyall LJ, Dunlap JT, Smolenskaya VN, Stahly BC, Stahly GP 2004. Crystal engineering approach to forming cocrystals of amine hydrochlorides with organic

acids. Molecular complexes of fluoxetine hydrochloride with benzoic, succinic, and fumaric acids. J Am Chem Soc 126(41):13335-13342.
88. KG Mooney MMHK, Stella VJ 1981. Dissolution kinetics of carboxylic acids I:effect of pH under unbuffered condtions. J Pharm Sci 70:13-22.
95. Good DJ, Rodríguez-Hornedo Nr 2010. Cocrystal Eutectic Constants and Prediction of Solubility Behavior. Cryst Growth Des 10(3):1028-1032.
109. Maheshwari C, Andre V, Reddy S, Roy L, Duarte T, Rodriguez-Hornedo N 2012. Tailoring aqueous solubility of a highly soluble compound via cocrystallization: effect of coformer ionization, pHmax and solute-solvent interactions. Crystengcomm 14(14):4801-4811.
110. Reddy LS, Bethune SJ, Kampf JW, Rodríguez-Hornedo Nr 2008. Cocrystals and Salts of Gabapentin: pH Dependent Cocrystal Stability and Solubility. Cryst Growth Des 9(1):378-385.
111. Black SN, Collier EA, Davey RJ, Roberts RJ 2007. Structure, solubility, screening, and synthesis of molecular salts. Journal of Pharmaceutical Sciences 96(5):1053-1068.
112. Chen AM, Ellison ME, Peresypkin A, Wenslow RM, Variankaval N, Savarin CG, Natishan TK, Mathre DJ, Dormer PG, Euler DH, Ball RG, Ye Z, Wang Y, Santos I 2007. Development of a pharmaceutical cocrystal of a monophosphate salt with phosphoric acid. Chemical Communications (4):419-421.
113. Velaga SP, Basavoju S, Boström D 2008. Norfloxacin saccharinate–saccharin dihydrate cocrystal – A new pharmaceutical cocrystal with an organic counter ion. Journal of Molecular Structure 889(1–3):150-153.
114. Paluch KJ, Tajber L, Elcoate CJ, Corrigan OI, Lawrence SE, Healy AM 2011. Solid-state characterization of novel active pharmaceutical ingredients: Cocrystal of a salbutamol hemiadipate salt with adipic acid (2:1:1) and salbutamol hemisuccinate salt. Journal of Pharmaceutical Sciences 100(8):3268-3283.
115. Harrison WTA, Yathirajan HS, Bindya S, Anilkumar HG, Devaraju 2007. Escitalopram oxalate: co-existence of oxalate dianions and oxalic acid molecules in the same crystal. Acta Crystallographica Section C 63(2):o129-o131.
116. Engel GL, Farid NA, Faul MM, Richardson LA, Winneroski LL 2000. Salt form selection and characterization of LY333531 mesylate monohydrate. International Journal of Pharmaceutics 198(2):239-247.
117. Gould PL 1986. Salt selection for basic drugs. International Journal of Pharmaceutics 33(1):201-217.
118. Higuchi TC, K. A. . 1965. Phase-Solubility Techniques. In Reilley C, editor Advances in Analytical Chemistry and Instrumentation, ed. p 117-212.
119. German WL 1936. LXIII. The thermodynamic primary and secondary dissociation constants of maleic and fumaric acids. London, Edinburgh and Dublin philosophical magazine and journal of science 22(149):790.
120. Bethune SJ. 2009. Thermodynamic and kinetic parameters that explain crystallization and solubility of pharmaceutical cocrystals. Pharmaceutical Sciences, ed., Ann Arbor, MI: University of Michigan.
121. Lindahl A, Ungell A-L, Knutson L, Lennernäs H 1997. Characterization of Fluids from the Stomach and Proximal Jejunum in Men and Women. Pharm Res 14(4):497-502.

122. Serajuddin A, Jarowski CI 1985. Effect of diffusion layer pH and solubility on the dissolution rate of pharmaceutical acids and their sodium salts II: Salicylic acid, theophylline, and benzoic acid. Journal of Pharmaceutical Sciences 74(2):148-154.
123. Bassi P, Kaur G 2010. pH modulation: a mechanism to obtain pH-independent drug release. Expert Opinion on Drug Delivery 7(7):845-857.
124. Higuchi T, Bolton S 1959. The solubility and complexing properties of oxytetracycline and tetracycline III. Interactions in aqueous solution with model compounds, biochemicals, metals, chelates, and hexametaphosphate. Journal of the American Pharmaceutical Association 48(10):557-564.
125. Miyako Y, Tai H, Ikeda K, Kume R, Pinal R 2008. Solubility Screening on a Series of Structurally Related Compounds: Cosolvent-Induced Changes on the Activity Coefficient of Hydrophobic Solutes. Drug Development and Industrial Pharmacy 34(5):499-505.

Chapter 5

Importance of characterizing surfactant interactions with cocrystal components to modulate the cocrystal solubility advantage

Introduction

There are increased reports of cocrystals that offer superior pharmaceutical properties relative to the parent drug including but not limited to chemical stability, hygroscopicity, compactability, tensile strength, compaction, solubility, dissolution and bioavailability.[5,10,34,78] Any cocrystal that exhibits $S_{cocrystal} > S_{drug}$ is at risk for solution-mediated transformation to the less soluble drug form, which could complicate the formulation, processing, and evaluation of a cocrystal solid form. The higher the cocrystal solubility is relative to the drug, the greater the driving force for transformation.

Cocrystal solubility is highly dependent on solution composition and additives that interact differentially with the cocrystal components have a profound effect on the cocrystal solubility and $S_{cocrystal}/S_{drug}$. The surfactant SLS, and the polymer PVP are both reported to lower the $S_{cocrystal}/S_{drug}$ of carbamazepine cocrystals.[15-17,126] The surfactant sodium lauryl sulfate (SLS) was recently found to impart thermodynamic stability to the carbamazepine-saccharin (CBZ-SAC) and carbamazepine-salicylic acid (CBZ-SLC) cocrystals, which are otherwise unstable in solution.[15-17] PVP was found to lower the $S_{cocrystal}/S_{drug}$ of carbamazepine nicotinamide,[126] however the cocrystal was not thermodynamically stabilized (i.e. $S_{cocrystal}/S_{drug}=1$) by PVP. The mechanism responsible for these behaviors was the severe asymmetric solubilization of the cocrystal components.

In order to utilize cocrystals as a solid form it is essential to streamline the characterization of the cocrystal solution interactions with potential excipients, additives or solvents that may come into contact with a cocrystal during processing. The eutectic point measurement is a useful tool for determining the stability of a cocrystal relative to the parent drug, the cocrystal solubility, and $S_{cocrystal}/S_{drug}$ under different solution

conditions.[4,15,95] From one eutectic measurement in water and one eutectic measurement in the presence of surfactant (above the CMC), it is possible to measure $S_{cocrystal}$, $S_{cocrystal}/S_{drug}$ and estimate the micellar solubilization constants of the cocrystal components, K_s^{drug} and $K_s^{coformer}$.

The interactions of two Pluronic® surfactants with cocrystals of carbamazepine were characterized using eutectic measurements. F127 and P103 were selected as they have been shown to increase the solubility of monoclinic carbamazepine 4-fold with 5% (w/v) surfactant in solution.[53] F127 has also been used as a hydrophilic stabilizer to coat CBZIII resulting in enhanced dissolution.[127] The physicochemical properties of the surfactants studied are shown in Table 5.1.

Table 5.1 Physicochemical properties of Pluronic block copolymers.

Pluronic	MW (g/mol)	CMC (M)[128] at 30°C	Structure
P103	4950	$6.1x10^{-6}$	$EO_{17}PO_{60}EO_{17}$
F127	12600	$2.8\ x10^{-6}$	$EO_{100}PO_{65}EO_{100}$

Both surfactants form micelles at relative low concentrations according the their critical micelle concentrations (CMC), thus very small concentrations of surfactant are expected to affect the cocrystal solubility and $S_{cocrystal}/S_{drug}$.

Materials and methods

Materials

Anhydrous monoclinic carbamazepine (CBZ III), saccharin (SAC) and salicylic acid (SLC) were purchased from Sigma Chemical Company (St. Louis, MO) and used as received. CBZ III was stored at 5° C over anhydrous calcium sulfate. P103 and F127 were received as gifts from BASF Corp. Parsippany, NJ, USA and used without further purification. Water used in this study was filtered through a double deionized purification system (Milli Q Plus Water System from Millipore Co., Bedford, MA).

Cocrystal synthesis

Cocrystals were prepared by reaction crystallization. The carbamazepine-saccharin cocrystal (CBZ-SAC) was prepared by adding 1.12 g of CBZA and 0.87 g SAC to 10 ml of 0.05 m SAC solution in ethanol. The carbamazepine-salicylic acid cocrystal (CBZ-SLC) was prepared by adding 1.26 g CBZ III and 0.40 g of SLC to a 10 ml solution of

0.01 m SLC solution in acetonitrile. CBZ dihydrate (CBZ (H)) was prepared in water. Solid phases were characterized by XRPD

Measurement of cocrystal eutectic points

Cocrystal eutectic points were measured in water without surfactant and aqueous solutions containing 0.0269 m (13.3% w/w) P103 and 0.0098 m (12.3 % w/w) F127 at 25 ±0.1°C. 50-100 mg of cocrystal and 50-80 mg of CBZ (H) were suspended in 3 mL of aqueous media for up to 4 days. The pH at equilibrium was measured but not independently modified. Cocrystal stoichiometric solubilities were determined from the measured eutectic concentrations according to $S_{cocrystal}=\sqrt{[drug]_{T,eu}[coformer]_{T,eu}}$ and the cocrystal solubility advantage was determined according to $\frac{S_{cocrystal}}{S_{drug}}=\sqrt{\frac{[coformer]_{eu}}{[drug]_{eu}}}$. [16,18] A detailed discussion of eutectic point measurements has been discussed elsewhere.[4,95] Drug and coformer concentrations were analyzed by HPLC. Solid phases at equilibrium were confirmed by XRPD.

High performance Liquid Chromatography (HPLC)

The solution concentrations of CBZ and coformer were analyzed by Waters HPLC (Milford, MA) equipped with a UV-vis spectrometer detector. Empower 2, Waters' operation software, was used to collect and process the data. A C18 Atlantis column (5 μm, 4.6 x 250 mm; Waters, Milford, MA) at ambient temperature was used to separate drug and coformer. The mobile phase was composed of 55% methanol and 45% water with 0.1% trifluoroacetic acid and the flow rate was 1 mL/min using an isocratic method. Injection sample volume was 20 μL. Absorbance of CBZ, SLC, and SAC, was monitored at 284, 303, and 230, respectively. All concentrations are reported in molality (moles solute/kilogram solvent).

X-ray Powder Diffraction

XRPD diffractograms of solid phases were collected with a benchtop Rigaku Miniflex X-ray diffractometer (Danvers, MA) using CuKα radiation (λ = 1.54 Å), a tube voltage of 30 kV, and a tube current of 15 mA. Data were collected from 5 to 40 ° at a continuous scan rate of 2.5°/min.

Results

CBZ III has been shown to maintain a supersaturation of 3 with respect to the CBZ dihydrate (CBZ (H)) for up to 20 hours. There are over 50 cocrystals of CBZ; two cocrystals reported to exhibit a solubility advantage relative to drug include carbamazepine-saccharin (CBZ-SAC), and carbamazepine salicylic acid (CBZ-SLC). CBZ-SAC is reported to be 4.5 times more soluble than CBZ (H) in water (pH 2.2) and CBZ-SLC is 2.5 times more soluble in water. The cocrystal solubility and $S_{cocrystal}/S_{drug}$ in water have been studied by eutectic point measurements.[4,14] The ratio of cocrystal component concentration in equilibrium at the eutectic between drug and cocrystal, $[coformer]_{eu}$ to $[drug]_{eu}$, is a function of the cocrystal solubility advantage ($S_{cocrystal}/S_{drug}$). This ratio has been referred to as the eutectic constant, $K_{eu,}$ which is adopted from the racemic solid-state literature. The K_{eu} is related to the solution concentrations and $S_{cocrystal}/S_{drug}$ according to

$$K_{eu}=\frac{[coformer]_{eu}}{[drug]_{eu}}=\left(\frac{S_{cocrystal}}{S_{drug}}\right)^2 \qquad (5.1)$$

for a 1:1 cocrystal.[95]

This relationship is useful to characterize the cocrystal solubility relative to the parent drug from the solution composition in equilibrium at the eutectic point. For example, $[coformer]_{eu}>[drug]_{eu}$, indicates $S_{cocrystal}>S_{drug}$, $[coformer]_{eu}=[drug]_{eu}$, indicates $S_{cocrystal}=S_{drug}$,and $[coformer]_{eu} < [drug]_{eu}$ indicates $S_{cocrystal}<S_{drug}$. Figure 5.1 shows the CBZ-SAC component concentrations in equilibrium at the eutectic point in water, 0.0269 m P103 and 0.0098 m F127. Drug and coformer are solubilized by F127 and P103, which is evident from the increase in $[drug]_{eu}$ and $[coformer]_{eu}$ in surfactant solutions relative to water. The CBZ-SAC $S_{cocrystal}/S_{drug}$ in the surfactant solutions was ½ as much as the $S_{cocrystal}/S_{drug}$ in water at the same pH. The decrease in $S_{cocrystal}/S_{drug}$ indicates that drug is preferentially solubilized relative to the coformer. Therefore both P103 and F127 may be useful to lower $S_{cocrystal}/S_{drug}$ of the CBZ-SAC cocrystal to mitigate solution-mediated transformation.

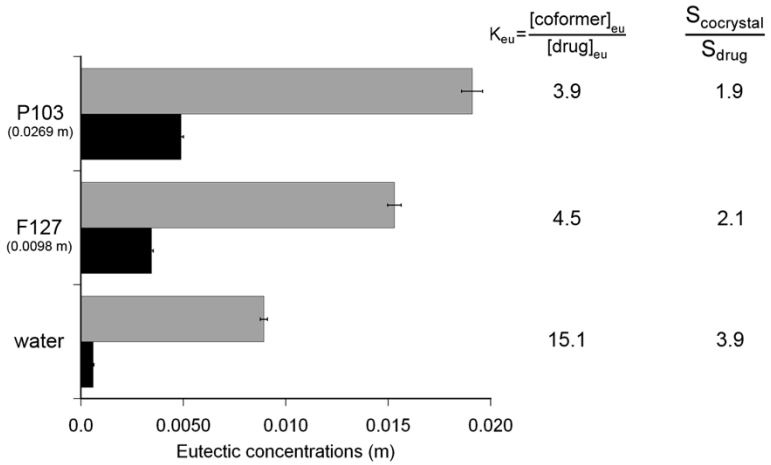

Figure 5.1. CBZ-SAC eutectic point composition in aqueous solutions containing the Pluronic® surfactants compared to water at pH 2.2, 25°C.

CBZ-SLC is only 2 times mores soluble than the drug in water (pH 3). The effect of P103 and F127 on the CBZ-SLC eutectic point compositions, was much different than that observed for CBZ-SAC. Figure 5.2 shows that the CBZ-SLC eutectic component concentrations are higher in the surfactant solutions than in water, indicating that both components are being solubilized in P103 and F127. However, $S_{cocrystal}/S_{drug}$ was higher in solutions containing P103, and F127 relative to water at the same pH, which has not been observed before in surfactant solutions and suggests that the coformer is preferentially solubilized relative to the drug.

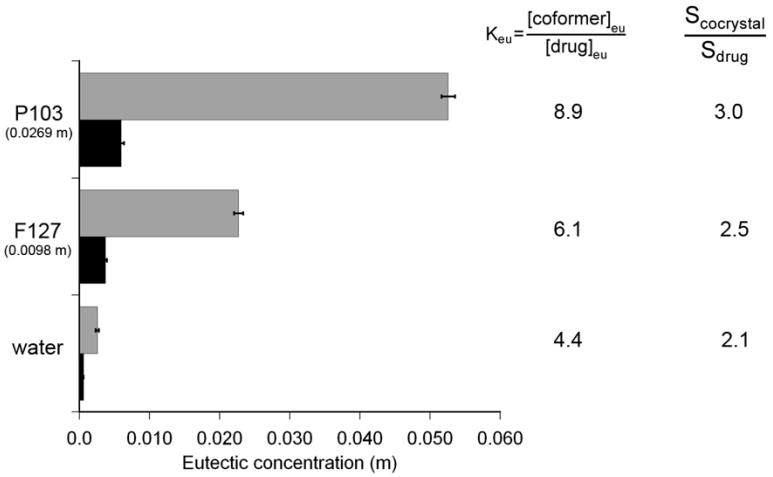

Figure 5.2. Solubilization of CBZ-SLC components by Pluronic surfactants in equilibrium at the eutectic point at pH 3, 25°C.

The K_s values of both cocrystal components were estimated from eutectic point measurements. The K_s of the nonionizable drug was determined according to

$$[CBZ]_{eu,T}=[CBZ]_{eu,aq}\left(1+K_s^R[M]\right) \quad (5.2)$$

where $[CBZ]_{eu,aq}$ is the drug eutectic concentration in an aqueous solution without surfactant, and [M] is the micellar concentration of surfactant.[15] The K_s of an acidic component such as saccharin or salicylic acid, HA, is determined according to

$$[HA]_{eu,T}=[HA]_{eu,un}\left(1+\frac{K_a^{HA}}{[H^+]}+K_s^{HA,T}[M]\right) \quad (5.3)$$

where $[HA]_{eu,un}$ is unionized coformer concentration in an aqueous solution without surfactant, and K_a^{HA} is the ionization constant of the acid.[15]

Table 5.2 shows the micellar solubilization constants estimated from the CBZ-SAC eutectic point measurements in surfactant relative to water according to equations (5.2) and (5.3). Carbamazepine was preferentially solubilized by both P103 and F127 ($K_s^{CBZ}>K_s^{SAC}$). However, the solubilization of saccharin by both P103 and F127 is quite large compared to the solubilization observed in other surfactants such as SLS, Tween 80, Myrj 52 and Brij 99, which range from 8-83 m^{-1} (Chapter 2). To achieve a critical stabilization concentration (CSC) such that the $S_{cocrystal}=S_{drug}$, the following relationship between drug and coformer solubilization must apply

$$K_s^{CBZ}>\frac{Ksp}{\left(CBZ_{aq}\right)^2}K_s^{HA,T} \quad (5.4)$$

according to the findings in chapter 2. At pH 2.2, $\frac{K_{sp}^{CBZ-SAC}}{\left(CBZ_{aq}\right)^2}=2$,[18] therefore the K_s^{CBZ} must be 2 times greater than the $K_s^{SAC,T}$ to achieve a CSC. Unfortunately, the solubilization constant, K_s^{CBZ}, is only 1.2 times higher than $K_s^{SAC,T}$, in both Pluronic F127 and Pluronic P103, and therefore neither surfactant achieves a CSC for CBZ-SAC.

Table 5.2 CBZ-SAC eutectic concentrations in equilibrium with solutions containing surfactant compared to water, 25 °C.

Surfactant	[M] (m)	pH	$[CBZ]_{eu}$ (mM)	$[SAC]_{eu}$ (mM)	K_s^{CBZ} (m^{-1})	$K_s^{SAC,T}$ (m^{-1})
None[a]	0	2.20±0.03	0.59±0.05	8.9±0.2	----	----
P103	0.0269	2.19±0.03	5.0±0.1	19.1±00.5	280±10	230±20
F127	0.0098	2.16±0.08	3.45±0.09	15.3±0.03	510±20	430±80

a) Ref[47,120]

The micellar solubilization constants of CBZ and SLC were determined from the eutectic concentrations in surfactant solutions relative to water according to equations (5.2) and (5.3). The solubilization of SLC was 3.7 times higher than that observed for

CBZ (H) in P103 and 2.5 times higher in F127. This is the first report of a surfactant preferentially solubilizing the coformer($K_s^{SLC,T} >> K_s^{CBZ}$), resulting in an increase in the measured $S_{cocrystal}/S_{drug}$ in a surfactant solution.

Table 5.3 CBZ-SLC eutectic concentrations in equilibrium with solutions containing surfactant compared to water, 25 °C.

Surfactant	[M] (m)	pH	$[CBZ]_{eu}$ (mM)	SLC_{eu} (mM)	K_s^{CBZ} (m^{-1})	$K_s^{SLC,T}$ (m^{-1})
None[a]	0	2.91±0.05	0.59±0.01	2.6±0.3	----	----
P103	0.0269	3.13 ± 0.04	5.9±0.4	50 ±10	350±30	1300±200
F127	0.0098	3.13 ± 0.07	3.8 ±0.2	22.7±0.7	570±40	1400±200

(a) Ref[47,120]

Predicted $S_{cocrystal}/S_{drug}$ dependence on [M] CBZ-SAC and CBZ-SLC

The solubilization constants calculated in the previous section were used to predict the cocrystal solubility and $S_{cocrystal}/S_{drug}$ dependence on micellar solubilization for CBZ-SAC and CBZ-SLC. The cocrystal solubility and $S_{cocrystal}/S_{drug}$ dependence on ionization and micellar solubilization were predicted using the reported the cocrystal solubility product, K_{sp}, the coformer ionization constant, pK_a, and the component micellar solubilization constants, K_s. The cocrystal solubility dependence on ionization and micellar solubilization for a cocrystal of the nonionizable drug R and an acidic coformer HA has been described as:

$$S_T^{RHA} = \sqrt{K_{sp}\left(1 + \frac{K_a}{[H^+]} + K_s^{HA,T}[M]\right) + (1 + K_s^R[M])} \tag{5.5}$$

The $S_{cocrystal}/S_{drug}$ dependence on ionization and micellar solubilization has been derived previously,[18] and is determined according to

$$\frac{S_T^{RHA}}{S_T^R} = \frac{\sqrt{K_{sp}\left(1 + \frac{K_a}{[H^+]} + K_s^{HA,T}[M]\right) + (1 + K_s^R[M])}}{S_{aq}^R(1 + K_s^R[M])} \tag{5.6}$$

for a 1:1 cocrystal of nonionizable drug R and acidic coformer HA where K_{sp} is the cocrystal solubility product, K_a is the ionization constant of the acidic coformer and $K_s^{HA,T}$ and K_s^R are the solubilization constants of the coformer and the drug respectively.

Table 5.4 shows the thermodynamic parameters that are required, in addition to the determined K_s values, to model the solubility dependence on micellar solubilization and ionization for both the CBZ-SAC and CBZ-SLC. The solubility-pH dependence of

both CBZ-SAC and CBZ-SLC has been evaluated previously by our group,[14,18] and was used to obtain the solubility product for both cocrystals.

Table 5.4 Cocrystal K_{sp}, solubility and $S_{cocrystal}/S_{drug}$ in water at 25±0.5 °C.

Parameter	CBZ-SAC	CBZ-SLC
Coformer pKa	1.6 [a]	3.0 [b]
K_{sp} [c]	(1.00±0.0.05) x 10^{-6} m^2	(1.13± 0.05) x10^{-6} m^2
$S_{cocrystal, H2O}$ [d]	(2.36±0.05) x10^{-3} m pH 2.2	(1.32±0.06) x10^{-3} m pH 3.0
$S_{cocrystal}/S_{drug}$ [d]	4.5	2.5

(a) Reference [89]
(b) Reference [104]
(c) Reported K_{sp} of CBZ-SAC evaluated from nonlinear regression of coformer eutectic dependence on pH (pH 1-3, 25 °C).[18] Reported K_{sp} of CBZ-SLC evaluated from linear regression of coformer eutectic dependence on pH (water pH 1-4, 25°C).[14]
(d) Reference [47,120]

The solubility of CBZ-SAC is predicted to increase with surfactant concentration, while the solubility advantage relative to the drug should decrease with increasing surfactant concentration due to preferential solubilization of the drug.

Figure 5.3 shows that the solubility of CBZ-SAC is predicted to increase with increasing concentrations of both P103 and F127. The cocrystal solubility is predicted to be higher in solutions of F127 relative to P103, as shown in Figure 5.3(a), due to the higher K_s values of both CBZ and SAC in F127 than in P103. The $S_{cocrystal}/S_{drug}$ of CBZ-SAC decreases with increasing surfactant as shown in Figure 5.3(b) due to the preferential solubilization of the drug over the coformer,. The $K_s^{CBZ}/K_s^{SAC} = 1.2$ for both P103 and F127, however due to the higher overall solubilization in the surfactant F127, $S_{cocrystal}/S_{drug}$ decreases at lower concentrations of F127 than P103. The $S_{cocrystal}/S_{drug}$ theoretically reaches a plateau of 1.7 at 0.16 m concentrations of both P103 and F127, however these surfactants often form viscoelastic gels at higher concentrations.

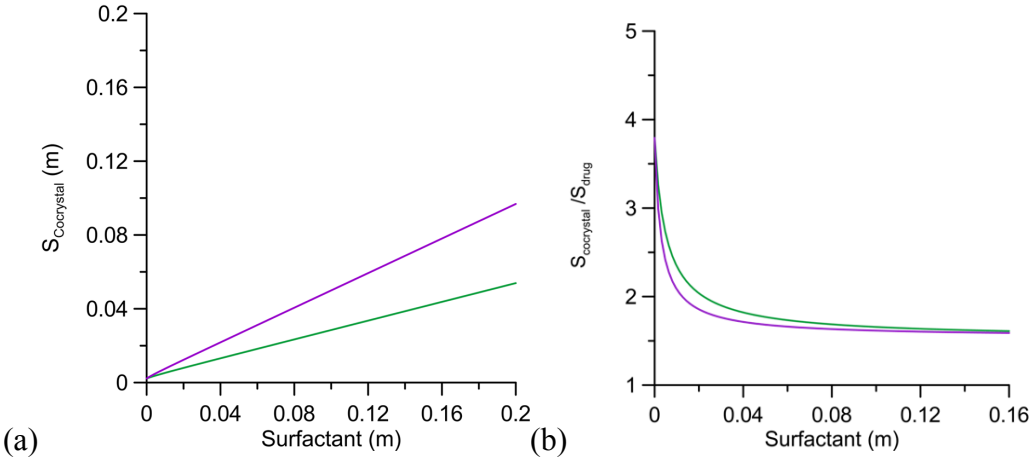

Figure 5.3. (a) $S_{cocrystal}$ and (b) $S_{cocrystal}/S_{drug}$ dependence on micellar surfactant concentration of P103 (—) and F127 (—) of 1:1 CBZ-SAC in deionized water (pH 2.2) Predicted curves were generated from equation (5.5) and (5.6) respectively using the K_s values in Table 5.2, K_{sp} =(1.00±0.05) 10^{-6} m^2,[18] and SAC pKa = 1.6.[89]

The CBZ-SLC solubility in both F127 and P103 presents an interesting case in which preferential solubilization of the coformer results in the increase of $S_{cocrystal}/S_{drug}$. Figure 5.4(a) shows the solubility of CBZ-SLC is predicted to increase with surfactant concentration in solution, and the dependence of CBZ-SLC solubility as a function of F127 and P103 is much greater than that observed for CBZ-SAC. Again, F127 is observed to solubilize the cocrystal components to a greater extent than P103 as determined by comparing the relative K_s values in Table 5.3.

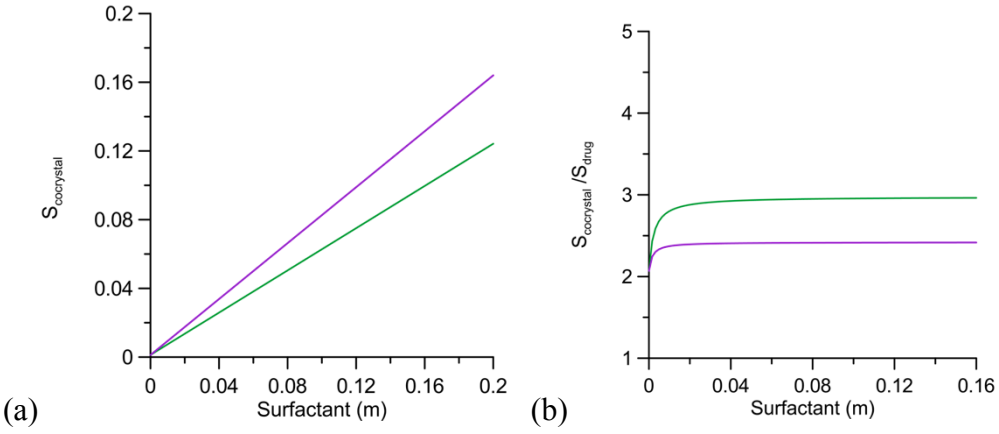

Figure 5.4(a) $S_{cocrystal}$ and (b) $S_{cocrystal}/S_{drug}$ dependence on micellar solubilization by P103 (—) and F127 (—) of 1:1 CBZ-SLC in deionized water (pH 3.0) Predicted curves were generated from equation (5.5) and (5.6) respectively using the K_s values in Table 5.3, K_{sp}=(1.13±0.05) 10^{-6} m^2,[14] and SLC pKa = 3.0.[104]

The $S_{cocrystal}/S_{drug}$ of CBZ-SLC is predicted to increase with increasing surfactant concentration due to the preferential solubilization of the coformer, however the $S_{cocrystal}/S_{drug}$ reaches a plateau of 3.0 and 2.5 for P103 and F127 respectively. The higher maximum $S_{cocrystal}/S_{drug}$ achieved by P103 is due to the greater difference in the solubilization constants; K_s^{SLC}/K_s^{CBZ}= 3.7 in P103 compared to K_s^{SLC}/K_s^{CBZ}=2.45 in F127. The experimental $S_{cocrystal}/S_{drug}$ shown in Figure 5.2 achieved the maximum $S_{cocrystal}/S_{drug}$. While P103 and F127 exhibit differential solubilization of the cocrystal components, these surfactants solubilized SAC and SLC to a higher extent than shown for other surfactants such as SLS,[15,16] Tween 80, Brij 99 and Myrj 52. Based on the presented eutectic measurements, P103 and F127 are not well suited for achieving a CSC for either CBZ-SAC or CBZ-SLC. Both P103 and F127 may be useful to increase the $S_{cocrystal}/S_{drug}$ of SLC cocrystals depending on the relative K_s^{drug}. The results presented here illustrate the importance of characterizing surfactant solution interactions with cocrystals.

Conclusions

Key parameters that affect $S_{cocrystal}/S_{drug}$ are the magnitude of K_s of the components in addition to the difference of K_s^{drug} and $K_s^{coformer}$. Simply adding a surfactant, or any formulation component which interacts differentially with the cocrystal components, has a significant impact on $S_{cocrystal}/S_{drug}$ The presented results illustrate a new level of control of $S_{cocrystal}/S_{drug}$ as surfactants that preferentially solubilize the coformer relative to drug, $K_s^{drug} < K_s^{coformer,}$ can be used increase the cocrystal solubility advantage. A target $S_{cocrystal}/S_{drug}$ can be achieved through careful surfactant selection and an understanding of how a given surfactant modulates cocrystal solubility as evidenced by eutectic point measurement. Cocrystal solubility increases with the micellar solubilization of the cocrystal components. The solubility advantage of a cocrystal ($S_{cocrystal}/S_{drug}$) depends on the relative solubilization of the drug compared to the coformer. Excipients such as polymers and surfactants may differentially interact with the cocrystal components; therefore it is crucial to characterize the solution interactions prior to including an additive in a cocrystal formulation, or a processing method. The eutectic measurement is very useful to characterize surfactant interactions with a

cocrystal and may help to guide excipient selection for the formulation development of a cocrystal.

References

4. Good DJ, Rodríguez-Hornedo Nr 2009. Solubility Advantage of Pharmaceutical Cocrystals. Cryst Growth Des 9(5):2252-2264.

5. Karki S, Friščić T, Fábián L, Laity PR, Day GM, Jones W 2009. Improving Mechanical Properties of Crystalline Solids by Cocrystal Formation: New Compressible Forms of Paracetamol. Advanced Materials 21(38-39):3905-3909.

10. Stanton MK, Kelly RC, Colletti A, Kiang YH, Langley M, Munson EJ, Peterson ML, Roberts J, Wells M 2010. Improved pharmacokinetics of AMG 517 through co-crystallization part 1: Comparison of two acids with corresponding amide co-crystals. Journal of Pharmaceutical Sciences 99(9):3769-3778.

14. Bethune SJ, Huang N, Jayasankar A, Rodriguez-Hornedo N 2009. Understanding and Predicting the Effect of Cocrystal Components and pH on Cocrystal Solubility. Cryst Growth Des 9(9):3976-3988.

15. Huang N, Rodriguez-Hornedo N 2011. Engineering cocrystal thermodynamic stability and eutectic points by micellar solubilization and ionization. Crystengcomm 13(17):5409-5422.

16. Huang N, Rodríguez-Hornedo N 2011. Engineering cocrystal solubility, stability, and pHmax by micellar solubilization. Journal of Pharmaceutical Sciences 100(12):5219-5234.

17. Huang N, Rodríguez-Hornedo Nr 2010. Effect of Micellar Solubilization on Cocrystal Solubility and Stability. Cryst Growth Des 10(5):2050-2053.

18. Alhalaweh A, Roy L, Rodríguez-Hornedo N, Velaga SP 2012. pH-Dependent Solubility of Indomethacin–Saccharin and Carbamazepine–Saccharin Cocrystals in Aqueous Media. Molecular Pharmaceutics.

34. Sanphui P, Goud NR, Khandavilli UBR, Nangia A 2011. Fast Dissolving Curcumin Cocrystals. Cryst Growth Des 11(9):4135-4145.

47. Huang N. 2011. Engineering Cocrystal Solubility and Stability via Ionization and Micellar Solubilization. Pharmaceutical Sciences, ed., Ann Arbor, MI: University of Michigan.

53. Kadam Y, Yerramilli U, Bahadur A 2009. Solubilization of poorly water-soluble drug carbamezapine in Pluronic® micelles: Effect of molecular characteristics, temperature and added salt on the solubilizing capacity. Colloids and Surfaces B: Biointerfaces 72(1):141-147.

78. Remenar JF, Peterson ML, Stephens PW, Zhang Z, Zimenkov Y, Hickey MB 2007. Celecoxib:Nicotinamide Dissociation: Using Excipients To Capture the Cocrystal's Potential. Molecular Pharmaceutics 4(3):386-400.

89. Kluza RB, Newton DW 1978. pKa values of Medicinal Compounds in Pharmacy Practice. Drug Intelligence & Clinical Pharmacy 12(9):546-554.

95. Good DJ, Rodríguez-Hornedo Nr 2010. Cocrystal Eutectic Constants and Prediction of Solubility Behavior. Cryst Growth Des 10(3):1028-1032.

104. Aydin R, Ozer, U 1997. Potentiometric and Spectroscopic Determination of Acid Dissociation Constants of Some Phenols and Salicylic Acids. Turkish Journal of Chemistry 21:428-436.

120. Bethune SJ. 2009. Thermodynamic and kinetic parameters that explain crystallization and solubility of pharmaceutical cocrystals. Pharmaceutical Sciences, ed., Ann Arbor, MI: University of Michigan.

126. Good D, Miranda C, Rodríguez-Hornedo N 2011. Dependence of cocrystal formation and thermodynamic stability on moisture sorption by amorphous polymer. Crystengcomm 13(4):1181-1189.
127. Sarkari M, Brown J, Chen X, Swinnea S, Williams Iii RO, Johnston KP 2002. Enhanced drug dissolution using evaporative precipitation into aqueous solution. International Journal of Pharmaceutics 243(1–2):17-31.
128. Batrakova E, Lee S, Li S, Venne A, Alakhov V, Kabanov A 1999. Fundamental Relationships Between the Composition of Pluronic Block Copolymers and Their Hypersensitization Effect in MDR Cancer Cells. Pharm Res 16(9):1373-1379.

Chapter 6

Conclusions and future work

This dissertation has investigated the influence of solution chemistry on the solubility and thermodynamic stability of cocrystals and cocrystalline salts relative to their constituents. Solution mechanisms that differentially affect the component solubilities can be used to engineer cocrystal (and cocrystalline salt) solubility and their solubility advantage relative to the parent drug (or salt). Through identification of the solution mechanisms that modulate the component solubilities (i.e. ionization, micellar solubilization and complexation), it is possible to derive mathematical models to anticipate the cocrystal (or cocrystalline salt) solubility behavior under a range of different solution conditions. These mathematical models can be applied to engineering the solubility to meet the required specifications for a given drug product.

The objectives of this dissertation were to (1) determine the key parameters and experiments required to guide surfactant selection to modulate cocrystal solubility, $S_{cocrystal}/S_{drug}$, and CSC, (2) develop mathematical models to predict the cocrystal solubility in a given physiologically relevant media from the knowledge of the aqueous cocrystal solubility and the component solubilities in the given media, (3) evaluate the relative component solubilization by physiologically relevant mixed micelles and the resulting effect on the $S_{cocrystal}/S_{drug}$ and observed supersaturation, (4) investigate $S_{cocrystal}/S_{drug}$ as a predictor of the relative supersaturation achieved among different media, (5) develop mathematical models to describe the cocrystalline salt solubility dependence on pH, counter-ion, coformer, stoichiometry and solution complexation, and (6) design methodologies and mathematical expressions to assess the equilibrium solubility of cocrystalline salts that generate supersaturation relative to the parent salt.

The indomethacin-saccharin cocrystal, which is 26 times more soluble than the drug at pH 2.1, converts within 2 minutes to the parent drug during powder dissolution. Micellar solubilization was found to thermodynamically stabilize indomethacin-saccharin

against transformation in solutions containing surfactant concentrations above the CSC. Surfactants were rationally selected to modulate the solubility and $S_{cocrystal}/S_{drug}$ of this cocrystal composed of the hydrophobic drug indomethacin, log P=4.4, and the hydrophilic coformer saccharin, log P = 0.9, based on the asymmetric solubilization of the cocrystal components. Therefore surfactants were selected based on the observed solubilization of the hydrophobic drug (K_s^{drug}) and the preferential solubilization of the drug relative to the coformer ($K_s^{drug} > K_s^{coformer}$).

Tween 80, Myrj 52, Brij 99, and SLS were all observed to achieve CSC; the nonionic surfactants solubilized indomethacin to a greater extent than SLS, and as anticipated, the nonionic surfactants achieved a lower CSC than SLS. The $S_{cocrystal}$ dependence on micellar solubilization and CSC were successfully evaluated by three methods: (1) by calculation from the intersection of $S_{cocrystal}$ and S_{drug} using the cocrystal K_{sp} in conjunction with values of cocrystal component ionization (K_a), micellar solubilization (K_s), surfactant CMC and solution pH, (2) by measurement of cocrystal eutectic points as a function of [M] from which the experimental cocrystal and drug solubility at a given pH can be obtained and (3) by calculation of the intersection of the drug and coformer eutectic concentration dependence on micellar solubilization. All three methods were in agreement when both drug and coformer solubilization were used to evaluate $S_{cocrystal}$ dependence on [M] and CSC by calculation, which show that $S_{cocrystal}$ and CSC can be *a priori* predicted from knowledge of cocrystal K_{sp}, component K_a values and component K_s values.

The cocrystal solubility dependence on micellar solubilization, and the CSC were under predicted when coformer solubilization was assumed to be negligible. All the surfactants studied solubilized saccharin to a small extent, and the CSC values predicted without consideration of coformer solubilization were half that of the CSC values observed. The nonionic surfactants were observed to solubilize the coformer to a greater extent than SLS, and still achieved lower CSC values; the drug solubilization (K_s^{drug}) was found to be the most influential parameter in rank-ordering surfactants to achieve a lower CSC. Cocrystal and drug phase solubility diagrams in surfactant solutions constructed from the measured drug and cocrystal solubilities in surfactant solutions, were useful to

identify the regions, or solution conditions in which the cocrystal is thermodynamically stable relative to the drug.

Below the CSC the cocrystal was more soluble than the drug, and micellar solubilization was observed to modulate the cocrystal solubility relative to the parent drug ($S_{cocrystal}/S_{drug}$). While cocrystal solubility increases due to micellar solubilization, the $S_{cocrystal}/S_{drug}$ decreases due to the preferential solubilization of the drug relative to the coformer. The surfactant concentration required to reduce the $S_{cocrystal}/S_{drug}$ of indomethacin-saccharin to half its value in aqueous media, at pH 2.1, was highly dependent on the K_s^{IND} and the surfactant CMC. The nonionic surfactants exhibited CMC values that were 1 to 2 magnitudes lower than that of SLS. Tween 80 exhibited the lowest CMC of the surfactants studied and required the least amount of surfactant to reduce the $S_{cocrystal}/S_{drug}$ to half its value. This has important implications for the evaluation of cocrystal solubility by dissolution in media containing surfactants; the $S_{cocrystal}/S_{drug}$ of indomethacin-saccharin is reduced by a third of its value at surfactant concentrations that are just slightly above the CSC. Assuming a cocrystal could maintain supersaturation without transforming, evaluating its solution behavior relative to the drug in the presence of a surfactant could conceal its true solubility advantage.

The $S_{cocrystal}/S_{drug}$ of indomethacin-saccharin increases with pH in the range of 1-3 due to the increased ionization of the coformer saccharin relative to the drug (which is primarily unionized in this pH range). In contrast, micellar solubilization decreases $S_{cocrystal}/S_{drug}$ due to the preferential solubilization of the drug relative to coformer. More surfactant is required to achieve CSC as pH increases because micellar solubilization must overcome the increase in $S_{cocrystal}/S_{drug}$ due to ionization. Therefore the pH range in which the CSC can be achieved depends on the coformer ionization relative to that of the drug and the magnitude of the micellar solubilization of the drug relative to the coformer. The CSC for the indomethacin-saccharin cocrystal was achieved in a pH range of 1-3 based on the mathematical models for the CSC dependence on ionization and micellar solubilization. Selecting an alternative coformer that has a higher pKa than saccharin could increase the pH range in which the CSC is achieved for a cocrystal of indomethacin.

A supersaturation of 7.5 cannot be maintained by indomethacin-saccharin, and lowering the $S_{cocrystal}/S_{drug}$ results in a lower supersaturation that is maintained for a longer time period. The mathematical model derived for the $S_{cocrystal}/S_{drug}$ dependence on micellar solubilization was useful to calculate the required surfactant concentration to achieve a target solubility and $S_{cocrystal}/S_{drug}$. Based on the mathematical models, 0.1% (w/w) Tween 80 was predicted to reduce the $S_{cocrystal}/S_{drug}$ from 26 (pH 2 buffer) to 6, this value was targeted as it is less than the maximum supersaturation that was generated by the cocrystal. The observed supersaturation in 0.1% Tween 80 was 4.4, which was sustained for 15 minutes before the solution concentrations began to drop. However, the cocrystal maintained a supersaturation of 2 for 2 hours.

Cocrystals provide an opportunity to create a supersaturating drug delivery system (similar to the amorphous form) with the advantage of maintaining a crystalline phase. However, when $S_{cocrystal}>S_{drug}$, the conversion to the less soluble parent drug may occur upon contact with aqueous media, either during processing, formulation, or when dosed in media; therefore utilizing surfactants, or any other additives that differentially interact with the cocrystal components may be useful to protect against conversion. Moving forward, these solubility models could be used to design appropriate solution conditions for cocrystal suspension formulations. For cocrystals to be a viable drug product, knowledge of their solution chemistry must be merged with current formulation and manufacturing practices.

There are several examples in which cocrystal solubility behavior, relative to the parent drug, is characterized by dissolution in media containing physiologically relevant mixed micelles of sodium taurocholate and lecithin. Regardless of the actual biorelevance of the media, if it contains micellar components that differentially solubilize the cocrystal components, it will affect $S_{cocrystal}/S_{drug}$, which was shown to affect cocrystal supersaturation and the driving force for transformation during dissolution in the second chapter of this thesis. Cocrystal solubility was evaluated in fed state simulated intestinal fluid (FeSSIF) to determine the influence of NaTC and lecithin mixed micelles on cocrystal solubility relative to acetate buffer, which is the same media without NaTC and lecithin. FeSSIF was selected due to its high concentrations of NaTC and lecithin, and its frequent use.

Carbamazepine-saccharin, carbamazepine-salicylic acid, carbamazepine 4-aminobenzoic acid and indomethacin-saccharin all exhibited higher solubilities than the parent drug in both FeSSIF and buffer. However, cocrystal solubilization was lower than that of the drug due to the preferential solubilization of the drug by FeSSIF; this occurs as the drug components were solubilized while the coformers were not ($K_s^{coformer} = 0$). Even though cocrystal solubilities were higher in FeSSIF relative to buffer, the preferential micellar solubilization of the drug was observed to reduce $S_{cocrystal}/S_{drug}$. Appreciable differences in $S_{cocrystal}/S_{drug}$ related to the magnitude of the drug solubilization. For example, carbamazepine was 1.8 times more soluble in FeSSIF relative to buffer while indomethacin was 16 times more soluble in FeSSIF relative to buffer. The preferential solubilization of indomethacin resulted in a reduction of $S_{cocrystal}/S_{drug}$ for IND-SAC while the solubilization of carbamazepine in FeSSIF was not substantial enough to reduce $S_{cocrystal}/S_{drug}$.

$S_{cocrystal}/S_{drug}$ was found to be a good predictor of the relative supersaturation observed between different media, in this case FeSSIF compared to buffer. Indomethacin-saccharin, which has a lower $S_{cocrystal}/S_{drug}$ in FeSSIF relative to buffer, exhibits a lower supersaturation in FeSSIF relative to buffer, which is maintained for four hours. The cocrystal achieved a higher supersaturation in buffer relative to FeSSIF, however this supersaturation could not be maintained due to solution-mediated transformation after 10 minutes. The indomethacin concentrations during dissolution were higher in FeSSIF relative to buffer, which was in agreement with the equilibrium solubility studies.

Because FeSSIF, and other "physiologically relevant" media, are more expensive than aqueous buffers and synthetic surfactants, it is useful to predict the cocrystal solubility in a given media based on the cocrystal K_{sp} and the component solubilities in a given media. Solubility predictions in different media provide valuable information while sparing the materials necessary to obtain a robust solubility characterization. Therefore, mathematical models were developed to predict the cocrystal solubility in FeSSIF based on the aqueous cocrystal solubility (K_{sp}) and the component solubilities in FeSSIF. The cocrystal solubilities predicted using the mathematical models were in excellent agreement with the experimental results. Previously, the increase in cocrystal

solubility in a synthetic micellar solution relative to a solution at the same pH without surfactant was found to correspond to the square-root of the ratio of drug solubility increase in the same solutions; this relationship was found to apply to the mixed micelles of NaTC and lecithin. The predicted cocrystal solubilization estimated from the observed drug solubilization in FeSSIF was also in excellent agreement with the measured values.

FeSSIF has been found to overestimate the solubility of BCS class II drugs under fed state conditions compared to human intestinal fluid, however future work investigating the effects of human intestinal fluid in the fed state on $S_{cocrystal}/S_{drug}$ is essential to evaluate whether bio-surfactants are capable of reducing $S_{cocrystal}/S_{drug}$ which may result in improved (or in some cases inferior) pharmacokinetic behavior. The derived mathematical equations allow for the cocrystal solubility and $S_{cocrystal}/S_{drug}$ prediction in any aqueous media containing a micellar component, from knowledge of the cocrystal K_{sp} and the component solubilities in the given media. Therefore, future work would involve applying these models to understand the pharmacokinetic behavior of a cocrystal in the fed versus fasted state. However, in order to evaluate this correlation, the solution conditions of both the fed and fasted state must be confirmed.

The cocrystalline salts of fluoxetine HCl are shown to exhibit different apparent solubilities in water, however prior to the work presented in this thesis, the solubility dependence of cocrystalline salts on pH, and solution concentrations of counter-ion and coformer had not been explored. The solution chemistry of the cocrystalline salts of fluoxetine HCl (1:1 benzoic acid, 2:1 fumaric acid and 2:1 succinic acid) were investigated to gain insights into the key parameters that are required to characterize the cocrystalline salt solubility under a variety of solution conditions.

Similar to salts and cocrystals, cocrystalline salts exhibit solubility product behavior that is dependent on the equilibrium solution concentrations of drug, coformer and counter-ion; the drug solution concentrations in equilibrium with a cocrystalline salt decrease with increasing counter-ion or coformer in solution. The solubility product behavior of HCl salts is often problematic due to the reduction in solubility in the concentrations of chloride that are present throughout the GI tract. Cocrystalline salts were observed to exhibit a weaker dependence on counter-ion relative to the parent salt, which may be useful to mitigate the common-ion effect. The order of solubility

dependence on chloride, from strongest to weakest, was observed to be salt >2:1 cocrystalline salt > 1:1 cocrystalline salt.

For the first time, mathematical models that describe cocrystalline salt solubility dependence on pH, counter-ion, coformer and stoichiometry are derived considering the heterogeneous solution equilibria describing cocrystalline salt dissociation and component ionization. Based on the derived mathematical models, chloride salts exhibit pH independent solubility below pH_{max}, and cocrystallization with a coformer with a pK_a below the pH_{max} of the salt is predicted to impart solubility-pH dependence to the salt plateau region due to the ionization of the coformer. The derived mathematical models allowed for the evaluation of the cocrystalline salt solubility product by nonlinear regression analysis of the cocrystalline salt solubility dependence on counter-ion.

The solubility-pH dependence of the fluoxetine HCl cocrystalline salts were predicted to increase with pH based on the derived mathematical models considering the cocrystalline salt solubility product, K_{sp}, and the coformer ionization constant(s) (K_a). Based on the derived solubility-pH models, a cocrystalline salt that exhibits a lower intrinsic solubility than the parent salt achieves a pH_{max} where the cocrystalline salt and parent salt solubilities are equal. Above the pH_{max}, the cocrystalline salt is expected to have a solubility advantage relative to the parent salt.

The cocrystalline salt solubility was observed to increase with increasing pH, when the solution-pH could be independently modified to the pH range in which a solubility increase was predicted. The coformers, particularly benzoic acid, exhibited a self-buffering effect such that the solution pH range in which the cocrystalline salt solubility was predicted to increase could not be achieved. The 2:1 fluoxetine HCl fumaric acid cocrystalline salt was evaluated in the pH range of 1.4 to 2.88, and above pH 2.88 the solution pH could not be independently modified. However, suspension of this cocrystalline salt in a pH 7 phosphate buffer generated a supersaturation of 2 relative to the parent salt.

The solubility product behavior of cocrystals has been useful to design screening and synthesis methods such as the reaction crystallization method; this method is also applicable to screen and synthesize cocrystalline salts by generating supersaturation with respect to the cocrystalline salts by increasing the component concentrations in solution.

Because cocrystalline salts exhibit solubility product behavior, the equilibrium solubility of a metastable cocrystalline salt can be accessed at the eutectic point between the salt and the cocrystalline salt in solutions containing excess coformer. The solutions must contain excess coformer because excess chloride is shown to increase cocrystalline salt solubility relative to the parent salt, while excess coformer decreases the cocrystalline salt solubility relative to the parent salt. The stoichiometric solubility can be determined from the component solution concentrations in equilibrium at the eutectic point based on the derived mathematical expressions.

Succinic acid was observed to increase the solubility of the fluoxetine HCl salt; therefore to characterize the solubility of the fluoxetine HCl succinic acid cocrystalline salt, the solution complexation of the ionized fluoxetine with the unionized succinic acid was quantified using an apparent complexation constant, K_{11}. A mathematical equation describing the cocrystalline salt solubility was derived incorporating 1:1 solution complexation. The proposed solubility model was in excellent agreement with both the solid phase stability studies and solubility studies carried out for this cocrystalline salt, which enabled an estimate of the equilibrium cocrystalline salt solubility in the absence of coformer.

The contribution of the cocrystalline salt lattice energy to the aqueous solubility was determined by evaluating the ideal solubilities of the salt and cocrystalline salts from their fusion temperature and enthalpy of fusion. Similar to cocrystals, the fusion properties of the cocrystalline salts studied were not predictive of their aqueous solubilities. The 1:1 fluoxetine HCl benzoic acid cocrystalline salt exhibited the lowest ideal solubility, however this was the least soluble cocrystalline salt. Though cocrystalline salts exhibit different fusion properties relative to the parent salt, their aqueous solubilities were dominated by solvent-solute interactions relative to lattice contributions.

Currently, cocrystals and cocrystalline salts are under-utilized as supersaturating solid forms due to a lack of understanding of their solution chemistry. The majority of the cocrystals presented in this work exhibit higher solubilities than the parent compound; therefore kinetic approaches would have grossly underestimated the true equilibrium solubility, and would give no indication to the solubility behavior under different solution

conditions. The solubility models presented in this thesis allow for the identification of solution conditions that will enable the cocrystal and cocrystalline salt solubility advantage relative to the parent compound. The eutectic point measurements used in this work were useful to characterize both cocrystal and cocrystalline salt solubility under equilibrium conditions. Eutectic measurements in media with and without surfactant provide valuable information concerning the surfactant interactions with cocrystal components, which can be used to calculate the surfactant necessary to achieve a CSC or a target $S_{cocrystal}/S_{drug}$. The cocrystal solubility and supersaturation can be engineered by taking advantage of any solution mechanism that alters cocrystal solubility relative to the parent drug.